SKB

TECHNICAL REPORT 97-30

ZEDEX – A study of damage and disturbance from tunnel excavation by blasting and tunnel boring

Simon Emsley[1], Olle Olsson[2], Leif Stenberg[2],
Hans-Joachim Alheid[3], Stephen Falls[4]

1 Golder Associates, Maidenhead, United Kingdom
2 Swedish Nuclear Fuel and Waste Management Co., Figeholm, Sweden
3 Federal Institute for Geosciences and Natural Resources, Hannover, Germany
4 Queens University, Kingston, Ontario, Canada

December 1997

SVENSK KÄRNBRÄNSLEHANTERING AB
SWEDISH NUCLEAR FUEL AND WASTE MANAGEMENT CO

P.O.BOX 5864 S-102 40 STOCKHOLM SWEDEN
PHONE +46 8 459 84 00
FAX +46 8 661 57 19

ZEDEX - A STUDY OF DAMAGE AND DISTURBANCE FROM TUNNEL EXCAVATION BY BLASTING AND TUNNEL BORING

Simon Emsley[1], Olle Olsson[2], Leif Stenberg[2], Hans-Joachim Alheid[3], Stephen Falls[4]

1 Golder Associates, Maidenhead, United Kingdom
2 Swedish Nuclear Fuel and Waste Management Co., Figeholm, Sweden
3 Federal Institute for Geosciences and Natural Resources, Hannover, Germany
4 Queens University, Kingston, Ontario, Canada

December 1997

ZEDEX - A STUDY OF DAMAGE AND DISTURBANCE FROM TUNNEL EXCAVATION BY BLASTING AND TUNNEL BORING

Simon Emsley

Golder Associates, Maidenhead, United Kingdom

Olle Olsson

Leif Stenberg

Swedish Nuclear Fuel and Waste Management Co., Figeholm, Sweden

Hans-Joachim Alheid

Federal Institute for Geosciences and Natural Resources, Hannover, Germany

Stephen Falls

Queens University, Kingston, Ontario, Canada

DECEMBER 1997

A JOINT STUDY FUNDED BY

ANDRA- UK NIREX LTD-SKB

FOREWORD

Important contributions to the realization of work performed and the production of this report have been given by the following organizations and individuals:

- ANDRA, France, André Cournut, Karim Ben Slimane and Jean-Francois Durand-Smet
- Bundesanstalt fur Geowissenschaften und Rohstoffe (BGR), Germany, Hans-Joachim Alheid, Klaus-G Hinzen, M. Knecht and D. Böddener
- Colenco Power Engineering Ltd, Switzerland, Ondrej Voborny, Eric Tauzin and Oliver Jaquet
- Conterra AB, Sweden, Bengt Leijon
- Geomechanics Research Centre, Canada, Derek Martin, J Alcott and S Yazici
- Geosigma AB, Sweden, Seje Carlsten, John Olausson, Jan-Erik Ludvigsson, Agne Bern, Kent Rubinsson, Örjan Magnusson, Bengt Gentzschein and Allan Stråhle
- Geoväst, Sweden, Robert Gass
- Golder Associates, Germany, Christian Enachescu
- Golder Associates, Sweden, Jan Hermansson and Sven Follin
- Golder Associates, UK, Simon Emsley and John Wozniewicz
- JAA AB, Australia, Nick Litterbach, Max Lee and Mike Struthers
- JAA AB, Sweden, Bengt Stillborg, Göran Nilsson and Mats Holmberg
- Juliusz Sandecki, Lund, Sweden
- Keele University, UK, Paul Young, Ruth Murdie and Ian Stimpson.
- Kärnborrning AB, Sweden
- Laboratorie de Geomécanique, Ecole Nationale Supérieure de Géologie (ENSG), France, Francoise Homand, Corinne Bauer and Stephane Pepa
- Malå GeoScience, Sweden, Christer Gustafsson
- Luleå University of Technology, Sweden, Jonny Sjöberg, Gunnar Rådberg, Xiangchun Tan and Shaoquan Kou
- Mesy GmbH, Germany, F Rummel
- NAGRA, Switzerland, Stratis Vomvoris, Berndt Frieg and Peter Blhmling
- Norwegian Geotechnical Institute (NGI), Norway, Nick Barton, Lloyd Tunbridge, Fredrik Löset, Pawel Jankowski and Fan-Nian Kong
- Office for In situ Ingenieur Seismik (I.S.I.S), Germany, Sharon K. Reamer
- PNC, Japan, Hiroya Matsui
- PRG-Tec Ltd, Finland, Pekka Rouhiainen
- Roy Stanfors Consulting, Sweden, Roy Stanfors
- Scandiaconsult, Sweden, Raymond Munier
- SINTEF, Norway, Arne Myrvang
- SKANSKA AB, Sweden
- SKANSKA AB, Sweden, Bengt Niklasson

- SKB, Sweden, Göran Bäckblom
- SKB, Äspö Hard Rock Laboratory, Sweden, Olle Olsson, Mats Ohlsson, Gunnar Ramqvist and Leif Stenberg
- Swedish Rock Engineering, SveBeFo, Sweden, Mats Olsson and Lena Reidarman
- Sydkraft Konsult AB, Sweden, Ingemar Markström and Kristian Annertz
- UK Nirex, UK, David Mellor and Nick Davis
- Vattenfall Hydropower, Sweden, Christer Ljunggren and Hans Klasson
- VBB Viak, Sweden, Torbjörn Forsmark and Gert Rudolf
- Vibrometric Oy, Finland, Calin Cosma, Seppo Honkanen, Pekka Heikkinen and Nicoleta Enescu
- Queen's University, Canada, Stephen Falls and Gerhard Pratt
- YSO Consultants, France, Yvan Sifre and Pascal Bernasconi

ABSTRACT

The ZEDEX project was undertaken as a joint project by ANDRA, UK Nirex and SKB with significant contributions from BMBF and Nagra. The objectives of the project were to understand the mechanical behaviour of the Excavation Disturbed Zone (EDZ) with respect to its origin, character, magnitude of property change, extent and its dependence on excavation method. Supporting studies to increase understanding of the hydraulic significance of the EDZ and to test equipment and methodology for quantifying the EDZ were also performed. In the ZEDEX project excavation with "normal" smooth blasting, blasting with low-shock explosives and tunnel boring (TBM) was studied. The drifts are located in the Äspö Hard Rock Laboratory at a depth of 420 metres, the profiles are circular and 5 metres in diameter.

The results from the ZEDEX Project have shown that there is a damaged zone, close to the drift wall dominated by changes in rock properties which are mainly irreversible and that there is a disturbed zone beyond the damaged zone that is dominated by changes in stress state and hydraulic head and where changes in rock properties are small and mainly reversible. The changes in rock properties and rock stress with distance from the rock wall of the excavation is gradational and there is hence no distinct boundary between the two zones.

The damaged zone caused by the excavation methods applied has been identified by several measurement techniques. Monitoring of Acoustic Emission (AE) events is the most sensitive method which indicates minor damage due to crack opening and slip. For the Drill&Blast (D&B) drift significant AE-activity was observed up to 1 metre from the drift wall while the corresponding extent for the TBM drift is a few tens of centimetres. Changes in seismic velocity indicate a larger increase in crack density. The dye penetration tests performed in the slots cut from the drift has shown the extent of macro fracturing, which in the floor of the D&B drift has extended to about 50 centimetres. The hydraulic measurements performed in the damaged zone showed little if any change in permeability of the rock matrix.

The disturbed zone is characterised by elastic displacements and no induced fracturing. There are only very few AE-events observed in the disturbed zone and these have been found to correspond to slip on existing fractures. The AE-event density in the disturbed zone is also similar for both the TBM and D&B drifts. The hydraulic tests performed before and after excavation have not revealed any significant changes in hydraulic properties due to excavation.

The results from ZEDEX indicate that the role of the EDZ as a preferential pathway to radionuclide transport is limited to the damaged zone. The extent of the damaged zone can be limited through application of

appropriate excavation methods. By limiting the extent of the damaged zone it should also be feasible to block pathways in the damaged zone by plugs placed at strategic locations.

SAMMANFATTNING

ZEDEX- projektet har genomförts som ett internationellt samarbetsprojekt mellan ANDRA, UK Nirex och SKB med bidrag från BMBF och Nagra. Projektets mål har varit att studera den störda zonen (EDZ) med avseende på orsaken till förändringar i bergets egenskaper, förändringarnas storlek, störda zonens utbredning samt dess beroende av brytmetod. Kompletterande studier för att öka förståelsen av den hydrauliska betydelsen av EDZ genomfördes liksom test av metoder och utrustning för att mäta EDZ. I projektet har "normal" drivning medelst sprängning, försiktig sprängning och tunnelborrning (TBM) studerats. Tunnlarna är belägna i Äspölaboratoriet på 420 m djup, har cirkulär profil och är 5 m i diameter.

ZEDEX projektets resultat visar att det föreligger en skadad zon, närmast bergytan som karakteriseras av irreversibla förändringar i bergets egenskaper och att det är en störd zon utanför den skadade zonen som domineras av förändringar i bergspänningar och hydrauliskt tryck och där förändringarna i bergets egenskaper är reversibla. Förändringarna i bergets egenskaper och bergspänningar förändras gradvis som funktion av avståndet från bergytan och det finns ingen distinkt gräns mellan den skadade och störda zonen.

Den skadade zonen förorsakad av sprängningarna har identifierats med flera mätmetoder. Registrering av akustisk emission (AE) är den känsligaste metoden, vilken indikerar mindre skador förorsakade av spricköppning och rörelser längs med sprickor. Den sprängda tunneln visade tydlig AE aktivitet upp till 1 meter från tunnelväggen medan motsvarande aktivitet för TBM tunneln kunde observeras ett fåtal centimeter utanför tunnelväggen. Förändringar i seismisk hastighet visar en ökning i spricktäthet. Infärgning av sågade slitsar i berget visar utbredningen av makrosprickor, som i golvet på den sprängda tunneln hade en utbredning på ungefär 50 centimeter. De hydrauliska mätningarna utförda i den skadade zonen visade små om alls några förändringar i bergmatrisens permeabilitet.

Den störda zonen karakteriseras av elastiska förskjutningar och inga inducerade sprickor. Det har bara observerats ett fåtal akustiska emissioner i den störda zonen och dessa har visat sig bero på förskjutning på existerande sprickplan. Tätheten av AE är också likvärdig för både TBM och den sprängda tunneln i den störda zonen. De hydrauliska mätningarna utförda före och efter sprängning har inte visat på några större ändringar i hydrauliska egenskaper förorsakade av tunnelbrytningen.

Resultatet av ZEDEX indikerar att transport av radionuklider i EDZ är begränsad till den skadade zonen. Utbredningen av den skadade zonen kan begränsas med användning av särskilt anpassade brytmetoder. Genom att

begränsa skadezonens utbredning är det också möjligt att blockera transportvägar i skadezonen med hjälp av strategiskt placerade pluggar.

TABLE OF CONTENTS

EXECUTIVE SUMMARY

BACKGROUND AND OBJECTIVES

This report presents the results of the ZEDEX (Zone of Excavation Disturbance EXperiment) project undertaken at the Äspö Hard Rock Laboratory (HRL), Sweden, between April 1994 and July 1996. The project was undertaken in two phases with the first experimental phase being completed in 1995 and reported by Olsson *et al.* (1996b). The analysis of those results showed that further data collection and more thorough analysis of the existing data would be beneficial for a better understanding of the extent and properties of the disturbed zone for different excavation techniques. Consequently a second phase was undertaken with the experimental acquisition work performed between January and July 1996. The results and analyses from the second phase were integrated with those from the first phase. This report presents the combined data and results for both phases of the project.

The ZEDEX project was undertaken as a joint project by ANDRA, UK Nirex and SKB with significant contributions from BMBF and Nagra. The objectives of the project were to understand the mechanical behaviour of the Excavation Disturbed Zone (EDZ) with respect to its origin, character, magnitude of property change, extent and its dependence on excavation method. Supporting studies to increase understanding of the hydraulic significance of the EDZ and to test equipment and methodology for quantifying the EDZ were also performed.

SKB's decision to test Tunnel Boring Machine (TBM) excavation methods in addition to drill and blast excavation for the main access tunnel of the Äspö HRL provided an opportunity for studying EDZ properties and extent for two principally different excavation methods. In combination with ANDRA's interest to develop optimised blast designs which could reduce the extent of the EDZ and UK Nirex interest to test methods for quantifying the EDZ, this provided a basis for setting up the ZEDEX Project as a joint international undertaking.

The rationale for undertaking this project is that it is considered that the properties of the disturbed zone, that develop around excavations created by the construction of a repository, may affect the efficiency and effectiveness of plugs placed to seal underground openings and provide enhanced hydraulic conductivities which may be detrimental to performance assessment. Safety or performance assessment undertaken indicates that the extent and magnitude of the EDZ has an effect on safety or performance of the repository system. The measurement of the EDZ around particular excavations may therefore be used to demonstrate whether the extent or

magnitude of property changes within the EDZ has any affect on the safety of the system.

It is generally accepted that any underground excavation or opening is surrounded by zones that have been damaged and disturbed due to the redistribution of rock stresses that occur as a consequence of the excavation. The abbreviation EDZ is often used to describe the zone around an excavation and is used variously for the term "Excavation Disturbed Zone" as well as for "Excavation Damage Zone". In this report the term EDZ is taken to mean the disturbed zone that includes the failed and damage zones closest to the wall that are caused by the excavation method (Read, 1996). In the failed zone the rock has completely disintegrated; whilst the damaged zone is characterised by changes in rock properties and changes in state (for example, stress field, hydraulic head). In the disturbed zone the material properties remain almost unchanged whereas changes in state are considered to be dominant.

Previous documented work has shown that the excavation of a tunnel will cause a disturbance to the rock mass surrounding the tunnel. The character and magnitude of the disturbance depends on the tunnel shape and size, the method of excavation used to excavate the tunnel, the stress state and the properties and nature of the rock mass and how these react to the presence of the air filled void. The hypothesis established at the outset of the project was that it was anticipated that the near-field (< 2 metres) disturbance should be reduced by the application of an appropriate excavation method (smooth blasting or tunnel boring). It was also predicted that the far-field disturbance (> 2 metres) would be essentially independent of the excavation method.

The ZEDEX Project included tests of normal smooth blasting, similar to that used for excavation of the Äspö HRL tunnel to a depth of approximately 420 metres, together with smooth blasting based on the application of low-shock energy explosives together with an optimised drilling pattern. The ZEDEX project comprised investigations before, during and after excavation of the drifts. The results from the two blast designs were compared with those from the TBM excavation. This systematic approach provided the ability to monitor the progressive development of the EDZ.

EXPERIMENTAL CONFIGURATION AND SCOPE

The site for the study was located at the very beginning of the TBM drift at a depth of 420 metres below ground. The experimental drift for the drill and blast operations was located parallel and 23 metres from the TBM drift. This location was determined by the location of the TBM drift and the requirement that the two test drifts should be situated in relatively homogeneous Äspö diorite so that the geological conditions for both drifts would be similar, facilitating a meaningful comparison.

The TBM test drift constitutes part of the main access tunnel of the Äspö HRL. The test section is 35 metres long and located directly after the TBM assembly hall. A drift was excavated from the end of the assembly hall to access the drill & blast (D&B) test drift with the blast design being optimised during the excavation of this drift. The first two rounds in the D&B test drift were not part of the test and were used to reduce the effects of the anomalous stress field caused by the drilling niches and D&B access drift and to allow plane strain conditions. The following four rounds were used for testing the smooth blasting technique based on low-shock energy explosives and the remaining five rounds were used for testing the effects of normal blasting. The shape of the blasted drift was designed to be circular with a flat floor and with the same diameter (5 metres) as the TBM drift. A number of boreholes were drilled axially and radially relative to the test drifts to assess the properties and extent of the EDZ. These boreholes were used to undertake a range of measurements that included seismic tomography, borehole radar, hydraulic testing and Acoustic Emission (AE) monitoring. After excavation of the drifts a number of short (3 metres) radial boreholes were drilled in each drift to assess the extent of the damage zone in the near-field, measurements included velocity logging and high resolution hydraulic measurements. A set of longer (~15 metres) boreholes was drilled radially from the drift to investigate properties of the disturbed zone, in the far-field, at a larger distance from the drift wall.

During the second phase of the project additional 8 metre long radial boreholes were drilled in a ring around both drifts, two rings located in the D&B drift and one in the TBM drift. Additional measurements were undertaken in these boreholes that included high resolution hydraulic measurements, seismic velocity logging, seismic tomography and anisotropy measurements. In two of the rings, one in each drift, three additional boreholes were drilled parallel to one of the existing boreholes, in order to perform seismic velocity anisotropy studies. Additionally, three boreholes were drilled for stress measurements, two of the boreholes were positioned in the pillar between the drifts and one was directed SE of the D&B drift to obtain measurements of the virgin stress field. A fourth borehole was subsequently drilled in the pillar between the drifts to undertake confirmatory stress measurements, this borehole is close and sub-parallel to the other two boreholes, in the pillar, used for stress measurements.

INITIAL CHARACTERISATION

The initial characterisation of the ZEDEX volume is partly based on measurements performed before the excavation of the drifts. The data showed that the two test drifts were located in grey medium grained Äspö diorite with irregular sheets of red fine grained granite cutting the drifts at various locations. The rock mass is intersected by three dominant sets of fractures, some of which were water bearing with considerable outflow. The D&B drift is only intersected by two water conducting fractures while the TBM drift was intersected by a larger number of water conducting fractures.

Borehole radar, seismic reflection and geotechnical logging were all useful in delineating these features. The main fracture sets are all steeply dipping, striking NW and NE.

Geotechnical logging used to determine the rock mass quality gave quite uniform results of good quality rock in the TBM drift but showed more variability in the D&B drift.

Seismic tomographic imaging showed variability in velocity and attenuation interpreted to be associated with fracturing. One or two features in the tomograms were seen to correlate with mapped fractures in the TBM drift. However, identifying smaller features from tomographic imaging alone was generally more problematic. The average P-wave velocity of about 6 kms^{-1} indicated a very good quality rock mass. Seismic anisotropy measurements showed good correlation with fracture orientations. The reflection analysis of the tomographic data indicated the presence of reflectors that were present prior to the excavation of the drift, but the post excavation data suggested that the reflectors were no longer present suggesting that the excavation of the drifts had removed the causative features.

Stress measurements have been performed in the pillar between the D&B and TBM drifts to study the variation in stress as a function of distance from the tunnel wall. The magnitudes of the stresses measured at the ZEDEX site were lower than expected based on an extrapolation of trends seen throughout the Äspö HRL based on earlier measurements. However, after comparative measurements had been made using different overcoring methods values obtained at the ZEDEX were judged to be reliable. The magnitude of the main principal stress (σ_1) was estimated to be approximately 20 MPa orientated approximately NW and horizontal. The magnitudes of σ_2 and σ_3 were estimated to be 11 and 10 MPa, respectively.

RESULTS

Measurements During Excavation

During TBM excavation, vibration measurements showed that only about 0.03 % of the energy used to excavate the drift and bore through the rock was radiated into the surrounding rock as seismic energy. Maximum particle velocities determined 3 metres from the drift wall during cutting were only about 1 mms^{-1}. For the D&B drift, it was estimated that 4-7 % of the energy applied in the form of explosives was converted into seismic energy. Accelerations measured 3 metres from the drift wall reached values in excess of 500 g in peaks of very short duration. The seismic energy input to the rock mass was somewhat lower for rounds excavated using the smooth blast design than the normal blast design. These data showed that the TBM requires much more cumulative energy to create a similar length of drift compared to a drill and blast round. However, the time required for excavation and the minimal seismic efficiency of the TBM means that drill

and blast methods may input somewhere in the region of a million times more power into the rock as seismic waves or ground vibration.

Acoustic Emission (AE) monitoring was performed when TBM excavation was stopped overnight at 9, 15, 22 and 25 metres measured from the start of the TBM drift. When the TBM stopped at 9 metres the majority of the recorded and subsequently located AE activity (232 events) defined a narrow zone directly in front of the position of the TBM face. Additionally other events were located around the drift, generally within 1 metre of the drift perimeter and ahead of the drift face. For the TBM drift the majority of AE-events occurred at the face within a few tens of centimetres from the advancing face.

In the D&B drift AE monitoring was undertaken after each blast round. The spatial distribution of AE events was similar for both drifts but the AE-event density was approximately a factor of 10 higher for the D&B drift compared to the TBM drift and was high out to one metre from the drift wall.

Analysis of the Acoustic Emission (AE) events have shown that AE-events occurred at deviatoric stress levels of approximately 25 MPa which is well below the typical range of crack-initiation stresses. Source mechanism analysis of AE events showed that the great majority of events could be fit to shear-slip mechanisms. Other mechanisms considered were explosive (crack-opening) events and implosive (crack-closure) events. The highest proportion of implosive events were recorded from rounds R2 and R6 which were described as partially failed rounds, i.e. a blast round that failed to completely excavate the design volume of rock. The majority of the activity from these rounds occurred in the blasted but intact volume, which may have cracks initially opened by the blast gases and the implosive events may represent the closure of such cracks. There was also some evidence that the damage also extended further into the walls around the failed rounds than for successful blasts. Of the nine rounds within the D&B drift only four did not require corrective action, the others were considered to have failed or partially failed.

Convergence measurements were made at two sections, 9 and 24 metres, along the TBM drift. The results indicated predominantly horizontal convergence in both sections (3.6 and 1.3 millimetres, respectively), with little convergence in the vertical direction. This pattern of convergence is consistent with the *in situ* stress measurements which indicate a horizontal to vertical stress ratio of about 3:1. The magnitude of the displacements is consistent with the expected magnitudes of initial stress with a mass modulus in the range 50 to 60 GPa.

In the D&B drift, displacements were measured after each blast round. Measured displacements were generally less than 1 millimetre and most of the displacement occurred when drift excavation advanced one blast round. The small displacements measured were partly due to the fact that the convergence pins had to be installed about 2 metres behind the centre of the face due to its curvature.

During excavation of the D&B drift, there were two major misfires which had to be totally re-blasted. Four rounds had to be partly re-blasted as rock remained in the contour of the walls. Only four of the 9 rounds did not require any corrective action. The reason suggested for failed rounds were misfires due to sympathetic initiation of the charges in the cut. However, successful blasts sometimes also had some missing detonations in the cut. In general, failed rounds showed more damage than successful rounds when completely excavated.

Measurements After Excavation

The seismic tomography results showed no effects of excavation on the seismic properties of the rock at distances larger than 1.5 metres from the drift wall for any of the excavation methods. In the D&B drift a low velocity zone extending up to about 1 metre from the drift perimeter was observed.

A large number of hydraulic pulse test data were collected from 26 tested short radial boreholes. The re-analysis of pulse tests in 9 selected boreholes has produced a new set of permeability data that characterises the rock properties in the damaged zone. The principal conclusions suggested that any change of hydraulic properties in hard rock due to the EDZ is attributed to enhanced aperture and/or connectivity of discrete features and not to deformation or alteration of the rock matrix itself. This is in agreement with the geomechanical conceptual model of the ZEDEX study that indicated that the effects of EDZ would be seen as the propagation of discrete fractures which were either pre-existing (and re-activated) or newly developed discrete planes of weakness rather than an alteration or deformation of the rock matrix. As the damaged zone testing was only applied in boreholes drilled after the drift excavation a direct comparison of before/after *in situ* properties could not be undertaken and it is not clear whether the measurements reflect the effect of the excavation (EDZ). The results do, however, suggest that there is no well defined and significant increase of permeability of rock mass in the damaged zone in the vicinity of drift excavation which could be observed systematically in the analysed data. Also that there is no significant distinction between the damage extent in D&B and TBM boreholes.

Hydraulic pressure build-up tests performed before and after excavation have also been re-analysed and have contributed to the development of a better overall understanding of the formation response in the disturbed zone. These tests were made at distances of approximately 2 and 6 metres from the drift wall. The significance of changes in hydraulic properties of the disturbed zone was evaluated largely on the basis of observed changes in formation response. Significant changes in hydraulic properties of the far-field were detected in 13% of the tests, all of which are related to the D&B drift excavation. In the disturbed zone of the TBM drift, the observed changes were less evident and described as detectable in 16% of all tests.

The results of the measurements made in the short radial boreholes to assess the near-field damage (permeability, seismic velocity, acoustic impedance and fracture mapping) can be summarised as follows:

- The comparison of results from the different measurement types in general showed strong correlation.

- The vertical boreholes in the floor of the D&B drift indicated the presence of a larger zone of damage than observed in boreholes with other orientations. This can be explained by the high lifter hole charging and the large radius of the flat floor.

- The results of measurements made in the TBM drift and horizontal boreholes in the D&B drift are interpreted to show considerably less damage.

- The extent of the damaged zone in the D&B drift is estimated to be 0.8 metres in the floor and about 0.3 metres in the walls. In the TBM drift there is very little evidence of damage.

- The results showed no significant or consistent differences between the two blast designs.

The laboratory measurements provided a check on the *in situ* measurements in terms of providing data on rock properties by alternative techniques. In general, the laboratory measurements corroborated the results obtained *in situ* and provided greater confidence in the interpreted extent of the damage zone. In addition, the laboratory measurements provided data on parameters such as micro-crack porosity, compressibility and micro-cracking not directly obtainable from *in situ* methods.

CONCLUSIONS

The hypothesis established at the start of the ZEDEX Project was that it was anticipated that the effects of the excavation could be described in terms of near-field disturbance (at a distance of less than 2 metres from the drift wall) that could be reduced by the application of an appropriate excavation methods and also in terms of far-field disturbance that would be independent of the excavation method. However, the results from the ZEDEX Project have shown that this division is not appropriate. Based on the ZEDEX results a more appropriate division is that there is a damaged zone, close to the drift wall dominated by changes in rock properties which are mainly irreversible and that there is a disturbed zone beyond the damaged zone that is dominated by changes in stress state and hydraulic head and where changes in rock properties are small and mainly reversible. The changes in rock properties and rock stress with distance from the rock wall of the excavation is gradational and there is hence no distinct boundary between the two zones.

The ZEDEX experiment was performed in a rock mass with low stresses which resulted in mainly elastic behaviour and no induced damage due to stress concentrations at the drift perimeter. The damaged zone caused by the excavation methods applied has been identified by several measurement

techniques. Monitoring of AE-events is the most sensitive method which indicates minor damage due to crack opening and slip. Sparse AE-activity monitored in the disturbed zone is not expected to correspond to measurable changes in rock properties. However, a large number of AE-events indicates intense micro-cracking and is expected to produce a macroscopically detectable increase in crack density. For the D&B drift significant AE-activity was observed up to 1 metre from the drift wall while the corresponding extent for the TBM drift is a few tens of centimetres. Changes in seismic velocity indicate a larger increase in crack density. The dye penetration tests performed in the slots cut from the drift has shown the extent of macro fracturing, which in the floor of the D&B drift has extended to about 50 centimetres. The hydraulic measurements performed in the damaged zone showed little if any change in permeability of the rock matrix. The larger permeabilities observed have been associated with the induced and pre-existing fractures.

Two different blast designs were used during excavation of the D&B drift. Measurement results show only minor differences in terms of damage between the blast designs used. Differences in initial conditions, coupled with relatively small differences between results from the two drill and blast designs, make it difficult to draw any precise conclusions regarding the differences between the effect of excavation method between low-shock energy smooth blasting and normal smooth blasting. However, failed rounds of both designs have shown more damage than successful rounds.

The disturbed zone is characterised by elastic displacements and no induced fracturing. There are only very few AE-events observed in the disturbed zone and these have been found to correspond to slip on existing fractures. The AE-event density is also similar for both the TBM and D&B drifts. The hydraulic tests performed before and after excavation have not revealed any significant changes in hydraulic properties due to excavation.

The results from ZEDEX indicate that the role of the EDZ as a preferential pathway to radionuclide transport is limited to the damaged zone. The extent of the damaged zone, which is the hydraulically significant part, can be limited through application of appropriate excavation methods. By limiting the extent of the damaged zone it should also make it feasible to block pathways in the damaged zone by plugs placed at strategic locations.

There appears to be no experimental evidence in support of an increased permeability in the disturbed zone affected by the stress redistribution caused by the void, as suggested by Olsson and Winberg (1996). The stress redistribution will of course lead to changes in fracture aperture, both opening and closure. In a general three-dimensional fracture network it is unlikely that fractures would open and connect in such a way that a permeable path opened along the drift. The risk of a connected pathway is of course greater if drifts are oriented parallel to one of the main fracture sets.

The ZEDEX Project has been successful, particularly in the mechanical aspects and met the objectives set out for the project. A conceptual model

and hypotheses were established prior to the commencement of the project and these were tested by the data obtained and validated through modelling.

The project applied and tested an integrated suite of measurement techniques to the characterisation of the damaged and disturbed zones. Great emphasis was placed on the integration of the different data sets and the redundancy of data proved to be very useful and provided a consistency in the interpretation of the "boundary", albeit gradational in nature, between the damaged and disturbed zones developed around the drifts. Further it has demonstrated the link between damage and the excavation method and has shown that a difference, in terms of damage, can be determined. It has also indicated that there is some lithological control on damage, with the more "brittle" lithologies showing more damage.

The range of methodologies employed during the ZEDEX project has allowed equipment to be tested and to assess the applicability of certain equipment and methods to quantifying the EDZ and the change in properties in the EDZ around the drifts. Some of the equipment utilised was specially designed and constructed to address the problem of measuring the EDZ and the funding organisations anticipated that they would use the equipment developed within their own programmes. Most of the techniques applied have been successful in quantifying the extent of the EDZ or characterising the geological setting of the experiment.

1 INTRODUCTION

It is generally accepted that any underground excavation or opening is surrounded by zones that have been damaged or disturbed due to the redistribution of rock stresses that occur upon the creation of an underground excavation or as an effect of the excavation itself. The changes in stresses and rock properties around underground openings could influence the performance of a repository for long lived nuclear waste. Hence, the extent and properties of the excavation disturbed zone is normally considered in performance assessments of nuclear waste repositories (Sumerling, 1996). It is generally assumed that the disturbed zone will have increased hydraulic conductivity compared to the undisturbed host rock and hence it could constitute a preferential pathway for radionuclide transport. There is however considerable uncertainty with respect to the extent and magnitude of property changes of the disturbed zone (Olsson and Winberg, 1996). In performance assessments conservative, i.e. worst case, assumptions are used. To provide a basis for more realistic descriptions of the disturbed zone more experimental work has been required.

The Zone of Excavation Disturbance EXperiment (ZEDEX) was undertaken at the Äspö Hard Rock Laboratory (HRL), Sweden between April 1994 and July 1996 and this report presents the results of this experiment. The ZEDEX investigations were performed in order to obtain a better understanding of the properties of the disturbed zone and its dependence on the method of excavation. The investigations were undertaken in two phases, with the first being performed between April 1994 and June 1995 and reported in the Äspö HRL International Cooperation Report 96-03 (Olsson *et al.*, 1996b). Following the successful completion of the first phase of the project a supplementary and complementary experimental programme (The ZEDEX Extension Project) was designed to obtain additional information, with this being undertaken between January and July 1996.

The abbreviation EDZ is often used to describe the zone around an excavation and is used variously for the term "Excavation Disturbed Zone" as well as for "Excavation Damage Zone". In addition the expression "Disturbed Rock Zone (DRZ)" is also used to describe this zone. All these terms are used synonymously and often without clear definitions in the literature. A recent example of the inconsistent usage of these terms is the "Proceedings of the Excavation Disturbed Zone Workshop" held in Winnipeg in 1996 which contains many papers where the excavation damage zone is discussed. The proceedings include a paper by Fairhurst & Damjanac (1996) "The Excavation Damage Zone - An International Perspective" in which the term Excavation Damage Zone is used to describe the region of rock adjacent to an underground excavation while Martin *et al.* (1996), in the same workshop proceedings, used the terms

"damage and failure zone" to describe the zone around underground excavations in high stress environments.

According to Read (1996) the zone around an underground opening can be divided into three parts: 1) a disturbed zone in which the material behaviour is essentially unchanged, but the stress state is perturbed by the opening, 2) a smaller excavation damaged zone characterised by changes in both the pre-excavation stress state and in the material behaviour of the rock mass, 3) a failed zone in which rock slabs detach completely from the rock mass as a result of progressive failure. In this report, in an attempt to avoid confusion and establish a clear nomenclature for the various zones which may develop around an underground excavation, the term EDZ is taken to mean the *disturbed* zone that *includes* the failed and damaged zones closest to the wall that are caused by the excavation method. Further, in this report the terms the failed, damaged, and disturbed zones have been defined according to Read (1996) and are used when the respective parts of the EDZ, experimental observations, results, and interpretations are discussed.

It is considered that the development of these zones and which zone is more pronounced at individual sites is dependent on the magnitude of the *in situ* stresses, the material properties, the geometry of the opening and the excavation method. Therefore, in order to obtain an understanding of the development of such zones in relation to the above factors and determine which zone is more pronounced at a specific underground site the ZEDEX project was performed. The objective of the project was to obtain a better understanding of the changes in property and state within the damaged and disturbed zones, produced as a consequence of the excavation of drifts in a hard rock environment, by measuring the extent and magnitude of excavation induced changes relative to virgin rock conditions. This report discusses the measurements performed, their interpretation and an integration of the results obtained from the two phases. The integrated results being interpreted to define the zones referred to above which together comprise the EDZ and the results are presented in relation to the damaged and disturbed zone terms. The objectives, rationale, experimental concepts, scope of work, project organisation and resource requirements were specified in Test Plans produced before the commencement of the work (SKB, 1994, 1995).

1.1 BACKGROUND

Previous documented work has shown that the excavation of a drift will cause a disturbance to the rock mass surrounding the drift. The character and magnitude of the disturbance is a function of the resulting stress redistribution due to the existence of the air filled void represented by the drift, the method of excavation used to excavate the drift and the properties and nature of the rock mass (Chandler, *et al.*, 1996). The extent of the

disturbed zone, encompassing the damaged zone, around the excavation is dependent upon the strength and deformation modulus of the rock mass, the *in situ* rock stress, the nature and properties of the discontinuity network, the geometry of the excavation and the excavation method. The properties and state of the disturbed zone surrounding excavations are considered to be of importance to repository performance, as the zone may provide preferential pathways for radionuclide transport or may affect the efficiency and effectiveness of plugs placed to seal underground openings.

Consequently in order to obtain a better understanding of the properties of the disturbed zone and its dependence on the method of excavation, the Agence Nationale pour la Gestion des Déchets Radioactifs (ANDRA), France, UK Nirex Ltd. and the Swedish Nuclear Fuel and Waste Management Co. (SKB), Sweden decided to perform a joint study to characterise disturbed zone effects. The project is named Zone of Excavation Disturbance EXperiment (ZEDEX). Significant in kind contributions to the project were also provided by Bundesministerium für Bildung, Wissenschaft, Forschung und Technologie (BMBF), Germany and Nationale Genossenschaft für die Lagerung Radioaktiver Abfälle (NAGRA), Switzerland.

SKB has constructed the Äspö Hard Rock Laboratory (Äspö HRL), near Oskarshamn, SE Sweden (Figures 1-1 and 1-2), to provide an opportunity for research, development and demonstration in a realistic and undisturbed underground rock environment down to the depth planned for a future deep repository. The Äspö HRL also provides an opportunity to conduct research and supporting studies in the fields of excavation disturbance, ground water flow, transport of solutes and the demonstration of techniques for repository construction, sealing and the simulation of all steps in the deposition sequence.

The excavation of drifts for a future deep repository for spent nuclear fuel maybe undertaken utilising a full-face Tunnel Boring Machine (TBM). Consequently SKB decided in 1993 that it would be beneficial to gain experience with TBM excavation techniques and that a TBM should be used for the excavation of the final 420 metres of the Äspö HRL tunnel. This provided an opportunity to compare the Excavation Disturbed Zone (EDZ) in the first part of this TBM drift with the EDZ caused by the use of drill & blast (D&B) excavation methods under similar conditions.

Äspö provides SKB and other national radioactive waste management agencies with the opportunity to test equipment and methods under actual conditions before applying the techniques to their own facilities such as the planned ANDRA underground laboratories.

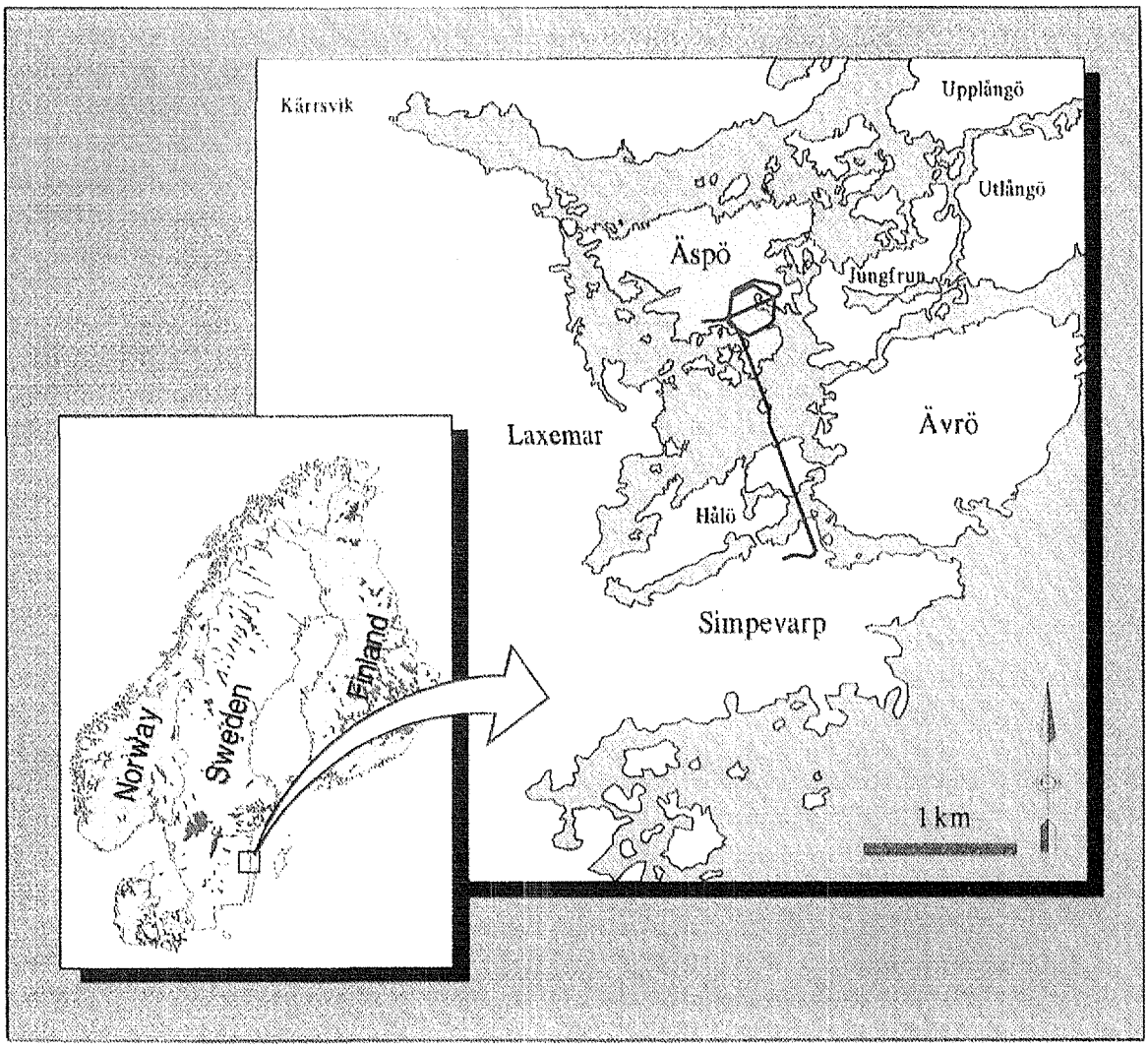

***Figure 1-1**. Location of the Äspö Hard Rock Laboratory.*

1.2 OBJECTIVES

The objectives of the ZEDEX project were (SKB, 1994):

- To understand the mechanical behaviour of the Excavation Disturbed Zone (EDZ) with respect to its origin, character, magnitude of property change, extent and its dependence on excavation method.
- To perform supporting studies to increase understanding of the hydraulic significance of the EDZ.
- To test equipment and methodologies for quantifying the EDZ.

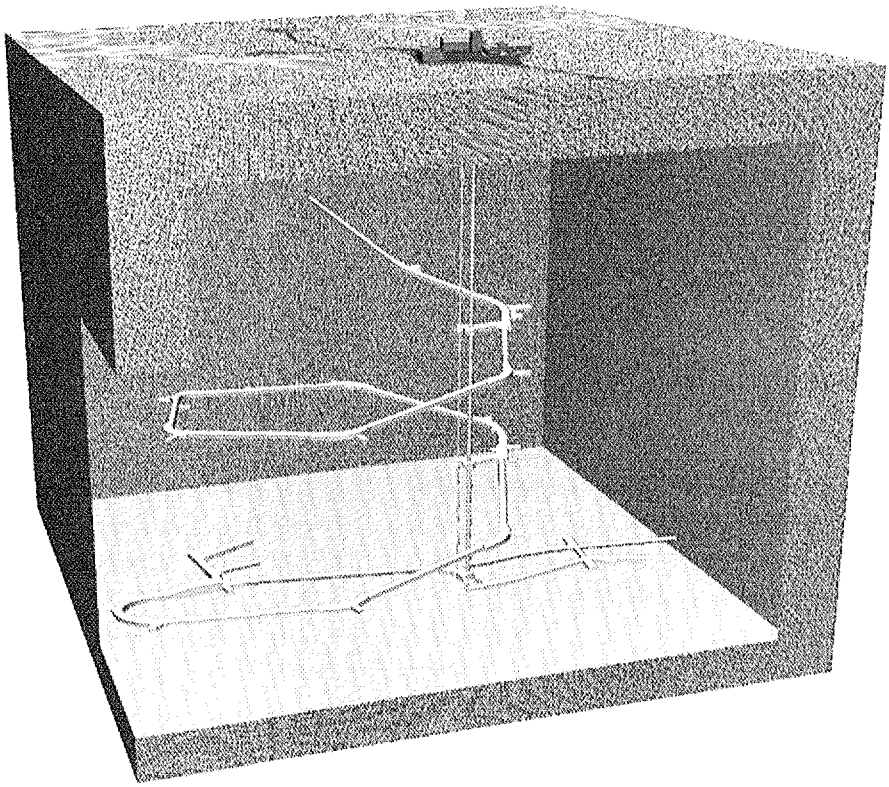

Figure 1-2. *Outline of the Äspö Hard Rock Laboratory.*

The ZEDEX project comprised investigations before, during and after excavation of drifts excavated by Tunnel Boring Machine (TBM) and by drill and blast methods (D&B). It included tests of the following excavation techniques:

- Normal smooth (NS) blasting, similar to that used for excavation of the Äspö HRL tunnel to a depth of approximately 420 metres,
- Smooth blasting based on the application of low-shock energy explosives (LSES) in the perimeter and cushion holes and an optimised drilling pattern and
- Tunnel boring

The project did not include, as a major aim, the comprehensive study of possible changes in hydraulic properties in the disturbed zone caused by the two excavation methods. The main reason for this was that it was anticipated that it would not be possible to resolve the issues of hydraulic effects in the disturbed zone within the time and funding constraints of the project. However, a limited hydraulic testing programme was included and pertinent analysis and results are presented.

The main emphasis of the project was placed on measuring the extent of the immediate excavation induced damage zone and the total disturbance created by the excavation and understanding the mechanisms that cause damage and disturbance, in order to apply the findings to the expected

conditions in the planned facilities of the respective funding organisations. The extent of the damage and disturbance were initially referred to in terms of near-field and far-field effects, the differentiation being based on distance from the wall of the excavation but it was recognised that the "boundary" between these zones was unlikely to be distinct but gradational in nature.

1.3 RATIONALE

It is considered that the disturbed zones that develop around excavations created by the construction of a repository may provide preferential pathways for radionuclide transport and may also affect the efficiency and effectiveness of plugs placed to seal underground openings. The extent and magnitude of the property changes in the EDZ may, therefore, be of significance to the safety assessment and the long term performance of the containment system. The ZEDEX programme was therefore undertaken to determine the properties of the disturbed zone and their dependence on excavation methods in a realistic and undisturbed underground rock environment. From such experimental work it was considered that the project may show whether the EDZ could have implications for safety of a repository at a particular site.

In a repository or underground research laboratory, data collected in drifts will also be used for detailed characterisation of the repository site and for repository design. It is considered that the properties of the disturbed zone must be considered in this process and in the design and selection of the backfill material and sealing methodology and, further, in the assessment of its long-term performance.

For these reasons it is important to understand how the method of excavation could affect the properties and extent of the disturbed zone and to have the ability to characterise the rock mass and disturbed zone. This knowledge is necessary in deciding how to minimise or negate such effects, if they are greater than threshold levels determined from performance assessment and to select the most appropriate excavation method, or combination of methods, that should be used for the construction of a future repository.

Clearly the excavation process should be undertaken in such a manner that construction does not have a significant negative impact upon repository performance. In this context there is a need to demonstrate how the extent of the EDZ can be reduced by the selection of the optimum drilling and charging pattern for a drift excavated by D&B methods.

The ZEDEX project has therefore attempted to complement and expand on the results from similar experiments carried out, for example at the Canadian Underground Research Laboratory (URL). Furthermore, the

results will also be used to help fulfil the requirement of selecting and developing equipment for the measurement of EDZ properties and extent of the disturbed zone. The experience gained during this project in the use of such techniques can then be applied to other facilities including the planned ANDRA underground laboratories.

The experiments undertaken as part of this project have relevance to repository design, construction and performance in that it has been attempted to relate physical measurements of disturbance to excavation method and geological conditions.

1.4 PREVIOUS EDZ STUDIES

In this sub-section a brief summary of previous EDZ studies is presented and this indicates that in most countries where the deep underground storage of radioactive waste is being considered EDZ studies have or are being undertaken or planned as part of the research programmes.

In the United States *in situ* experimental work, involving the characterisation of the EDZ for radioactive waste programmes, has been performed by USDOE in the Climax Mine and in the Edgar Mine.

The main objective of the Spent Fuel Test-Climax (SFT-C) was to experimentally assess the suitability of granite for the retrievable storage of spent fuel and to assess the rock mass response to the thermal load of a simulated repository. Measurements were made of the mechanical response to a central mine-by between two previously excavated drifts (Heuze, 1981). Model calculations of rock mass thermal and mechanical response was performed for each stage of the experiment; excavation, heating and cooling. Calculations of the mechanical response were initially made with continuum models and later with discrete joint models. The models predicted expansion of the pillars between the rooms, whilst the measurements performed *in situ* showed contraction. Results of modelling of the temperature field as a function of time showed good correspondence with *in situ* data. It was also shown that available finite difference codes could accurately simulate temperature conditions that would be present in future test areas and full scale repositories. The geological structure (heterogeneity) appeared to cause more disturbance during the excavation phase than during the heated phase (Patrick, 1986).

The experiments carried out at the Edgar Mine by the Colorado School of Mines (CSM) had the objectives of developing and evaluating blast rounds in order to minimise damage to the rock mass surrounding underground openings and to develop techniques for characterising the nature and extent of the excavation response in the rock. The characterisation showed that the controlled blasting had limited the extent of blast damage to 0.5-1 metres from the wall of the room. Stress models applied, adequately

predicted the trend and magnitude of measured stresses, but did not account for the variability in the measured data and this was attributed to non-elastic movements. In a post-analysis, discontinuous deformation analysis techniques were employed to fit distinct block movements to account for measured displacement vectors. Ubbes *et al.* (1989) concluded that for the determination of the properties of the EDZ the actual number of fractures is less important than whether or not the fractures are open.

At Stripa, Sweden a number of experiments have been performed over the years. Whilst these did not necessarily have the characterisation of the EDZ as a primary experimental objective, they did nonetheless require the EDZ to be addressed in order to explain the experimental results. These experiments included the Macro-Permeability Test (MPT), the Buffer Mass Test (BMT), the Site Characterisation and Validation Experiment (SCV) and the Rock Sealing Project (RSP). The MPT was undertaken to assess the bulk permeability of a large volume of rock and showed that a skin zone with a hydraulic conductivity about one third of the bulk rock hydraulic conductivity had to be assigned in order to match the model to the pressure data measured in the radial boreholes. The Buffer Mass Test was performed to study water uptake in highly compacted bentonite and later, the Rock Sealing Project was carried out in an enclosed part of the same drift to evaluate the hydraulic properties of the EDZ and the ability to seal the EDZ by grouting (Börgesson *et al.*, 1992). The results of the experiment and associated modelling indicated that the hydraulic conductivity of the part of the EDZ (0.0-0.8 metres from drift wall) which is directly affected by blasting is of the order of 1.0×10^{-8} ms^{-1} whilst the conductivity in the floor is twice that in the wall, which is attributed to the use of higher energy explosive charges. The part of the EDZ which was affected by stress redistribution (extending approximately from 0.8-3.0 metres from the drift wall) was attributed a hydraulic conductivity of 3×10^{-9} ms^{-1} with an anisotropy ratio (radial:axial) of 1:40. In the SCV experiment (Olsson, 1992) it was shown that the inflow to the drift was affected by a low conductivity skin around the drift.

At the AECL Underground Research Laboratory (URL) research directed at understanding the factors and the mechanisms controlling rock mass response to excavation has been the focus of two major experiments. The Room 209 test was performed to determine the hydraulic and mechanical response of a rock mass containing a narrow zone of permeable fractures, to estimate the mechanical and hydraulic properties of the rock mass and to assess the ability to model the hydraulic and mechanical response of the rock mass (Simmons, 1992). It was found that the tunnel floor was more damaged than the rock in the wall and the roof and that the extent of damage in the floor was found to be at least 1 metre, which was attributed to a higher charge density and explosive energy used in the floor blast holes. The results of hydraulic conductivity tests indicated that the blast induced fractures were not hydraulically connected and that there was no significant axial conductivity along the tunnel (Martin *et al.*, 1992). Modelling of the rock mass response was performed and it was concluded that the mechanical response of the rock mass (without the fractured zone) was adequately simulated by the elastic two- and three-dimensional models

used (Simmons, 1992). The hydraulic response of the fractured zone was not well simulated by the models used in predictions of the response to tunnel advance.

The main objective of the Mine-by Experiment performed at the 420 metre level of the URL was to show safe constructability at this depth in highly stressed granitic plutons (Read and Martin, 1991). Specific objectives were to improve the understanding of *in situ* rock mass behaviour and failure mechanisms, to evaluate the excavation damage around underground openings and to contribute to studies on the viability of the borehole alternative for emplacement of waste containers. The first phase of the experiment, the Excavation Response test, was to excavate a circular test tunnel in an orientation selected to maximise the in-plane stress ratio in order to promote development of excavation damage. A notch developed in the crown and floor of the tunnel by progressive failure and an understanding of the failure process has been reached through the use of both monitoring and laboratory testing.

ANDRA was involved in a smooth blasting experiment carried out in 1991 at the URL in Canada. The main result of the experiment showed that it was possible to reduce the extent of the damaged zone significantly (from >1 metre to 10 or 20 centimetres) using gas energy explosives combined with appropriate blast designs. A compilation of the experience of EDZ related studies performed at the URL is given by Read (1996).

In the research performed within the Grimsel Test Site, a test of excavation effects was performed in 1983. This included measurements of excavation response around a 30 metre long, 3.5 metre diameter TBM drift. Changes in the measured parameters and particularly in the permeability were attributed to elastic deformation of the excavated rock mass and changes in hydraulic boundary conditions due to the drift (Lieb *et al.*, 1989).

Additional EDZ experiments have been undertaken at the Kamaishi Mine, Japan; the Asse salt mine, Germany; the HADES, Underground Research Laboratory, Mol, Belgium within clays and in Finland in a shallow research tunnel at Olkiluoto.

During 1991 SKB performed an experiment to study the extent and character of the disturbed zone at the Äspö HRL. The aim of this experiment, the "Blasting Damage Investigation", was to study the extent of the zone damaged by blasting for three different drill and blast schemes. The experiment showed that the damage in the floor of the drift was more extensive than in the walls for all drill and blast schemes used (Pusch and Stanfors, 1992). The distribution of induced fractures in the contour were mainly controlled by two parameters; the precision in contour hole drilling and the local geology (Christiansson and Hamberger, 1991). In the three blasting schemes there was a damage zone of 0.3 metres in the wall and 1.7 metres in the floor for scheme 1, 0.3 metres in the wall and 0.6 metres in the floor for scheme 2 and 0.5 metres in the wall and 2.1 metres in the floor for scheme 3 respectively.

1.5 PROJECT ORGANISATION

The project was controlled by a Steering Committee with one member from each participating organisation. The members of the Steering Committee were; André Cournut, ANDRA, David Mellor, UK Nirex Ltd and Göran Bäckblom, SKB (Olsson *et al.*, 1996a).

The project was run by a Project Manager (Olle Olsson, SKB) who reported to the Steering Committee. The Project Manager was assisted by technical experts from ANDRA (Karim Ben Slimane, Jean-Francois Durand-Smet) and UK Nirex Ltd (Nick Davies) who were responsible for the technical contributions by their respective organisations.

There was an on-site Co-ordinator (Gunnar Ramqvist, SKB) with responsibility of co-ordinating on-site activities. There was also an on-site Data Manager (Mats Ohlsson, SKB) with responsibility to file all data collected in the Äspö HRL Project database.

The responsible organisations and contractors for each project activity were specified in an Activity List. Organisations and individuals that have participated in the project are listed in the Foreword.

2 GEOLOGICAL SETTING

2.1 REGIONAL SETTING

The regional setting of Äspö has been established from an interpretation of geological field investigations and geophysical survey data, on a 25 x 25 kilometre scale. This shows that the Äspö area is mainly of a granitic composition with different types of Småland granite dominant in the study area. The presence of some E-W elongated massifs of basic rocks have been inferred by positive magnetic and gravity anomalies (Gustafson *et al.*, 1988).

Information from all geological and geophysical investigations corroborates a tectonic picture of the Äspö area dominated by one almost orthogonal system of 1st order lineaments (N-S and E-W). These lineaments are of the order of 20 to 50 kilometres in length and often coincide with low magnetic zones (some hundred metres wide) with a central fracture zone up to some tens of metres wide. In addition to the system of 1st order lineaments, there are also 2nd order lineaments trending NW and NE and forming another, almost orthogonal, system. The 2nd order lineaments are mostly of the order of 100 to 200 metres wide and extend from 1 to 20 kilometres in length. Lineaments trending NNW and NNE (3rd order lineaments) are interpreted as being a conjugate shear set to the tensional fracture zones trending N-S. The location of the main lineaments in the neighbourhood of Äspö are shown in Figure 2-1 (Rhén *et al.*, 1997).

2.2 GEOLOGICAL SETTING OF THE ÄSPÖ SITE

2.2.1 Lithology and Alteration Features

The dominant rocks at Äspö belong to the 1700-1800 M year old Småland granite suite, with mafic inclusions and dykes probably formed in a continuous magma-mingling and magma-mixing process (Gustafson *et al.*, 1988). The result of these processes is a very inhomogeneous rock mass, ranging in mineralogical composition from true granites to dioritic or gabbroic rocks. Rather large, irregular, bodies of diorite/gabbro have been located in boreholes at great depth in the site area. Fine grained granite and pegmatite also occur frequently on Äspö as more or less well defined dykes or veins intersecting the older rocks. Aplite, pegmatite and dolerite

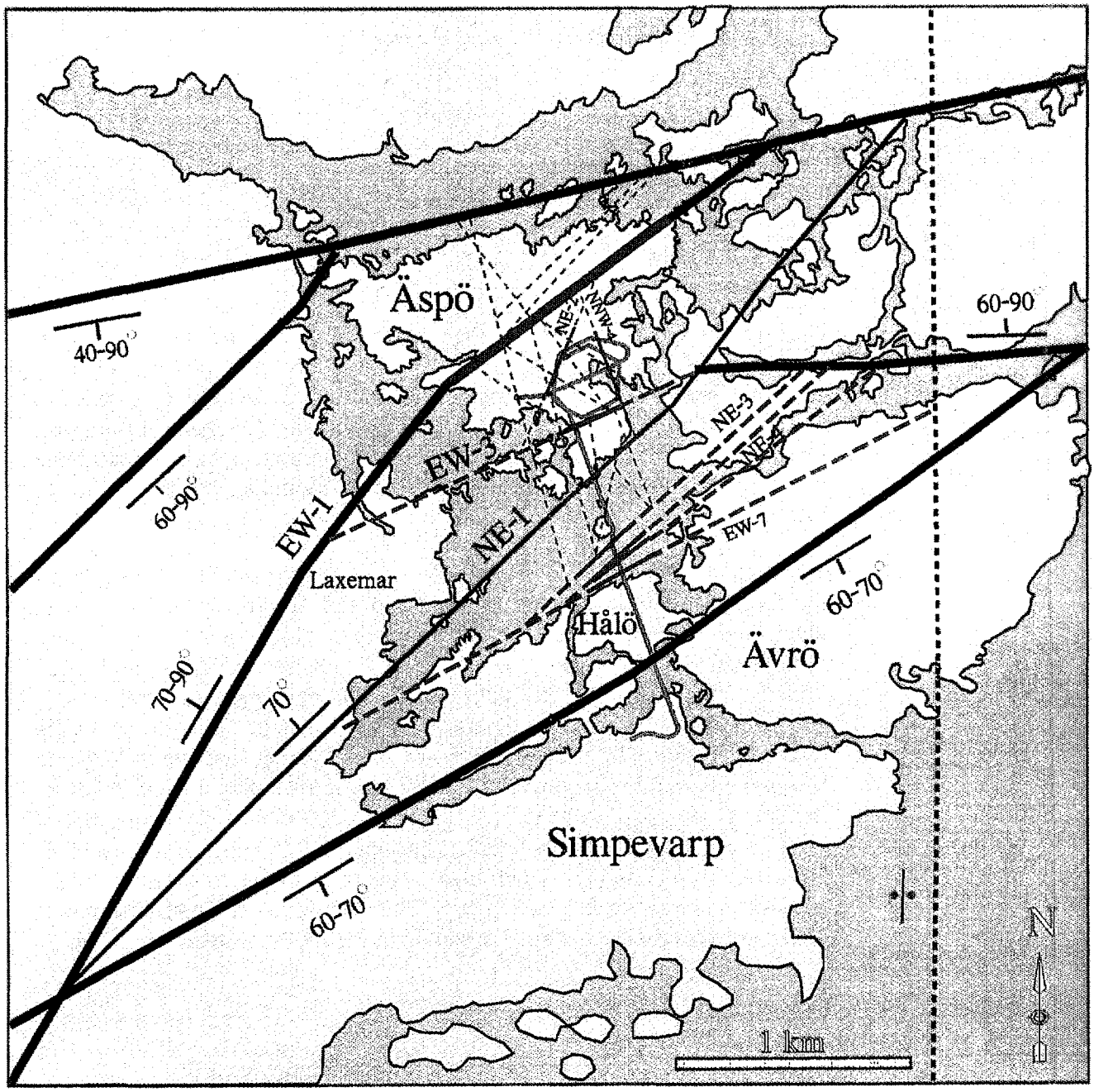

Topographically, geologically and aerogeophysically indicated extensive structure (>approx. 10 km)

Less extensive structure (3-5 km)

Aerogeophysically indicated extensive structure (>approx. 10 km)

60-70° Strike and dip

Certain (in tunnel or borehole)

Probable (geophysically/geologically indicated)

Major fracture zone in the Äspö HRL model

Certain

Possible

Minor fracture zone in the Äspö HRL model

Figure 2-1. *Fracture zones in the Äspö HRL (red) fit in the pattern of regional structures (black).*

Figure 2-2. *Map of the solid rocks of the island of Äspö. Modified from Kornfält et al. (1988) in Rhén et al. (1997).*

have only been observed as very narrow dykes, seldom more than a few centimetres wide.

Minor inclusions of mafic rock types (greenstones) are common within the granite. Narrow shear zones, resulting from different deformation intensities, are present at all scales. Mylonite zones up to several metres wide sometimes occur.

Figure 2-2 shows the distribution of rock types at the surface of Äspö (Rhén *et al.*, 1997).

The classification of the rocks of Äspö are divided into four units (Wikberg *et al.*, 1991):

- The typical Småland granite is dominant down to a depth of 100-150 metres in the Äspö drift south of the Äspö Island. Macroscopically, the unaltered Småland granite is grey to reddish grey, medium to coarse grained and somewhat porphyritic, with a generally massive texture.

- The Småland granite grades into the more mafic Äspö diorite at depth in the Äspö drift. The grey-reddish grey, medium grained porphyritic Äspö diorite contains less quartz and microcline balanced by a higher plagioclase and biotite content compared to the Småland granite. Petrographically, the Äspö diorite is a quartz-monzodiorite, granodiorite or quartz monzonite.

- Fine grained, red to greyish red granite occurs very frequently on the Äspö island as well defined dykes intersecting the older rocks but also as irregular veins and sheets. The dykes usually vary in width between 0.1 metres and up to 5 metres. They are generally orientated NE-SW. Most of the typical fine grained granite dykes are strongly deformed, which has resulted in brittle deformation.

The most common rock type in the greenstone group is a greyish black, fine grained, often rather homogeneous, mafic rock probably of volcanic origin which is always strongly altered.

2.2.2 Fracture zones

A NE-ENE trending, steep, penetrating foliation is the most dominant structural element in the 1700-1800 M year old Äspö granitoids and seems to be the oldest sign of ductile deformation related to a sub-horizontal NNW-SSE compression.

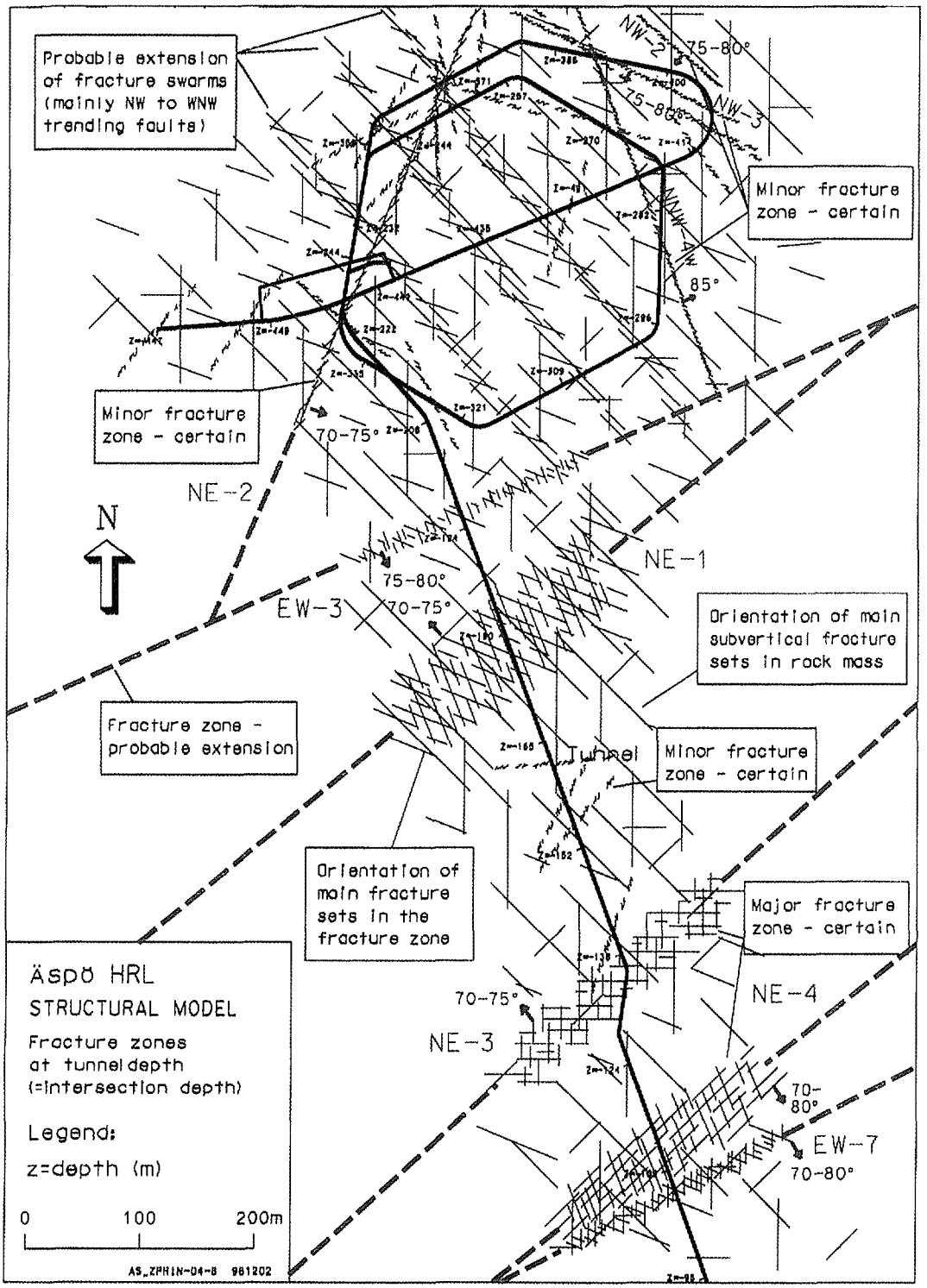

***Figure 2-3**. Structural model of the Äspö site area (Rhén et al., 1997).*

Intensified strain associated with amphibolite-facies metamorphism is evident as gneissic zones trending NE-ENE, dipping to the NNW. Elevated to a higher structural level between 1700-1400 M years ago, these old gneissic zones were reactivated as mylonitic NE trending shear zones, especially in central Äspö, in a ductile-semiductile deformation phase.

Strong foliation and mylonites are common in the Äspö shear-zone, EW-1 (Figure 2-1), where more than 10 metre long bodies of mylonite occur, trending E-W and dipping steeply to the north. Regional evidence suggests that the E-W trending mylonites are older than those trending NE. Small scale mylonitic shear planes less than about 1 centimetre wide and up to a few metres long, with a wide range of orientations, are found in many parts of the island.

The first brittle faults probably developed in the region in response to the emplacement of younger granites. These faults and older ductile zones were reactivated several times. The rock mass became increasingly brittle as it was uplifted and exposed about 1000 M years ago. Parts of the epidotic vein system reactivated and its fractures were later filled by chlorite, zeolites and calcite.

Fracture zones on Äspö have a wide range of orientations and styles and most of them result from the reactivation of older structures. The style of each fracture zone tends to depend on the nature of the older structure being reactivated, such as E-W gneissic zones, NE or E-W trending mylonites and gently dipping alteration zones. Fracture zones with N, NE or E-W trends, on Äspö normally had ductile precursors whereas those trending NW apparently did not.

Except for the fracture zone which reactivated the NE trending Äspö shear zone EW-1 (Figure 2-1), there is no fracture zone of a regional extent crossing the island. Fracture zones trending ENE and NE which border Äspö to the north and south have been interpreted from geophysical data.

On a more local scale, outside the Äspö shear zone EW-1, fracture zones are mainly orientated in an E-W direction (Figure 2-3). Whilst the outcrop mapping of fractures performed on the Äspö island showed a dominant set of fractures orientated NW with dips 70°-90°. Additionally, narrow fracture zones trending approximately N-S to NW are common and found to be hydraulically important, with most of the fracture zones and fractures orientated in a N-S direction forming an en-echelon pattern. A few gently SW dipping fracture zones have also been mapped underground in the Äspö-Hålö area.

2.2.3 Mineralogy of Fracture Infill Materials

The dominant fracture filling minerals are chlorite (38%), calcite and chlorite (32%), calcite (12%), epidote and/or chlorite and calcite (7%) and other combinations, together with or without quartz, Fe-oxyhydroxide and other accessories (11%).

The longest fractures are often filled with quartz, epidote and/or mylonite and often show evidence of having been reactivated during faulting to form gouge or breccia. These fractures were later filled with calcite and Fe-oxyhydroxide as a result of the circulation of water. The shortest fractures are filled with chlorite, calcite or a combination of both.

2.2.4 Water conductive fractures

Narrow fracture zones trending approximately N-S to WNW are reported to be hydraulically important with the predominant orientation of water conducting fractures being WNW striking and sub-vertical (Hermansson, 1995 and Munier, 1995). A subordinate set of water conducting fractures is oriented NE and sub-vertical and some water conducting fractures oriented close to N (NNW to NNE) have also been observed. The transmissivity of the water conducting fractures varies over several orders of magnitude from 3.5×10^{-5} m^2s^{-1} down to 1.7×10^{-9} m^2s^{-1}. Whilst the rock matrix has a hydraulic conductivity of less than 1×10^{-11} ms^{-1}.

3 EXPERIMENTAL SETTING AND MEASURMENTS PERFORMED TO DEFINE THE EDZ

3.1 BACKGROUND

The ability to address the objectives established for the project required the TMB and drill & blast (D&B) drifts to be excavated under similar conditions to allow a meaningful comparison to be made between the effects of the two excavation methods. The initial conditions of the rock mass within which the drifts were excavated had to be determined prior to excavation such that the progressive development of the EDZ could be evaluated.

Consequently, the layout and sequencing of the experimental programme was designed such that investigations were conducted before, during and after the excavation of the drifts. The first set of measurements, undertaken before excavation, were performed to determine the initial conditions and establish a baseline to enable comparisons to be made with data obtained later in the programme. Measurements were conducted contemporaneously with the excavation process to monitor and determine the effects of excavation. After completion of the excavations measurements were carried out to show, by comparison with the initial conditions, the development of the EDZ. Some of the post excavation measurements were repeats of those performed before excavation whilst others were specifically focused in the near-field damaged zone and required boreholes to be drilled from the drifts into the surrounding rock volume.

3.2 LOCATION AND CONFIGURATION OF THE EXPERIMENT

The site for a comparative study of excavation disturbance using different excavation methodologies had to be located somewhere in the vicinity of the planned TBM drift, as this was the only place where TBM excavation could be performed at reasonable cost. The study of excavation induced disturbance of the rock mass required boreholes to be drilled at appropriate locations before excavation commenced to allow testing to be undertaken. The only possible location for the required boreholes around the TBM drift was at the very beginning of the drift. This necessitated the experimental drift for the drill and blast operations to be located adjacent to the TBM

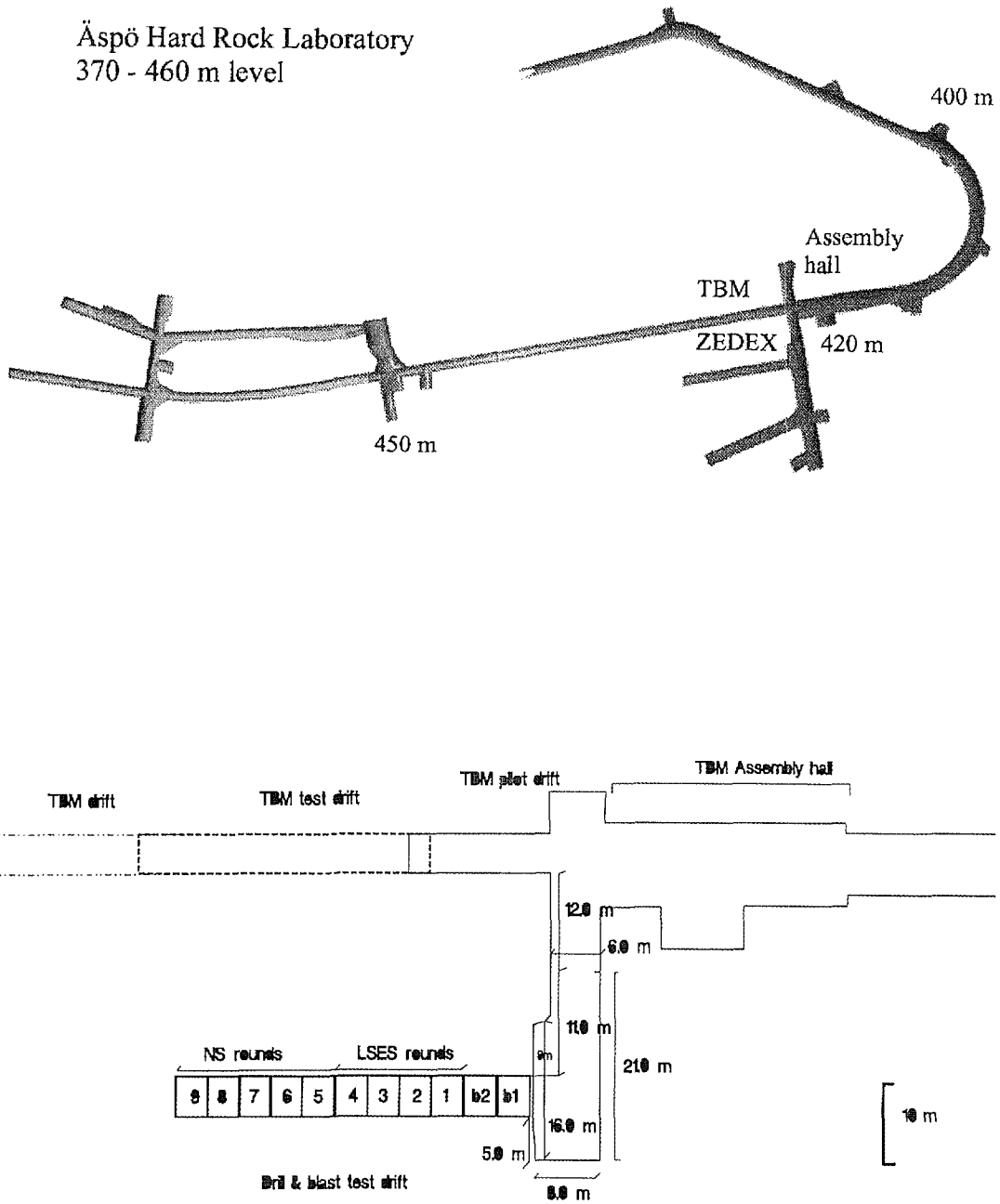

Figure 3-1. *Top) The test drifts are located adjacent to the TBM assembly hall of the Äspö HRL tunnel at a depth of 420 metres. Below) Detail on test drift location and usage.*

Assembly Hall at a similar, approximate, depth of 420 metres below ground (Figure 3-1). Further, the orientation of both drifts was planned to be at a high angle to the main horizontal stress direction to generate high stresses around the drifts, which it was considered, could cause measurable stress induced damage.

The drill and blast (D&B) drift was, therefore, planned to be parallel to the TBM drift and located approximately 25 metres away. The rationale behind this design was that the two test drifts should be located in relatively homogeneous Äspö diorite to ensure that the geological conditions for both drifts would be similar, facilitating a meaningful comparison of the results of the experiments to be made. The (D&B) drift was excavated by eleven rounds; the first two rounds did not form part of the test and were excavated to reduce the effects of the anomalous stress field caused by the access drift and to provide plane strain conditions. The following four rounds were used to test the smooth blasting technique, based on low-shock explosives (LSES), previously developed by ANDRA at the AECL Underground Research Laboratory and the remaining five rounds were used for testing the effects of normal blasting (NS). The shape of the blasted drift was designed to be circular with a flat floor and the diameter was designed to be about the same as the TBM drift, i.e. 5 metres.

A number of boreholes were drilled axially and radially (post excavation) relative to the test drifts to assess the properties and extent of the EDZ. The locations of the boreholes in plan and vertical section are shown in Figures 3-2 and 3-3, respectively. Prior to the excavation of the test drifts two sets of boreholes were drilled axially around the positions of the test drifts. Boreholes C1 to C7 were drilled around the TBM drift and boreholes A1 to A7 were drilled around the D&B drift. Boreholes for acceleration or vibration measurements (diameter 86 millimetres) were drilled parallel to and at a distance of 3 metres from each test drift (boreholes A1 and C1). Around each drift, six boreholes (three to the sides, one above and two directed below the drift (boreholes A2-A7 and C2-C7) were drilled with lengths of 40-50 metres to facilitate acoustic emission monitoring, directional radar, seismic tomography and hydraulic permeability measurements to be made before, during and after excavation of the drifts.

A set of longer boreholes were drilled radially from the drifts to investigate properties of the disturbed zone at a greater distance from the drift wall. Three of these holes, B2, B4 and B6, were drilled from the TBM drift towards the D&B drift before excavation of the drift and were used to measure displacements and changes in rock properties at the D&B drift before, during and after excavation.

After excavation of the drifts a number of short radial boreholes were drilled in each drift to assess the extent and properties of the EDZ in the near-field. In the D&B drift radial boreholes 3 metres long were drilled in the left wall (orientated horizontally and inclined downwards 45°) and vertically downwards in the floor. In the TBM drift radial boreholes were drilled in the right wall (oriented horizontally and inclined downwards 45°)

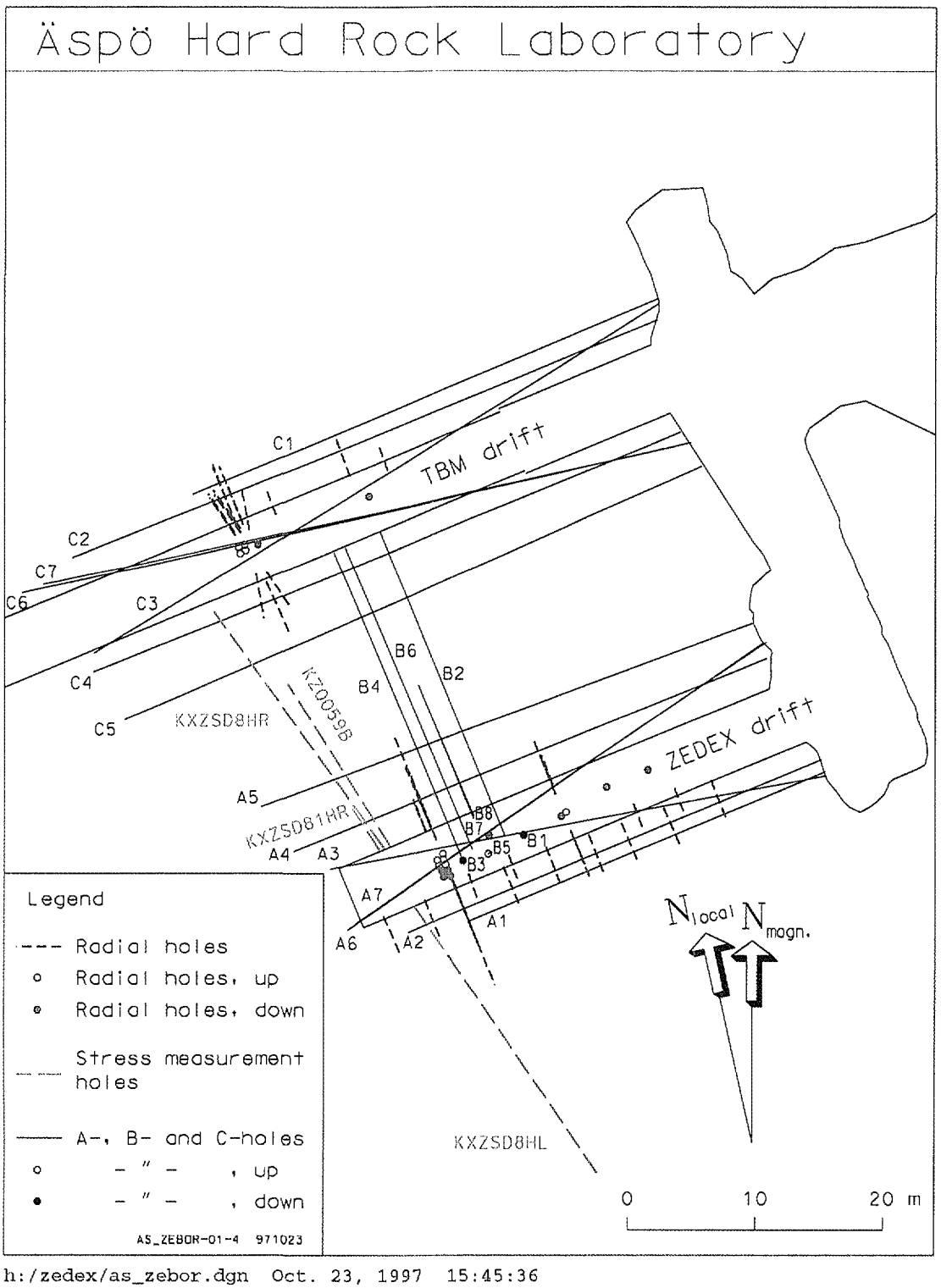

Figure 3-2. *Horizontal section showing location of boreholes in relation to the test drifts.*

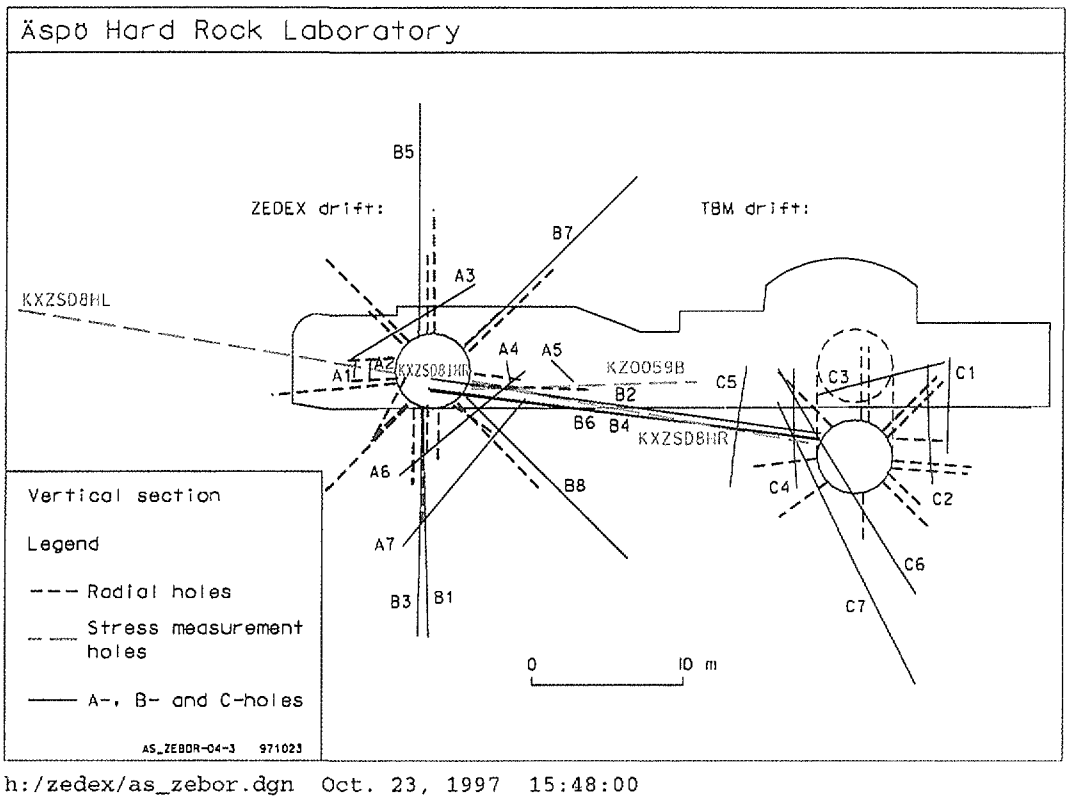

Figure 3-3. *Vertical section showing location of boreholes in relation to the test drifts.*

and vertically down in the floor. An additional five radial boreholes were drilled after the excavation of round R6 for the D&B drift, three for measuring displacements (B5, B7 and B8) and two to undertake seismic tomographic surveys (B1, B3).

In the second phase of the project an additional six radial boreholes, 8 metres long, were drilled in each of the rounds R4 and R7 in the D&B drift and in section 2 (at chainage 3210) in the TBM drift such that they formed a complete "fan" around the drifts (Figure 3-4). The orientations of these boreholes were; horizontal in left and right walls, inclined downwards 45° and inclined upwards 45° in both sides, vertically downwards in the floor and vertically upwards in the roof. Additionally 3 sets of three boreholes were drilled in round R7 in the D&B drift and section 2 in the TBM drift to perform seismic velocity anisotropy studies. These boreholes were parallel to a radial borehole such that there was a set of four boreholes for the study at each of the three locations in the two rounds (Figure 3-5). A naming convention was developed for the radial boreholes which was based on the position and orientation of the boreholes (Figure 3-4) and was used throughout the report.

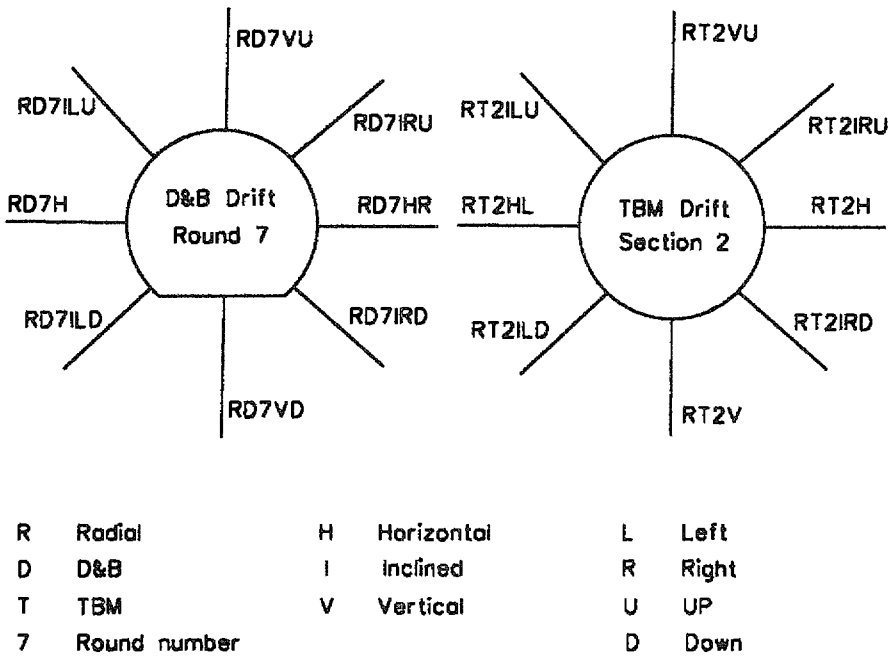

Figure 3-4. *Location of the sets of boreholes drilled in Round R7 (D&B drift) and section 2 (TBM drift) and naming convention used for the radial boreholes.*

A further three boreholes were drilled for stress measurements, two were positioned in the pillar between the drifts and one was directed SE of the D&B drift to obtain measurements of the virgin stress field. An additional borehole was drilled after completion of the ZEDEX Project in the pillar between the drifts to undertake confirmatory stress measurements, this borehole was drilled close to and sub-parallel to the other two boreholes used for stress measurements.

The primary usage of the boreholes and the diameter of each borehole are given in Table 3-1.

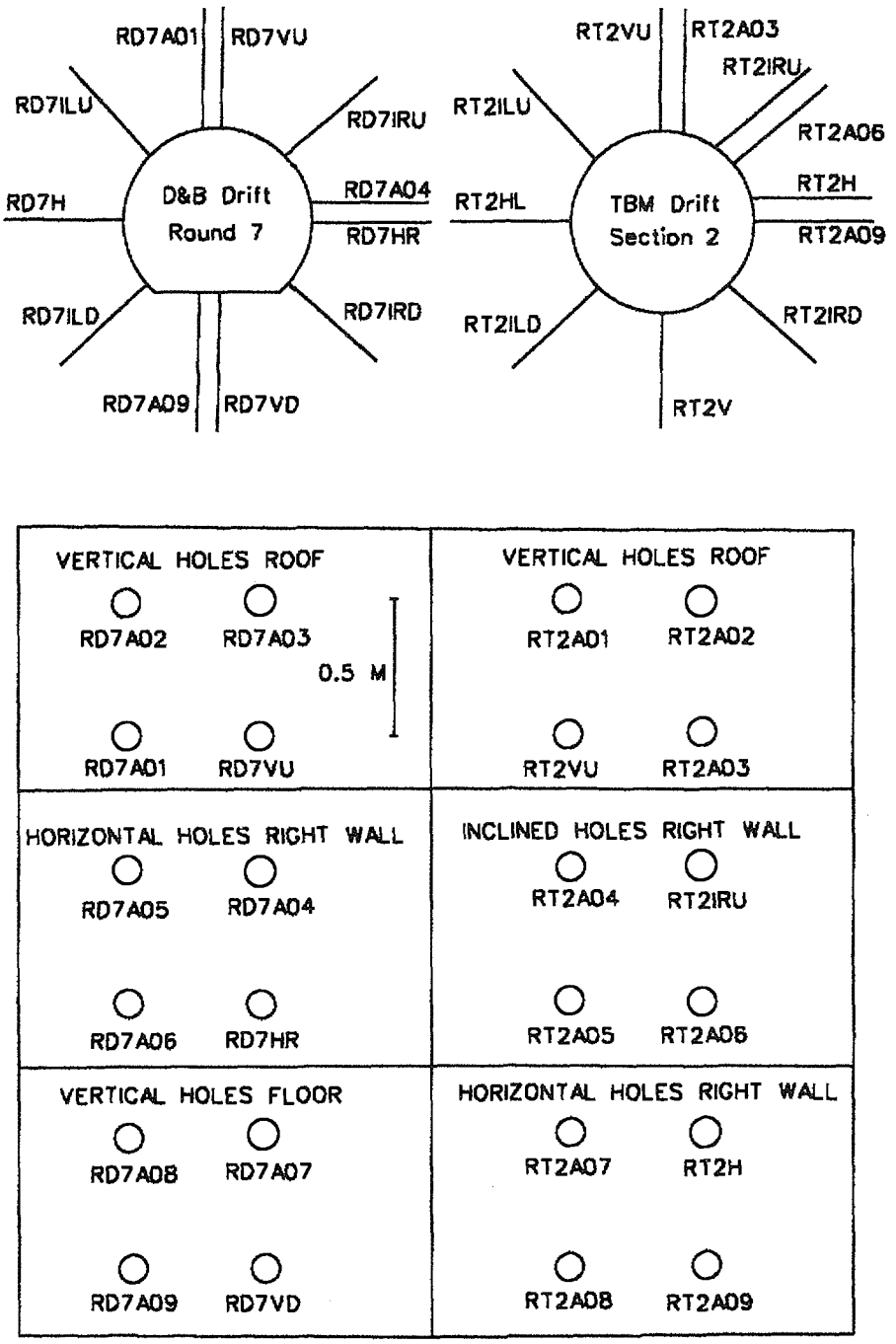

Figure 3-5. *Location of the sets of boreholes drilled in Round R7 (D&B drift) and section 2 (TBM drift). The boxes show boreholes used for seismic velocity anisotropy studies.*

Table 3-1. Borehole usage and diameters.

Borehole number	Purpose	Orientation, location	Diameter (mm)	Length (m)
A1	vibration monitoring, temperature	horizontal, side wall	86	30.2
A2	AE, directional radar	horizontal, side wall	56	35.1
A3	AE, directional radar	inclined, arch	56	40.1
A4	AE, seismic, permeability	horizontal, side wall	56	40.2
A5	seismic, permeability	horizontal, side wall	56	41.1
A6	AE, seismic, directional radar	plunging, floor	56	40.1
A7	seismic	plunging, floor	56	40.1
B1	seismic	radial, down; from D&B	56	15.1
B2	seismic, permeability	radial, horizontal; from TBM	56	26.2
B3	seismic	radial, down; from D&B	56	15.2
B4	seismic, permeability	radial, horizontal; from TBM	56	26.2
B5	MPBX	radial, up; from D&B	76	15.4
B6	MPBX	radial, horizontal; from TBM	76	26.1
B7	MPBX	radial, 45° up; from D&B	76	16.1
B8	MPBX	radial, 45° down; from D&B	76	15.1
C1	vibration monitoring, temperature	horizontal, side wall	86	40.0
C2	AE, directional radar	horizontal, side wall	56	50.0
C3	AE, directional radar	inclined, arch	56	52.2
C4	AE, seismic, permeability	horizontal, side wall	56	50.3
C5	seismic, permeability	horizontal, side wall	56	49.9
C6	AE, seismic, directional radar	plunging, floor	56	55.3
C7	seismic	plunging, floor	56	55.0
C8	stress	horizontal (not at drift)	86	20
KXZSD8HR	stress	horizontal, right	86	24.3
KXZSD81HR	stress	horizontal, right	86	3.9
KXZSD8HL	stress	horizontal, left	86	24.6
KZ0059B	stress	horizontal, right	86	15
Radial	seismic, permeability	radial: up, down, inclined up, inclined down, horizontal	86	3-8

3.3 SUMMARY OF THE MEASUREMENT TECHNIQUES

The methods used to determine the extent and magnitude of the EDZ and the progressive development, were required to provide data on the parameters listed below. The measurements, summarised in the following sections, were undertaken before, during and after the excavation with some targeted on the near-field damaged zone, others on the far-field disturbed zone, whilst some of the techniques monitored or provided information on the EDZ as defined in this report:

- input energy during excavation
- elastic and non elastic properties of the rock mass and their response to excavation
- hydraulic conductivity
- natural and induced fracturing
- acoustic energy release
- stress state
- temperature

The following techniques were applied to the characterisation of the EDZ predominantly in the far-field (disturbed zone):

1. Seismic tomography was used to map P- and S-wave seismic velocity and attenuation in several planes around the tunnels. Seismic velocity is a function of the elastic properties and density of the rock mass. Attenuation is affected by the inelastic response of the rock, particularly as a result of the presence of fractures. Variations of seismic velocity with the direction of wave propagation relate to the preferential directions of fractures and other elements of rock structure such as foliation, if present.

2. Far-field stress was measured 15-20 metres from the excavations and throughout the HRL. Prior to the project the closest measurement was performed more than 100 metres from the ZEDEX region, although after excavation stress measurements were performed in the pillar between the two drifts and in the virgin rock surrounding the D&B drift.

3. Hydraulic properties were measured before and after excavation in C4 and C5, A4 and A5 and B2 and B4 utilising pressure build-up tests. Difference flow measurements were performed in A4, A5 and C5 after excavation to determine transmissivity.

4. Radar and seismic reflection processing were used to help map the presence and orientation of fractures. The velocity of electromagnetic waves (radar) obtained from reflection measurements could also be used to estimate the average water content of a given rock volume.

5. Measurements of ground vibration or acceleration during excavation were made to estimate the magnitude of the energy released into the rock mass during excavation.

The following techniques were applied close to the drift walls, in the near-field (damaged zone) after excavation to provide detailed information on the EDZ:

1. P-wave seismic velocity and acoustic resonance measurements in short radial holes.

2. Seismic velocity anisotropy studies.

3. High resolution permeability measurements in short radial holes with a packer spacing of 50 millimetres.

4. Mapping of the cores of short radial holes. Distinguishing induced fractures from natural fractures.

5. Mapping of the half barrels in the D&B drift.

6. Detailed laboratory studies of samples from the short radial holes were performed to examine crack damage using a variety of methods.

The range of some parameters measured overlaps between the near-field and far-field (covering the full extent of the EDZ):

1. Acoustic emission monitoring was used to detect the spatial and temporal distribution of microcrack activity associated with excavation. This monitoring was primarily intended to detect AE activity near the tunnel. The AE method can, however, also provide information on the extent of the zone where joint movements occur in the far-field.

2. Displacements were measured that were a combination of both the elastic response and the brittle response of the rock mass to the excavation. Convergence measurements were also undertaken in the near-field, while borehole extensometer measurements extended the near-field measurements into the far-field.

3. Geological and fracture mapping was undertaken, including core logging and borehole TV using a front viewing colour camera and a side looking scanning TV camera (BIPS). Geological and fracture information, as well as Q and RMR values were produced.

3.4 SUMMARY OF THE INVESTIGATION PROGRAMME

An outline of the investigations performed during the project is presented in summary form in this section and Table 3-1 indicates where the techniques, utilising boreholes, were undertaken in relation to the excavation of the drifts and should be read in conjunction with Figures 3-2 and 3-3 to visualise the location of the boreholes. The techniques applied during the two phases of the project are tabulated in Table 3-2 that includes borehole usage and timing of the measurements in relation to the excavation of the drifts. It also indicates when the activity was undertaken in terms of the phase of the project. A brief summary of the equipment used is presented in the following section.

Table 3-2. Summary of techniques applied during the project, borehole utilisation, timing, in relation to the excavation of the drifts and the phase of the project during which the activity was undertaken.

Technique	Boreholes Utilised	Before	During	After	Phase
Directional borehole radar	C2, C3 and C6	✓			1
	A2, A3 and A6	✓			1
High resolution seismic tomography	C4-C5	✓		✓	1
	C6-C7	✓		✓	1
	A4-A5	✓		✓	1
	A6-A7	✓		✓	1
	B2-B4	✓		✓	1
	B1-B3			✓	1
	Borehole fans RD7 and RT2			✓	2
Permeability measurements (pressure build-up tests)	C4 and C5	✓		✓	1
	A4 and A5	✓		✓	1
	B2 and B4	✓		✓	1
Geological core logging	All			✓	1 and 2
Geological mapping of drifts	not applicable			✓	1
Borehole TV logging	All			✓	1
Borehole TV logging BIPS	All Phase 2			✓	2
Stress measurements	KA3068A	✓			1
	KXZSD8HR			✓	2
	KXZSD81HR			✓	2
	KZXSD8HL			✓	2
	KZ0059B			✓	2
Vibration and acceleration monitoring	C1 and A1		✓		1
Temperature monitoring	C1 and A1		✓		1

Technique	Boreholes Utilised	Before	During	After	Phase
Acoustic emission monitoring and ultrasonic velocity measurements	C2, C3, C4 and C6 (array)		✓		1
	A2, A3, A4 and A6 (array)		✓		1
Convergence measurements (pins)	not applicable		✓		1
MPBX extensometers	B5, B7 and B8		✓		1
	B6		✓		1
Geotechnical logging of drifts and cores				✓	1
Difference flow measurements	A4, A5 and C5			✓	1
High resolution permeability measurements	short radial holes and borehole fans RD7 and RT2			✓	1 and 2
Laboratory testing	not applicable			✓	1 and 2
Velocity measurements in core samples under uniaxial load	samples from RD7VU and RT2VU			✓	2
Downhole P-wave velocity logging	short radial holes			✓	1
Acoustic resonance measurements	short radial holes			✓	1
Micro-velocity logging (high frequency)	borehole fans RD7 and RT2			✓	2
Mini-sonic velocity logging (low frequency) and downhole logging	borehole fans RD7 and RT2			✓	2
Seismic refraction	not applicable			✓	2
Detailed mapping of half barrels	not applicable			✓	1
Detailed crack analysis of samples from the walls and face of the TBM	not applicable			✓	2
Dye Penetration tests	not applicable			✓	1
Tunnel radar	not applicable			✓	1
3D velocity anisotropy	three sets of four boreholes in RD7 and RT2			✓	2
Surveying of borehole positions and collar locations	All	✓		✓	1 and 2
Boundary element stress modelling	not applicable	✓		✓	1 and 2

To determine the rock mass properties existing before the excavation of the TBM and D&B drifts the following measurements were performed:

- Directional radar in boreholes C2, C3 and C6 (TBM) A2, A3 and A6 (D&B).

- High resolution seismic tomography in borehole sections C4-C5 and C6-C7 (TBM), A4-A5, A6-A7 (D&B) and B2-B4.

- Permeability measurements (pressure build-up tests) with a packer spacing of 3.5 metres in boreholes C4 and C5 and A4 and A5 and with a packer spacing of 1.0 metre in boreholes B2 and B4.

- Core logging.

- Borehole television logging with a forward looking camera.

- Stress measurements in borehole KA3068A located near the TBM Assembly Hall.

During excavation of the drifts the following measurements were performed to determine parameters that included; for example energy release and the response of the rock mass to excavation.

- Vibration and acceleration measurements were monitored by instrumentation in borehole C1 and A1.

- Temperature was measured in borehole C1 and A1.

- Acoustic emission monitoring and ultrasonic velocity measurements were made by instrumentation in boreholes C2, C3, C4 and C6 (TBM) and A2, A3, A4 and A6 (D&B).

- Convergence pins were installed at the drift front of the TBM drift at two locations. Readings were made at the time of installation and after excavation had been completed to measure displacements. In the D&B drift convergence pins were installed at the face for all rounds except R2, a failed round that required re-blasting and R9 the last round of the D&B drift. Readings were taken at all locations after each round of advance.

- MPBX extensometers were installed in boreholes drilled from round R6 (B5, B7 and B8). All MPBX's (including one installed in B6 before excavation began) were read after each round of advance.

After excavation and drilling had been completed the following investigations were performed to determine the resultant changes in properties, some of which were undertaken during phase 2 as indicated in Table 3-2.

- Geological and geotechnical mapping of the test drift and of cores; while this cannot directly determine changes in property, the methods may assist in determining where such changes may be located and assist with the interpretation of other data sets.

- Permeability measurements (pressure build-up tests) with a packer spacing of 3.5 metres in boreholes C4 and C5.

- Permeability measurements (pressure build-up tests) with a packer spacing of 1 metre in boreholes B2 and B4 and in boreholes A4 and A5 with a packer spacing of 3.5 metres.

- Difference flow measurements in boreholes A4, A5 and C5.

- High-resolution seismic tomography in borehole sections C4-C5, C6-C7 and B2-B4 and A4-A5, A6-A7, B2-B4, B1-B3 and fans of boreholes in round R7 and section 2.

- High-resolution permeability measurements in the short radial holes and fans of boreholes in round R7 and section 2 in the TBM drift, with packer separations of 50 millimetres.

- Logging and laboratory testing of cores from short radial holes.

- Downhole P-wave velocity and acoustic resonance measurements in the short radial boreholes. Interval velocity logging and 3D velocity anisotropy studies in round R7 of the D&B drift and section 2 of the TBM drift.

- Seismic refraction surveys, with one profile in round R7 and another in section 2 in the TBM drift.

- Stress measurements, both in the pillar between the two test drifts and also in virgin rock.

- Detailed mapping of blast induced damage located around half barrels exposed in the D&B drift.

- Borehole television logging with a forward looking camera and side looking camera (BIPS).

- Tunnel radar.

- Dye penetration tests in slots cut in the D&B and TBM drifts.

- Crack discrimination in rock samples from the walls and face of the TBM drift.

- Surveying of borehole positions and collar locations.

The research performed on this rock volume also included numerical boundary element stress modelling.

3.5 SUMMARY OF THE EQUIPMENT AND TECHNIQUES

A brief summary of the equipment used is presented in the following section, more detailed information on the equipment and methodologies employed may be obtained from International Cooperation Report 96-03 (Olsson *et al.*, 1996b), the papers/publications cited below or the other supporting documentation.

The following techniques were applied to the characterisation of the EDZ predominantly in the far-field (disturbed zone):

- The high resolution seismic tomography surveys were carried out using purpose built borehole sondes. Full details of the instrument have been reported by Cosma and Honkanen (1994). The main components of the equipment are a borehole source containing a down hole power module to drive a piezoelectric transducer and a multi-receiver borehole probe containing eight piezoelectric transducers spaced 0.15 metres apart.

- Measurements of stress magnitude and orientation were made by overcoring using CSIRO hollow inclusion cells. Three measurements were made in borehole KA3068A. Additional measurements were made using the Borre probe (described by Hallbjörn *et al.*, 1990) in boreholes KXZSD8HR and KXZSD81HR drilled in the pillar between the two drifts and in borehole KXZSD8HL in virgin rock surrounding the drifts. These latter measurements have been checked by new stress measurements performed by overcoring using CSIRO hollow inclusion cells in borehole KZ0059B, in the pillar between the two drifts.

- Permeability measurements were performed by undertaking pressure build-up tests using a double packer system. The inflatable rubber packers were 1 metre long and the packer spacing was 1 metre for tests in the radial B-boreholes and 3.5 metre for the axial C- and A-boreholes.

- Difference flow measurements were performed in A4, A5 and C5 after excavation to determine transmissivity. The main component of the difference flow measurement equipment is the downhole TVO flowmeter, calibrated for a range of 0.1 - 500 ml/min. The flowmeter is designed to measure groundwater flow into or out from a borehole section of 3.5 metres length, isolated by rubber disks. All flow into or out from the monitored section was monitored by a pressure transducer that was recorded by a data logger.

- Borehole radar measurements were performed using the RAMAC system. Directional antenna were used with a nominal frequency of 45-50 MHz and the transmitter-receiver separation was 7.0 metres. The received signal were sampled at 600 MHz, with 512 sample points and each signal was stacked 32 times to reduce noise (Emsley *et al.*, 1996).

- Acceleration and vibration measurements were performed using triaxial transducers at four stations at three metre intervals in boreholes C1 and A1. Different sensors were used for monitoring vibrations during excavation using the TBM (velocity transducers) compared to those used to monitor the effects of blasting in the D&B drift (accelerometers) due to the different sensitivities required. Signals were recorded using a signal analyser and also using a transient recorder.

The following techniques were applied for a detailed characterisation of the EDZ close to the drift walls, in the near-field (damaged zone) after excavation, some of the measurements were performed during the second phase (Table 3-2):

- Down-hole seismic measurements in short radial holes utilised a borehole probe containing an accelerometer. The seismic signal was generated by a pendulum hammer, which was fixed to the wall of the drifts (Bauer *et al.*, 1996b). The signals were recorded with a signal analyser.

- Seismic velocity anisotropy studies were undertaken using two micro-velocity logging borehole probes (high frequency) in crosshole logging mode to determine anisotropy. The velocity probes consisted of 1 MHz transducers, one as a transmitter and the other as a receiver. Both P- and S-waves were generated and received by the transducers with the received signal digitised and stored on a computer. To perform interval velocity measurements the micro-velocity probes contained two 1 MHz transducers 10 centimetres apart.

- Interval seismic measurements were also performed using the BGR mini-sonic probe (low frequency) (Alheid and Knecht, 1996). This contained the sources, pneumatic hammers and two receivers separated by 10 centimetres, each consisting of two piezoelectric accelerometers. The received signals were recorded by a four channel digital storage oscilloscope. Down-hole measurements were also made using this probe as the receiver unit and a piezoelectric actuator was used as a source that was clamped to the drift wall close to the borehole. The piezoelectric actuator was also used as a source for refraction surveys conducted along the drift walls.

- Borehole resonance/impedance measurements were performed using the BORET device (BOrehole REsonance Tool) used an acceleration transducer as the energy source applied to the borehole wall and

measures the force and acceleration response on the borehole wall directly at the point where the source is applied (Bauer *et al.*, 1996b). The signals were acquired using a two channel signal analyser. The impedance function was acquired directly in the frequency domain. A total of 32 signals were acquired and stacked at each borehole location to increase signal coherence.

- High resolution permeability measurements were performed using the SEPPI probe, developed by the Laboratoire de Mécanique de Lille and the Laboratoire de Géomécanique de Nancy (Bauer *et al.*, 1996a). It contains a small injection chamber (50 millimetre), the test section, mechanical packers and two standard packers. To obtain measurements close to the wall, an extension tube can be fixed to the drift wall within which the outermost packer can be partly inflated.

- Core logging was performed to SKB standards (Sehlstedth *et al.*, 1990) and provided lithology and fracture data and was complemented by geotechnical logging using the Q and RMR system of rock mass classification (Barton, 1996). The logging gave background information for interpreting measurements of EDZ properties. Logging of the core from the radial holes provided data on fracturing close to the drift wall and data on lithology and natural discontinuities that was used to determine the optimal positions for MPBX anchors.

- Laboratory measurements were made on cubic samples, 4 centimetres in size, prepared from cores from different depths in the various boreholes. Measurements were made under saturated and dry conditions and included: isotropic compression tests, permeability measurements, P-wave velocity measurements, mercury porosity, unconfined compressive strength, Young's modulus and thin sections for micro-crack analysis (Bauer *et al.*, 1996b).

Some of the techniques and methods used were designed such that they would obtain data or measurements that encompassed the full extent of the EDZ and are not considered in terms of the near- or far-field subdivisions, such techniques are summarised below:

- Acoustic emission monitoring was undertaken using four borehole sondes, each housing five ultrasonic transducers, evenly spaced 1.2 metres apart, (four receiving and one transmitting) operating in the frequency range 40 kHz to 100 kHz. Receiving transducers had integral 40 dB preamplifiers. The transmitting transducers were also used to undertake 3D velocity surveys. AE events were recorded, using trigger logic, on four computer-controlled 4-channel digital oscilloscopes and downloaded to removable hard disks for storage and later processing (Falls and Young, 1996). The accuracy of event locations with respect to data acquisition and processing are about 100 millimetres.

- Convergence measurements were made using a *Soil Instruments* Tape Convergence Meter. Reference studs were installed as close to the face as possible, typically within 300 millimetres of the face for the TBM drift whilst in the D&B drift the studs were no closer than 2 metres from the deepest point of the face due to the irregular shape of the face. For the TBM and D&B drift three convergence lines, horizontal and inclined at 60° from horizontal, were measured at each location except for rounds R5 and R6 of the D&B drift there were five convergence lines.

- Multiple point borehole extensometers (MPBX's) were used to determine the radial distribution of displacement towards the tunnel periphery as a result of excavation and further tunnel advance. MPBX's were installed in borehole B6 after excavation of the TBM drift but before excavation of the D&B drift and in borehole B5, B7 and B8 after excavation of round R6 of the D&B drift, where the disturbed zone measurements were focused. Each MPBX had seven anchors and the range of MPBX measurements is ± 10 millimetres displacement with an accuracy of 0.2 millimetres.

- Mapping of drifts provided data on induced and natural fracturing and lithology along the test drifts to assess excavation damage on the drift perimeter surface and to document geological heterogeneity in the test drifts. Drift mapping was undertaken according to normal SKB standards complemented by collection of rock-mass quality Q- and RMR- data (Barton, 1996). During mapping, fractures that were longer than 0.5 metres were documented. Whilst these techniques are unable to determine changes in properties they may assist in determining where such changes are likely to be concentrated.

- A tunnel radar survey was performed on both walls, floor and roof of the TBM and D&B drift to detect water bearing fractures using NGI's step frequency GPR system. Two types of antennae were used; a short dipole antenna (0.4 metres) with a centre frequency of 350 MHz and antenna separation of 0.3 metres and a long dipole antenna (1.2 metres) in length with a centre frequency 120 MHz and antenna separation of 1.0 metres. The spacing between measurement points was 0.1 metres. The resolution was expected to be about 0.5 metres for the dimension of a fracture plane.

- Borehole TV inspection using a front viewing colour camera and subsequently a side-looking scanning TV-camera (BIPS) provided data on natural fractures, fracture infillings and inflow of water into the open hole. In addition, data were obtained on the small scale orientation of natural fractures and other geological structures and were used to aid in orienting core samples. Induced fractures were unlikely to be recorded with the camera (Emsley *et al.*, 1996).

4 INITIAL CONDITIONS AND EXCAVATION TECHNIQUES

The initial conditions of the rock mass within which the drifts were excavated was determined prior to excavation utilising the measurements techniques discussed and described in Chapter 3 and provided a baseline to determine the effects the excavation had on the rock mass. It can be considered that the progressive development of the EDZ is caused and/or controlled by a range of factors that include the geological setting, the mechanical properties of the rock mass, the stress state, existing fracture patterns and the excavation parameters and progress. These factors combine in complex ways and appear as the effects of the excavation which may be considered in terms of damage or disturbance. The effects, measured and interpreted based on the observed change in relation to the initial conditions, are discussed in Chapter 5.

4.1 GEOLOGICAL SETTING AND INITIAL CONDITIONS OF THE ZEDEX VOLUME

The detailed description of the ZEDEX rock volume and stress state, discussed in this section of the report and elsewhere, is based on drift mapping data from the TBM drift, the D&B drift and parts of the Assembly hall. The state of stress was determined by the extrapolation of stress measurements made within the Äspö HRL and from measurements made after excavation, within the pillar between the two drifts and in the virgin rock mass. Core logging data and results from borehole TV, with the results from the seismic and radar investigations contributed to the geological interpretation of the volume.

Based on the data available at the time that the excavation was planned, the assembly hall for the TBM machine and the start of TBM drift would be located close to a NNW trending fracture zone identified as NNW-4w (Figure 2-3). This location was selected such that the geological conditions would be as homogeneous as possible for the ZEDEX drifts. Additionally, the requirement for grouting should be limited or avoided and it was considered that this location should meet this requirement.

4.1.1 Lithology and fracturing

The dominant rock type in the vicinity of the TBM and D&B drifts is grey medium grained Äspö Diorite (Figures 4-1 and 4-2). There is an early penetrative and planar foliation in the diorite, which is marked by the orientation and shape of feldspar crystals and meta-basaltic inclusions. The

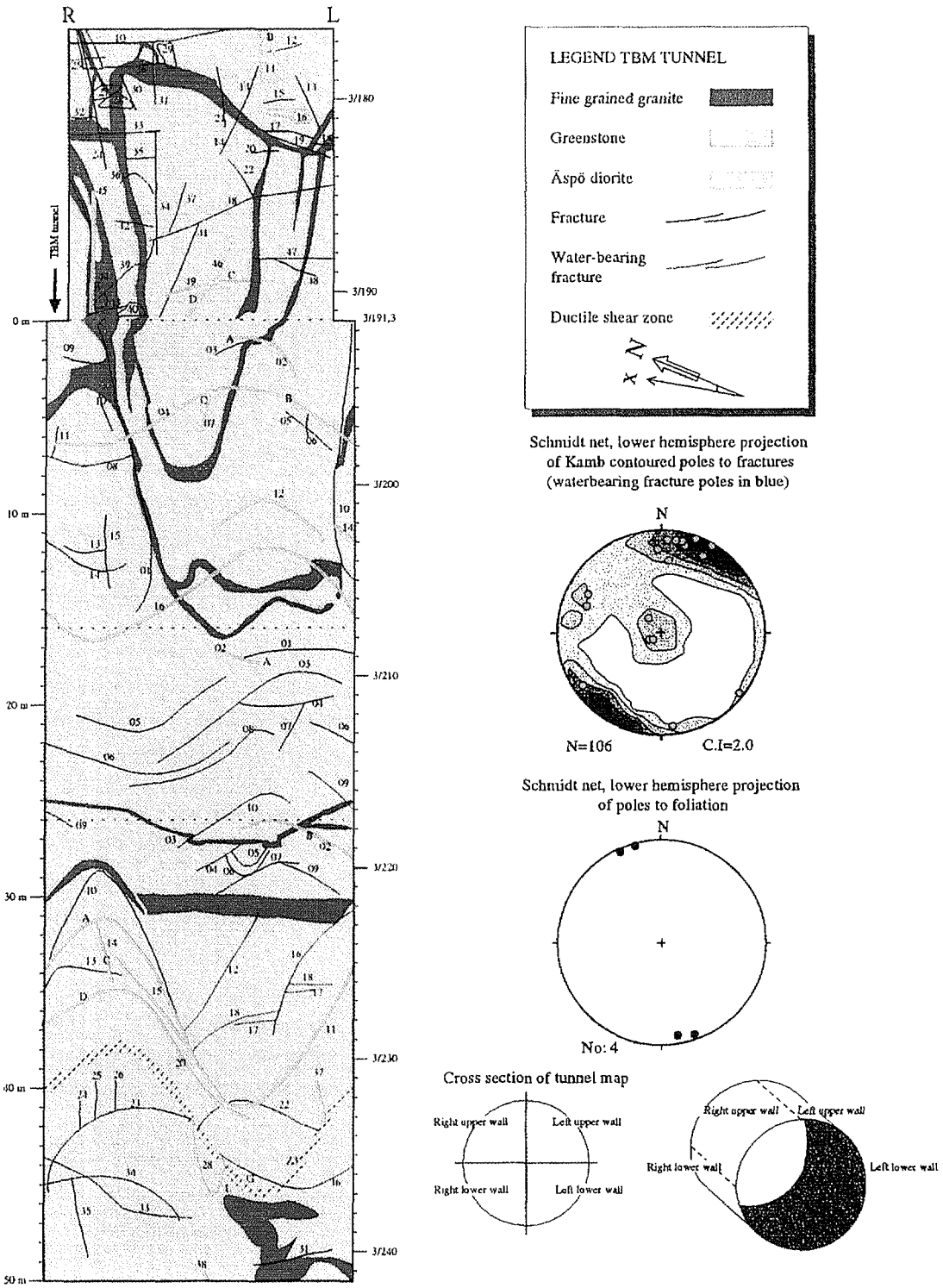

***Figure 4-1**. Diagram of the geology and structures mapped in the TBM drift (Rhén, 1995).*

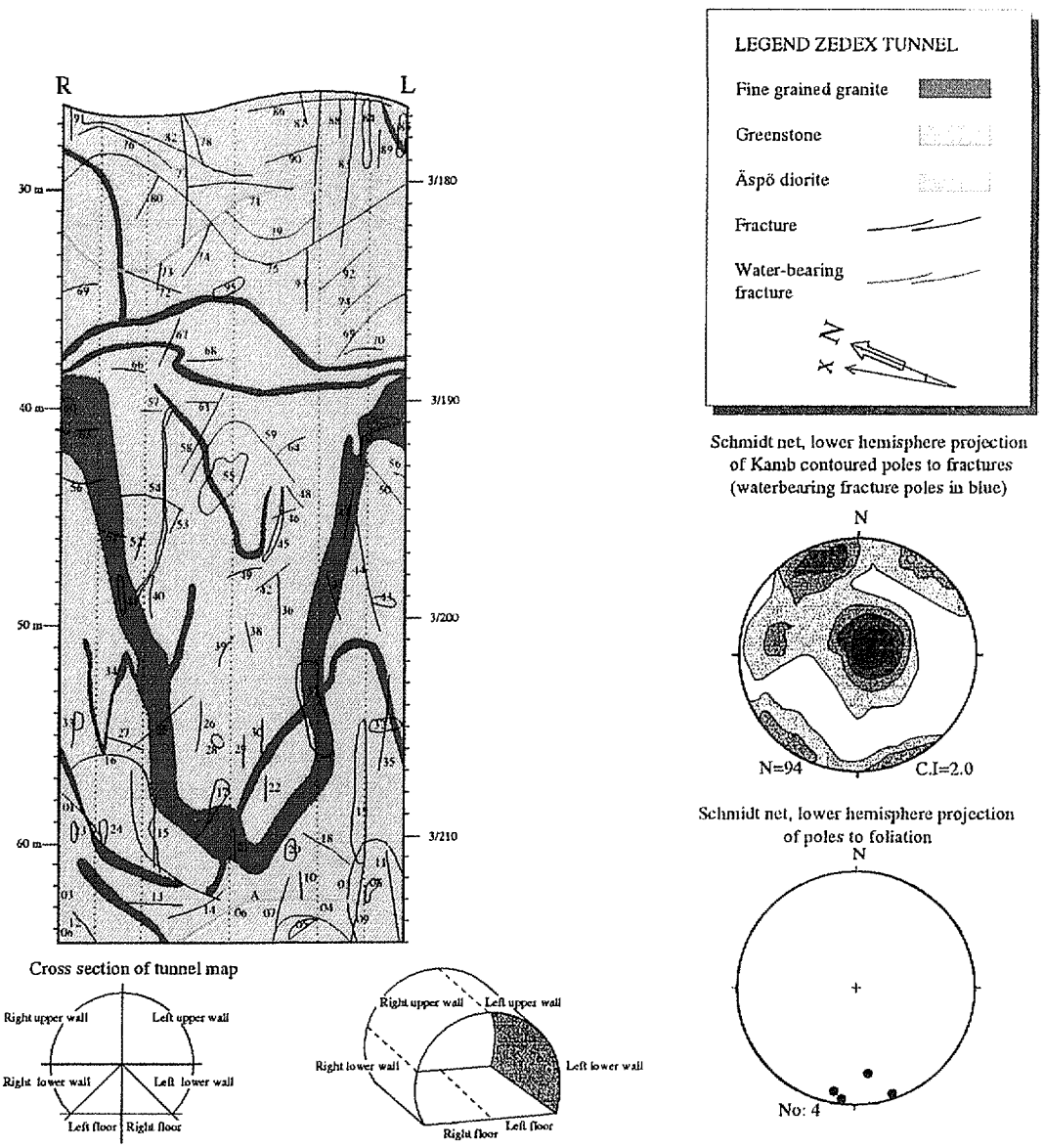

Figure 4-2. *Diagram of the geology and structures mapped in the D&B drift (Rhén, 1995).*

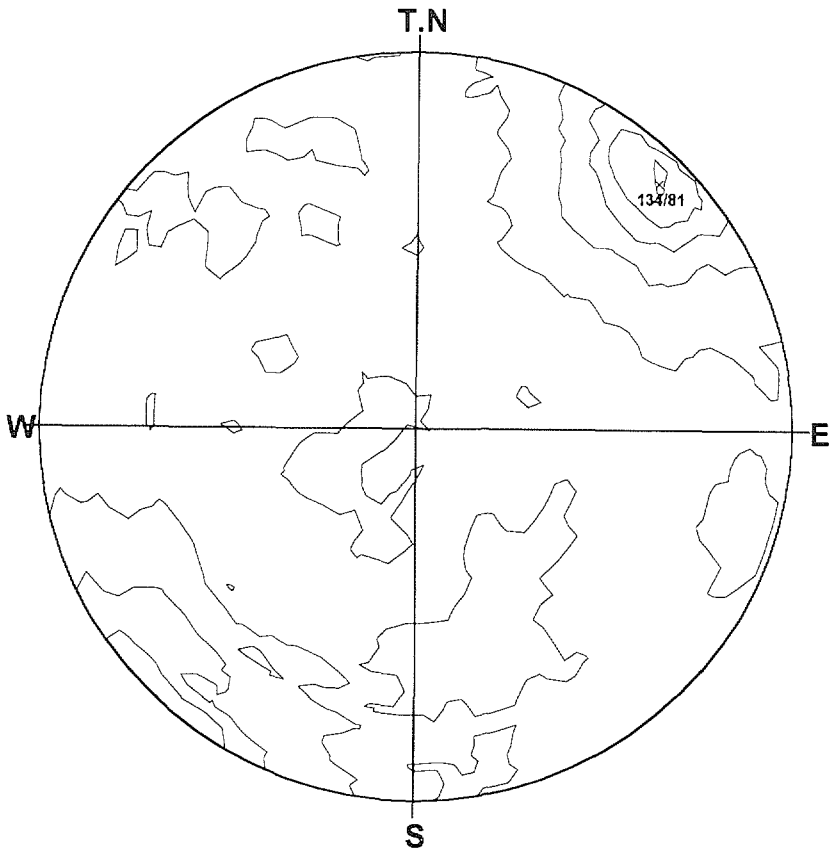

Figure 4-3. *Stereographic plot of oriented TV observed fractures from the C-boreholes (714 fractures).*

foliation generally dips about 80°-90° towards NNW and is sometimes distorted and intensified by, younger, zones of ductile shear. The variation of the foliation direction in the Äspö granitoids varies over a range of angles of about 20° within 95% confidence limits. Shear zones have a negligible impact on the foliation in the investigated drifts since none of the observed shear zones exceed one centimetre in width.

The general lithological composition, based on borehole core logging and drift mapping, suggests that the two drifts are similar (92-95% of Äspö diorite and 5-8% of fine grained granite). The TBM drift is intersected by three narrow (0.5 to 1 metres) veins of fine grained granite. The D&B drift is intersected by a NW striking shallow dipping fine grained granite vein 2-3 metres wide, which runs along nearly the whole length of the drift. Investigations may have been affected locally by these lithological differences, particularly the near-field experiments, which are generally performed at a small scale.

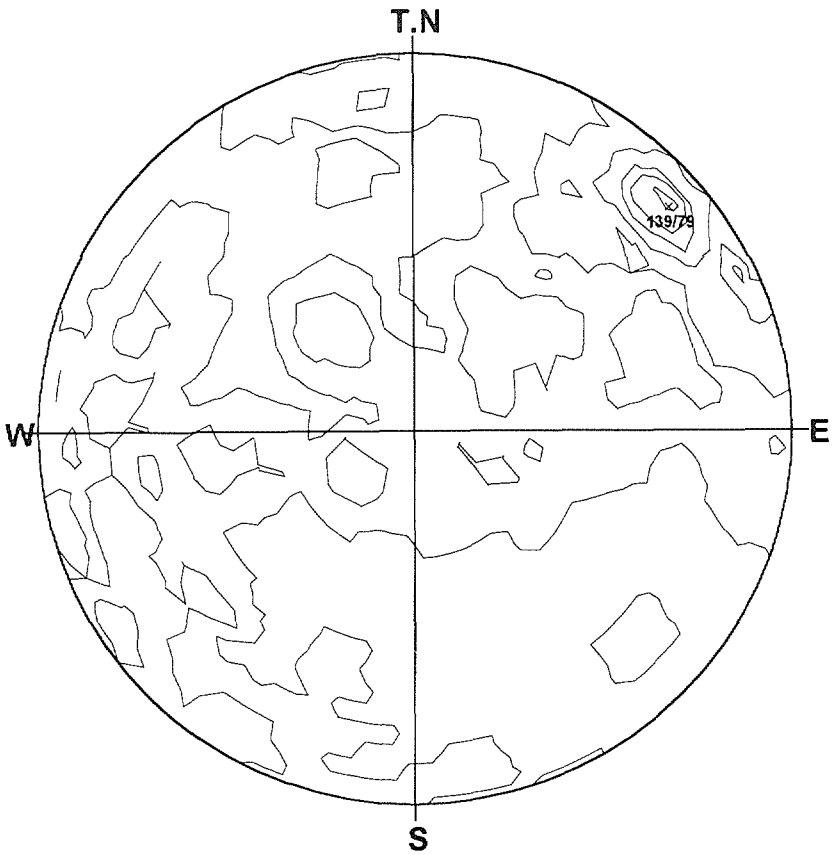

Figure 4-4. *Stereographic plot of oriented TV observed fractures from the A-boreholes (170 fractures).*

Fracturing is more intense in the TBM drift than in the D&B drift. The latter contains only two water bearing NW striking fractures: one at the start (round R1) and one near the end of the drift (round R9). No other important fractures were observed in the D&B drift. However, the TBM drift contains many NW striking fractures and most of them are water bearing. TV-logging of C- boreholes (C1-C7) showed an orientation of the fractures with a strike of 134° from Äspö North and a dip of 81° towards the West (Figure 4-3). The corresponding values for the A-boreholes where 139°/79° (Figure 4-4). About four times more fractures were observed in the C-boreholes (714 fractures) compared to the A-boreholes (170 fractures). An integration of the fracture observations obtained from TV-logging and mapping of the fracturing is shown as a simplified model in a plane in Figure 4-5 and as a section through the TBM drift in Figure 4-6.

The fracture infill materials are generally calcite or chlorite and less frequently epidote. Oxidation products and grout are also commonly seen.

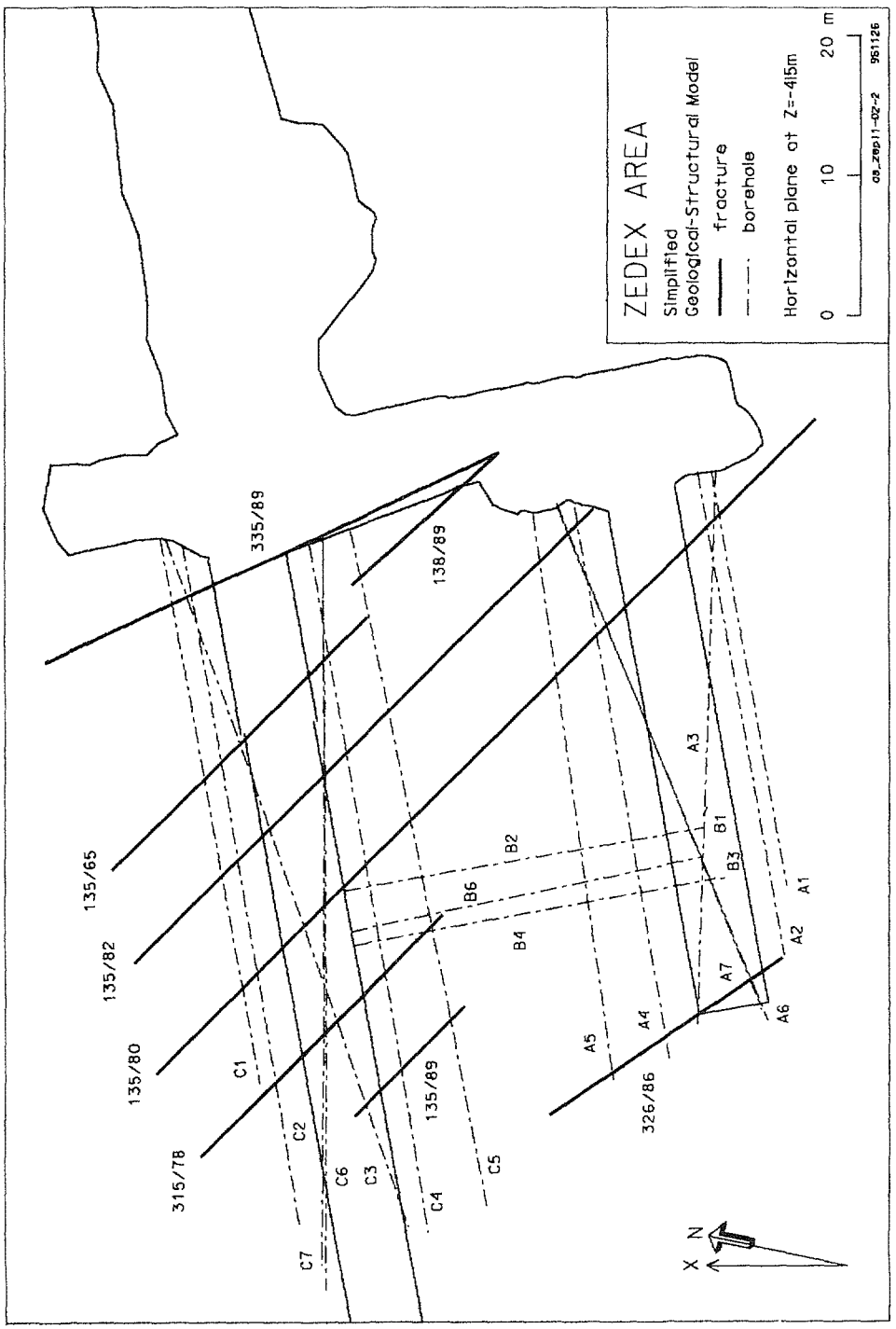

Figure 4-5. *Integration of oriented TV observed fractures and geologically mapped fractures on a plane at -415 metres.*

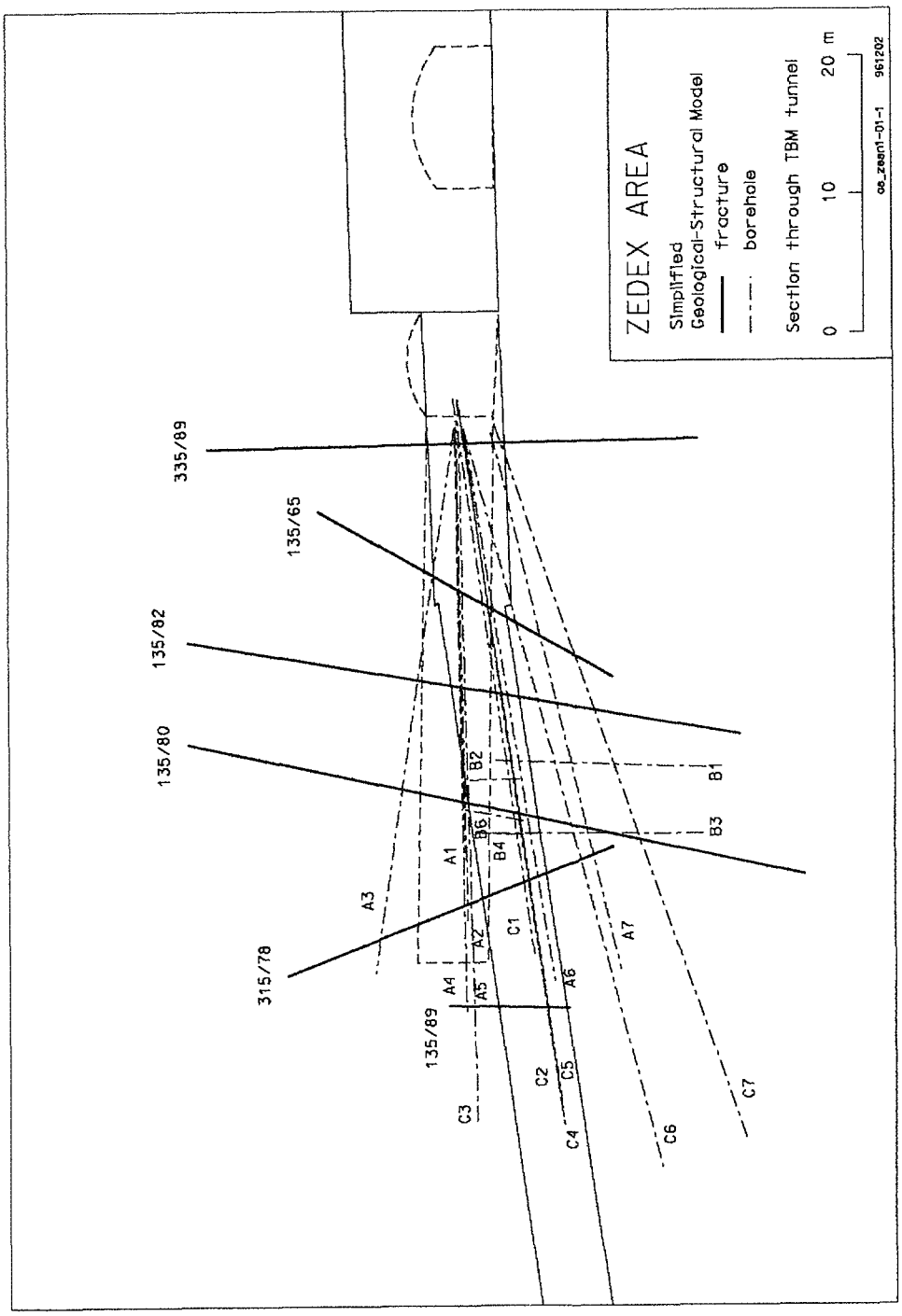

Figure 4-6. *Integration of oriented TV observed fractures and geologically mapped fractures on a section centred along the TBM drift.*

From drift mapping, most of the fractures appear to have a strike length limited to a few metres, although some persist over tens of metres. Several of the fracture sets exhibit water outflow.

Borehole and tunnel radar measurements and seismic tomography have been used to locate structures away from the drifts and boreholes. Four major NW trending features and one NE trending feature were identified from the drift mapping and radar reflections, with good correlation between the two methods. The location of radar and seismic reflectors at the ZEDEX site before excavation of the drifts are shown in Figure 4-7.

4.1.2 Seismic Velocity and Attenuation

P-wave and S-wave velocity and attenuation measurements were made on two planes around the TBM drift by undertaking tomographic surveys. Measurements in a horizontal plane south of the TBM drift were made between boreholes C4 and C5 and in a vertical plane beneath the drift between boreholes C6 and C7.

The horizontal tomographic measurements performed between C4 and C5, showed an average P-wave velocity of 6060 ms^{-1}, varying by ± 100 ms^{-1} (Figure 4-8). The mean S-wave velocity was 3460 ms^{-1} with a variation of ± 120 ms^{-1}. The anisotropy calculated for this section was approximately 6%. The direction of maximum velocity was about 120-130° (NW-SE) and the slow direction was at 30-40° (NE) and it is noted that the slow direction is roughly perpendicular to the predominant NW striking sub-vertical joint set. The σ_1 stress direction is approximately parallel to the fast velocity direction in the horizontal plane. However, experience in other granitic rocks, such as the Lac du Bonnet Granite, shows that there is very little *in situ* velocity anisotropy directly induced by high differential stress, unless jointing is more marked than at this site.

Tomographic images derived from surveys performed show NW trending features, aligning with both fractures and the anisotropic fast direction (see further Figure 5-63).

The tomographic measurements made between C6 and C7, forming a vertical plane, before the excavation of the TBM drift showed an average P-wave velocity of 5960 ± 150 ms^{-1} and a mean S-wave velocity of 3390 ± 150 ms^{-1}. These values are somewhat slower than those derived for the horizontal plane. The direction of the maximum velocity was approximately vertical. The anisotropy was 3.5 % in this case.

P- and S-wave tomographic velocity measurements were made in four planes around the D&B drift. Two of these planes were horizontal and were formed between boreholes A4-A5 and B2-B4, whilst the other two planes were vertical and beneath the drift formed between boreholes A6-A7 and B1-B3.

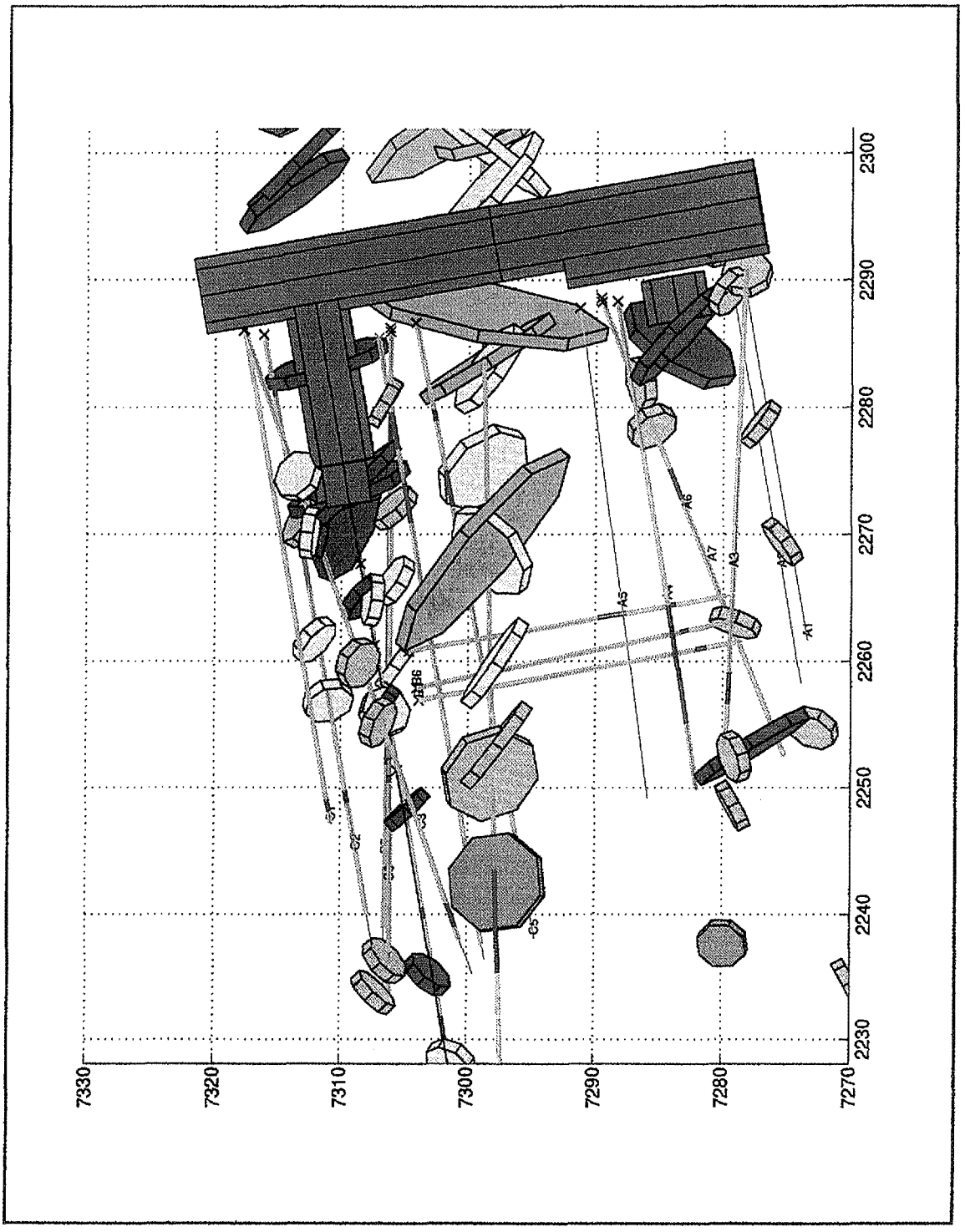

Figure 4-7. *Radar and seismic reflectors observed in boreholes around the TBM drift. Reflectors are plotted as octagonal disks. Radar, light green and orange; seismic, dark green. Purple disks along TBM and D&B drifts correspond to mapped fractures in the drifts.*

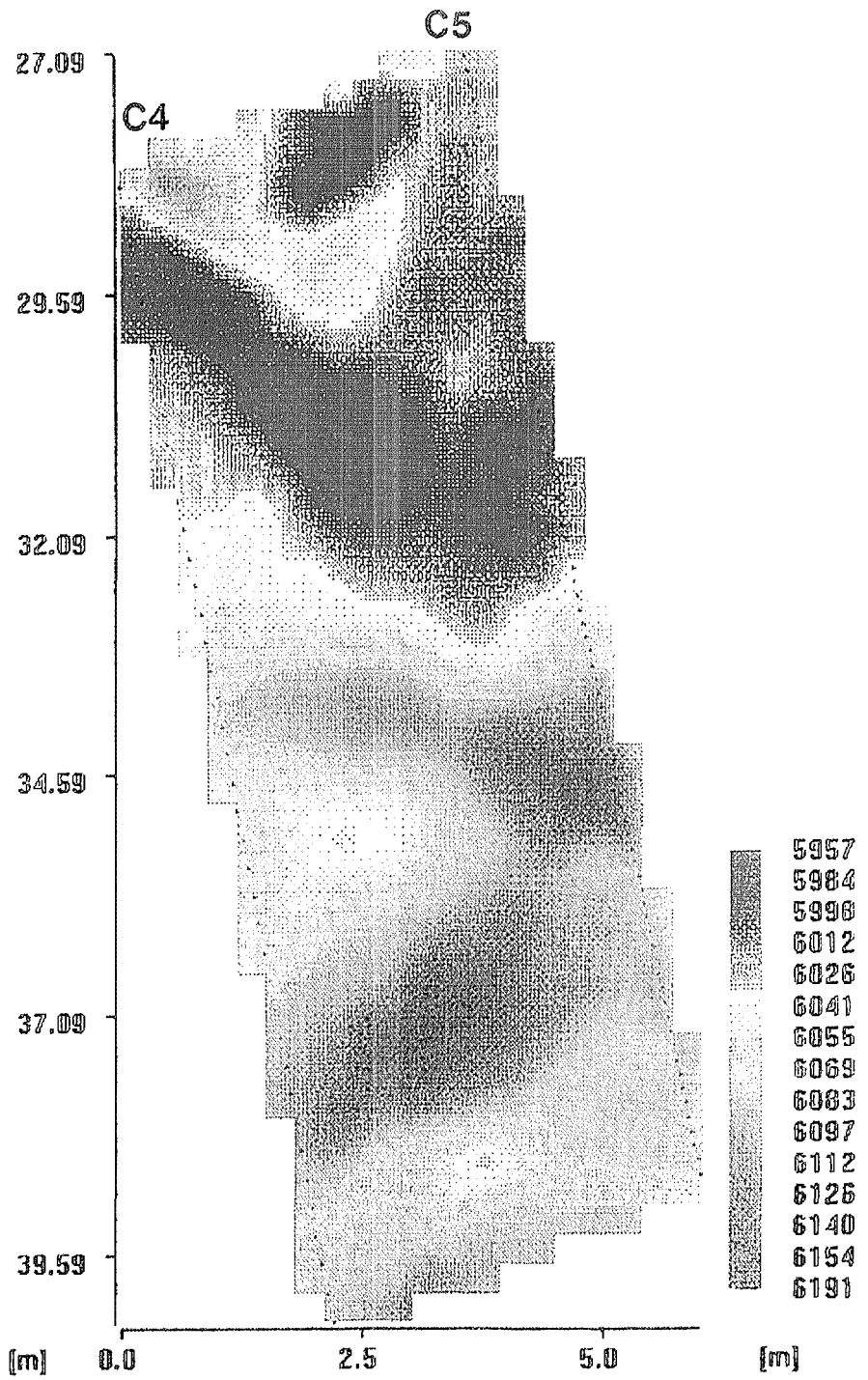

***Figure 4-8**. P-wave velocity tomogram of the horizontal plane between boreholes C4 and C5, before excavation.*

The mean P- and S-wave velocities for the horizontal sections (A4-A5 and B2-B4) before excavation were 6060±100 ms^{-1} and 3490±100 ms^{-1} respectively. For the vertical section (A6-A7), the corresponding velocities were V_P = 6260±100 ms^{-1} and V_S = 3520±100 ms^{-1}. The P-wave and S-wave velocities for the B1-B3 section, acquired after the excavation of the drift, were V_P = 5880±150 ms^{-1} and V_S = 3330±100 ms^{-1}. These velocities are from tomographic imaging results determined after correcting for velocity anisotropy. Anisotropy estimates gave values of the order of 2-3 %, except for the plane between A6-A7 that produced a value of 6.5 % anisotropy. It is possible that the higher velocities and anisotropy values in the A6-A7 section may be attributed to errors in the sensor co-ordinates. The tomographic data from the B1-B3 plane were independently processed, utilising a different code, one that had been applied to tomographic data from the Grimsel site and this produced a result consistent to those reported here.

The three-dimensional velocity measurements associated with the acoustic emission measurements seemed to show a self-consistent pattern of velocity anisotropy, with the fastest direction of V_P = 6063 ms^{-1} in the near vertical direction. In the horizontal plane the intermediate velocity axis (V_P=5993 ms^{-1}) was oriented NW and the slow velocity direction (V_P=5902 ms^{-1}) was oriented NE. The slow velocity direction is approximately normal to a commonly occurring NW striking near vertical fracture set.

A generalised relationship between structure, velocity and stresses in the D&B drift has been suggested (Young personal comm.) and is represented in Figure 4-9. It should be noted that σ_2 and σ_3 at the ZEDEX site and generally at Äspö (Leijon, 1995, Myrvang, 1997) are approximately equal and consequently their directions are not well defined (except from being perpendicular to σ_1).

Elastic properties of the rock mass were also calculated from the results of the survey by combining the P- and S-wave results. These show an average dynamic Young's Modulus of 78±2 GPa and an average dynamic shear modulus of 32±1 GPa.

The attenuation tomograms produced for the sections acquired do not correlate well with velocity tomograms and this has been observed in the results from other tomographic surveys in hard rock environments in which fractures are present cross cutting the image plane. As would be expected there is good agreement between the P-wave and S-wave attenuation tomograms. The inversion algorithm assumes that the attenuation of the signal, or signal reduction is purely a function of attenuation of the signal through transmission and does not consider other losses such as scatter. It is therefore considered that the attenuation results are probably dominated by and are a function of scattering rather than the attenuation of the signal as a function of transmission. There is some indication, although not strong and some putative correlation, that the high attenuation features may be

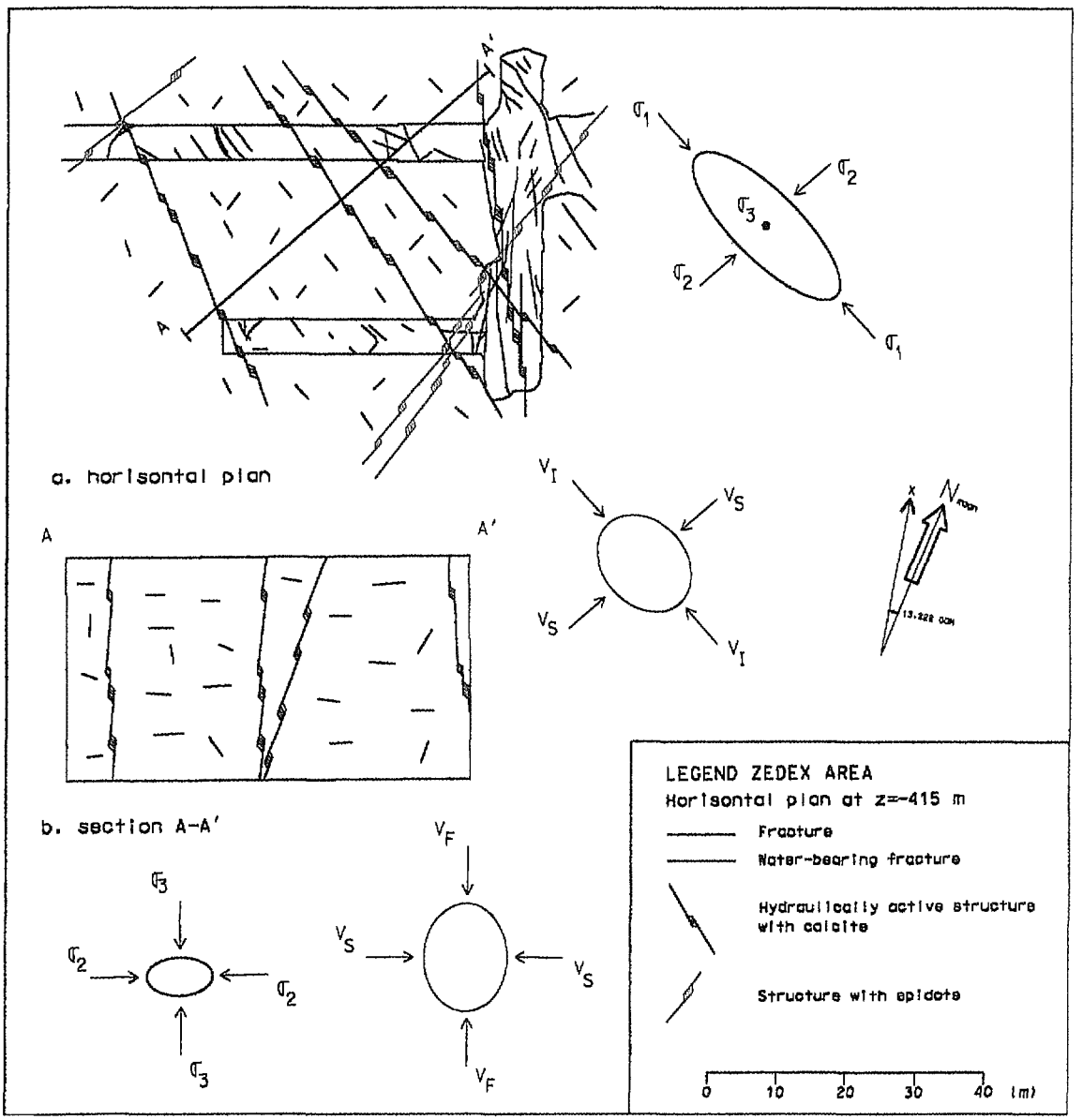

Figure 4-9. *Generalised relationship between structure, velocity and stresses in the D&B drift. V_F represents the fast velocity, V_I the intermediate and V_S the slow velocity. σ_1 represents the maximum principal stress, σ_2 the intermediate and σ_3 the minimum principal stress.*

related to fractures although, as mentioned, the interpretation of the image is complicated by what are considered to scattering effects.

4.1.3 Physical properties

Rock mechanical laboratory testing of cores from a borehole (KA3191F) drilled axially along and before the excavation of the TBM drift gave the values for the physical properties listed in Table 4-1. These values have been assumed to apply to the rocks of both the TBM and D&B drifts. Measurements were later performed on cores from boreholes A3-A6 and C3-C6. The results from these tests are provided in Table 4-2.

Numerical stress modelling undertaken before the compilation of these results used slightly different physical properties determined from biaxial tests carried out in conjunction with overcoring measurements. Young's modulus was taken as 61 GPa and Poisson's ratio as 0.32 (Sjöberg *et al.*, 1994). The uniaxial compressive strength of the rock material was assumed to be 170 MPa.

Other strength parameters may be determined in addition to the peak compressive strength. The strength of a rock is dependent on the crack density of the rock. In the laboratory, cracking initially begins at about 0.3 to 0.5 of the peak laboratory strength. This crack-initiation strength (σ_{ci}) has been determined using acoustic emission techniques to detect the onset of cracking. As the load accumulates beyond σ_{ci}, cracks accumulate, eventually reaching a critical value where dilation or volumetric strain reversal marks the onset of macroscopic failure. This critical value is referred to as the long-term strength (σ_{cd}) and is typically about 0.7 to 0.8 of the peak laboratory strength. Table 4-3 lists values determined for Äspö diorite derived by testing core samples obtained from boreholes drilled in the far-field disturbed zone. Under the increasing confining stress (σ_3), the values of σ_{ci} and σ_{cd}, which are expressed in terms of differential or deviatoric stress (σ_1-σ_3), also increase.

Table 4-1. Properties of Äspö diorite from rock mechanical laboratory testing (KA3191F).

	Mean value	Standard deviation
Uniaxial compressive strength (MPa)	195	31
Young's modulus (GPa)	69	5
Poisson's ratio	0.25	0.03
Tensile strength (MPa)	16	3
Internal friction (°)	45	3
Cohesion (MPa)	47	4

Table 4-2. Properties of Äspö diorite from boreholes A3-A6 and C3-C6.

	Mean value	Standard deviation
Density (kg/m^3)	2.76	0.033
P-wave velocity (km/s)	5.57	0.16
S-wave velocity (km/s)	3.26	0.13
Young's modulus, dynamic (GPa)	73	0.24
Poisson's ratio, dynamic	0.235	0.02
JCS, intact core (MPa)	41	22
JCS, joint surfaces (MPa)	29	14
Uniaxial compressive strength (MPa)	169	14
Young's modulus, static (GPa)	61	2
Poisson's ratio, static	0.22	0.04
Internal friction (°)	35	
Cohesion (MPa)	10-20	

Table 4-3. Additional strength properties of Äspö diorite

Parameter	
Unconfined crack-initiation strength (σ_{ci})	64 MPa
Unconfined long-term strength (σ_{cd})	146 MPa

4.1.4 Initial stress field

The stress field close to the ZEDEX test area were originally estimated based on all previous stress measurements performed at Äspö. Table 4-4 presents data obtained from (Lee *et al.*, 1993, Lee *et al.*, 1994, Litterbach *et al.*, 1994) and complied by (Sjöberg *et al.*, 1994). Additionally, Leijon (1995) compiled data from hydraulic fracturing studies and overcoring studies made with both CSIRO triaxial strain cells and Swedish State Power Board (SSPB) triaxial strain cells. These data showed trends in orientation and magnitude of the stress field as a function of depth from which the stress field at the ZEDEX site was extrapolated. These data were used as input for numerical stress modelling studies of the ZEDEX drifts. Leijon (1995) also noted that the SSPB measurements using the Borre probe tended to give lower estimates of the stress than the CSIRO strain cells.

At the ZEDEX site, the estimated σ_1 stress direction was close to the strike direction of the predominant sub-vertical fracture set at Äspö. The results for the σ_3 stress show good agreement with a trend commonly seen throughout the world in regions of horizontal compression in that the magnitude is approximately equal to the weight of overburden (approximately 11 MPa) and the direction is sub-vertical. However, the stress measurements were obtained relatively close (15-20 metres) to the

main HRL access tunnel and may have been affected by the presence of the tunnel. The magnitudes are thought to be reasonable, but the directions may be less accurate. Furthermore, stress data for these initial estimates were only available from locations more than 100 metres from the ZEDEX drifts.

Table 4-4. Estimated virgin rock stresses at the ZEDEX site at 420 metres depth (Sjöberg *et al.*, 1994).

Stress component	Magnitude (MPa)	Dip direction (Bearing) (°)	Dip(Plunge) (°)
σ_1	32	140	0
σ_2	17	50	25
σ_3	10	240	65

To obtain a first estimate of the stresses and displacements expected around the TBM drift, boundary element stress modelling of a cylindrical drift under the imposed stress field was undertaken using the above stress field estimate (Table 4-4) as input to EXAMINE^{3D}, a three dimensional modelling code (Curran *et al.*, 1993). The elastic properties of the rock determined from rock mechanics laboratory testing (Table 4-1) were also used in the model. It should be noted that the model does not take the jointed nature of the rock into account and assumes isotropic elastic behaviour.

The predictive 3D analysis undertaken by Sjöberg and Rådberg (1994) of the ZEDEX area, using EXAMINE^{3D}, showed that a completely undisturbed stress field could not be expected during excavation of the D&B drift. A distinct destressing occurs around the TBM Assembly Hall and the drilling niches which affects the stress field around the beginning of the D&B test drift. However, modelling indicated that after two to three blast rounds, the stresses acting on the D&B drift should be virtually the same as those acting on the TBM drift and consequently the first two blast rounds did not form part of the experimental programme. The intermediate and minor principal stresses (σ_2 and σ_3) in the region between the two drifts, were predicted to be less influenced by the excavation of the drifts.

During the ZEDEX Extension Project stress measurements were performed at the ZEDEX site in order to obtain stress data which could be correlated with excavation effects. The overcoring stress measurements were performed using the Borre probe (Hallbjörn *et al.*, 1990). Measurements were made in boreholes KXZSD8HR and KXZSD81HR located in the pillar between the D&B and TBM drifts and in borehole KXZSD8HL extending south from the D&B drift. The average principal stress magnitudes and directions obtained in the central part of the pillar and for undisturbed rock from measurements made in borehole KXZSD8HL are presented in Table 4-5.

Table 4-5. Average principal stress magnitudes and directions obtained in borehole KXZSD8HR and KXZSD8HL (Myrvang, 1997).

Borehole No.	Stress Component	Magnitude (MPa)	Dip Direction* (Bearing) (°)	Dip (Plunge) (°)
KXZSD8HR	σ_1	19.6	336	8
	σ_2	10.7	71	37
	σ_3	10.3	236	52
KXZSD8HL	σ_1	20.1	351	24
	σ_2	9.2	230	49
	σ_3	7.8	96	31

* Bearing is calculated clockwise from the Äspö x co-ordinate (local North).

The orientation of σ_2 and σ_3 varied widely over the measurement points, falling within a region approximated by a great circle perpendicular to the average σ_1 orientation (Figure 4-10). From Table 4-5, it can be seen that the magnitudes of σ_2 and σ_3 are quite similar to each other. Thus, the variation in orientation may reflect the observation that the σ_2 and σ_3 values are of similar magnitudes and are approximately equivalent. As a consequence of the small variation in values, the average σ_2 and σ_3 orientations listed hold little meaning, other than that they lie within a plane containing those orientations. However, the orientations of σ_1 were much more consistent (Figure 4-10).

The stress levels obtained with the Borre probe (Table 4-5) were significantly lower than had been anticipated (compared to those in Table 4-4) and the validity of the stress measurements was questioned. Much of the concern was due to the fact that these measurements had been performed with a different tool compared to the previous measurements. To investigate the difference, stress measurements were also performed with the CSIRO Hollow Inclusion Cell in borehole KZ0059B after completion of ZEDEX testing. This borehole is parallel to and less than 1 metre from KXZSD8HR. Comparable data were thus obtained from two parallel boreholes located less than 1 metre apart. A detailed comparison of the results (Myrvang, 1997) show that the overcoring strain obtained with both methods are of good quality and it is considered that the data provide a realistic estimate of stress state. The biaxial testing performed on overcored cores shows that the rock is reasonably linear elastic. However, the Borre tests gave reasonable values of Poisson's ratio while the CSIRO tests in this case gave unrealistically high values with an average of 0.42. A too high value of Poisson's ratio will give a too high stress value when used in the calculations. Hence, the stress data obtained with the Borre probe are considered to be reliable and provide a realistic estimate of the stress levels and directions at the ZEDEX site. Myrvang (1997) also

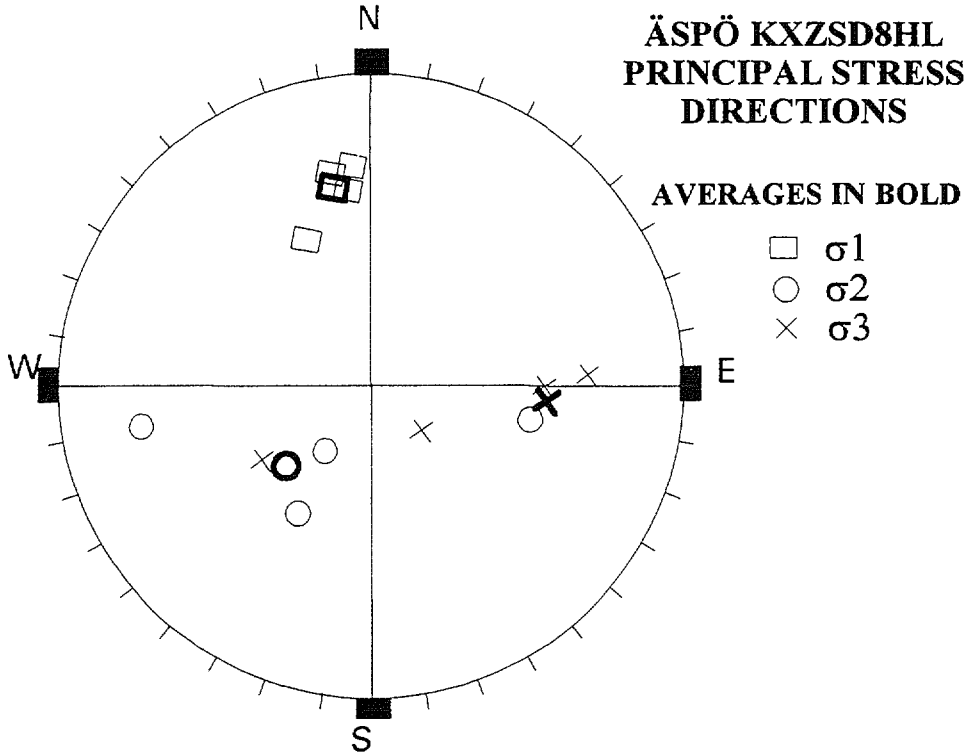

Figure 4-10. *Principal stress orientations from borehole KXZSD8HL. Lower hemisphere equal angle projection with azimuths relative to the Äspö x co-ordinate (local North).*

concluded that the variations in the stress field observed along the borehole seem to be caused by changing stress field conditions, possibly resulting from the presence of fractures close to the measurement locations, rather than inadequate measuring techniques. As the reliability of the performed stress measurements was not confirmed until after most ZEDEX work had been completed the stress data shown in Table 4-4 have been used for the majority of the analysis presented apart from the MAP3D modelling. As these data have been confirmed to be correct, a general reduction in the disturbance caused by stress should be expected. The general distribution of stress patterns would not be expected to change greatly as the ratio $K_0=\sigma_1/\sigma_3$ is approximately 3 for both cases.

Figure 4-11 shows the variation in magnitude of the principal stresses versus distance from the drifts. Although there is some scatter in the measurements, the trends observed are generally consistent with patterns expected in a pillar between tunnels. That is, stress values tended to be lower near the drift walls and higher near the centre of the pillar. The σ_1 stress orientation became more inclined toward vertical within 4 metres of the drift walls. The orientation of the maximum horizontal stress component was seen to be aligned more parallel to the TBM drift within 4 metres of the drift wall. Elastic modelling using the MAP3D programme (Wiles, 1996), was undertaken based on the stress values obtained from

KXZSD8HL shown in Table 4-5. The stress measurements from boreholes KXZSD8HR and KXZSD81HR were generally consistent with these models, but showed considerable scatter in magnitude around the modelled values (Figure 4-11).

Further analyses, in which large fractures were introduced into the elastic models, showed that both the magnitude and the orientation of the stress would vary considerably due to the presence of such fractures. However, large fractures had not previously been mapped in the immediate vicinity of the stress measurements sites, although a few potential measurement locations were not used due to the presence of healed or pre-existing fractures in the pilot borehole and a number of larger mapped fractures were present a few metres from the stress measurement boreholes. Consequently fractures may have had some influence on the stress results from the measurement locations.

Where the stress direction is parallel to the major fracture set this results in these fractures having a lower normal force acting across them than other fractures. Consequently the predominant fracture set would be expected to be more susceptible to opening or closing with the stress perturbations associated with the openings than other fracture sets that may be locked closed by the normal forces acting across them.

4.1.5 Rock mass quality

The rock mass quality was seen to be rather uniform throughout the cores (C1-C7) and around the TBM tunnel and belongs, in general, to rock mass Class B (good quality; Q-value of 10-40), Table 4-6 below and presented in Olsson *et al.*, (1996b). The RMR values were usually in Class II (RMR values 61-80). Only small sections belong to rock mass Q-Classes A (very good quality) and C (fair quality) and RMR Classes I and III respectively. Similarly the rock mass quality is fairly uniform throughout the cores (A1-A7, B1-B8) and the majority of the D&B drift belongs to rock mass Class B, which corresponds to a Q-value of 10-40 (good quality rock) (Olsson *et al.*, 1996b). Only a small section of the drift from chainage 30-34 metres belongs to rock Q-class C (fair quality rock) and RMR rating III. This section corresponds to the position of a large water conductive fracture.

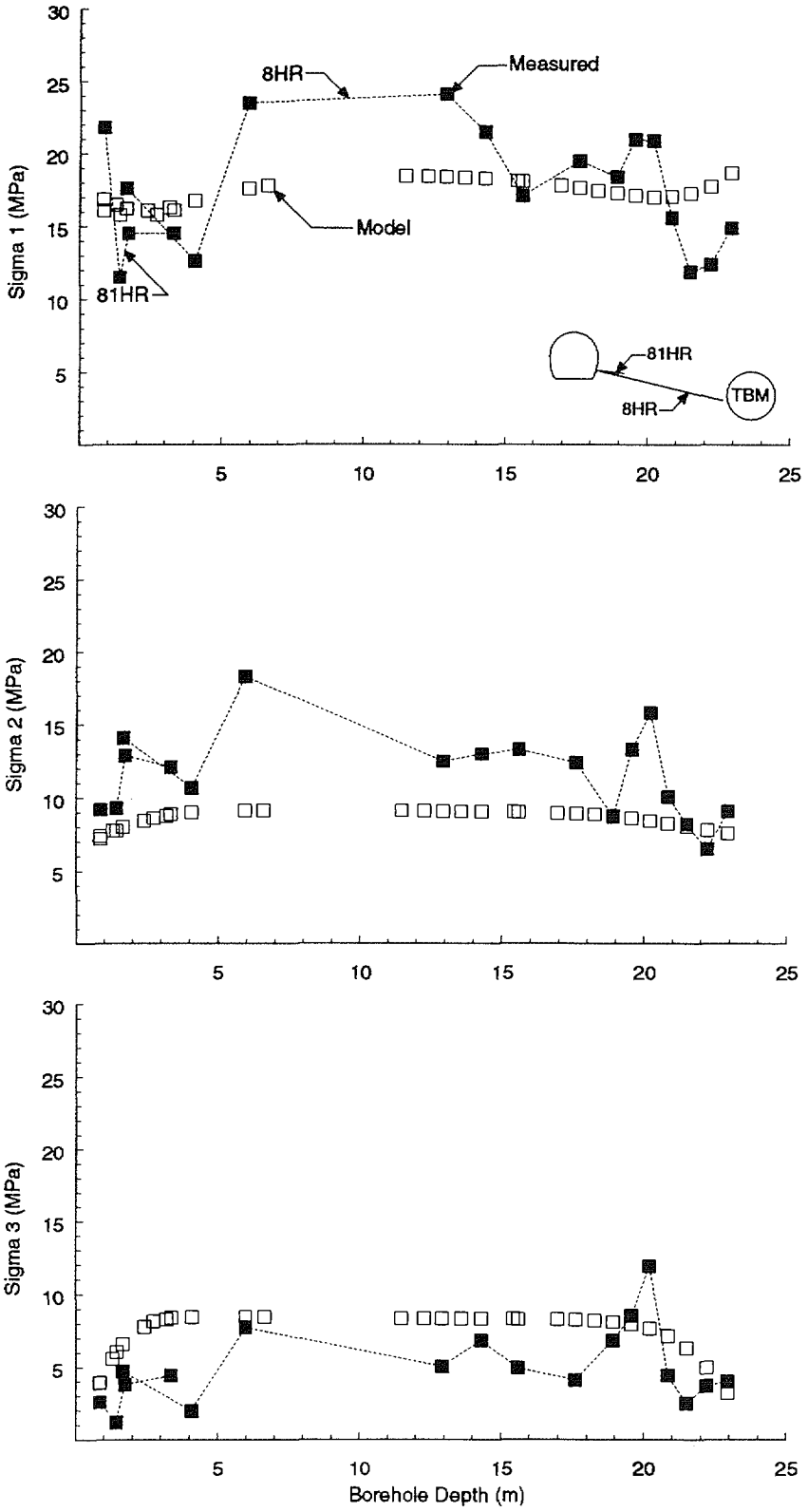

Figure 4-11. *Comparison between measured and predicted principal stress magnitude distribution in the pillar between the TBM and D&B drifts.*

In general the diorite has a slightly higher quality and rock mass rating than the granite. The joint alteration number is between 1 and 3 (no mineral fillings, only coatings). Joint roughness coefficient (JRC) varies between 8 and 10 with extreme values of 4 and 14. The JRC is a subjective term where the lower the number represents a "smooth" joint and higher number indicates a higher rugosity of the joint.

Table 4-6. Summary of Q and RMR values of the TBM drift, D&B drift and associated boreholes.

Borehole/ Drift	Diorite length (m)	Granite length (m)	Q Diorite Mean (Range)	Q Granite Mean (Range)	RMR Diorite Mean (Range)	RMR Granite Mean (Range)
C1-C7	322.83	29.82	19.1	14.7	70.9	65.3
TBM	50		(10-49)	(10-26)	(58-78)	(61-67)
			22.6		72	
			(20-26)		(70-75)	
A1-A7	222.48	34.34	29.3	24.8	76	76.2
			(19-41)	(15-33)	(72-78)	(72-82)
B1-B8	141.83	12.63	28.1	19.3	72	67
			(17-50)	(10-24)	(70-78)	(64-72)
Radial	59.25	12.60	22.2	23.2	70.7	71.3
Boreholes			(12-42)	(9-66)	(68-75)	(67-75)
D&B	38		21.8		72.4	
			(5-37)		(57-76)	

4.2 EXCAVATION TECHNIQUES AND PROGRESS

4.2.1 TBM Excavation

The TBM drift excavation began on June 16, 1994, using an Atlas Copco JARVA Mk15/1680 5.0 TBM. Some technical parameters of the TBM are listed in Table 4-7. The beginning of the TBM drift was at chainage 3191.28, corresponding to a starting position of X = 2269.755, Y = 7308.884 and Z = -418.033, in the Äspö co-ordinate system. Based on surveyed points on the perimeter of the drift the initial direction of the drift was 259.4° with a plunge of 8.7°.

Information of the progress of the excavation was documented in shift logs made by Skanska during the tunnel boring operations. Unfortunately the TBM logger did not function properly during the majority of the operation, except for the days of June 17 and 18, 1994. However, the position of the gripper pads can be determined as these form an almost continuous band

along the central line of the drift walls, as the grippers were placed slightly overlapping during the excavation process.

Table 4-7. TBM Parameters.

TBM Diameter	5.03 m
Rotation Rate	max. 10 RPM
Typical Penetration Rate	1200-2000 mmh^{-1}
Maximum Thrust Force	8300 kN
Typical Torque	40 kNm
Number of Cutters	34
Gripper load	25000 kN
Stroke length	1.52 m
Installed Power for breaking the rock	1680 MW

The average thrust on the TBM cutters was estimated to be 140 kN up to 190 kN per cutter. The penetration of the cutters is about 1 to 2 mm per rotation and at this penetration the contact length of the cutter was estimated to range from 18 to 26 mm. The average contact pressure on one of the cutters was estimated to vary between 280 MPa and 570 MPa which is of the order of 2 to 3 times higher than the uniaxial compressive strength of the rock.

4.2.2 Drill&Blast Excavation

Blast Design

The D&B drift was excavated perpendicular to the D&B access drift and sub-parallel to the TBM drift. A total of eleven rounds were blasted of which nine were included within the ZEDEX test. The D&B drift was designed to have the same geometry as the TBM drift, except for a flattened floor, with a cross section of 17.7 m^2 and an excavated total length of 38.5 metres.

Two different excavation techniques were used:

- Low-shock energy smooth blasting (LSES) for rounds B2 and R1 to R4 (Figure 3-1).
- Normal smooth blasting (NS) for rounds B1 and R5 to R9 (Figure 3-1).

The LSES blast design was tentatively optimised in the access drift. However, the access drift was directed perpendicular to the D&B drift which was not ideal. Unfortunately the LSES design could not be completely optimised because of restrictions in the use of some types of bulk explosives at Äspö.

Geometry

The drilling parameters were the same for all charged blast holes, with all blast holes having a diameter of 48 millimetres and a length of 3.6 metres. The drilling pattern was manually marked on the face and drilling was undertaken manually up to round R3. For rounds R4 to R9 an automatic Bever Control system was used which improved the performance and control of the drilling operations and provided information, in the form of a printout, showing that all shot holes had been drilled with the correct directions.

The cut design included three empty holes of 102 millimetres diameter which were expected to reduce the risk of sympathetic initiation of adjacent charges in the cut. The blast holes had a diameter of 48 millimetres. The drill pattern designed for the LSES design had three more holes than the NS design in the cushion row and the drilling pattern of the cut was also reversed between rounds.

Explosives

The main difference between LSES and NS designs was the amount and type of explosives in the cushion and lifter holes.

In the LSES technique, the cushion holes were charged with Emulite 100 which were 22 and 25 millimetres in diameter to produce lower shock energy levels compared to the production holes. The lifter holes were charged with Emulite 100, 25 millimetre diameter.

Whilst, in the NS design, the cushion holes were loaded with Dynamex with a diameter of 25 millimetres and Dynamex with a diameter of 32 millimetres which was used in the lifter holes.

The cut and production hole charges were similar in all rounds. To minimise the effects of shock energy, Gurit 17 millimetres was used in the perimeter holes in all rounds. The explosives and drilling pattern used for the LSES design (round R3) are summarised in Figure 4-12 and for the NS design (round R5) in Figure 4-13.

Initiation system

To control the blast firing times, high accuracy electronic detonators were used for initiation of the cushion and contour holes in the LSES rounds. This was combined with the conventional NONEL system, which was used in the remaining blast holes. For one round, electronic detonators were used for all the holes. The five NS blast rounds were completely initiated using NONEL detonators.

Drill&Blast excavation progress

The excavation progress for each round and the design used are summarised in Table 4-8. The amount of explosive energy in each type of hole was examined to determine the total explosive energy per round.

Table 4-8. Excavation progress for each round and the design used. E= Emulite, G=Gurit and DxM= Dynamex.

Blast	Date	Design	Spec. drill	Spec. char.	Explosives (kg)					Pull	Reblast	Remarks
			dm/m3	kg/m3	Cut + Prod.	Bottom	Cut	Cushion	Contour			
B2	10/01/95	LSES	4,70	1,83	47,1 DxM	17,4 E		22,7 E	16,3 G17	misfire	11/01/95	initiation disturbance in cut simultaneous detonations of # 0, 3 and 5 translation of holes # 6, 7 and 8
1	11/01/95	LSES	4,82	2,26	71,8 DxM	17,4 E		22,7 E	16,3 G17	full pull		2 more holes in production row # 4 (400 ms) missing in cut
2	12/01/95	LSES	4,82	2,26	71,8 DxM	17,4 E		22,7 E	16,3 G17	half pull	13/01/95	full cut pull, bad pull cushion and contour # 2 and 7 (200 and 700 ms) missing in cut 2 first holes : shock wave parallel to foliation
3	13/01/95	LSES	4,82	2,26	71,8 DxM	17,4 E		22,7 E	16,3 G17	full pull		all firing time detected inversion of the 2 first holes to be perpendicular to foliation
4	15/01/95	LSES	4,82	2,26	71,8 DxM	17,4 E		22,7 E	16,3 G17	half pull	17/01/95	full cut pull, bad pull cushion and contour # 9 (900 ms) missing - extra detonation (302 ms) must have detonated without free surface
5	16/01/95	NS	4,33	2,25	48,9 DxM	19,1 DxM	15,9 DxM	20,9 DxM	22,4 G17	full pull		# 2 (200 ms) missing in cut
6	17/01/95	NS	4,33	2,27	48,9 DxM	19,1 DxM	15,9 DxM	22,4 DxM	22,4 G17	misfire	18/01/95	first 4 holes OK, big spring inside no missing numbers in cut
7	26/01/95	NS	4,33	2,54	60,4 DxM	19,1 DxM	15,9 DxM	23,6 DxM	24,8 G17	full pull		
8	27/01/95	NS	4,33	2,54	60,4 DxM	19,1 DxM	15,9 DxM	23,6 DxM	24,8 G17	half pull	28/01/95	cut OK, rest of holes 1 m left
9	29/01/95	NS	4,33	2,54	60,4 DxM	19,1 DxM	15,9 DxM	23,6 DxM	24,8 G17	full pull		

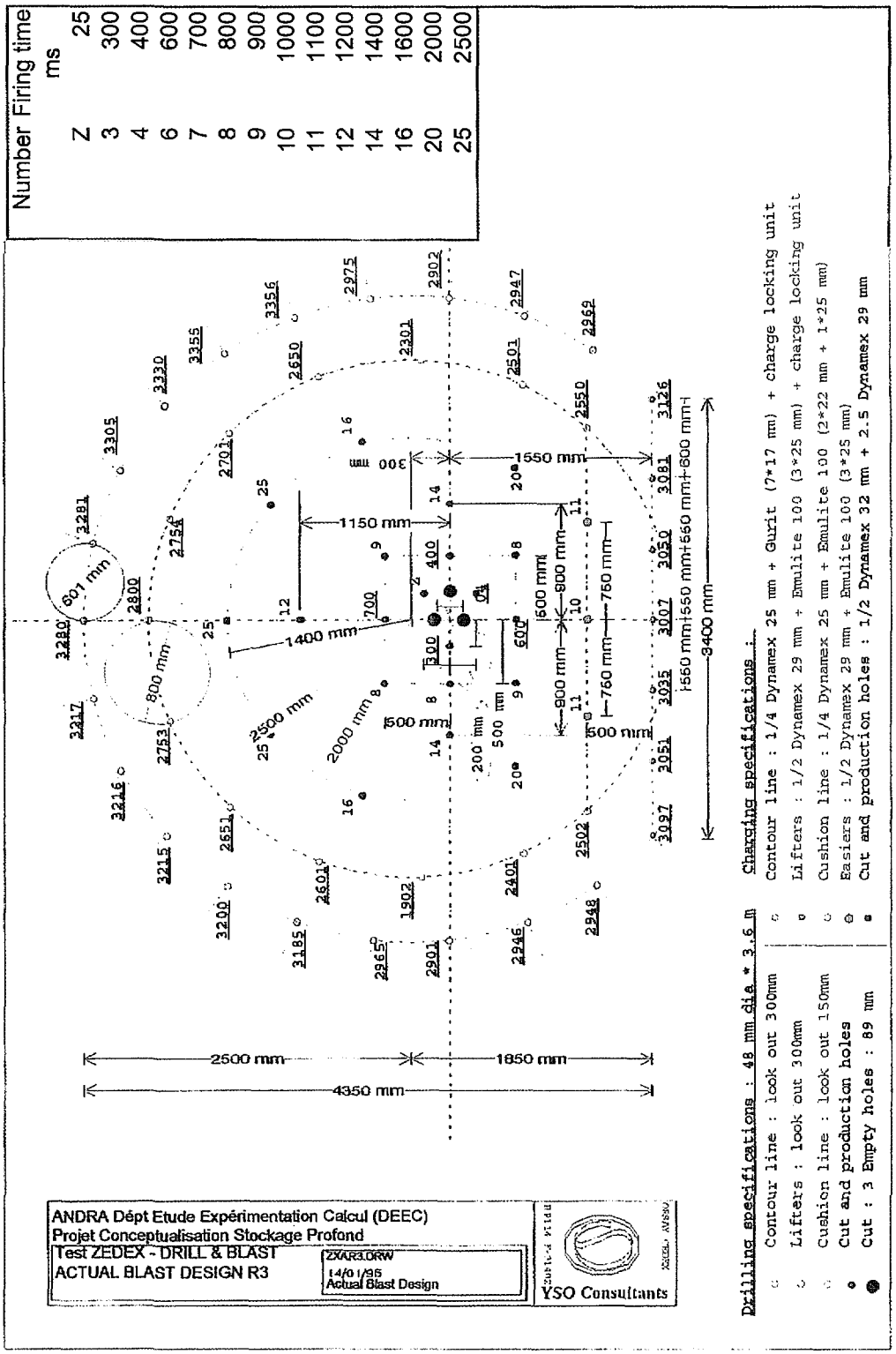

Figure 4-12. *Blast design for low shock energy smooth blasting (LSES) Round R3. Firing times of detonators are underlined. Sequence number for detonators are not underlined.*

Äspö Hard Rock Laboratory
Zedex - Zone of excavation disturbance experiment

Normal Smooth Blasting Design, Zedex drift **Blast 05 950116**
Bever used

Area	17,7	m2
Width	5,0	m
Height	4,4	m
Hole depth	3,5	m
Advance	3,2	m
Volume	57	m3
No. of large holes, 102 mm	2,0	no
Drill meter	210,0	m
Drillmeter large holes*5	35,0	m
Total drill meter	245,0	m
Spec. drilling	4,33	dm/m3
No. detonators / m3	1,06	no/M3
Spec. charge total	2,25	kg/m3

Result

Good

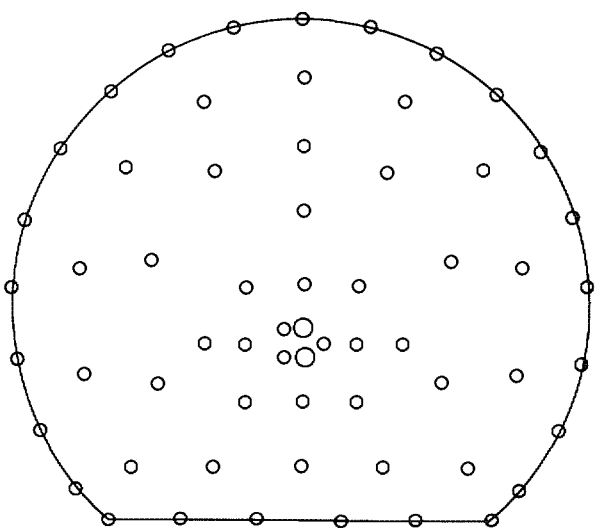

Explosive		
DxM 32*1110 mm	1,1	kg/m
DxM 29*1110 mm	0,9	kg/m
DxM 25*1110 mm	0,7	kg/m
Gurit 17*500	0,2	kg/m
	0,0	kg/m

	No. hole	DxM 32 mm		DxM 29 mm		DxM 25 mm		Gurit 17 mm		Kg/	Kg
Area m2 17,7	48 mm	m/hole	kg	m/hole	kg	m/hole	kg	m/hole	kg	hole	Total
Lifter	6	1,11	7,2	2,2	11,9	0,0	0,0	0,0	0,0	0,0	19,1
Perimeter	19	0,00	0,0	0,0	0,0	0,6	7,1	3,5	15,3	0,0	22,4
Wall/Roof helper	11	0,00	0,0	0,0	0,0	2,8	20,9	0,0	0,0	0,0	20,9
Cut	5	0,00	0,0	3,3	14,9	0,3	1,0	0,0	0,0	3,2	15,9
Cut & Production	19	0,55	11,3	2,2	37,6	0,0	0,0	0,0	0,0	2,6	48,9
Total	60	1,7	18,5		64,4		29,1		15,3		127,2

Figure 4-13. Blast design for normal smooth blasting (NS) Round R5.

Figure 4-14 shows the relative difference in explosive energy between the blasting rounds.

During LSES blasting, the cut was fully pulled (a pull is the designed excavated volume) for two of the rounds (R1 and R3), while cushion and contour row were only partly excavated for two of the rounds (R2 and R4). The acceleration measurements recorded during blasting showed that rounds R1, R2 and R4 were affected by missing detonations in the cut.

Round R3 was characterised by a full pull and this was the only LSES round that had no missing detonations. The drilling pattern of the cut was also reversed between rounds in order to have a shock wave direction between the two first holes to detonate perpendicular to the foliation of rock structure rather than parallel to it as was the case in round R2. It was believed that the round R2 pattern with early detonations aligned parallel to the foliation may have caused simultaneous initiation to occur.

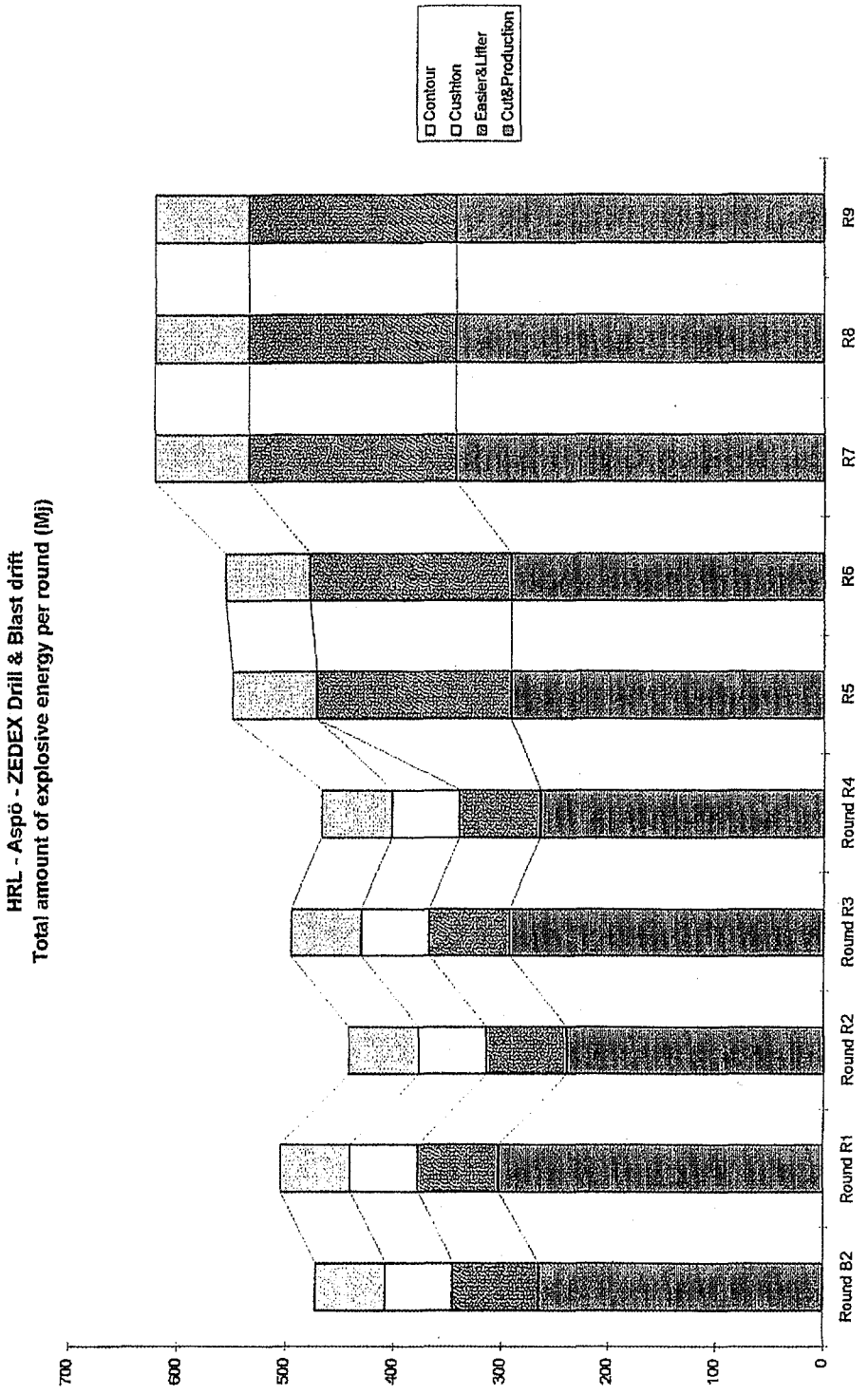

Figure 4-14. *Total amount of explosive energy per round (MJ).*

5 INTEGRATED INTERPRETATION OF RESULTS

The ZEDEX experiment was designed to improve understanding of the extent and character of the EDZ and its dependence on the method of excavation. To enable a direct comparison of the different excavation methods required the drifts to have similar geometries and to be excavated under similar initial conditions. The two test drifts therefore had comparable geometries and were excavated parallel to each other approximately 25 metres apart in fairly massive but variable Äspö diorite. Mapping of the drifts showed that some differences in lithology and fracturing were present.

In discussing the measurements and calculations undertaken as part of the project within the ZEDEX volume, we may classify the parameters studied as either:

1. causes and/or controlling factors of the excavation disturbance that include the geological setting, the mechanical properties of the rock, the stress state, existing fracture patterns and excavation parameters (Chapter 4) which combine in complex ways to cause the effects and

2. effects of those controlling factors that may be measured and may be discussed in terms of damage or disturbance that were detected by means of acoustic emissions, displacements, permeability changes, changes in seismic velocity and other measurements performed. These are discussed in Sections 5.2 through 5.4.

At the design and planning stages of the project, when the hypothesis was established, it was anticipated that the excavation disturbance could be described in terms of those effects that occur within the near-field, defined as the region within two metres from the excavation, where the largest disturbance was expected and beyond that, the far-field, where the disturbance was expected to be independent of excavation method. However, the results indicated that this arbitrary division was inappropriate. A more appropriate division is based on the recognition that there is a damaged zone, closest to the drift wall, dominated by changes in rock properties that are mainly irreversible. Beyond that there is a disturbed zone dominated by changes in stress state and hydraulic head, where any changes in rock properties are small and mainly reversible. The term EDZ is used to describe the total disturbed zone that includes the failed and damage zones closest to the wall that are caused by the excavation method and also the disturbed zone outside the damaged zone.

One of the causes and/or controlling factors mentioned above is the state of stress existing within the rock volume. The interaction between the stress state and the excavations may cause stress induced damage, that may in turn be measurable. To obtain an understanding of the stress state around

the excavations and develop a concept of what may be observed stress and displacement modelling was performed. This is discussed in Section 5.1 to establish the context within which the other measurements and interpretations can be set. The "effects" of excavation processes, the excavation response, are discussed in the following sections, with the observations and interpretation of the damaged zone presented in Section 5.3, while Section 5.4 presents an interpretation of the disturbed zone observations.

5.1 STRESS AND DISPLACEMENT MODELLING

The presence of an opening within a rock mass causes major changes to the stress field around that opening that result in disturbance to the rock mass. Detournay & St. John (1988) categorised possible failure modes around circular unsupported tunnels (Figure 5-1) and from this it can be seen that the rock mass around the ZEDEX drifts remains in a mainly elastic regime under the stress and material conditions determined for the Äspö site. It may therefore be considered that elastic displacement will occur and that no or minimal stress induced damage will occur.

Stress induced damage may, however, occur in regions of high differential stress (σ_1-σ_3), where the stress may be concentrated such that the crack initiation stress is surpassed. There may also be areas where the σ_3 stress may become tensile, surpassing the tensile strength of the rock causing failure. Another potential damage mechanism is stress relief, whereby the

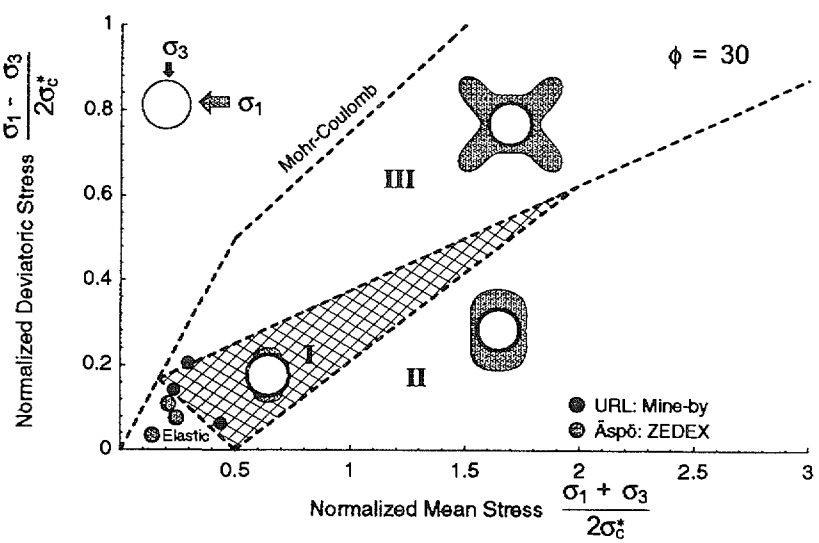

Figure 5-1. Relationship between failure modes and stress state for an unsupported circular opening, after Detournay and St. John (1988).

removal of the confining stress results in extension of existing cracks. In the presence of existing fractures, the shear and normal stresses acting on the fracture surface may change resulting in slip on the fracture.

Thus, an understanding of the stress field around the ZEDEX drifts is essential, as well as an understanding of the conditions under which the above mentioned disturbance mechanisms may occur. Furthermore, estimates of elastic displacement from modelling may be useful in understanding the observed displacements that occurred around the drifts in order to determine whether they can be explained by elastic strain, or whether inelastic displacement (crack damage) has occurred.

Detailed stress modelling close to the drifts was performed using EXAMINE^{3D}. In this case the calculations were based on a straight section of drift, without accounting for the influence of other parts of the excavation such as the TBM assembly hall. Previous modelling showed that these other drifts would have a limited effect on stresses in the volume used for the ZEDEX project investigations. The model of the D&B drift is for an idealised cross sectional shape, not accounting for the irregularities in the actual drift profile. Figure 5-2 shows the major compressive principal stress, σ_1, the minor compressive principal stress σ_3 and the differential stress (σ_1-σ_3) for cross sections several metres behind the drift faces of both drifts. The maximum compressive stress and the differential stress show similar spatial variation, although the differential stress is more concentrated close to the excavation surface. In both cases the maximum values are in the floor and roof of the drifts. In the D&B drift, the highest values were approximately 75 MPa in the corners of the floor, while in the roof of the drift, the peak values were about 70 MPa. In the TBM drift, the floor and roof of the drift had generally symmetrical stress fields with the highest values of σ_1 and differential stress (σ_1-σ_3) of approximately 70 MPa. The σ_1 stress trajectories were found to be tangential to the drift near the excavation surface. This value is just over one third of the unconfined compressive strength of the rock. In the region of the side walls of the drift the differential stress is as low as 12 MPa.

The minimum principal stress σ_3 is slightly tensile in regions above and below the springline of the drift (Figure 5-2). The most extensive regions of decreased σ_3 stress values are those regions inclined at about 45° above and below horizontal. In the D&B drift, there is a region of decreased σ_3 under the floor of the drift. The σ_3 stress trajectories were rotated perpendicular to the drift perimeter close to the drift where the values approach zero MPa.

5.1.1 Conditions for Stress-Induced Disturbance

The failure zone that forms around an underground opening is a function of the geometry of the opening, the far-field stress field and the strength of the rock mass. Detournay and St. John (1988) categorised possible failure

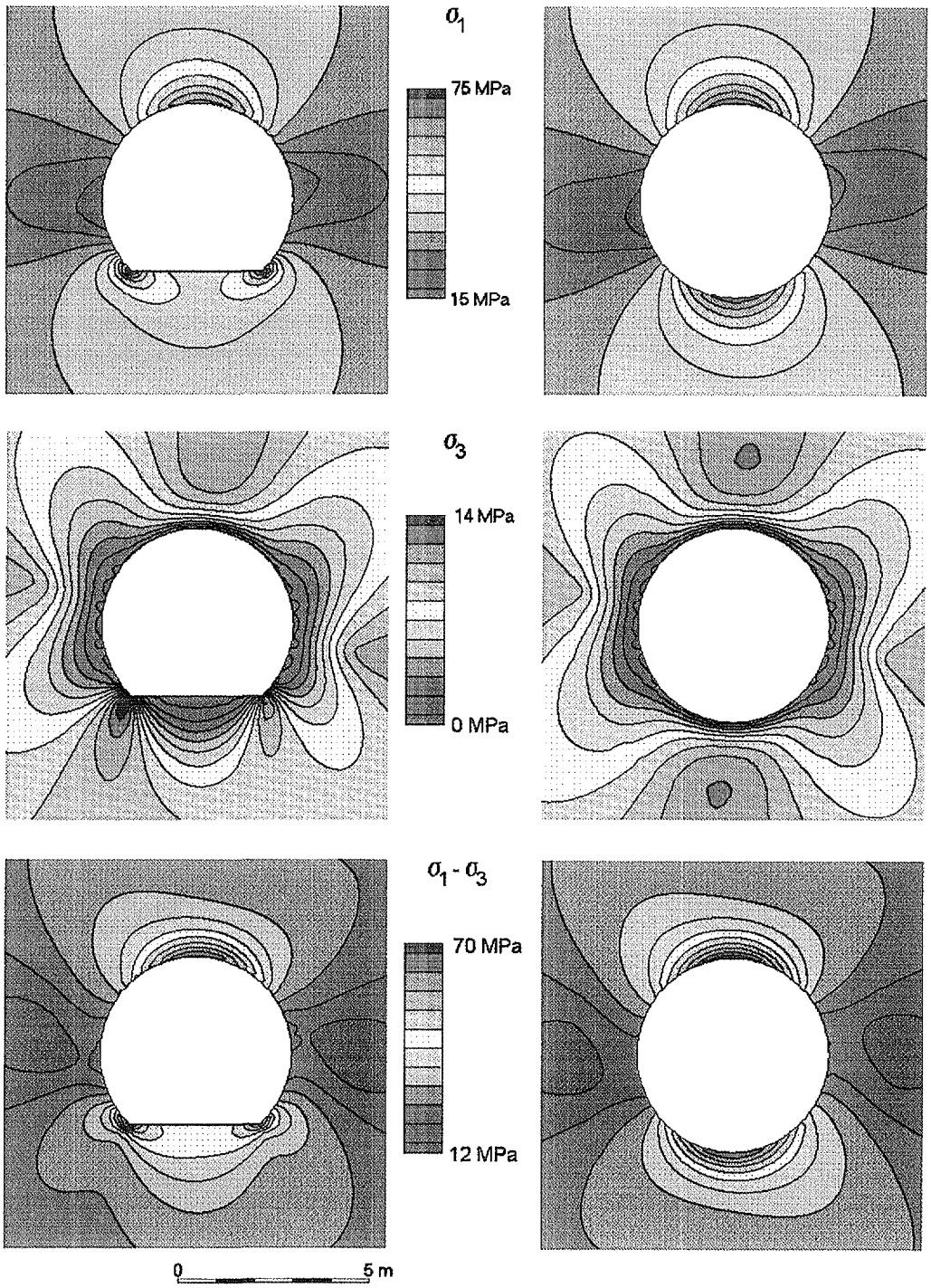

Figure 5-2. *Stress models for the D&B (left) and TBM drift (right). The maximum compressive principal stress (σ_1) is shown at the top, the minimum compressive principal stress (σ_3) is shown in the centre and the differential or deviatoric stress (σ_1-σ_3) is shown at the bottom. Minor undulations in stress close to the boundary are artefacts of the model.*

modes around a circular unsupported tunnel according to Figure 5-1. The mean and deviatoric stress shown in Figure 5-1 are normalised to the uniaxial compressive field strength σ_c^* which is approximately $0.5\sigma_c$ where σ_c is the laboratory uniaxial compressive strength. The rock mass properties for the Äspö Laboratory (ZEDEX Experiment) fall in the elastic region. This indicates that macroscopic failure would not be expected under these stress conditions. This is not to say that damage occurring as micro-cracking and small scale cracking would not occur. For comparison, the Underground Research Laboratory (URL: Mine-by Experiment), which is also currently being used for radioactive waste repository research, falls within Region I of Figure 5-1. Within Region I failure occurs by the development of a v-shaped "notch" and hence, the extent of the failure zone is quite localised. Only at large values of the deviatoric and/or mean stress does the failure shape become continuous.

Practical experience indicates that the greater the *in situ* stress magnitudes relative to the rock strength, the more severe the damage observed around underground openings. Hoek and Brown (1980) compiled observations from South Africa for square openings in brittle rocks and found that visible damage around the openings occurred when

$$\frac{\sigma_1}{\sigma_c} \geq 0.1 \tag{5-1}$$

where σ_1 is the far-field maximum stress magnitude and σ_c is the short term unconfined compressive strength. Martin (1997) translated the findings of Hoek and Brown (1980) to the maximum stress at the boundary of the opening and concluded that visible damage around the opening occurred when

$$\frac{\sigma_{max}}{\sigma_c} \geq 0.4 \tag{5-2}$$

where σ_{max} is the maximum tangential stress at the boundary of the opening. At the tunnel boundary, σ_{max} is essentially the local value of σ_1. The boundary element model in Figure 5-2 shows that $\sigma_{max} \approx 70$ MPa for the ZEDEX drifts and the ratio of $\sigma_{max}/\sigma_c \approx 0.4$. It is recognised that the actual stress is lower than σ_{max}. Hence, very minor damage may be evident in the regions of the maximum stress concentrations around the drifts. From Figure 5-2 it can be seen that the maximum stress concentrations occur in the roof and floor.

Another means by which crack growth may occur within a rock, is by the removal of the confining stress (σ_3). Virtually any undisturbed rock mass will have a population of micro-cracks that may act as stress concentrators in the presence of significant differential stress.

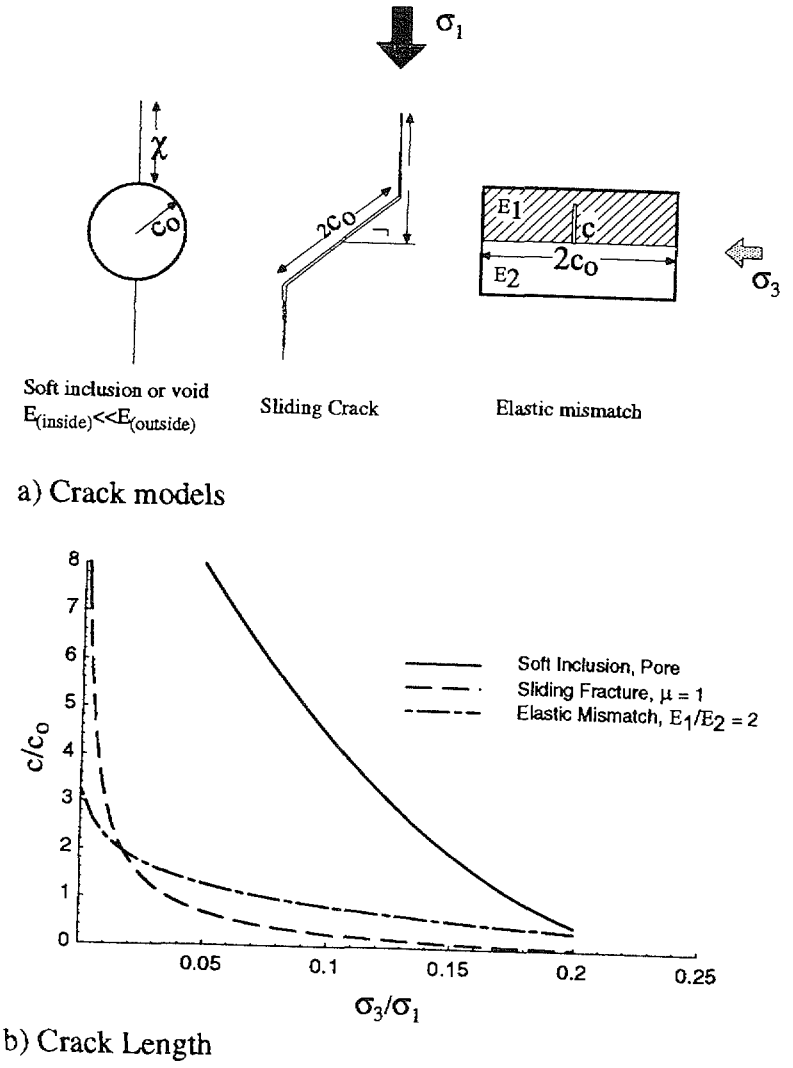

Figure 5-3. *Crack models and crack extension as a function of* σ_3/σ_1.

Both experimental studies (e.g., Hoek, 1965) and theoretical studies (Kemeny and Cook, 1991) have shown the effect of reducing the ratio σ_3/σ_1, on extending the length of existing cracks. Figure 5-3 is based on calculations made by Kemeny and Cook (1991) which show how crack length would increase in Äspö diorite by decreasing σ_3, while holding σ_1 constant at 30 MPa for three different tensile-crack extension mechanisms. The results for sliding cracks and neighbouring mineral grains with elastic mismatch are thought to be the most realistic models for crack extension in Äspö diorite. With the very low porosity at Äspö, we would not expect to see significant amounts of spherical pore space. The sliding-crack and elastic-mismatch mechanisms also show the closest agreement with the experimental findings of Hoek (1965). Hoek (1965) found that crack extension (c/c_0) became significant for $\sigma_3/\sigma_1 \leq 0.1$.

The stress induced damage that forms in a limited region next to the boundary of a tunnel is composed of cracks that can range in scale from micro (grain size) to macro (tunnel size). These cracks form as extension cracks and hence grow in a plane perpendicular to σ_3, because σ_3 is

approximately equal to the radial stress. Where $3 \geq K_0 \geq 1$; K_0 is the far-field ratio of σ_1/σ_3, the cracks will form parallel to the boundary of the tunnel. Within the ZEDEX volume the value of K_0 is approximately three implying that any stress induced damaged would form in a zone around the perimeter of the drift occurring as tangential cracks.

At the tunnel boundary, the confining stress is zero, however, depending on the ratio K_0, the shape of σ_3 contours may be highly varied. As seen from the modelled ZEDEX stress distribution (Figure 5-2), the greatest extent of decreased σ_3 values is at the regions surrounding vectors extending from the centre of the drift radially outward at approximately 45° above and below horizontal and in the floor of the excavation for the D&B drift.

The limits of damage due to stress relief can be estimated using the relationship found by Kemeny and Cook (1991) and Hoek (1965) showing that crack extension related to the removal of σ_3 begins to become significant as the ratio σ_3/σ_1 decreases below about 0.1. Figure 5-4 shows the σ_3/σ_1 ratio based on the modelled stress from Figure 5-2. The most extensive reduction in σ_3/σ_1, below 0.1, around the TBM drift, occurs in the regions inclined at 45 degrees above and below horizontal. The D&B drift also has an extensive region of reduced σ_3/σ_1 in the floor of the drift; but the irregular actual shape of the D&B drift, compared to this idealised model, means that stress can be modelled with less certainty for that drift.

Another form of disturbance that may be expected due to excavation induced stress redistribution is the interaction of the stresses with existing fractures. Normal forces may act to close or open existing fractures and shear stresses may act to cause slip on such fractures. These possibilities

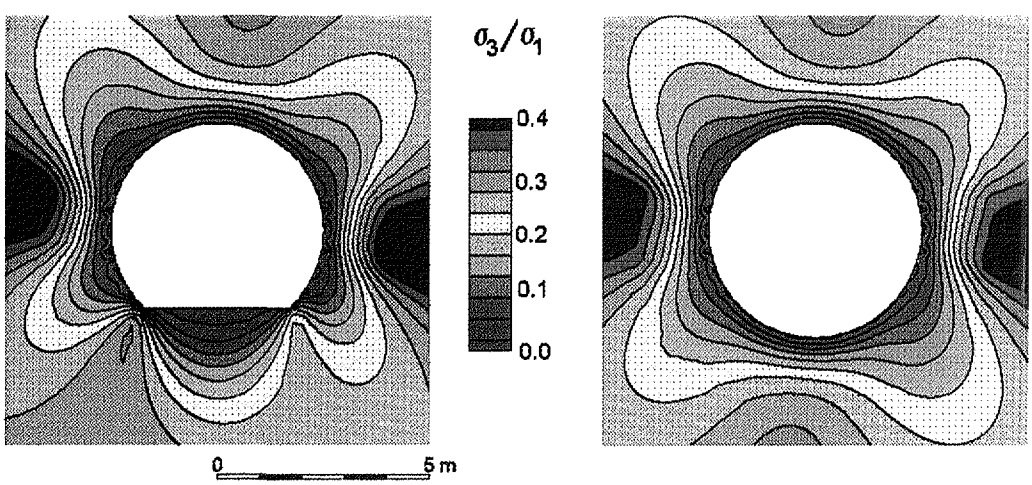

Figure 5-4. *The ratio σ_3/σ_1 for the D&B drift (left) and the TBM drift (right). Crack extension may be expected in under the conditions $\sigma_3/\sigma_1 <$ 0.1.*

would have implications on the hydraulic properties of the rock mass. An analysis of the shear and normal forces acting on a plane parallel to the predominant fracture set intersecting the TBM drift using the MAP3D modelling package (Wiles, 1996) has been performed. The potential for slip on fractures was evaluated by comparing modelled shear stresses to shear strength calculated across such a fracture. The shear strength (τ) was determined as:

$$\tau = S_o + \sigma_n \tan\phi \qquad (5\text{-}3)$$

where S_0 is the cohesion, σ_n is the normal stress acting on the plane and ϕ is the friction angle. For an open fracture, cohesion was assumed to be zero. Most fractures have friction angles that vary from peak values approaching 60° to residual values of 30°. The factor of safety (FOS), defined as the ratio of shear strength to shear stress acting across a fracture, has been evaluated. Results for different values of friction angle are shown in Figure 5-5. Using a FOS < 1 as a criterion for where slip might occur, the results indicated that, in specific regions, slip may have occurred up to 2.5 metres from the drift perimeter. That is, for the predominant fracture set, we would expect slip to be essentially confined to the damaged zone.

The normal forces acting on such a plane were also modelled as shown in Figure 5-6. The results indicate that a region of increased normal stress should be present in the roof of the drift and decreased normal stress in the side walls. These variations in normal stress could result in crack closing and opening respectively. This has implications for the seismic velocity and hydraulic properties such that a velocity decrease should be observed in the side walls with an increase in hydraulic properties; with the opposite effects observed in the roof.

5.2 MEASUREMENTS OF EXCAVATION RESPONSE

During the excavation of the drifts a number of measurements were undertaken, in boreholes close to the drifts and behind the advancing face during excavation. Rock quality data were also gathered in an attempt to determine the effects of excavation on the rock mass or show where such changes maybe expected. These measurements included; vibration and acceleration measurements; temperature measurements that were performed to determine the efficiency of the excavation methods; and displacement measurements. Acoustic emission monitoring was also undertaken to show the effects of the excavation in terms of either the generation of cracks or movement on pre-existing cracks, the results from this monitoring are presented later in Section 5.3 and 5.4.

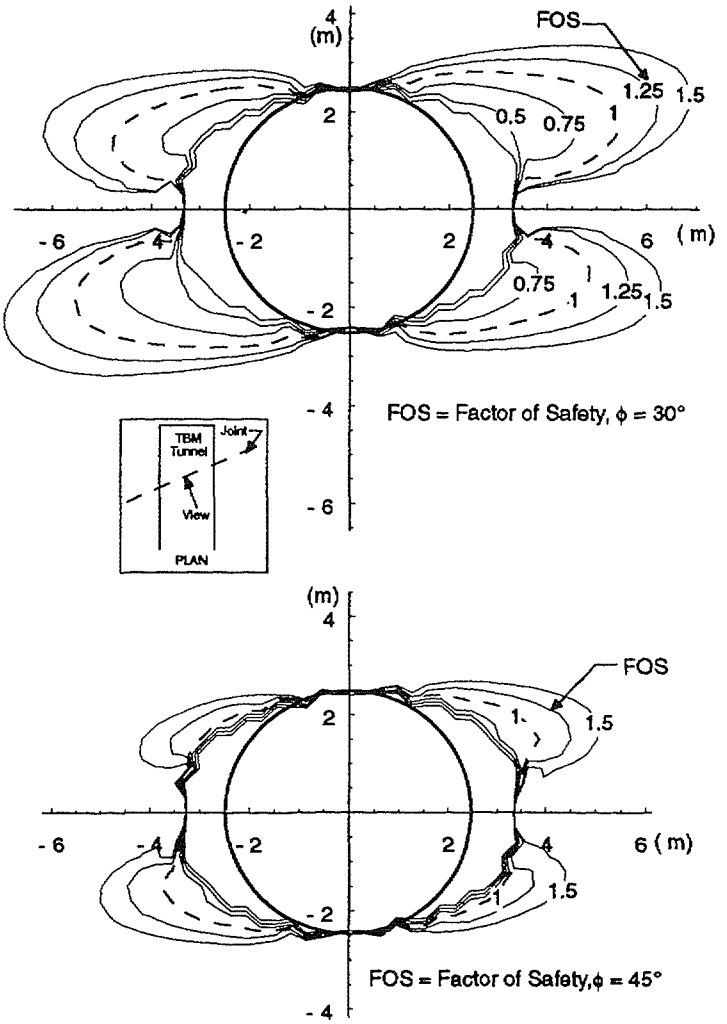

Figure 5-5. *Factor of safety against frictional sliding on a plane intersected by the TBM drift. The plane is aligned parallel to the main fracture set.*

Following excavation rock quality information, in the form of Q and RMR logging data were acquired to assess the effects of the excavation on the rock mass.

The above measurements, with the exception of the acoustic emission data, Q and RMR data are discussed in this sub-section.

5.2.1 Vibration and Acceleration Measurements

Vibration monitoring was used to examine the amount of seismic energy radiated into the rock during the excavation process. The vibrations generated by the TBM machine were measured in borehole C1, drilled parallel to and 3 metres away from the TBM drift. The vibration

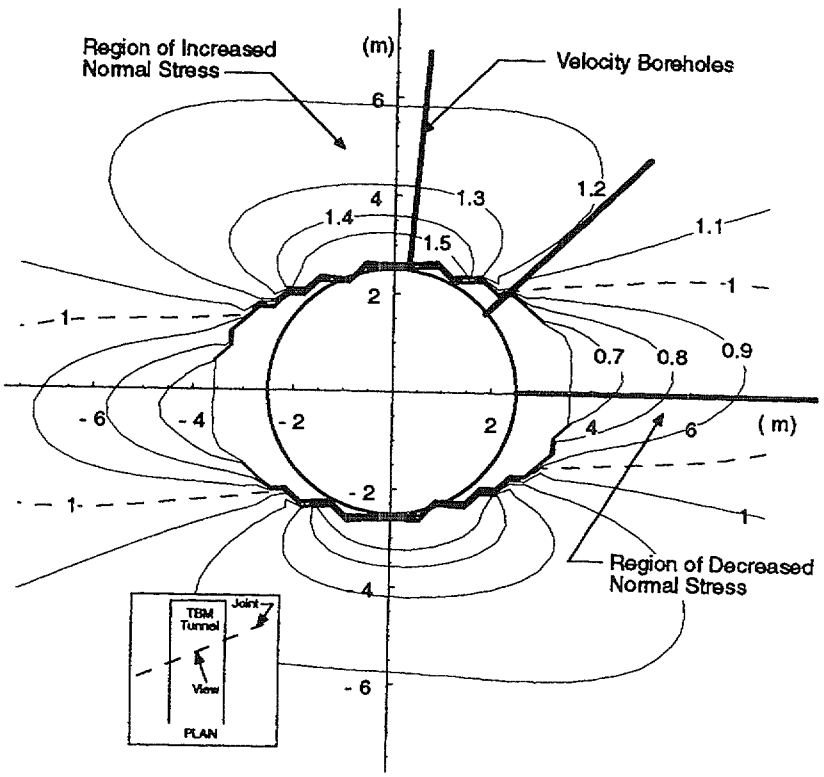

Figure 5-6. *Normal stress on a plane parallel to the main fracture set. The magnitudes are normalised to the far-field normal stress such that the contour 1 represents no change in magnitude.*

measurements were made using triaxial velocity transducers deployed at four stations, each of which were 3 metres apart and data were recorded in both the time and frequency domains.

The measured spectra, recorded during TBM operations, were observed to have the same or similar frequency contents for periods when the TBM head was merely rotating and periods when it was actually cutting. The only observed difference was in the amplitudes, which were higher when the TBM was cutting. The maximum vibration level was reported to be 1 mms^{-1}. The TBM required about 2 to 3 hours of actual cutting time to excavate a 3.5 metres length of drift. From these measurements the cumulative radiated seismic energy was calculated to be about 3.6 MJ. The energy expended by the TBM over this 2 to 3 hour period is about 13 500 MJ. During TBM cutting, the estimated radiated seismic energy was calculated for a one second period giving a power of approximately 400 W. Comparing this to the maximum TBM power consumption of 1 to 2 MW, the seismic efficiency was estimated to be only about 0.03%. This minute fraction of the total energy of the system, would not be expected to cause damage to the rock away from the excavation.

In the D&B drift, seismic acceleration measurements were performed in borehole A1 to monitor the firing sequences and to evaluate the level of seismic energy released into the surrounding rock mass. Four three-component accelerometers were used to measure the vibrations at distances between 5.3 and 21.4 metres from the centre of the blast rounds.

In some of the accelerograms the 500 g full-scale range of the transducers was exceeded. The maximum cumulative seismic energies from the blast rounds exhibited a definite radiation effect with significantly more energy radiated towards the back of the blast than to the front.

Blast rounds R1 to R3 (LSES) produced the lowest levels of cumulative seismic energy (CSE) (Figure 5-7), blasts R4 (LSES), R5 (NS) and R7 (NS) displayed intermediate levels of CSE and rounds R6 to R8 (NS) produced the highest CSE values which were 2.5 to 3 times larger than rounds R1 to R3. Data for R9 could not be used as the accelerometers were located too far from the blast round to provide meaningful data. Figure 5-7 shows that any missing or bad pull will result in increased seismic efficiency. The two full pull LSES rounds R1 and R3 gives lower level of CSE compared to the two half pull rounds R2 and R4. The two full pull NS rounds R5 and R7 gives lower level of CSE compared to the NS rounds R6 and R8 (misfire and half pull respectively). The increased seismic efficiency is expected to result in greater damage on the remaining rock.

The CSE values for each round and for an equivalent length of the TBM drift are given in Table 5-1. The total input energy (explosive energy or TBM energy expenditure) is also given, along with the seismic efficiency, defined as the percentage of total input energy transformed into seismic energy. The radiated seismic energy values calculated for each round in the D&B drift compared to the explosive energies, indicated seismic efficiency values ranging from 3.7 to 11.3 %. The blasts can be divided into three groups (Table 5-1) which display, respectively, low (A), intermediate (B) and high (C) levels of cumulative seismic energy when considering the power of the blast. The blast sequence occurs over about 4 seconds and the cumulative time of energy release within this period is only a fraction of a second. Thus, for the brief explosions the power may be in the range of 100 to 1000 MW.

From Table 5-1 it can be concluded that the TBM requires much more cumulative or total energy to create a similar length of drift compared to a drill and blast round. However, the time required for excavation and the minimal seismic efficiency of the TBM means that drill and blast methods may have a peak power output which is somewhere in the range of a million times greater than the TBM which is radiated into the rock as seismic waves or ground vibration. Clearly the drill and blast methods have a greater potential to damage the rock due to seismic energy release than the TBM. However, the anticipated effects of such levels of seismic energy release have not been quantitatively evaluated.

Table 5-1. Input energy, radiated seismic energy and seismic efficiency for the different excavation methods.

Type of blast	Excavation method / Group	Power or Explosive energy (MJ)	Radiated seismic energy(MJ)	Seismic efficiency (%)
-	TBM	13500	3.6	0.03
LSES	A - R1	505.1	18.9	3.7
LSES*	A - R2	442.1	24.8	5.6
LSES	A - R3	495.6	24.0	4.8
LSES*	B - R4	467.3	29.6	6.3
NS	B - R5	550.0	35.4	6.4
NS	B - R7	622.3	31.6	5.1
NS*	C - R6	556.8	63.0	11.3
NS*	C - R8	622.3	47.0	7.6

* partially failed blast round

Using the recorded data it has been possible to assess the actual firing sequence achieved in the D&B drift. A comparison between the designed blast sequence and measured firing times revealed differences between the times and also some missing detonations. The missing detonations could have resulted either from misfires or sympathetic initiation.

Thermodynamic calculations show that there was a large amount of energy in the cut which could cause sympathetic initiation to occur. Several mechanisms may be responsible for sympathetic initiation:

- Drilling deviations such that the boreholes may converge and cartridges may be too close together (explosives like Dynamex are very sensitive).
- Dynamic pressures from previous detonations transmitted through the foliation can affect the detonator in adjacent holes.
- Influence of the central damaged zone induced by the cut of the previous blast round. As illustrated in Figure 5-8, in the damaged zone, two linked, fully loaded, adjacent holes could be initiated at the same time.

The results from the acceleration measurements during blasting for round R1 are presented in Figure 5-9. The nominal firing times and the deviation between these times and the arrival time of P-waves of individual charges are also shown. This shows that there is a significant difference in the precision of the NONEL system and the electronic detonators used. Due to the importance of precise blasting of the cut for the success of the entire blast, it has been concluded that the exclusive use of electronic detonators in the first four blast rounds should have produced more successful results.

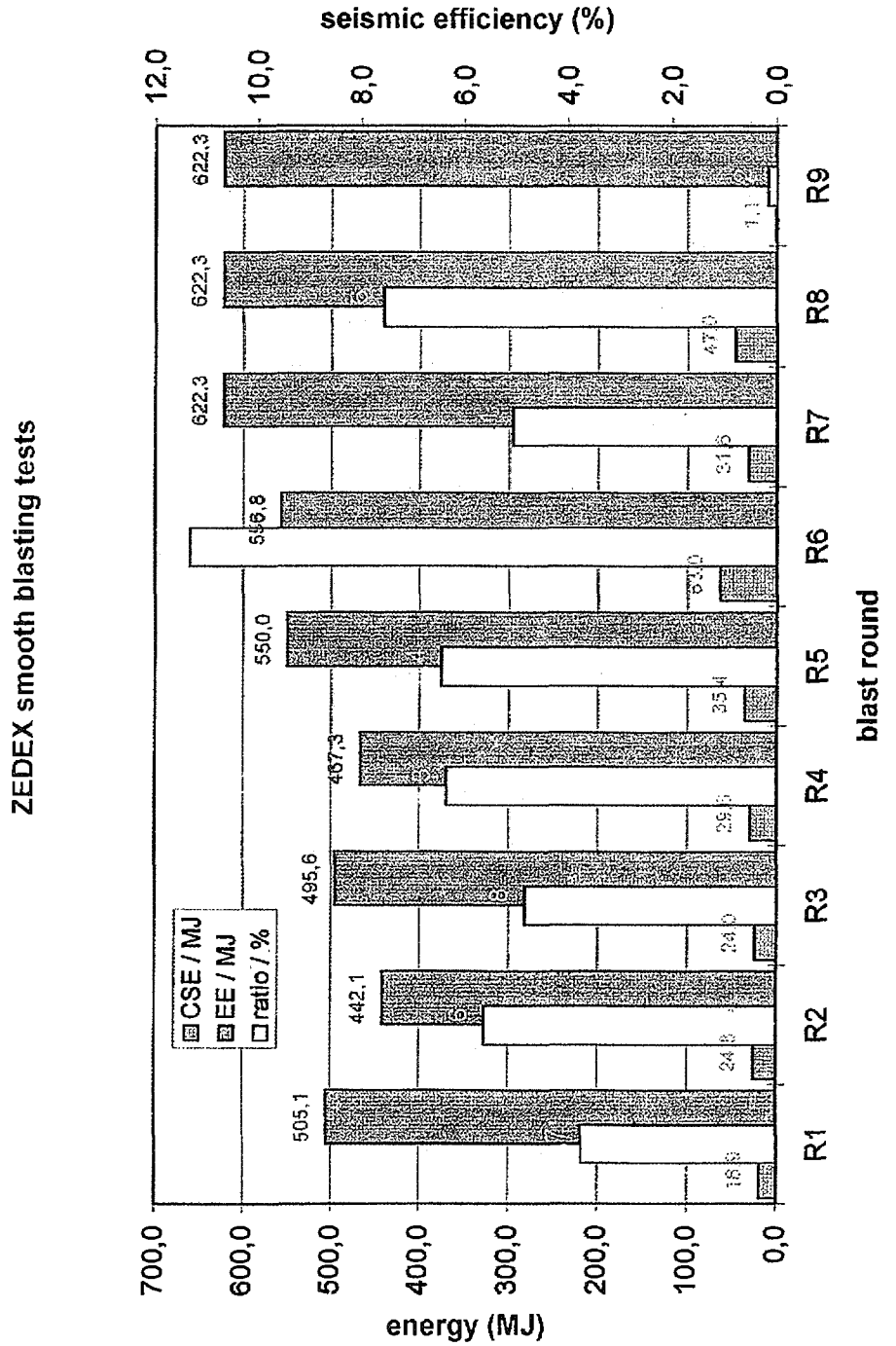

Figure 5-7. *Explosive energy values (red) compared to radiated seismic energy values (blue) - Seismic efficiency (yellow) the data from round R9 are unrealistic because the accelerometer stations were located in a shadow zone.*

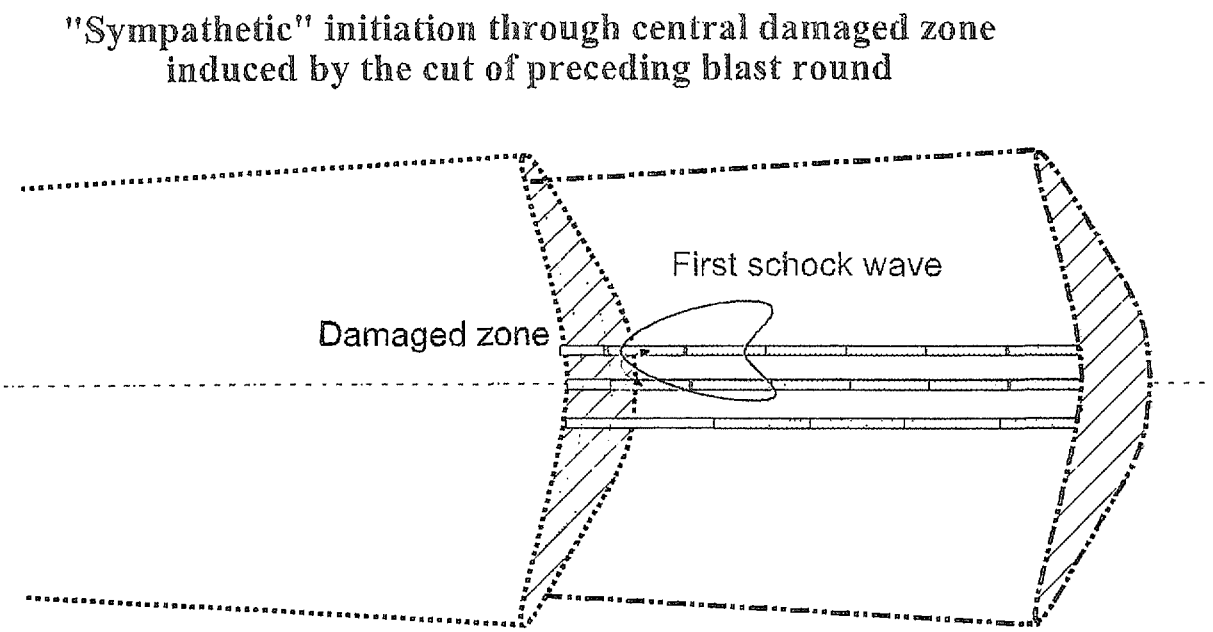

Figure 5-8. *"Sympathetic initiation" through central damaged zone induced by the cut of the preceding blast round.*

5.2.2 Temperature

The excavation of the drifts may cause a localised temperature increase which may therefore cause thermal expansion of mineral grains which may in turn cause stress perturbations and crack damage in the regions of high thermal gradients. Therefore during the excavation of the drifts temperature measurements were undertaken.

Temperature was measured in borehole C1 drilled parallel to and located 3 metres from the TBM drift. The observed temperature variations were, however, negligible, about 0.1°C and cannot be correlated with specific TBM events. Observed temperature variations were most probably due to changes in water flow in the borehole caused by the excavation.

Temperature was also measured in the air volume immediately ahead of the TBM and behind the face during convergence measurements. The temperature was approximately 20°C, which was only about 5°C higher than the background temperature. The change in temperature 3 metres from the drift would therefore be expected to be minimal for such a small increase at the drift face.

Similar temperature measurements were made in borehole A1 around the D&B drift during excavation using an array of 4 temperature sensors. No

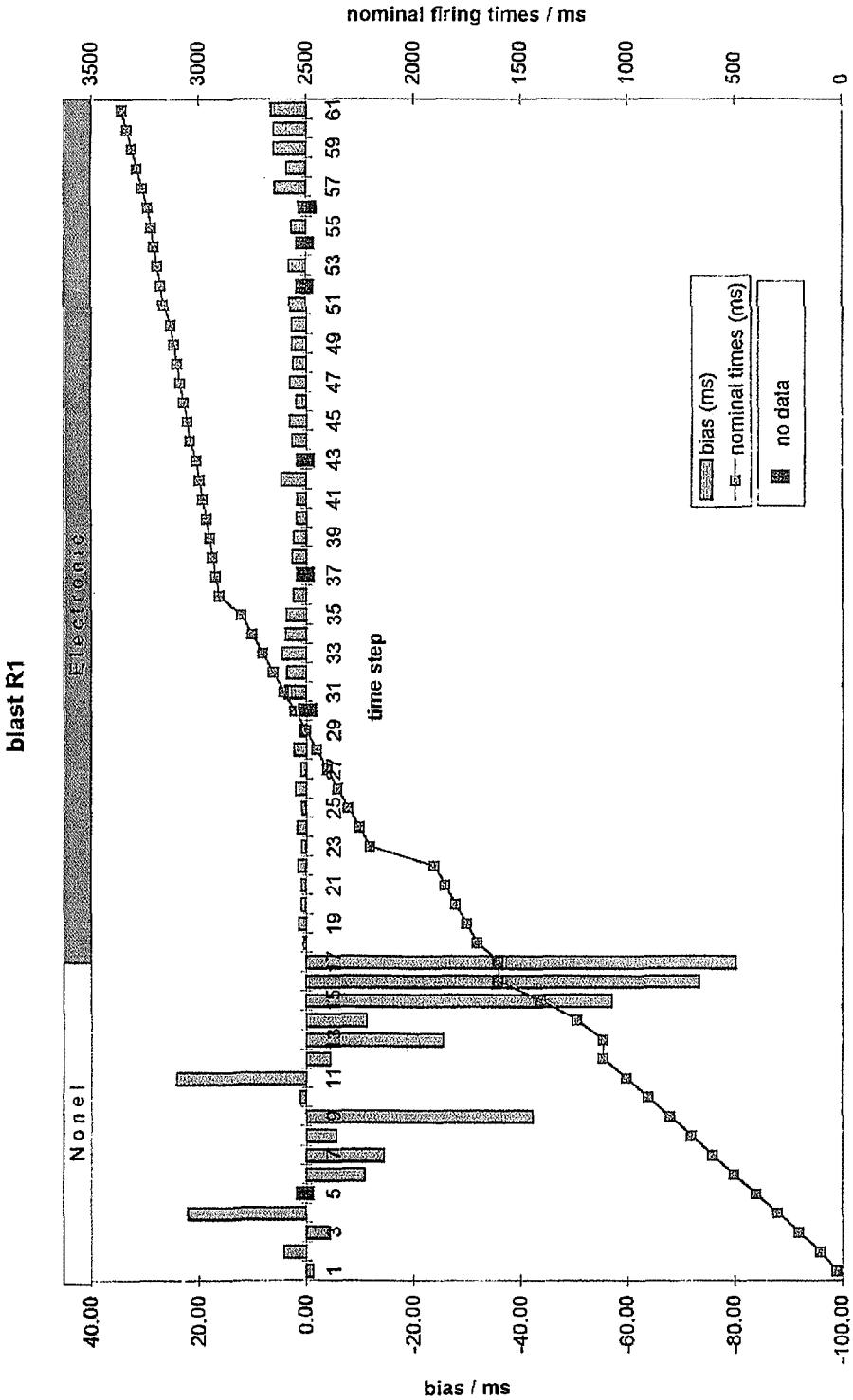

***Figure 5-9**. Difference in nominal and actual firing times for round R1.*

changes in temperature were observed that could be related to the blasting operations in the D&B drift.

5.2.3 Displacements

Displacement measurements may be used to evaluate the disturbance caused by an excavation. The creation of a circular tunnel in a stress field with differential stress ratio $K_0 \leq 3$, as at the ZEDEX site, should result in elastic convergence occurring around the tunnel. If crack damage has occurred, an additional component of inelastic strain resulting in further convergence would be expected.

The results of the convergence measurements for the TBM drift are summarised in Table 5-2. The measurements represent the elastic and non-elastic displacements following advance of the face from its position when the arrays were installed. Each array was installed as close as possible to the face (20-30 centimetres), but it was anticipated that about 50% of the elastic displacements would have occurred prior to installation and the first readings being taken.

The EXAMINE^{3D} programme was also used to calculate the displacements that would be expected from elastic strain around the drifts. These results are compared to convergence readings in Tables 5-2 and 5-3 for the D&B drift. Modelled convergence values in the TBM drift were calculated by comparing the displacement 0.2 metres behind the face, to the displacement several metres behind the face. For the drill and blast drift a similar procedure was undertaken, making initial calculations two metres behind the deepest point in a concave face of the drift and a second set of calculations one blast round further back.

The results indicate predominantly horizontal convergence in both sections, with little displacement in the vertical direction. This pattern of displacements is relatively consistent with results of BEM displacement based on the estimated *in situ* stress conditions and elastic properties of the rock. Although this is a simple model, the measured displacements have only exceeded the modelled values for one convergence measurement line. This may be taken as an indication that the elastic model has predicted the mechanical response reasonably well.

The results show some correlation with Q-values, the higher convergence occurred in the region with lowest Q. The drift mapping does not indicate any particular correlation with fracturing on a local scale but on the larger scale there may be some correlation between the maximum displacement observed by the convergence measurements at 9 metres in the TBM drift and the proximity of two large continuous fractures observed within 4 metres of either side of that array. No such continuous fractures were mapped at the position of convergence measurements at 24 metres.

Convergence around the D&B drift was measured during excavation at each new face following rounds R1 and R3 to R8 (Table 5-3). The

convergence arrays installed after rounds R5 and R6 allowed measurements across 5 diameters, while all other arrays were measured across only 3 diameters. One of the diameters was intended to be horizontal and the others were inclined at 60° (or at 30° intervals in the case of the 5-diameter arrays). Practical considerations in the drift, including avoiding the floor and protection of the pins from the following blast, dictated the final positions of reference pins. Due to the concave shape of the face caused by misfires, the arrays were typically installed about 2 metres behind the centre of the face.

The convergence measurements around the D&B drift indicated convergences of less than 1 millimetre across the diameters, with a standard deviation typically of 0.1 millimetres for each set of readings (Table 5-3). There was little significant displacement after the first round. The horizontal direction shows the most convergence and the inclined directions show an intermediate convergence. The correlation is, however, only clearly defined after the first blast. The difference between the expected elastic convergence for an array 2 metres behind the front of a concave face and an array 3.5 metres (one blast round) further back were calculated and showed that the total expected elastic convergence is about three times the difference between these two readings. That is, two thirds of the convergence would have taken place before the convergence array was installed for the first reading.

Table 5-2. Measured and calculated convergence values in the TBM drift.

Section (TBM drift length)	Displacement (mm)		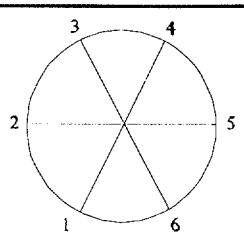
	1-4 (60°)	2-5 (0°)	3-6 (60°)
9 m	0	3.6	0.6
24 m	0.5	1.3	0.2
BEM Model	0.7	1.9	0.8

The measured convergence did not exceed the modelled elastic convergence for the horizontal diameter. On average the values were lower than those determined from BEM. However, the 60° diagonals showed relatively high convergence, in some cases exceeding the modelled value. This may be an indication that some inelastic strain due to crack damage has occurred in the diagonal directions as would be anticipated for these regions of maximum σ_3 stress reduction. The rock around the convergence anchors in the corners of the floor may have experienced inelastic strain due to damage caused by the high differential stress in these regions.

Several of the rounds may have experienced problems due to the presence of fractures, the necessity for re-blasts, damaged convergence pins, and the distance of the initial readings from the irregularly shaped drift face. The results from blast round R8 show remarkable agreement with the BEM results.

The displacements measured in the D&B drift (Table 5-3) were generally consistent along the length of the drift indicating no significant difference between the LSES excavation and NS excavation. Convergences measured for the D&B drift are of the same order of magnitude as the measurements made at 9 and 24 metres in the TBM drift (Table 5-2). The differences in magnitude and direction are not considered unusual given the likely effect of non-elastic displacements due to fracturing in the rock, likely variations in rock mass modulus and the fact that the convergence pins were installed much further behind the face than optimal in the D&B drift compared to the TBM drift. The stress anisotropy inferred from displacement measurements is not as marked in the D&B drift as in the TBM drift, which suggests that more of the measured displacement in the D&B drift was due to damage in a thin skin around the drift wall and only a proportion due to elastic closure.

Table 5-3. Displacements measured across 'diameters' after one round of excavation.

Round	Displacement (mm)				
	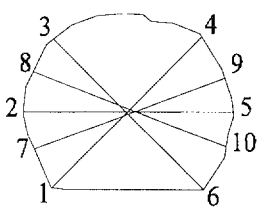				
	1-4 (60°)	7-9 (30°)	2-5 (0°)	8-10 (30°)	3-6 (60°)
R1	0.62		0.38*		0.33
R3	0.45		0.83		0.57*
R4	0.61		0.73		0.17
R5	0.52	0.76	0.69	0.55	0.49
R6	0.22	0.17	0.15	0.31	0.05
R7	0.18		0.44		0.31
R8	0.29		0.83		0.36
Average	0.41	0.47	0.58	0.43	0.32
BEM Model	0.29	0.62	0.94	0.74	0.36

* partial displacements measured due to damaged convergence pins

Displacements were also measured using four Multiple Point Borehole Extensometers (MPBX) which were installed more than 2 metres behind the face because of the space requirements for drilling the holes (Figure 5-10). Three of the MPBX were installed in boreholes near the face after round R6, B5 (vertically up), B7 (45° up) and B8 (45° down), with this round being the focus of these measurements. Additionally measurements were made using a MPBX installed in borehole B6, which was inclined 10° down. This had been installed from the TBM drift prior to excavation of the D&B drift. Anchors were installed at about 1 metre into the rock and then at 0.5, 1, 1.5 and 3 diameters from the drift wall. Measurements were taken after each blast.

The results of the MPBX measurements indicate that most of the measurable displacement took place within one round and were between 0.2 and 0.3 millimetres of convergence at the drift wall. This magnitude of displacement is generally consistent with the expected elastic displacement, although the vertical borehole yielded somewhat higher values than predicted by modelling. The displacements were generally distributed evenly with depth indicating that they were primarily elastic, although displacements at a few locations were indicative of local displacements along fractures. MPBX measurements in borehole B6 showed that there was no significant displacement (<0.02 millimetres) at distances up to 15 metres from the drift wall. There was no evidence of significant creep over a period of three weeks.

5.3 DAMAGED ZONE EFFECTS AND OBSERVATIONS

5.3.1 Acoustic Emissions

Acoustic emission (AE) activity in rocks results primarily from the sudden release of strain energy associated with cracks and micro-cracks. This may take the form of crack opening, closing, extension, shear slip, or some combination thereof. In this study 10 x 10 x 10 metre volumes around both drifts were monitored to determine whether AE activity was occurring around the drifts and if so, to determine the spatial and temporal distribution of AE activity. To help understand the causes of any such crack activity, the crack initiation conditions have been examined along with source-mechanism studies.

The AE rate versus time for a similar monitoring period in each drift is shown in Figure 5-11. In each case, the drift face was just approaching the edge of the sensor array. There was a clear exponential decay in the AE rate curves with time. For both the LSES and NS smooth blasting excavation technique approximately 1000 events per minute were detected immediately after the blasts, rapidly decaying to tens of events per minute.

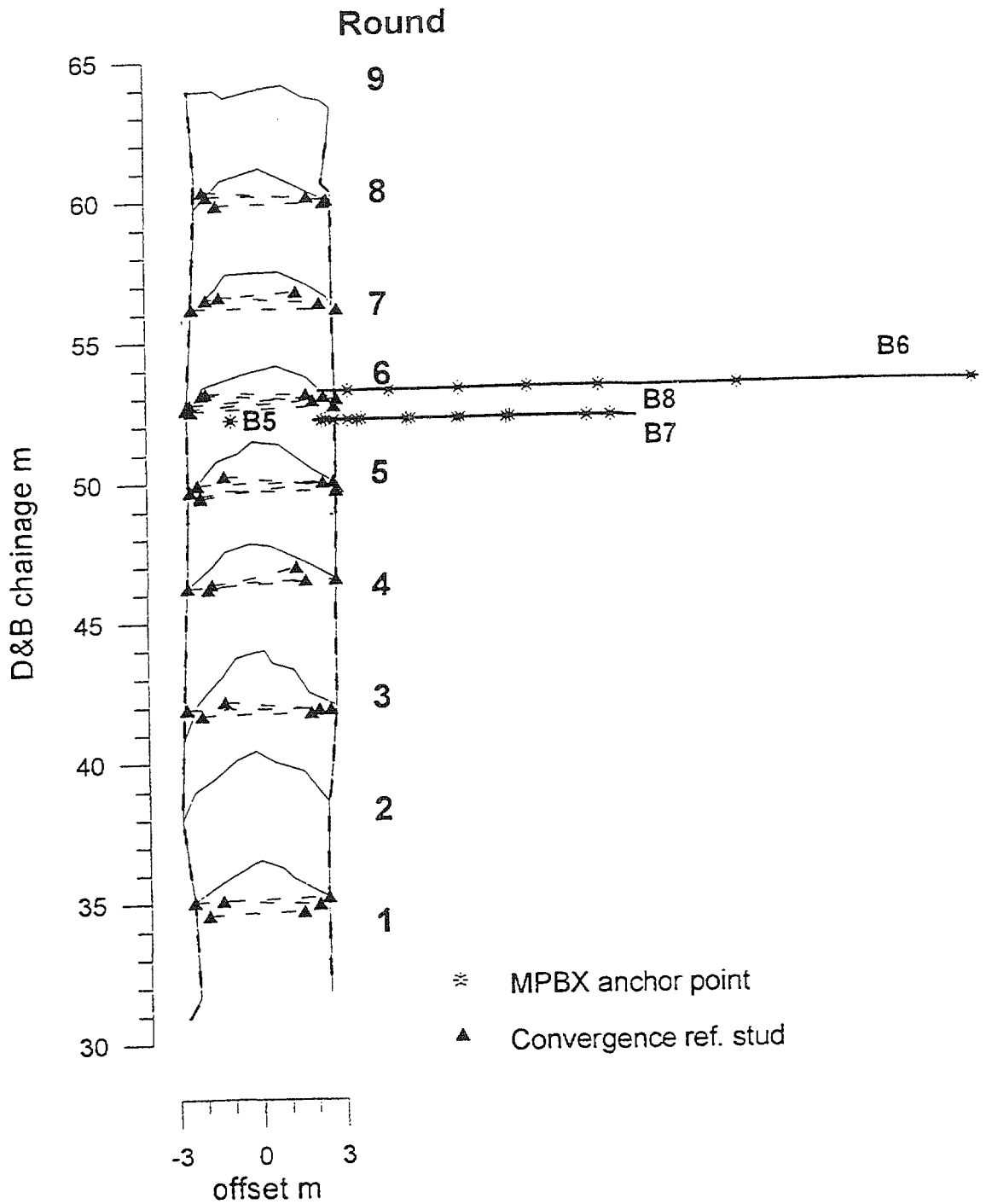

Figure 5-10. *Plan of drift face profiles, location of the convergence reference studs and location and numbering of the MPBX installations from the D&B drift.*

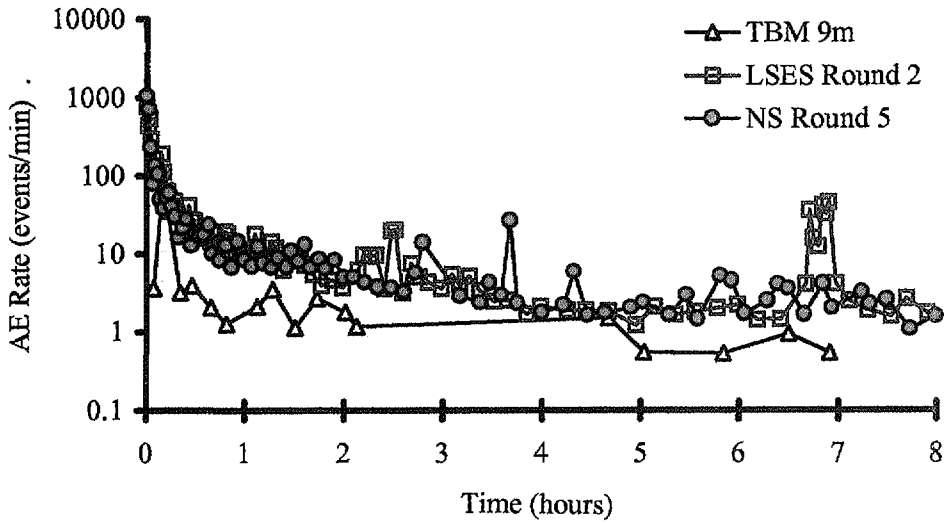

Figure 5-11. *Rate of AE activity following the 9 metres TBM stop, LSES blast round R2 and NS blast round R5.*

Plots of AE event rate for different positions of the drift faces showed similar trends, with an exponential decay and much lower AE rates for the TBM excavation than the D&B drift. Further, the two blasting methods used to excavate the D&B drift showed similar levels of AE activity. Background monitoring, performed before the TBM or D&B excavations began, did not detect any AE events within the study regions.

Throughout the monitoring periods the recorded AE rate was approximately ten times less for the TBM excavation method than for the D&B methods. It is recognised that as a result of the TBM drift blocking ray paths from the face to the sensor array resulting in fewer events being recorded, whilst the array positions were more optimised for the D&B drift, however, this does not affect the difference in AE event greatly. Of greater significance is the threshold level used for triggering AE event recording which was lower for monitoring the TBM than for the later D&B and this has therefore enhanced the AE rate recorded during TBM monitoring. If both data sets had been recorded with the same threshold level, i.e. those settings used for monitoring the D&B, the recorded AE rate would have been even lower when monitoring the TBM. This is a strong indication that brittle damage was greatly reduced using TBM excavation techniques compared to drill and blast methods applied under similar initial conditions.

AE source location results for selected excavation periods are presented as contoured event density plots in Figures 5-12 to 5-17, with views from above the drifts and looking along the drifts towards the excavation face. The resolution, as defined by the size of the grid elements used to create the plots, is 6.7 centimetres. The length values on the plots are in metres, starting at a local datum for each drift.

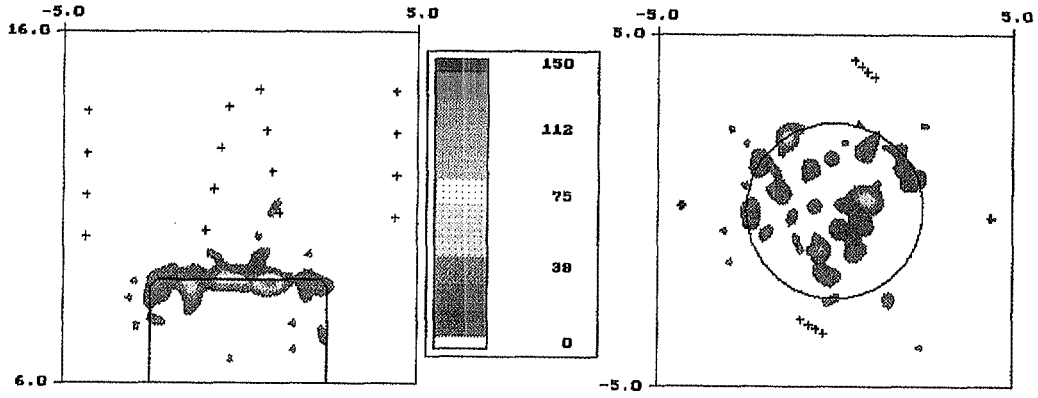

Figure 5-12. *Event density of AE data recorded when the TBM was stopped at 9 metres.*

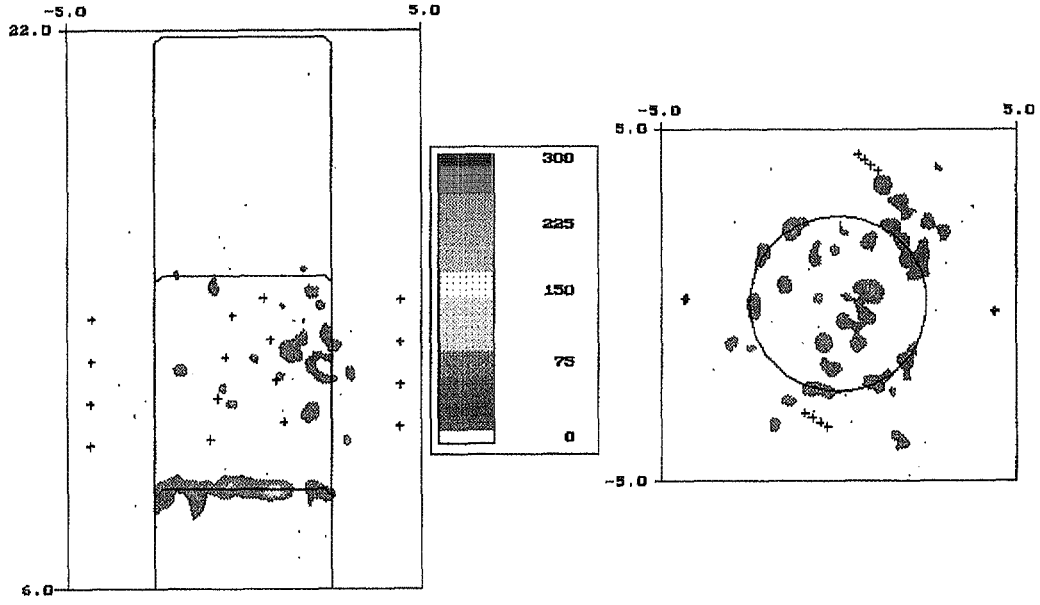

Figure 5-13. *Cumulative event density of AE data recorded when the TBM was stopped at 9 metres, 15 metres and 21.8 metres.*

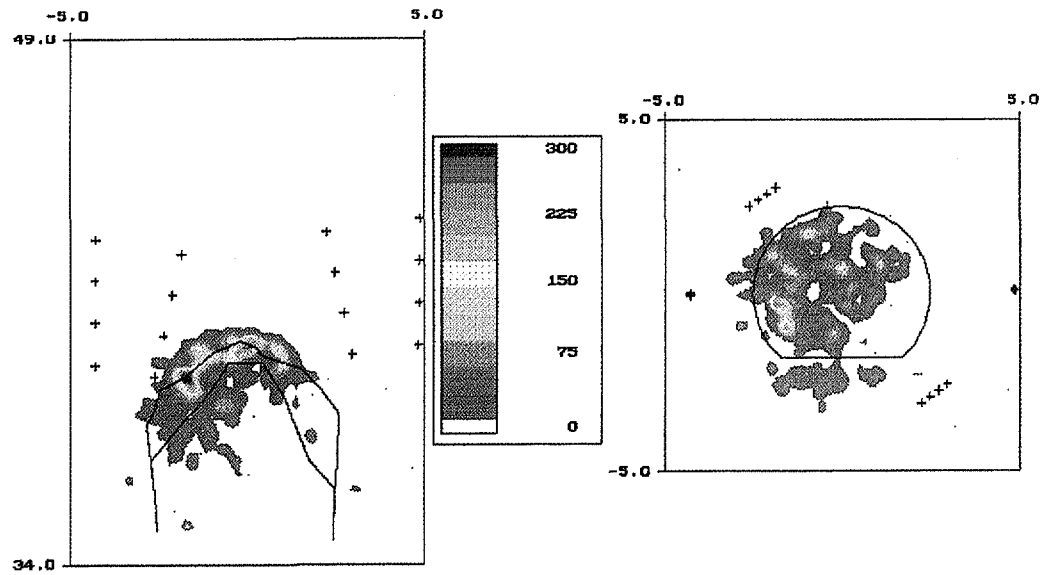

Figure 5-14. *Event density of AE data recorded after LSES blast round R2 in the D&B drift.*

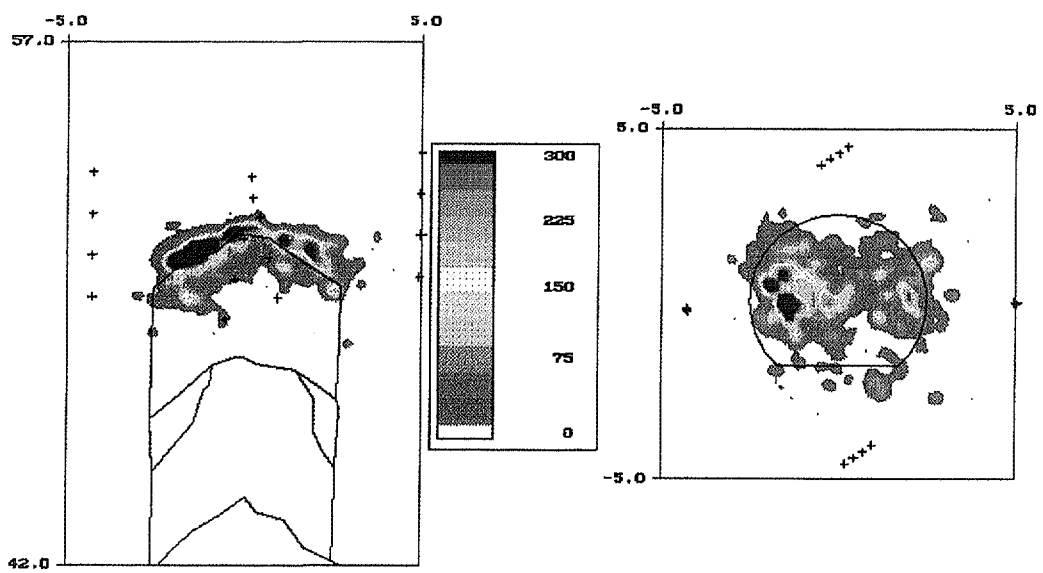

Figure 5-15. *Event density of AE data recorded after NS blast round R5 in the D&B drift.*

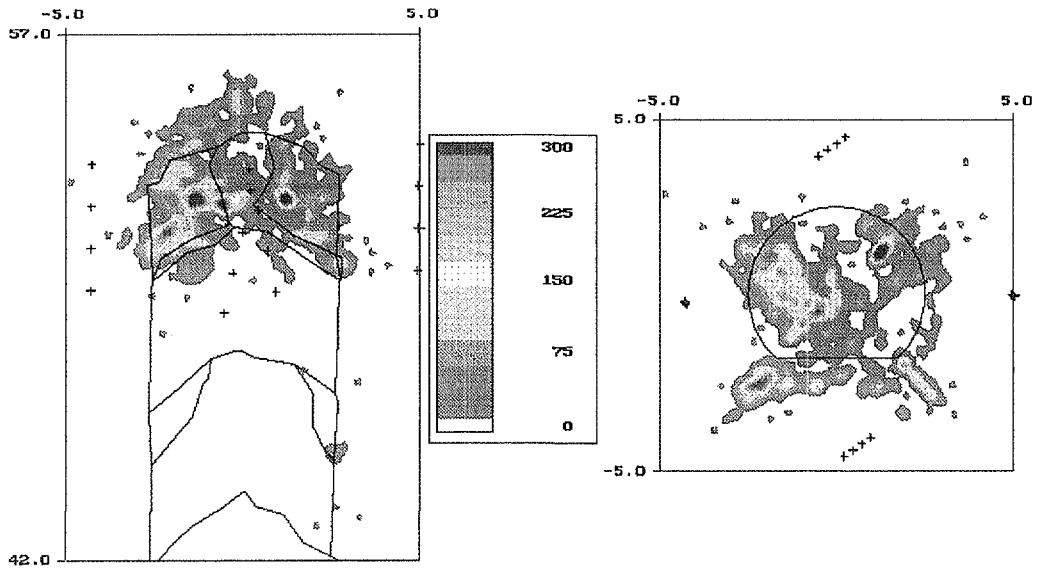

Figure 5-16. *Event density of AE data recorded after NS blast round R6 in the D&B drift.*

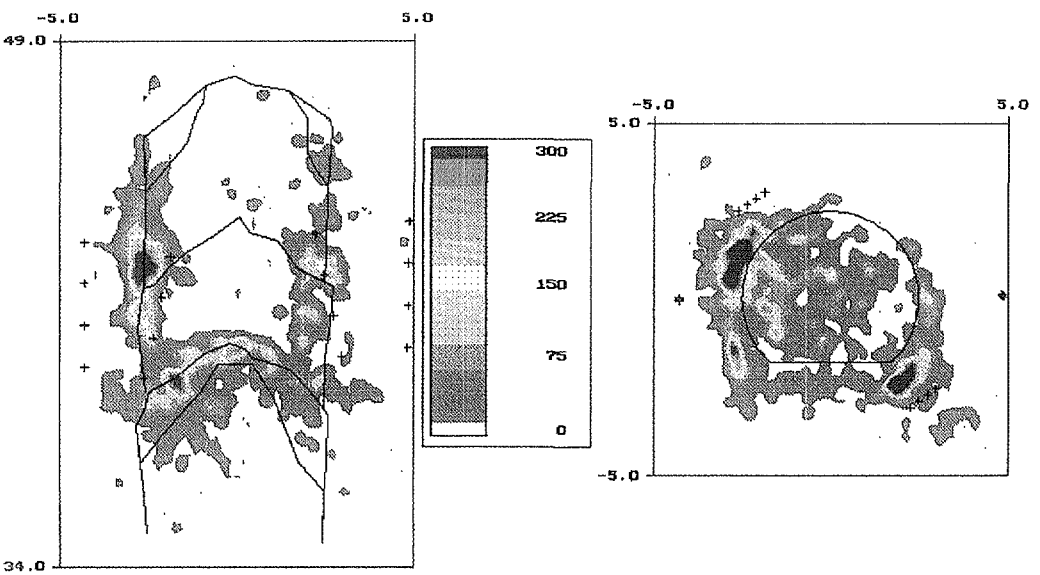

Figure 5-17. *Cumulative event density of AE data recorded after LSES blast rounds R2, R3 and R4 in the D&B drift.*

Some of the spatial patterns of recorded AE activity may reflect the effects of the sensor array geometry with respect to the drifts. Before the drift passed into the array, there was a clear path between any events at the drift face and all the sensors. Events behind the face, occurring in the drift walls, had ray paths to certain sensors that were blocked by the drift, this was also true for many events once the drift has passed through the array, particularly those at the face. For an event to be used in source location, criteria were set such that it must be detected on at least six sensors, which were in at least two boreholes.

Results from monitoring while the TBM drift face was at 9 metres from the starting point are shown in Figure 5-12. There were 232 events located from this interval, mostly within a thin skin, a few centimetres ahead of the face of the drift. The results from monitoring during intervals when the drift face was at 15 metres and 21.8 metres from its start point are shown in Figure 5-13, along with the events from the 9 metres stop. The events detected within the volume of interest during the intervals after the 15 metres and 21.8 metres stops had similar spatial distributions, but with subsequently fewer detected events as the drift face progressed further beyond the array. During the 15 metres stop, 115 events were located, with 78 events from the 21.8 metres stop. At this stage and in later monitoring periods, the drift blocked most of the direct raypaths between the face activity and the sensors, resulting in many fewer events being recorded from that region. Furthermore, the drift blocked many raypaths between events located close to the drift walls and sensors on the opposite side of the drift. As a result, there were arrival time picks on fewer channels so that the source locations are not as well constrained as during the previous monitoring intervals.

Events were generally less than one metre from the drift perimeter with the greatest concentration of events falling within a few centimetres of the drift perimeter and face (Figure 5-18). This thin skin of damage that occurred at the drift face and around the perimeter of the drift constituted one set of events. A second set seems to be characterised by more distal events, often occurring in clusters of activity up to several metres from the drift surface. While some of these events occur within the damaged zone, as defined here, the class of events and the conditions under which they occur extend into the disturbed zone and these will be discussed in more detail in Section 5.4.

The 425 events used to create Figure 5-13 represent only a small fraction of the AE activity that occurred. The acquisition system only recorded data if an amplitude threshold was surpassed on several channels simultaneously. There was much AE activity occurring, which triggered only two or three sensors and these were interpreted as being small events close to specific sensors. Many thousands of events were detected by the sensors in borehole C6, which passed below and were the closest of all the instrumented boreholes to the TBM drift. This suggests that there was considerable small scale micro-crack activity that occurred close to the drift wall. Such activity can only be studied in detail using a system dedicated to monitoring a smaller volume of rock than in this experiment.

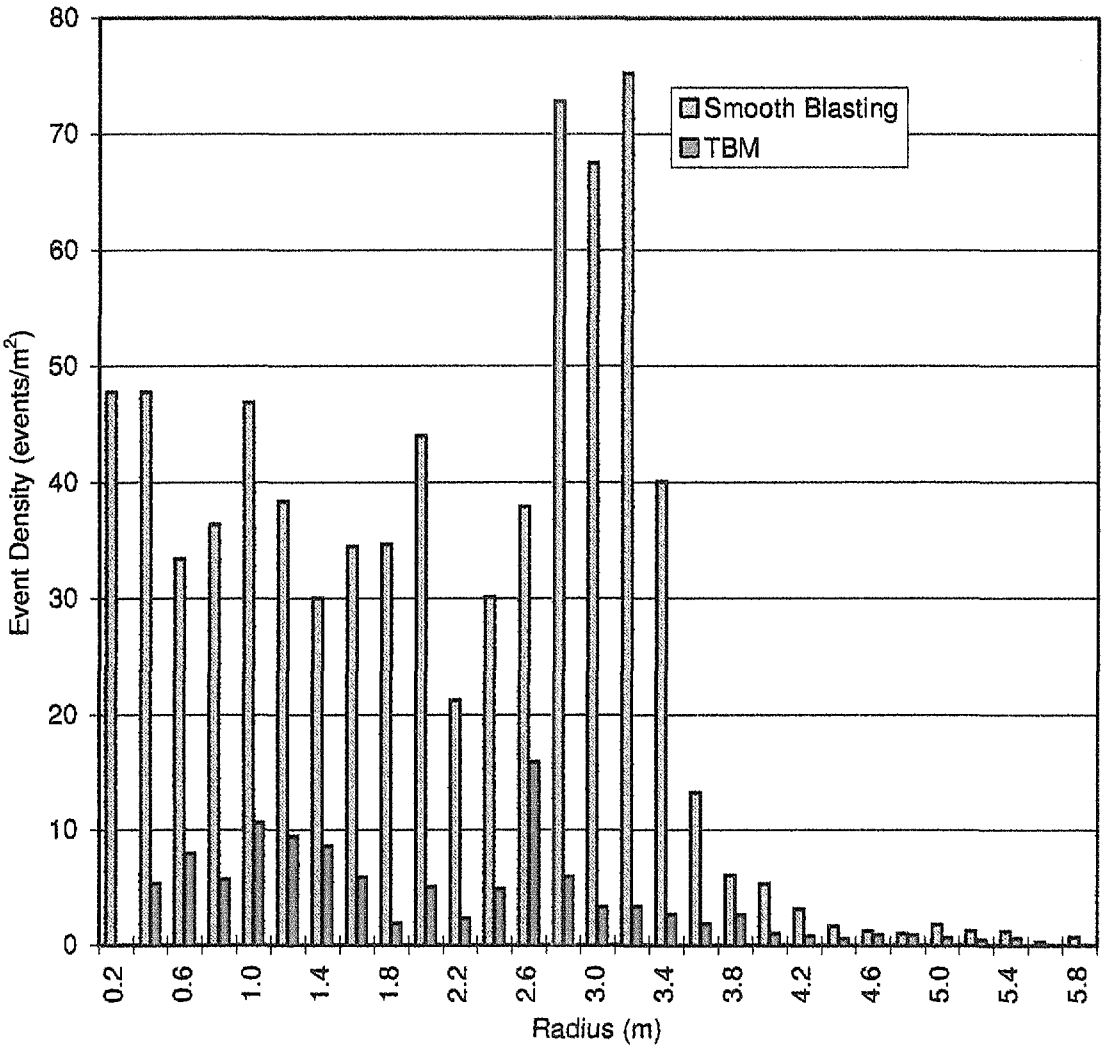

Figure 5-18. *Average AE event density as a function of radial distance from the centre of the drift for the TBM (9, 15 and 21.8 metres stops) and LSES (rounds R2, R3 and R4) monitoring.*

An inspection of the data recorded during the excavation of the D&B drift, shows that several blast rounds required re-blasting to remove rock that remained intact after the initial blast, this is shown in outline on the plan views of the AE event density plots. Figures 5-14 and 5-15 show AE events recorded from rounds R2 and R5 for the LSES and NS blast monitoring respectively, these positions represent a similar drift position to the 9 metres TBM stop relative to the sensor arrays. In both cases the events were concentrated ahead of the face, however, for round R2, which was unsuccessful in removing all the blasted material, the AE events were located in a wider band that included the rock at the face. This suggests that for unsuccessful blasts, most damage was confined to the blasted volume. This was particularly evident in NS round R6, in which most of the rock remained in place with AE spread throughout the blasted volume (Figure 5-16).

The AE distribution associated with rounds R2, R3 and R4 is shown in Figure 5-17. In the latter two rounds the recorded activity was concentrated about the perimeter of the drift distributed in a zone within about one metre of the drift wall (Figure 5-18). The activity associated with both rounds R3 and R4, showed a cluster of events at about 39 metres extending radially into the surrounding rock. This coincides with the position of a near vertical vein of fine grained granite cutting across the drift axis. The excavation of round R4 resulted in a small number of events near the walls of the drift around the volume excavated by round R3. However, the number of events recorded was too small to make a meaningful comparison between the location of AE activity occurring immediately after the blast with that which occurred a day later. Although there is some evidence, from laboratory velocity studies under load (Section 5.3.2), to suggest that thin veins of granite showed more crack damage than the surrounding, less brittle diorite. Thus, it would appear that damage may to some extent be controlled by lithology.

To determine whether the EDZ progressively extended further into the drift wall with time the combined activity from rounds R3 and R4 were examined in order to obtain a large data set (1303 located events). The activity from each round was divided such that there was a set of events that occurred early in the monitoring period and a set from the later part of the monitoring period, corresponding roughly to the first three hours of each monitoring period and the remaining five hours. Histograms of event density versus radius were created for the early and late period (Figure 5-19). This suggests that there was no significant progressive migration of AE activity into the rock over the first few hours following a blast.

The stress conditions around the drifts were considered in an attempt to understand the damage process. In unconfined compression tests, the crack initiation stress is defined by the onset of stable crack growth which generally occurs at 0.3-0.6 σ_c, where σ_c is the unconfined compressive strength (Brace and Byerlee, 1968). Martin *et al.* (1995) used numerical modelling to estimate the stresses acting at microseismic event locations around the URL Mine-by tunnel. They defined the *in situ* crack initiation stress as the differential stress (σ_1 - σ_3) the rock was under at the event locations, assuming that the microseismicity represented the initiation of the failure process. For the microseismic events in the regions experiencing breakout around the Mine-by tunnel, they found that cracking occurred at $\sigma_1 - \sigma_3 \approx 70$ MPa. This is about 0.3 σ_c, which is slightly lower than the laboratory value of 0.4 σ_c (Martin *et al.*, 1995).

The stress at AE event locations around the ZEDEX drifts was estimated using the EXAMINE^{3D} numerical stress modelling programme (Figure 5-20). The average *in situ* crack initiation stress was $\sigma_1 - \sigma_3 \approx 25$ MPa. This is about 0.12 σ_c, which is well below the typical range of crack initiation stresses. Similar values were estimated for the events around both the TBM and D&B drifts. A Hoek-Brown failure envelope is also shown in Figure 5-20 for reference. This may be seen as evidence that initiation of new cracks due to increased differential stress was not a major cause of AE

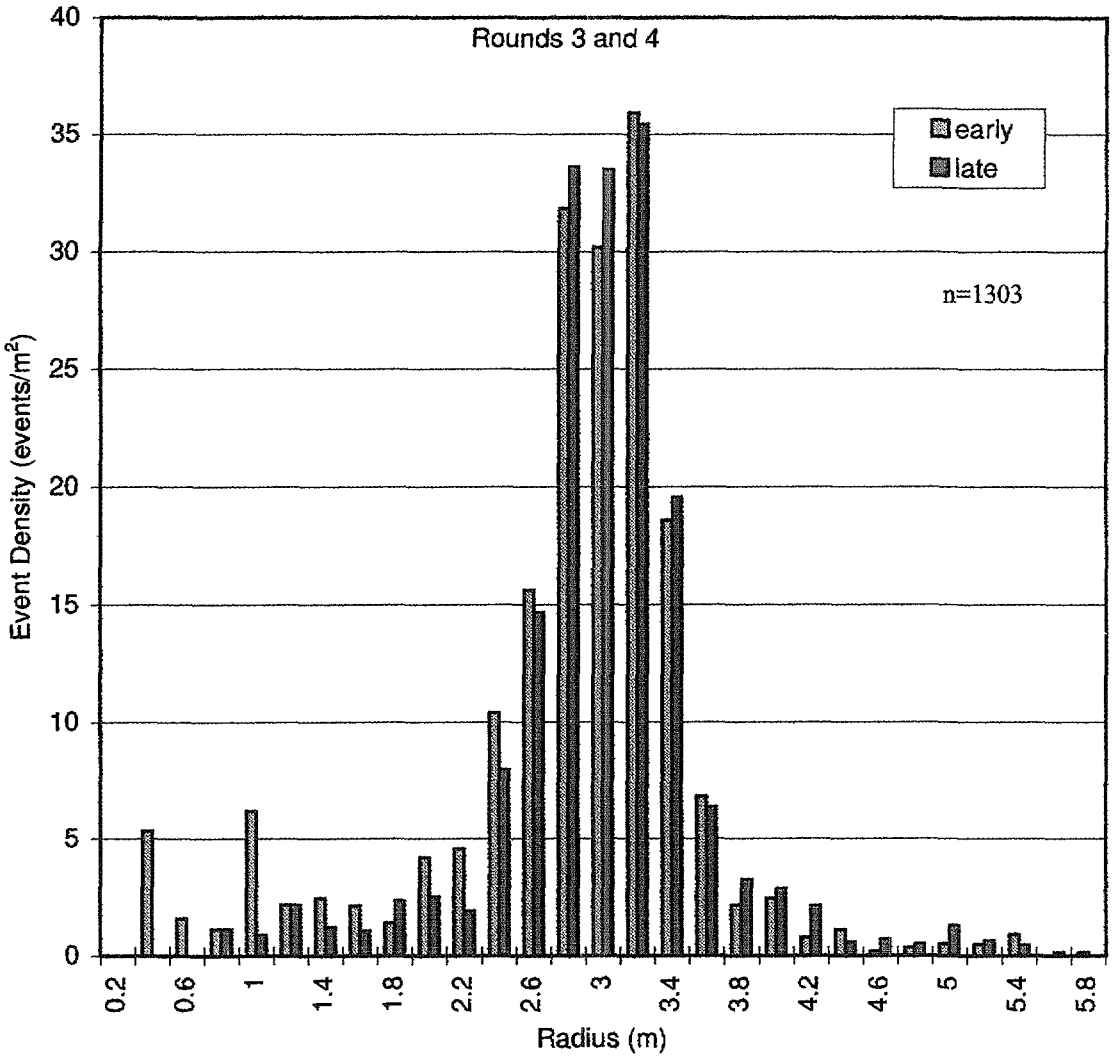

Figure 5-19. *AE Event density versus radius for rounds R3 and R4. The distribution of events recorded in the first 3 hours after the blasts are compared to the distribution of events recorded in the following hours.*

damage. Many of the events fall within the zone of critically reduced confining stress ($\sigma_3/\sigma_1 < 0.1$) shown in Figures 5-4, indicating that stressrelief may be playing a role in damage. The much greater event density for the D&B excavation compared to the TBM excavation and the interpreted wider damaged zone, indicated that the blasting may have directly damaged the rock to a greater extent than TBM excavation reducing the strength of the rock. This would have facilitated further micro-cracking and AE activity. This is not unexpected given the higher power input to the rock mass by the D&B methods.

Source mechanism analysis of AE events showed that the great majority of events could be fit to shear-slip mechanisms. Other mechanisms considered were explosive (crack-opening) events and implosive (crack-closure) events. The data quality and small number of events for the TBM drift prohibited a statistically meaningful sub-division of the proportions of different source mechanisms.

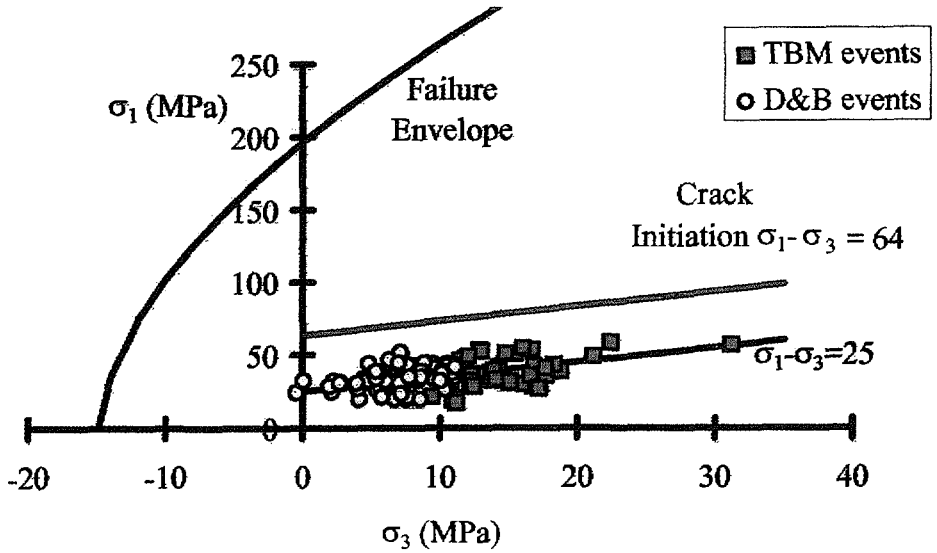

Figure 5-20. *Differential stress at AE source locations in the TBM and D&B drifts. A Hoek-Brown failure envelope for Äspö diorite is shown for reference as is the unconfined laboratory crack initiation stress ($\sigma_{ci} = \sigma_1 - \sigma_3 = 64$ MPa).*

A total of nearly 1200 events, from around the D&B drift, having 6 or more P-wave first motion polarities, were examined. Of these, the sub-division of the failure mechanisms was 89% shear-slip, 9% implosive and 2% explosive. However, many events which included volumetric change at the source (implosive or explosive) may have been complex events incorporating a component of shear slip and may have been characterised as shear events. The relatively high proportion of implosive or crack closure events in comparison to the URL or laboratory tests (Carlson and Young, 1993 and Falls, 1993) in comparison to explosive events was somewhat unexpected. Figure 5-21 shows the proportions of event types from different times during the monitoring of certain blast rounds. The partially failed rounds R2 and R6 had the highest proportion of implosive events, particularly immediately after the blasts. Much of the activity from these rounds occurred in the blasted but intact volume, which may have had cracks initially opened by the blast gases. The implosive events may represent the closure of such cracks.

5.3.2 Seismic Measurements

Several seismic techniques were used to evaluate the dynamic rock properties in the damaged zone of the ZEDEX drifts. The objective of the seismic surveys was to assess the amount of micro-crack damage caused by the excavation of the TBM and D&B drifts. Generally seismic energy travels more slowly in damaged rock than in undamaged rock (Boadu & Long, 1996). Further, seismic velocities will also tend to be higher in rock under compression, where the pre-existing fractures or micro-cracks have been closed under load (Young

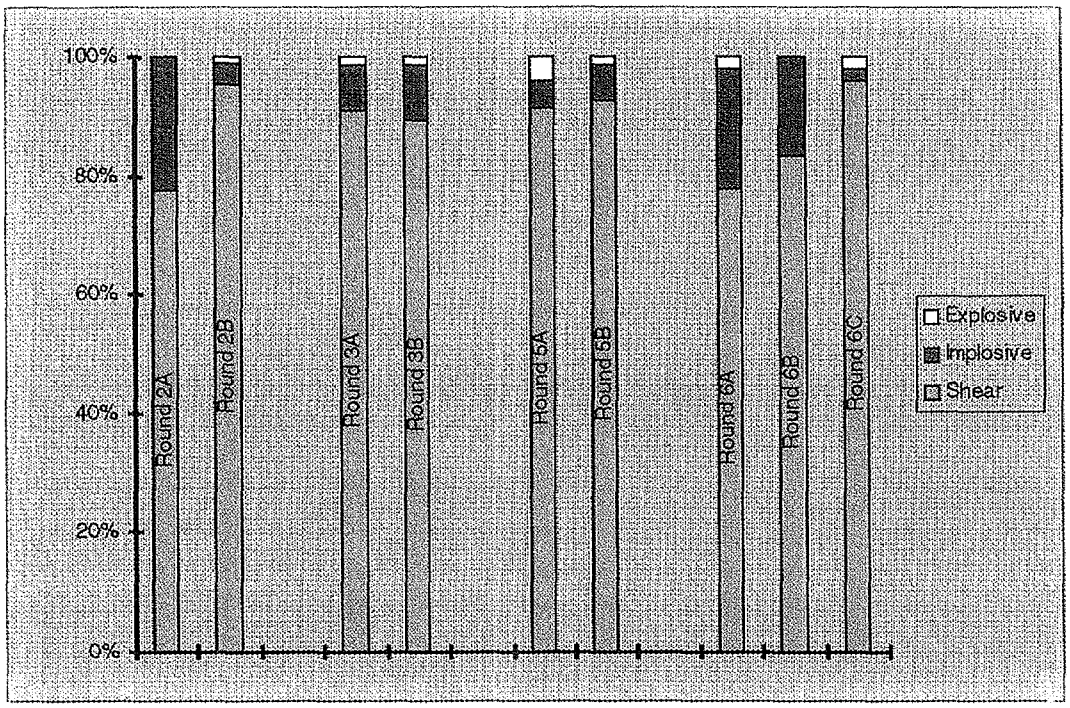

Figure 5-21. *Relative abundance of AE event source types within data sets that were temporally sub-divided.*

and Maxwell, 1992). Additionally the saturation of the rock may influence seismic velocities, especially the compressional wave velocities whereas shear wave velocities are less affected (Hudson, 1981).

The measurements were performed to assess the changes in velocity with increasing depth/distance from the drift walls. It was anticipated that within the damaged zone, close to the drift walls, the velocities would be lower and would increase and approach the seismic velocity of the undisturbed rockmass away from the drift.

Some of the methods used measured the one dimensional radial velocity distribution along boreholes (downhole and interval measurements), measurements from the drift walls (seismic refraction measurements) or using core samples (laboratory measurements). The seismic refraction measurements were undertaken, along the walls of the drifts, to test whether this method could be used to assess excavation damage without the requirement for boreholes. Other techniques which were used, measured the velocity distribution between boreholes to obtain the two or three dimensional velocity distribution. Such methods included seismic velocity anisotropy measurements, seismic tomographic surveys and the ultrasonic measurements performed using the Acoustic Emission monitoring system.

Radial Seismic Measurements - TBM and D&B Drifts

The one dimensional radial velocity distribution was determined using downhole and interval measurements performed in boreholes. The results and interpretation derived from these acquisition programmes is presented below.

Downhole Seismic Measurements

The downhole measurements were performed during both phases of acquisition; the first used a pendulum hammer and during the second a piezo-electric actuator was used as the seismic source. In both cases the source was placed on the drift wall close to the borehole collar in combination with piezo-electric accelerometers (mini-sonic probe) as downhole receivers. From the average velocities measured between source and receiver the local velocities at depth within the borehole was calculated.

Interval Velocity Measurements

Measurements of the interval velocities were performed along single boreholes. The seismic velocities are measured along a short borehole interval, typically about 10 centimetres long. The technique requires a borehole probe with a source and one or two receivers. The measurements started at the drift surface and the probe was moved progressively down the borehole. This method produces seismic velocities as a function of distance from the drift surface.

Two different types of equipment were used; the micro-velocity logging system (high frequency) and the mini-sonic probe (low frequency). The tools differ in frequency range, source characteristics and coupling against the borehole wall. From the micro-velocity logging system (high frequency) P- and S-wave velocities were derived with the interpretation mainly concentrated on P-wave velocities. With the mini-sonic probe (low frequency) only S-wave velocities were evaluated.

TBM drift

Downhole P-wave velocities were measured in two of the short radial boreholes of section 1 (boreholes RT1H, RT1I) and seven of the short radial holes of section 2. Water flow prevented measurements in the vertical holes. The results for section 2 for depths up to 1 metre are presented in Figure 5-22 as an example. At depths greater than 1 metre the velocity variation appears to be low. The average velocity of 5900 ms^{-1} calculated for depths greater than 1 metre is considered to represent the compressional wave velocity of intact rock.

Calculated velocities were considerably lower than the average background velocity. Close to the drift wall the velocities were as low as 2070 ms^{-1}. In Figure 5-22 the $V_P = 5600$ ms^{-1} isoline is hatched and compressional wave velocities lower than $V_P = 5600$ ms^{-1} are considered to represent significant deviations from the velocity of the intact rock. The results suggested that the

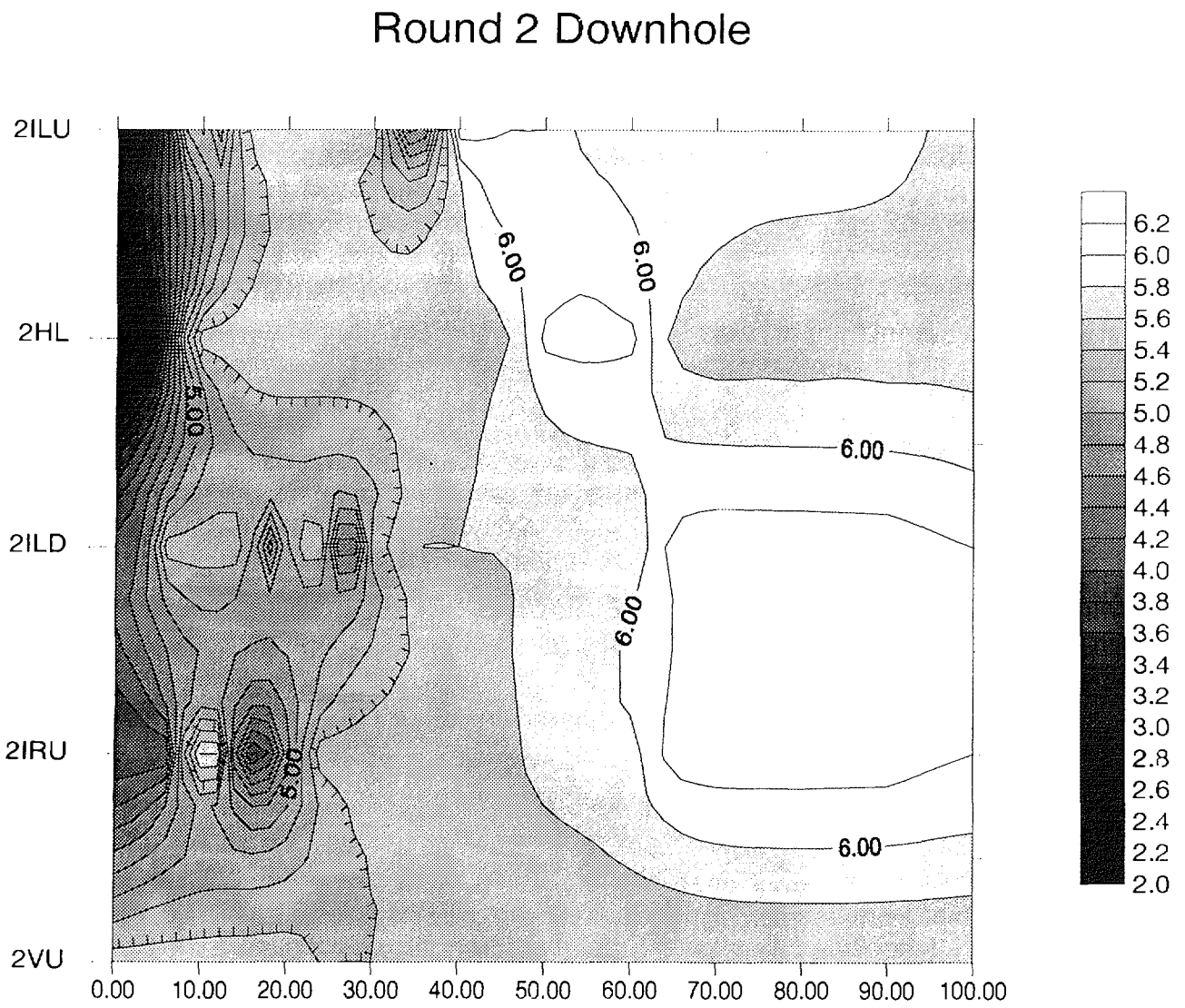

Figure 5-22. *Summary of compressional wave velocities from downhole seismic measurements up to depths of 100 centimetres in section 2 (TBM). The location of the boreholes is given in Figure 3-5.*

velocities were significantly lower within the first 10 - 30 centimetres of each borehole. However, the inclined boreholes showed a more pronounced low velocity zone than the horizontal boreholes and the vertical up hole showed virtually no reduction in velocity. In summary the P-wave low velocity zone is small surrounding section 2 in the TBM drift.

Micro-velocity logging (high frequency) was performed in several of the boreholes that were also used for anisotropy studies (Figure 3-5). All four of the vertical up holes, two of the inclined right up and two of the horizontal right holes in section 2 were logged with the micro-velocity logging tool. The results from the micro-velocity logging (high frequency) are shown in Figure 5-23 where the velocity trends from parallel boreholes are superimposed. It may be seen that the increase in velocity from the drift wall to the average velocity is not smooth and local heterogeneities in the rockmass may account for some of the changes in the shape of the graphs. Generally the fine grained granite has a higher velocity (about 200 ms^{-1}) than the diorite and the greenstone has a slightly lower velocity than the diorite. The abrupt low velocity excursions can sometimes be correlated with veins. The shear wave logs, which are not shown here, follow the same trends as the corresponding compressional wave logs.

The curves from the vertical and inclined holes from the TBM drift are almost flat and indicate that there is no or very little damage in these areas of the drift. The graphs of velocity derived for the horizontal holes could suggest that the drift wall is damaged at this point. However, there are a number of veins in the holes near the borehole collar.

Interval velocity measurements with the mini-sonic probe were performed in six of the short radial holes of section 2. Water flow in the vertical down and inclined right down holes prevented measurements in these boreholes. The results of the mini-sonic (low frequency) measurements of section 2 (TBM) are presented in Figure 5-24. The figure gives an expanded view of the first 100 centimetres and in addition the V_S = 2900 ms^{-1} isoline is hatched. Shear wave velocities lower than 2900 ms^{-1} are considered to represent significant deviations from the mean shear wave velocity of 3060 ms^{-1}, measured at greater depths, that may be considered to represent the intact rock. Three of the 6 measured holes (Figure 5-3) exhibit no low velocity zone (RT2ILD, RT2HL and RT2VU), two holes (RT2HR and RT2IRU) showed low velocity zones extending less than 5 centimetres from the drift wall. Only borehole RT2ILU shows a zone of velocity reduction, extending up to 10 centimetres from the drift wall.

The results suggest that velocity reductions were generally below 8%, extending only a short distance from the drift wall. Both methods showed no low velocity zone in the vertical up holes and a more pronounced reduction in the inclined and horizontal right holes. The mini-sonic probe (low frequency) shows reduced velocities only within the first 5 to 10 centimetres of the start of each borehole whereas the micro-velocity logging (high frequency) indicates a reduced velocity of up to 1 metre in the horizontal holes. Generally the low velocity zone is extremely small or even not present in section 2 around the TBM.

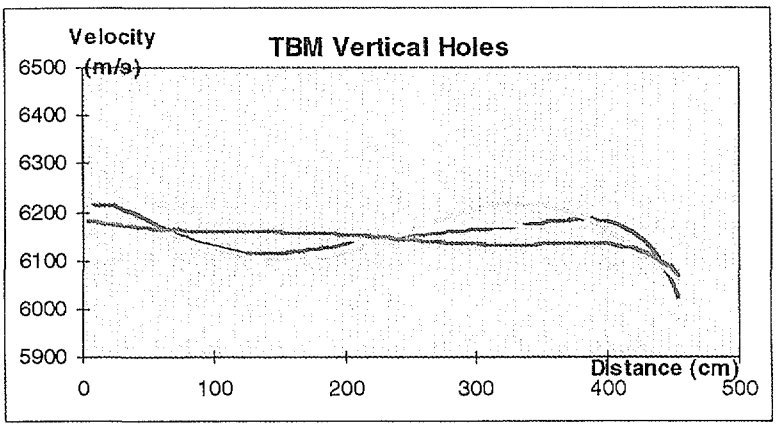

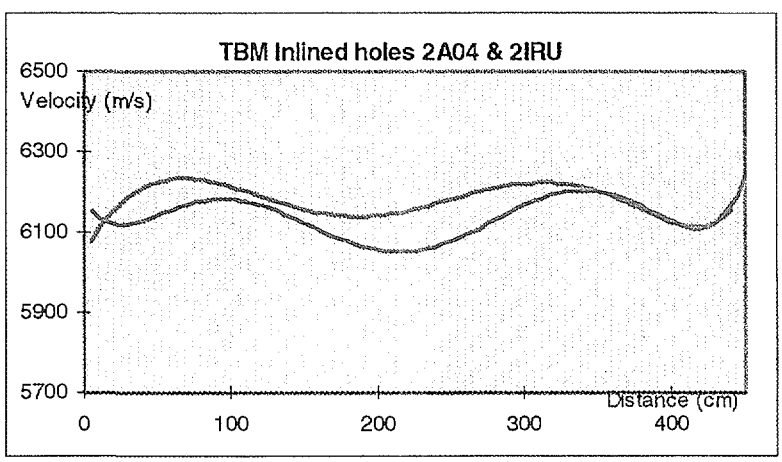

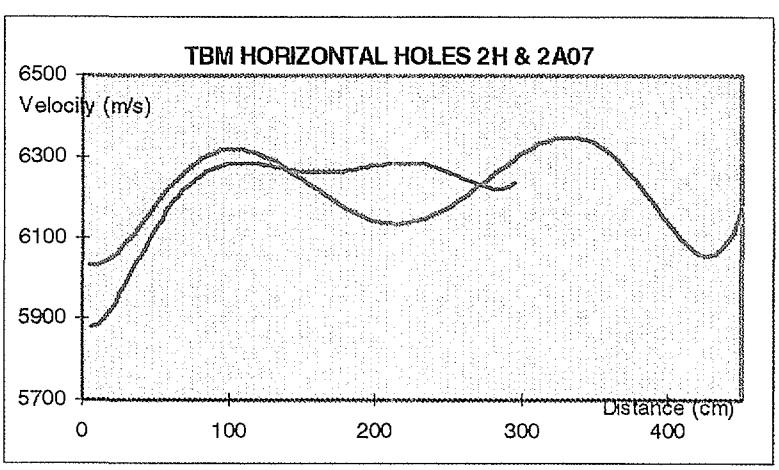

Figure 5-23. *The trends from compressional wave velocity logs from all holes surveyed in the TBM section 2 with the micro-velocity probe. The location of the boreholes is given in Figure 3-5.*

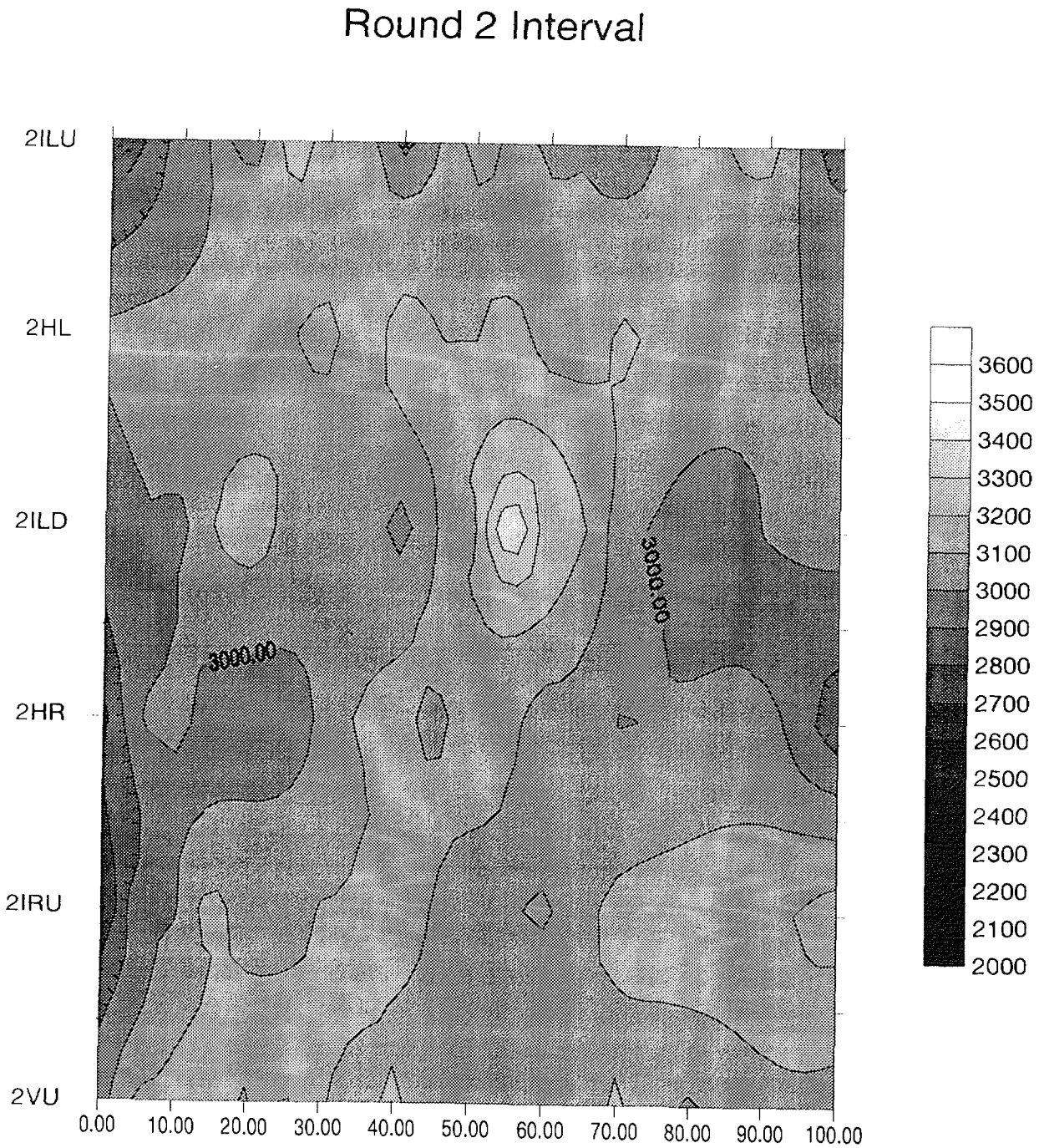

Figure 5-24. *Summary of shear wave velocities from interval measurements with the mini-sonic probe up to depths of 100 centimetres in section 2 (TBM). The location of the boreholes is given in Figure 3-5.*

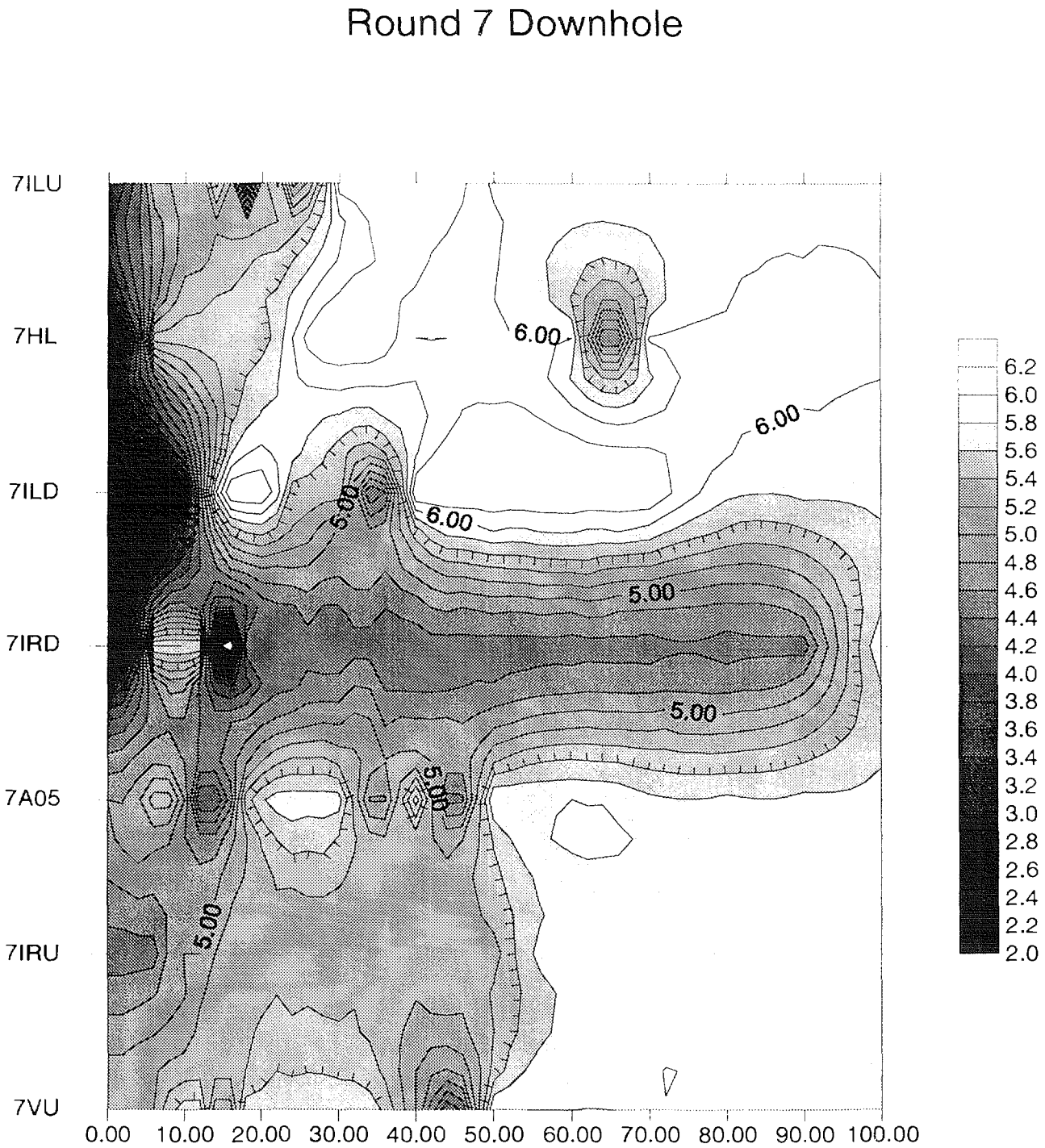

Figure 5-25. *Summary of compressional wave velocities from downhole seismic measurements up to depths of 100 centimetres in round R7 (D&B). The location of the boreholes is given in Figure 3-5.*

The low P-wave velocities (2070 ms^{-1}) obtained with downhole seismic measurements are unrealistically low for granitic rock. The lowest values are even below the S-wave velocities measured with both interval velocity tools and this is physically impossible. Hence, the results from the downhole measurements are not considered reliable.

D&B drift

Downhole seismic measurements were performed in all 17 short radial boreholes drilled during the first experimental phase (Olsson *et al.*, 1996b). In the second series of measurements, eight boreholes from round R4 and seven boreholes from round R7 were logged (Figure 3-5). The results from round R7, to a depth of 100 centimetre, are presented in Figure 5-25 as an example.

The P-wave velocity of the undisturbed rock was modelled to have a value of about 5900 ms^{-1}. In Figure 5-25 the 5600 ms^{-1} isoline has been hatched and compressional velocities lower than 5600 ms^{-1} are considered to represent significant deviations from the velocity of the intact rock. In round R7 two boreholes had low velocity zones of up to 25 centimetres (RD7HL and RD7ILD) and 3 boreholes indicated a low velocity zone of up to 50 centimetres (RD7ILU, RD7A05 and RD7VU). The boreholes RD7IRD and RD7IRU show low velocity zones of more than 50 centimetres. The low velocity zone of borehole RD7IRD is characterised by single fractures close to the surface.

From all the measurements performed in the D&B drift the greatest spatial extent of reduced seismic velocity is observed in the vertical down boreholes with zones of reduced velocity extending to distances of approximately 1 metre for borehole RD3V and RD7IRD. For the horizontal and inclined boreholes, the velocity reduction is considered to have an extent, in general, of less than 50 centimetres. The low velocity zone was more pronounced on the left hand side (when looking to the end of the drift) of the D&B drift in round R4 (RD4HL, RD4ILD and RD4VD) and on the right hand side in round R7 (RD7IRD, RD7A05, RD7IRU, RD7VU).

The extent of the low velocity zones as determined from downhole measurements during the second measurement phase are summarised in Table 5-4. The depth values are the depths at which the compressional wave velocities first reach 5600 ms^{-1}.

Interval velocity measurements were performed in all eight radial boreholes of round R4 and in seven radial boreholes of round R7. Micro-velocity logging (high frequency) was performed in several of the boreholes used for anisotropy studies. All four of the vertical up holes, two of the horizontal right and one vertical down borehole in round R7 (Figure 3-5) were logged with the micro-velocity logging (high frequency) probe. The results from the micro-velocity logging (high frequency) are shown in Figure 5-26 where the velocity trends from parallel boreholes are superimposed. The general characteristics are similar to those discussed for the TBM drift. In the

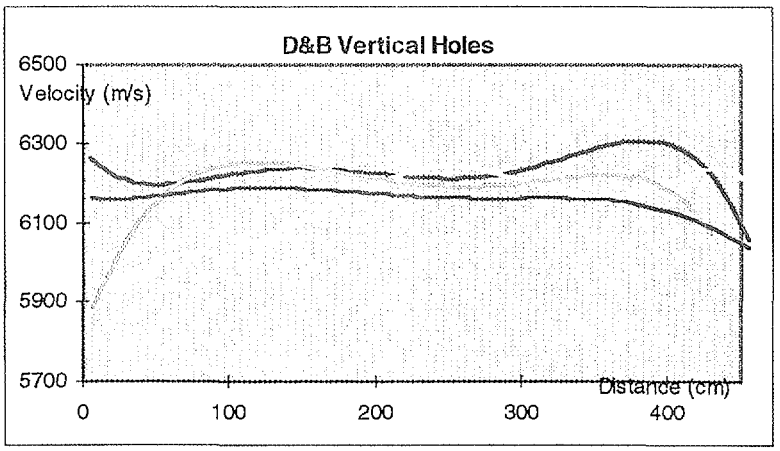

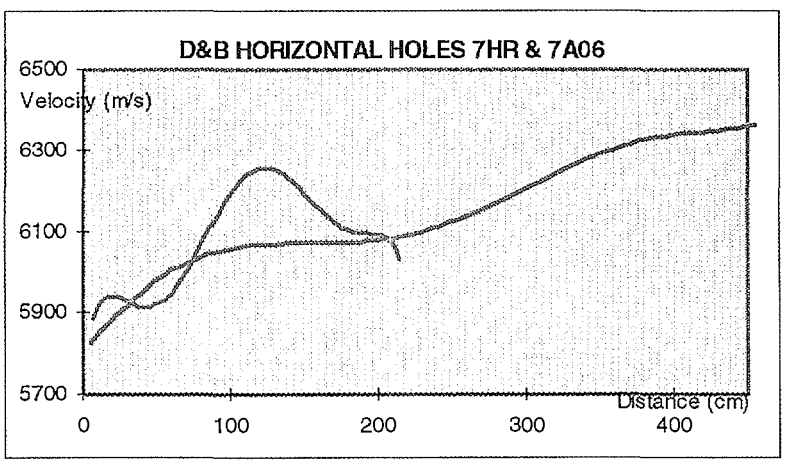

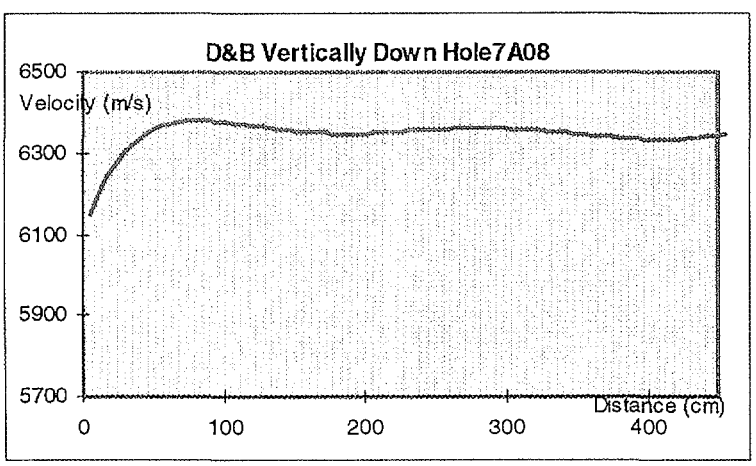

Figure 5-26. *The trends from compressional wave velocity logs from all holes surveyed in round R7 of the D&B drift with micro-velocity (high frequency) probe. The location of the boreholes is given in Figure 3-5.*

D&B drift the most obvious damage was seen in the floor of the drift, where the borehole walls were too cracked to allow the probe to be inserted. The rise to the average velocity in the borehole where measurements were obtained indicated this to be within only about 30 centimetres. The four boreholes directed vertically upward showed inconsistent trends. Two of the boreholes indicated damage whilst the other two showed no indications of damage. This could be explained by the random nature of the blasting process in that the damage seen is blast induced.

The results of mini-sonic logging (low frequency) measurements performed in round R7 are presented in Figure 5-27 as an example. The figure gives an expanded view of the first 100 centimetres, the 2900 ms^{-1} shear wave velocity isoline is hatched as in Figure 5-24. In round R7 two boreholes showed no low velocity zone (RD7VU and RD7IRU) and 4 boreholes showed a low velocity zone of less than 5 centimetres (RD7ILU, RD7HL, RD7ILD and RD7A05). Boreholes RD7IRD and RD7HR showed low velocity zones of 25 and 30 centimetres respectively. These low velocity zones were characterised by single fractures close to the surface.

The micro-velocity (high frequency) log showed reductions of up to 5%, whilst the mini-sonic (low frequency) measurements indicated reductions in velocity of up to 10%, with both methods showing similar general velocity trends. The results of all measurements performed in the second experimental phase are summarised in Table 5-4. The depth values given from mini-sonic (low frequency) measurements are the depths at which the shear wave velocities first reached 2900 ms^{-1}.

Table 5-4. Extent of low velocity zone as derived from downhole measurements; interval seismic measurements with mini-sonic probe (low frequency) and micro-velocity probe (high frequency).

Round	Borehole	Low Velocity zone from Downhole measurements (centimetres)	Low Velocity Zone from mini-sonic probe (low frequency) (centimetres)	Velocity trend from micro-velocity log (high frequency)
Round 4 (D&B)	RD4ILU	50	< 5	-
	RD4HL	> 50	5 - 10	-
	RD4ILD	90 - 100	< 5	-
	RD 4VD	> 50	5 - 10	-
	RD 4IRD	30	10 - 15	-
	RD 4HR	20 - 25	5 - 10	-
	RD 4IRU	40	< 5	-
	RD 4VU	25 - 30	0	-
Round 7 (D&B)	RD 7ILU	25 - 30	< 5	-
	RD 7HL	20 - 25	< 5	-
	RD 7ILD	15 (40)	< 5	-

Round	Borehole	Low Velocity zone from Downhole measurements (centimetres)	Low Velocity Zone from mini-sonic probe (low frequency) (centimetres)	Velocity trend from micro-velocity log (high frequency)
	RD 7A08	-	-	velocity rises 300 ms^{-1} for the first 0.3 m
	RD 7IRD	90 - 100	25	-
	RD 7A05	20 - 50	< 5	-
	RD 7A06	-	-	velocity rises 400 ms^{-1} for the first 1 m, then decreases again
Round 7 (D&B)	RD 7HR	-	30 /single cracks	velocity rises 600 ms^{-1} for the first 4.5 m
	RD 7IRU	50 - 55	0	
	RD 7A01	-	-	almost flat
	RD 7A02	-	-	velocity rises 300 ms^{-1} for the first 2.5 m
	RD 7A03	-	-	velocity rises 300 ms^{-1} for the first 1 m
	RD 7VU	10 - 50	0	almost flat
TBM	RT2ILU	15	5 - 10	
	RT 2HL	10	0	
	RT 2ILD	35	0	
	RT 2A07	-	-	velocity rises 250 ms^{-1} for the first 1 m
	RT 2HR	-	< 5	velocity rises 400 ms^{-1} for the first 1 m
	RT 2A04	-	-	almost flat
	RT 2IRU	20 - 25	< 5	almost flat
	RT 2A01	-	-	almost flat
	RT 2A02	-	-	almost flat
	RT 2A03	-	-	almost flat
	RT 2VU	-	0	almost flat

From Table 5-4 it can be seen that the methods used produce different estimates for the extent of the damaged zone. The downhole method produces low velocity zones of significantly larger extent and magnitude than the interval velocity methods. The downhole method measures velocity over an increasing distance between source and receiver producing average velocities from which local velocities are calculated. These measurements are therefore of lower resolution and sensitivity than the

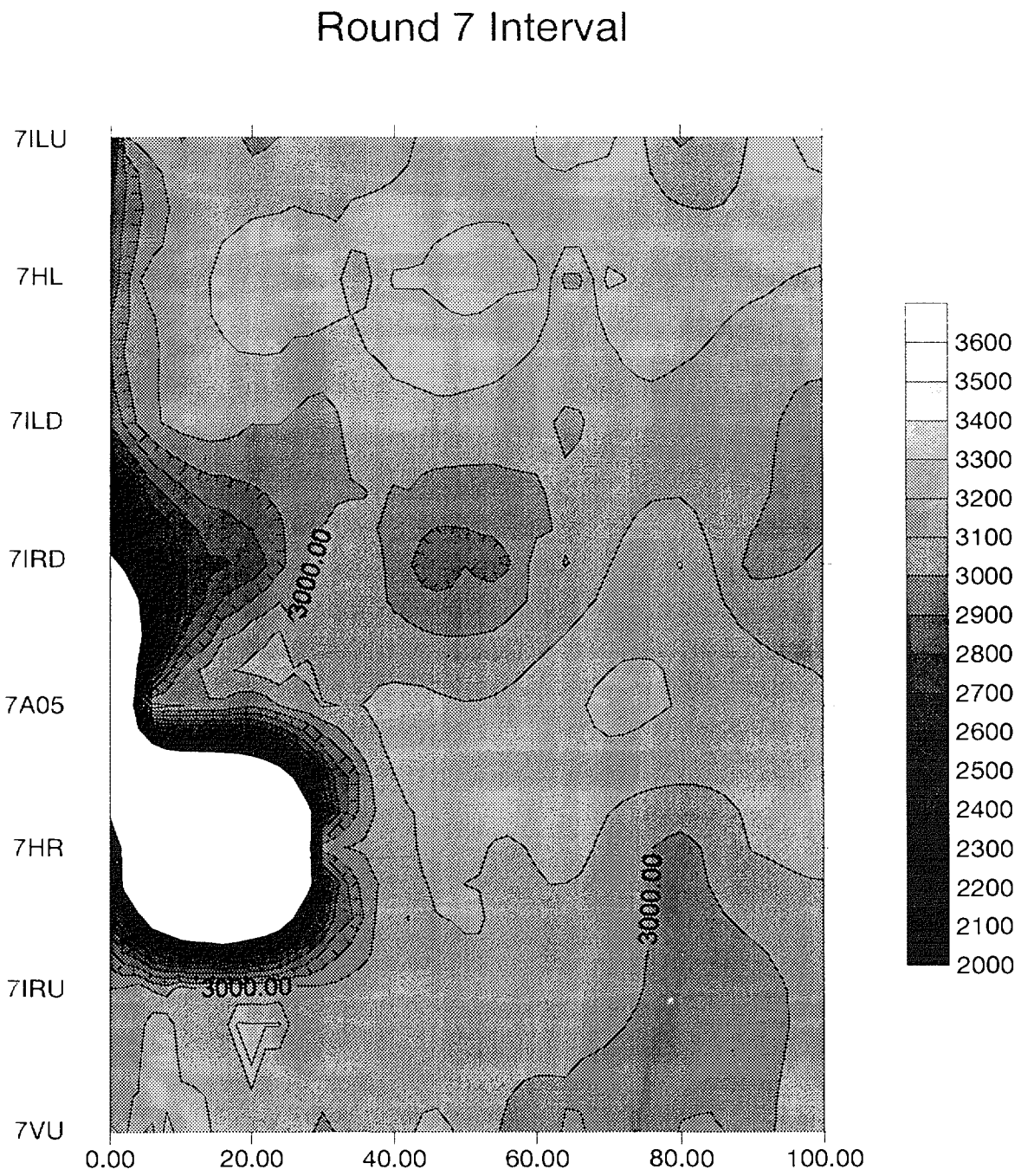

Figure 5-27. *Summary of shear wave velocities from interval measurements with the mini-sonic (low frequency) probe up to depths of 100 centimetres in round R7. The location of the boreholes is given in Figure 3-5.*

interval velocity methods. The extremely low velocities obtained with the downhole method close to the drift wall in some cases could be due to sensor location or timing errors. These types of errors are most significant for the shorter measuring distances, i.e. close to the drift wall. Hence, most confidence should be given to the results obtained from the interval velocity measurements.

Refraction Seismic Measurements - TBM and D&B Drifts

Refraction seismic measurements were performed on one profile in the D&B drift and paralleled the drift axis. The profile was close to borehole RD7A05 drilled in round R7 and had a profile length of 264 centimetres. A second profile was surveyed in the TBM drift and paralleled the drift axis. This profile was close to borehole RT2HL in section 2 and had a length of 300 centimetres.

Both profiles detected a small low velocity zone. The maximum velocities of 5800 ms^{-1} (TBM section 2) and 6000 ms^{-1} (round R7) were reached at depths of 10 and 15 centimetres respectively. At greater depth the measured velocity distribution is flat.

Borehole Resonance Measurements - TBM and D&B Drifts

Borehole resonance measurements were performed using a borehole probe with a piezo-electric actuator and a combination of acceleration and force transducers. Changes in the resonant frequency and amplitude were interpreted to infer rock damage. Borehole resonance measurements were performed in some boreholes in which downhole seismic measurements had also been performed. The method turned out not to be sensitive enough to determine the extent of the excavation damaged zone and therefore the results have not been presented here.

Laboratory Measurements

Various laboratory measurements were performed on oriented core samples from the short radial holes and on 5 samples taken from the drift face. The laboratory measurements discussed here are related to P- and S-wave velocities.

Ultrasonic wave velocities

Ultrasonic wave velocity measurements were performed on dry and saturated core samples. It is assumed that values greater than 1 indicate micro-cracking or stress relaxation. The ratio V_{Psat}/V_{Pdry} is very close to 1 for the horizontal borehole RD3H indicating a low level of cracking (Figure 5-28). In boreholes RD2I, RD6I and RD7I, the ratio decreases significantly from 1.2 to 1 with distance from the wall. It is considered therefore that micro-cracking exists due to damage or stress relaxation near the wall. The ratio of the velocities derived for RD7V is nearly constant and equal to 1.05 and this was unexpected.

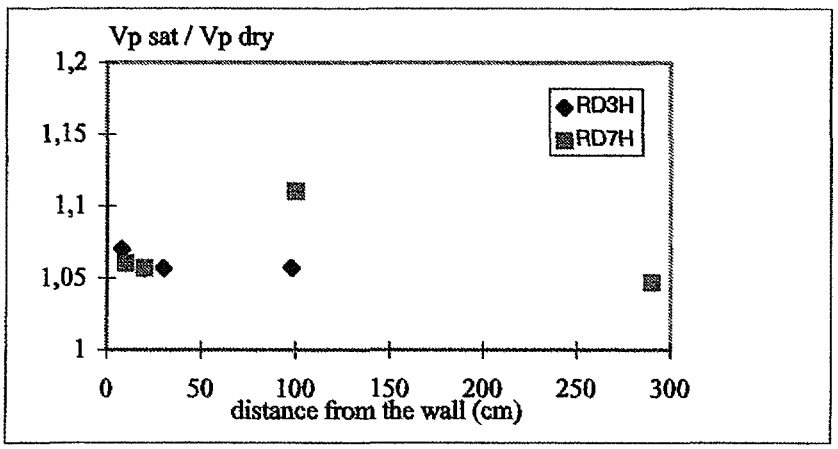

a)

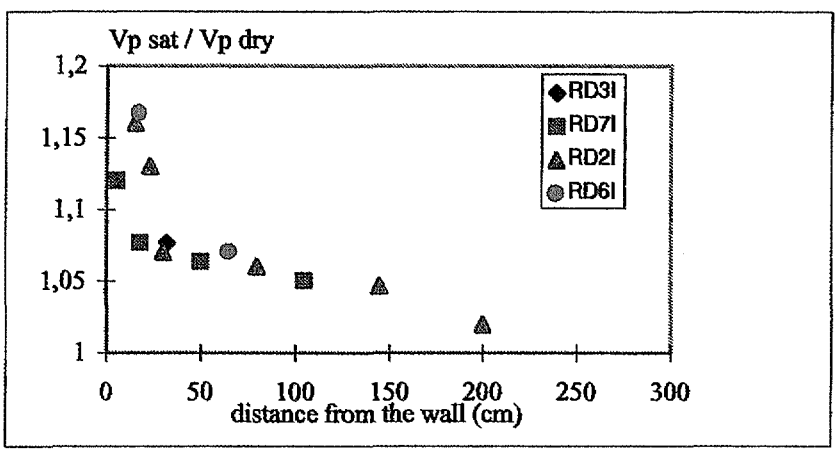

b)

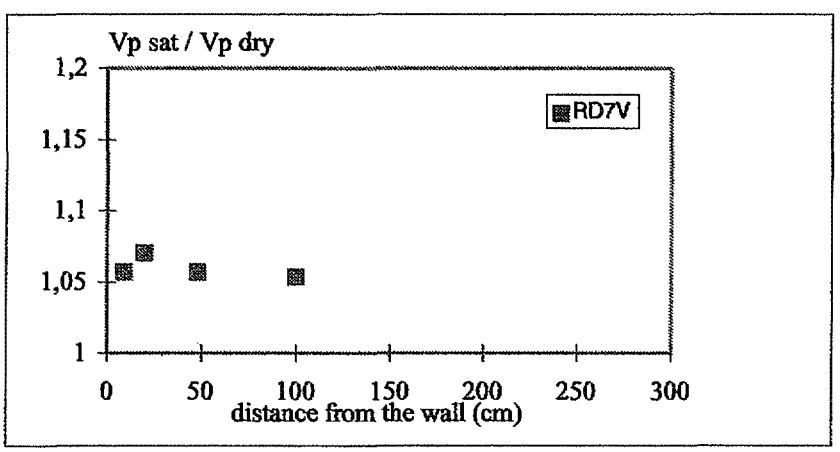

c)

Figure 5-28. *Variation of the $V_{P\ sat}/V_{P\ dry}$ ratio versus distances from the wall a) horizontal boreholes, b) inclined boreholes, c) vertical boreholes.*

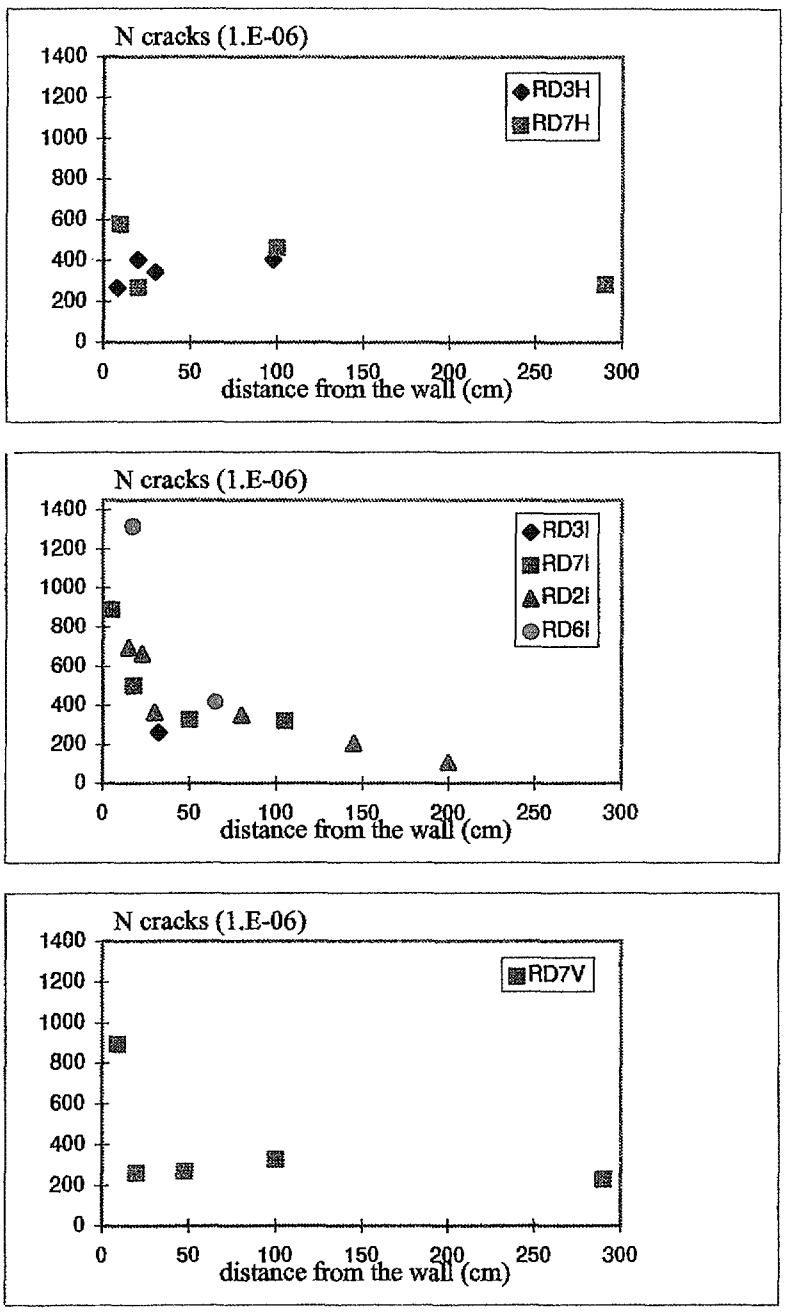

Figure 5-29. *Crack porosity derived from isotropic compression tests versus distance from the wall of the D&B drift a) horizontal boreholes, b) inclined boreholes, c) vertical boreholes.*

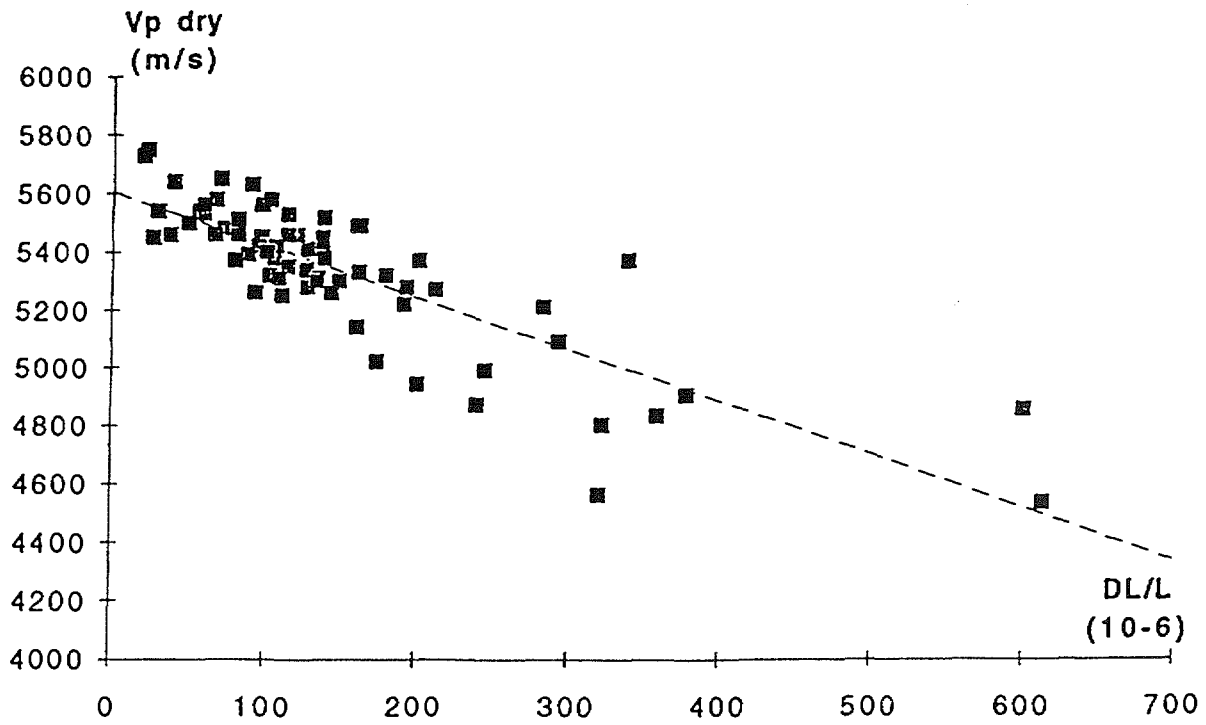

Figure 5-30. *Variation of V_P versus axial strain DL/L ($\Delta L/L$) including microcracking in the Äspö diorite.*

Velocity Variations During Isotropic Compression Tests

Crack porosity and P-wave velocities were determined during isotropic compression tests (Bauer *et al.*, 1996b). These showed that crack porosity generally decreases as a function of the distance from the wall (Figure 5-29).

The P-wave velocity was shown to be well correlated with axial strain which includes micro-crack deformation in the Äspö diorite for cores from around the drifts (Figure 5-30). Re-calculation of the principal deformation axis orientation did not indicate a preferential deformation direction, which suggests that a crack orientation cannot be defined.

Velocity Measurements in Core Samples Under Load

Twenty one samples were taken from cores from two boreholes RD7A02 and RT2A03. These boreholes were orientated vertically upward from round R7 in D&B drift and round R2 in the TBM drift respectively. The cores were sampled to reflect the lithologies and the changes with distance from the drift walls. The samples were uniaxially loaded up to 60 MPa and velocity measurements were taken along the axes of the samples at 10 MPa increments.

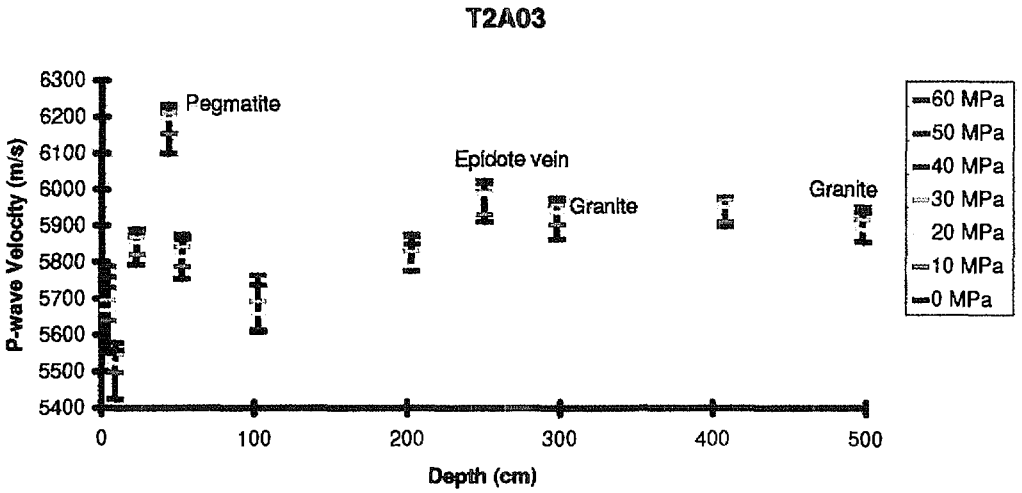

Figure 5-31. *Velocity variation with the application of uniaxial load for samples from different depths from core RT2A03 in the TBM drift.*

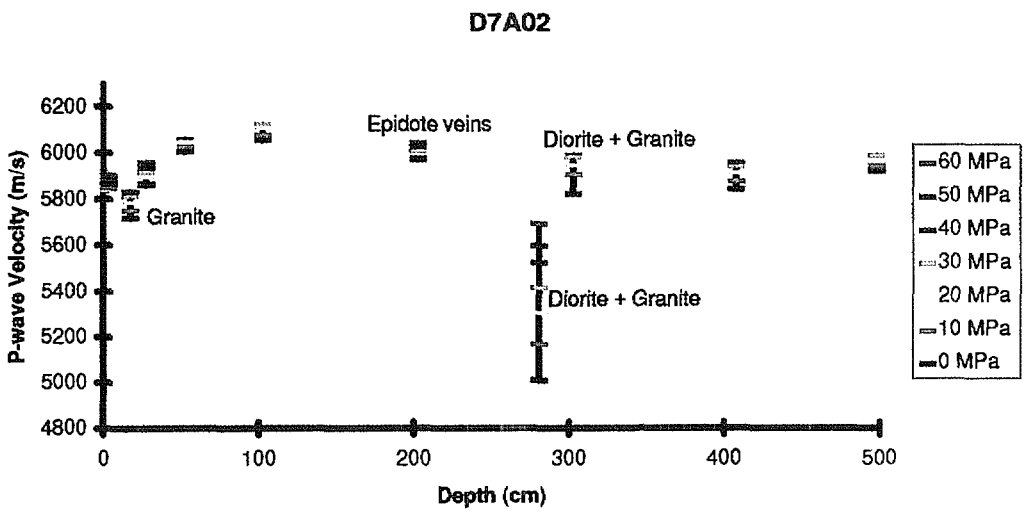

Figure 5-32. *Velocity variation with the application of load for samples at different depths from core RD7A02 in the D&B drift.*

In Figures 5-31 and 5-32 the P-wave velocity versus distance from the drift roof are plotted for RT2A03 and RD7A02 respectively at different loading increments. Unless otherwise labelled the samples were Äspö diorite. The results indicated that there were both spatial and lithological variations in velocity. The sample of quartz-rich pegmatite had a substantially higher velocity than the diorite. Granite samples had generally similar P-wave velocities except where granite occurred as thin veins or as small lenses 2 to 4 centimetres in dimension within the diorite. In these cases, the velocity was lower, with a large increase caused by loading. This may be due to an elastic mismatch between the diorite and granite, causing the more brittle granite to crack more on stress relief. Disregarding the variations due to

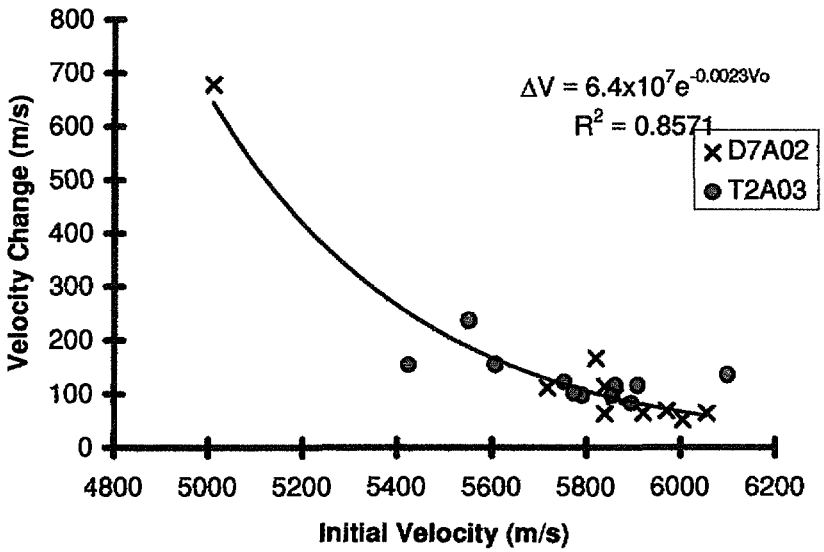

Figure 5-33. Relationship between change in velocity with the application of 60 MPa uniaxial stress, and the initial unstressed velocity within core samples.

different rock types, there appears to be a slight decrease in velocity towards the drift walls. However, this trend is much more subtle than some of the other velocity variations.

There is evidence that the low velocities of the unloaded samples, are a result of the presence of micro-cracks, which close upon application of load. Figure 5-33 shows a plot of increase in velocity with application of 60 MPa uniaxial load versus the initial velocity. Samples with initially low velocities show the larger increase in velocity with load.

It may therefore be suggested that the change in velocity may be a better indicator of crack damage than the velocity of the unstressed sample. In addition velocity changes are easier to quantify than absolute velocities and should be less influenced by variations due to mineralogical differences. Both P-wave and S-wave data showed similar trends but the change in S-wave velocity is generally less than for P-waves. The greatest change in velocity with load and therefore the greatest initial crack density, was found within the first 10 centimetres for the TBM drift and the first 30 centimetres for the D&B drift. Whilst these changes are subtle compared to some of the variation in other parts of the cores they are correlatable with the other data sets that indicate the damaged zone to be of very limited extent.

Anisotropy around the Drifts

Cross hole velocity measurements were undertaken, using the high frequency micro-velocity logging probes, by pulsing seismic energy between two transducers. The measurements were performed in four parallel boreholes and were designed to give an even and full coverage of data over a lower hemisphere stereonet.

Three sets of four boreholes were used in both the TBM and D&B drifts. The boreholes are generally 5 metres in length and drilled in a square configuration 50 centimetres apart (Figure 3-5). In the TBM drift the sets were located in section 2, oriented vertically up, inclined right 45° up and horizontal right. In the D&B drift the boreholes were located in round R7. The sets were oriented vertically up, horizontal right and vertically down. Six sets of readings were made in the TBM drift and five sets were made in the D&B drift. Figure 5-34 shows the P-wave velocity stereonets for the vertically up holes in the TBM drift. Table 5-5 summarises the fast and slow directions of the P-wave stereonets.

Table 5-5. Summary of the fast and slow P-wave velocity directions for all the stereonets. 'Parallel' indicates in the direction of the strike of the drift, 'Perpendicular' indicates orthogonal to the drift wall and 'Tangential' indicates parallel to the drift wall, but perpendicular to the strike.

Drift	Borehole Set	P-wave fast direction	Comments	P-wave slow direction	Comments
TBM	Vertical 0 - 0.8 m	300/70	perpendicular to drift wall	all horizontal	parallel to drift wall
	Vertical 1 - 2 m	300/70	perpendicular to drift wall	all horizontal	parallel to drift wall
	Vertical 3.5 - 4.5 m	300/70	perpendicular to drift wall	all horizontal	parallel to drift wall
	Inclined 0 - 0.8 m	330/50	tangential to drift wall	100/30	parallel to drift wall
	Inclined 1 - 2 m	350/40	tangential to drift wall	100/30	parallel to drift wall
	Horizontal 0 - 0.8 m	030/10	perpendicular to drift wall	110/30	parallel to drift wall
D&B	Vertical 0 - 0.8 m	too	borehole	dependent	
	Vertical 1 - 2 m	too	borehole	dependent	
	Vertical 3.5 - 4.5 m	too	borehole	dependent	
	Horizontal 0 - 0.8 m	000/20	perpendicular to drift wall	110/0	parallel to drift wall
	Horizontal 1 - 2 m	030/20	perpendicular to drift wall	110/0	parallel to drift wall

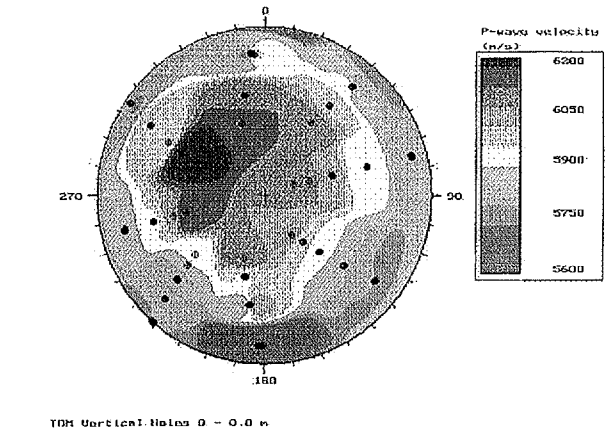

a)

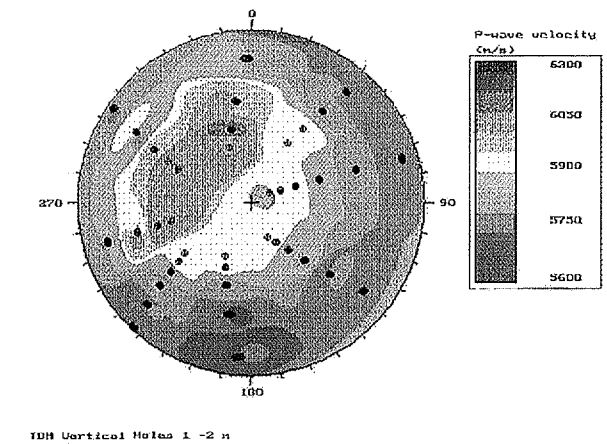

b)

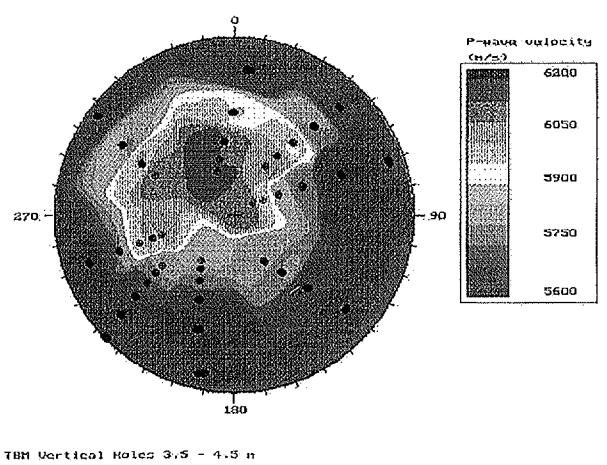

c)

Figure 5-34. *Examples of the stereonets produced by the crosshole surveying. These are taken from the vertical holes in the TBM drift. a) 0 - 0.8 m depth, b) 1 - 2 m depth and c) 3.5 - 4.5 m depth into the boreholes.*

The fast direction consistently appears to be perpendicular to the borehole walls, indicating micro-cracking parallel to the drift walls. Only with the inclined holes in the TBM drift is the fast direction tangential to the drift wall.

The range of degree of anisotropy varied with distance from the drift perimeter. The maximum difference in velocity (about 600 ms^{-1}) between fast and slow velocities is seen in the deepest holes in the D&B drift. The smallest range (about 300 ms^{-1}) appears in the rock mass 1-2 metres away from the drift walls. Close to the drift walls the velocity difference rises again.

Tomography around the Drifts

Detailed seismic tomography surveys were performed in two fans of radial boreholes around the D&B drift (round R7) and the TBM drift (section 2). The measurements were carried out using a piezoelectric transducer as seismic borehole source and a multi-receiver probe. The measurements were performed as eight crosshole layouts between pairs of adjacent boreholes. A variable increment between source and receiver positions with depth produced a more densely covered zone close to the drift.

TBM Drift

A ray diagram of the eight crosshole sections measured around the TBM drift is shown in Figure 5-35.

From the eight crosshole sections six produced normal velocity distributions. The two remaining sections, between the vertical down (VD) and the horizontal right (HR) boreholes, display an abnormal anisotropy and a high velocity feature. This anisotropy may be an artefact due to small positioning errors. The six "normal sections" produced the tomogram shown in Figure 5-36. The measurements gave a maximum velocity of 6050 ms^{-1} with an anisotropy of 2% and showed that the direction of the high velocity is vertical. Changes in seismic velocities due to excavation damage were not evident. The zone of lower velocities that was imaged is only a few centimetres wide and may be a function of ray bending near the drift.

D&B Drift

The whole eight section data set obtained in the D&B drift produced the P-wave velocity distribution shown in Figure 5-37. The velocity distribution is remarkably smooth with the exception of the immediate vicinity of the drift. Generally the P-wave velocity increases to values over 5900 ms^{-1} in the first 20 to 50 centimetres and stays between 5900 ms^{-1} and 6000 ms^{-1}. A zone of smaller contrast extends to 1.5 to 2.5 metres and has a different shape for the upper and lower part of the fan of boreholes. P-wave velocity anisotropy was not observed in these data.

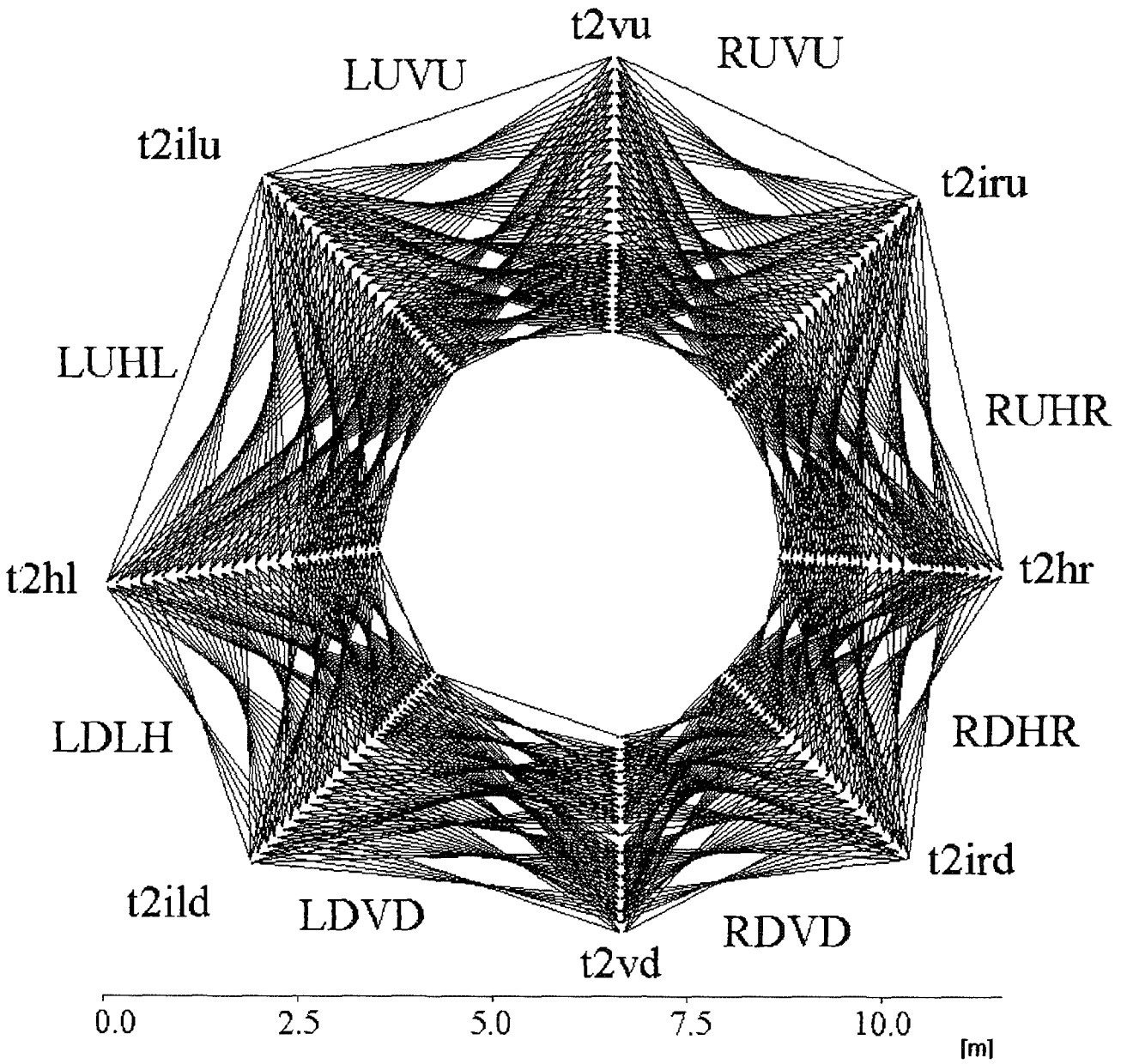

Figure 5-35. *Ray diagram of the eight crosshole sections measured around the TBM drift. The location of the boreholes is given in Figure 3-5. Every section is identified by the corresponding pair of boreholes. The first borehole in the name of the section is the source borehole.*

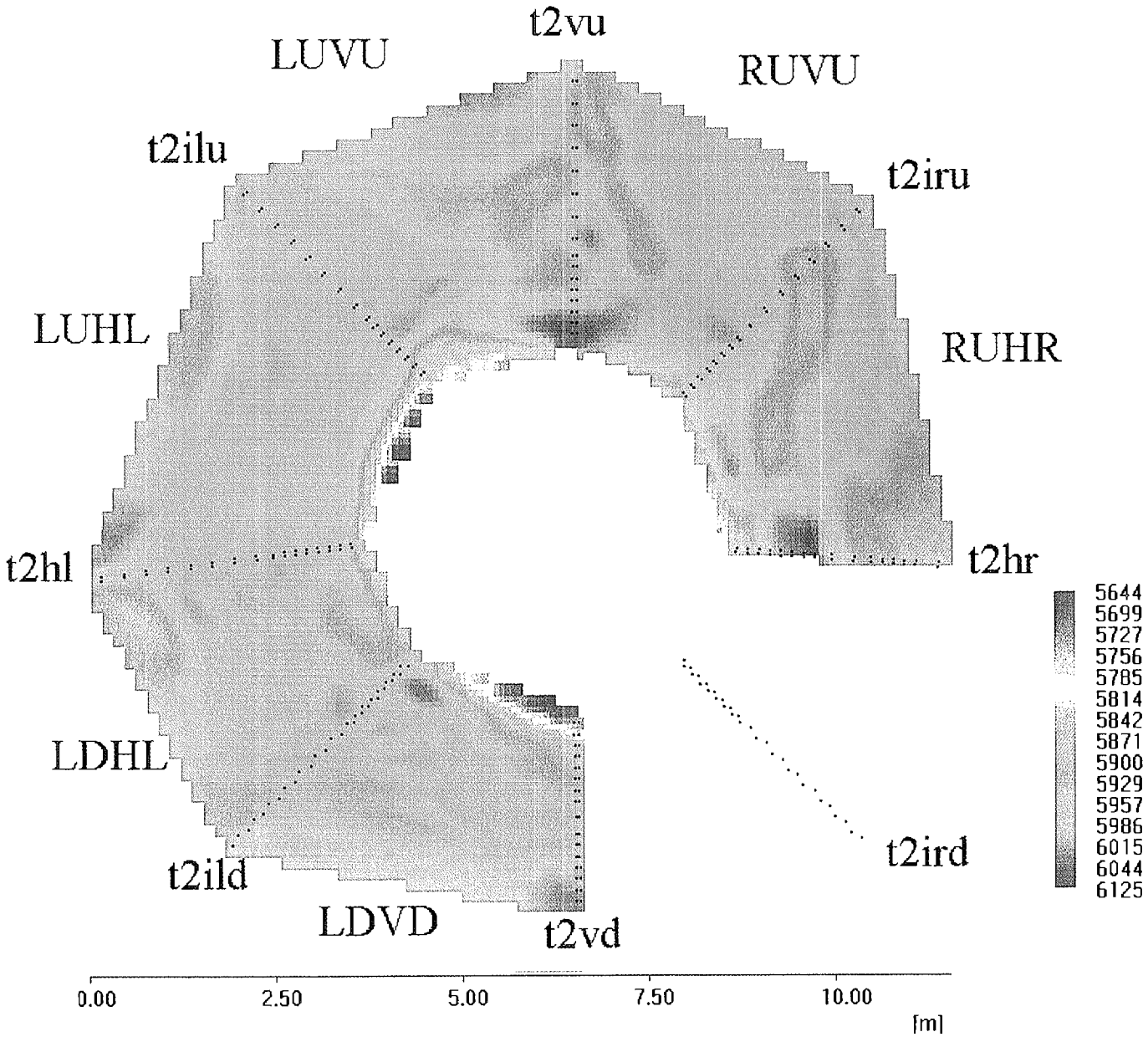

Figure 5-36. *P-wave velocity of six crosshole sections of TBM section 2. The location of the boreholes is given in Figure 3-5.*

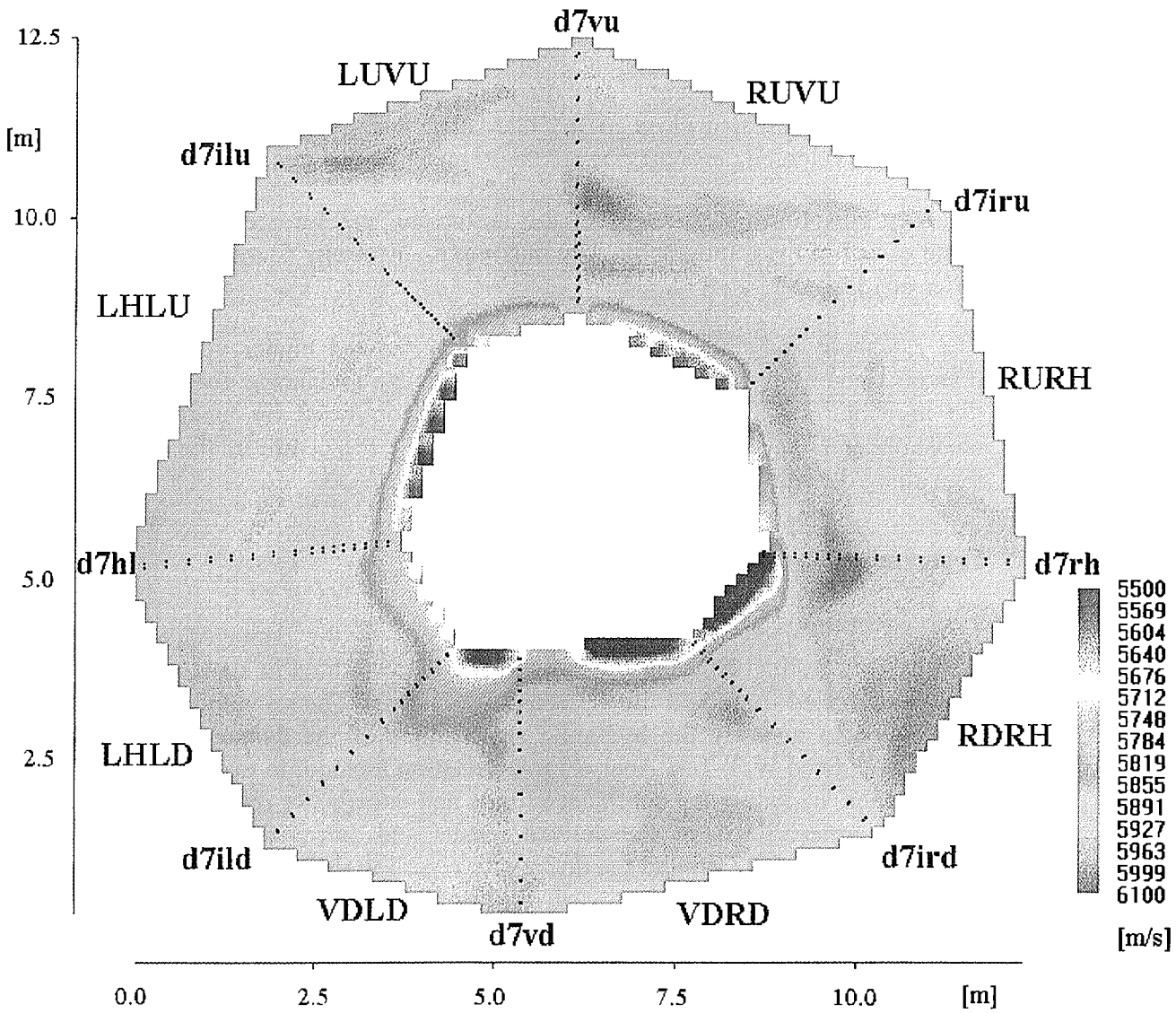

Figure 5-37. *P-wave velocity of eight crosshole sections of D&B round R7. The location of the boreholes is given in Figure 3-5.*

Conclusions of the Damaged Zone Seismic Measurements.

All of the seismic methods showed low velocities close to the drift surfaces. The extent of this low velocity zone seems to be small with some results seeming to overestimate the low velocity zone, probably due to measurement errors and low resolution (the downhole method).

Generally the low velocity zone is extremely small (about 10 centimetres) or even not present around the TBM drift. The D&B drift exhibits a larger low velocity zone of about 30 centimetres. Some single holes showed low velocities to a depth of 100 centimetres especially in vertical down boreholes. The zone was more pronounced in round R4 than round R7. The larger low velocity zone seen from the downward orientated boreholes may be due to more energy used in the excavation method used in the D&B drift and stress relief due to the flat shape of the floor. However, the disturbed zone reflection seismic analysis (Section 5.4.2) showed that some reflectors were present before the excavation of the D&B drift some of which were situated close to the later drift walls. Thus some larger "local" low velocity zones may be due to pre-existing features.

Velocity anisotropy was found in the anisotropy measurements and to some extent in the tomography. The maximum anisotropy found is of the order of 15 %.

The crosshole and tomographic measurements showed higher velocities than obtained by the borehole logs. This may be due to damage directly at the borehole wall, an assumption which was confirmed by laboratory measurements that showed higher velocities along the centre of the core than along the side of the core.

5.3.3 Hydraulic Measurements

In order to characterise the hydraulic properties of the damaged zone permeability testing using the pulse method was performed in short radial boreholes drilled from both the TBM and D&B drifts. The re-analysis was undertaken to quantify the hydraulic significance of the damaged zone using a validated Well Test Analysis interpretation method; to evaluate the significance, including the confidence limits and uncertainty related to the derived permeabilities, of the derived results and assess the hydraulic behaviour of the EDZ around the drifts with regard to different excavation methods.

Pulse Tests

The hydraulic assessment of the damaged zone was undertaken in a number of short (3 metres) radial boreholes drilled after the excavation of each drift. Twelve boreholes were tested after the completion of the drifts but the number of boreholes tested was considered to be insufficient for a meaningful characterisation of the hydraulic properties of the damaged zone and an additional 15 boreholes, forming radial rings, were drilled and

tested. In the D&B drift the boreholes were located in the LSES section (rounds R3 and R4) and NS section (round R7) of the drift. Additional holes were located in the "failed" and re-blasted rounds R2 (LSES) and R6 (NS). In the TBM drift the boreholes were located in two sections each having three boreholes.

The equipment used for the high-resolution permeability measurements was the SEPPI probe, developed by the Laboratoire de Mécanique de Lille together with the Laboratoire de Géomécanique de Nancy. The pulse tests were performed at 50 millimetre intervals to a depth of 0.5 metres, then at 10 centimetre intervals to 1.0 metre depth, followed by 20 centimetre intervals to the end of the borehole. The pressures in the inflatable packers and in the guard zone were not monitored during the execution of the pulse tests. Constant pressure injection tests were also performed by maintaining a constant pressure and measuring the flow rate. But it is unlikely that a steady state had been reached during the test and consequently these tests have not been analysed.

Analysis and Interpretation

The pulse tests were originally analysed based on a diffusivity equation with the solution obtained using a finite difference method (Bauer *et al.*, 1996a). The tests were re-analysed using Colenco's modular Well Test Analysis package MULTISIM (Tauzin, 1996; Tauzin & Johns, 1997), an interactive well test interpretation package. Included in the package is the analytical inverse modelling programme MULTIFIT (Johns, 1995) designed for low permeability formations. Both packages have been extensively validated.

Analysis Methodology

A selection of pulse tests were re-analysed from the 26 boreholes tested based on; borehole orientation, significant permeability variation and a number of successful tests derived from previous analyses. In total, 9 out of the 26 tested boreholes were selected for re-analysis. These included; 10 tests from boreholes RD3VD (LSES), RD4VD (LSES) and RD7VD (NS) from the D&B drift; all six boreholes from section 2 of TBM drift and round R7 of D&B drift (NS) were selected; and the remaining tests from RD7VD (NS).

Diagnostic plots using 'classical' log-log plots without superposition were used for the pulse tests to estimate the wellbore storage dominated period duration.

The estimate and/or selection of the input parameters is important to the analysis and a summary of the parameters used is presented in Table 5-6. The homogenous radial flow model was selected as an appropriate flow model from log-log diagnostic plots, given the lack of any evidence for more complex flow dimension and the small radius of investigation of the tests. The impact of the wellbore storage effects and specific storage on parameter uncertainty was assessed in the sensitivity analysis. The

borehole history is an important source of uncertainty for every analysis. Since the pressure history and its impact on static formation pressure is unknown, two bounding scenarios (low p_{his}, high p_{his}) were considered in the analysis to cover the uncertainty.

Table 5-6. Input parameters used in the re-analysis of ZEDEX pulse tests

Parameter	Value	Source
Flow Model	homogeneous radial flow	assumed from log-log plots
Interval length	50 mm	measured
Borehole radius	43 mm	nominal
Fluid density	1000 kg/m^3	from project data
Fluid viscosity	1.2E-3 Pa.s	from project data
Porosity	0.41 %	estimated
Formation compressibility (rock and water)	1.0E-9 1/Pa	estimated
Wellbore storage coefficient	computed	calculated from measured ΔV, Δp
Borehole history	varied	unknown, two bounding scenarios were considered

Table 5-7 summarises the re-analysis procedure performed with three different levels of analysis applied in accordance with the behaviour of the pulse transient.

Table 5-7. Summary of pulse-tests analyses.

Analysis Procedure / Borehole ID and Location (drift)		Log-log diagnostic	Log-log diagnostic and Quick analysis	Log-log diagnostic and Detailed analysis
RD3VD	D&B	0 tests	0 tests	10 tests
RD7VD	D&B	0	7	11
RD7ILD	D&B	0	0	5
RT2HL	TBM	6	5	7
RT2IRD	TBM	3	8	2
RD4VD	D&B	0	0	10
RD7A05	D&B	1	5	5
RD7ILD	D&B	1	8	4
RD7IRD	D&B	0	6	5
Total number of tests analysed		11	39	59

The quick analysis were performed, using direct MULTSIM simulations taking a high pressure history into account, to derive an upper bound to the permeability that leads to the same pressure drop, rather than to fit the data. Detailed analyses were carried out for the pulse tests getting out of wellbore storage effects to obtain the best fit to the data. Estimates of permeability or permeability and formation pressure were obtained by non-linear regression over the pulse sequence. Regressions were systematically performed taking into account the two borehole histories, in order to assess parameter uncertainty due to the unknown borehole history. Confidence limits were provided for the permeability estimates, based on the non-linear regression results and the sensitivity analyses. The average fit quality can be categorised as:

- Good fit: RD7A05, RT2HL, RT2IRD and RD7IRD
- Fair to good: RD7ILD (second phase), RD3VD and RD4VD
- Fair: RD7ILD (first phase)

In general, the best fit was obtained when assuming a high value for the pressure history, whilst a poor fit was obtained using a fixed formation pressure of 100 kPa. In the non-linear regression, the formation pressure was kept as a free parameter, resulting in values well above 100 kPa (up to 800-900 kPa at the end of boreholes). These values are very uncertain when considering the borehole history uncertainty. It is not clear whether the resulting values correspond to a real formation pressure because the tests are affected by the borehole history.

The quality of data did not, in general, allow a positive identification of a flow model and most "fits" were obtained with a simple homogeneous radial flow model. In cases, where a fit could not be obtained with this flow geometry, or where the log-log plots indicated a different flow dimension (e.g. RD7ILD - Test 4, linear flow), a composite flow model and/or flow dimensions was used. However, these flow models did not yield a significant improvement, except for the tests Nos. 9 and 10 in RD3VD, which fitted with a radial composite flow model.

Sensitivity analyses were performed on selected pulse tests with the objective of deriving confidence limits and estimating the impact of parameter uncertainty on the permeability estimates. The pressure history value was identified as a prime source of uncertainty and the sensitivity of the derived permeability to this parameter is high. In turn, the sensitivity to the duration of pressure history is low, given the short duration of the tests performed. The sensitivity study showed that assigning a longer duration to the borehole history has no impact on the simulations. The wellbore storage coefficient, has a large impact on the test results. Any variation of this coefficient leads to changes in the derived permeability value by the same ratio. The sensitivity of results to the specific storage is generally low.

Synthesis of the Results

The integration and assessment of results was performed by comparing the results along and between the individual boreholes to assess the hydraulic significance of the EDZ in the immediate vicinity of drift perimeter. All results are displayed as permeability profiles along boreholes in Figures 5-38 to 5-45. As can be seen in the re-analysis of the pulse tests leads to higher permeability values throughout when compared to previous results (Olsson *et al.*. 1996b). In most of the cases, the previous values are smaller than the lower limit of the confidence range indicated for the new permeability values. Given this uniform trend it is concluded that the previous analyses systematically underestimated the permeability. The permeability profiles serve as a basis for identifying characteristic trends in the permeability distribution along the boreholes and are briefly discussed below, with comments on the hydraulic properties of the EDZ presented in Table 5-8.

A number of core samples were tested in the laboratory and in total, 41 standard permeability tests were performed in a triaxial cell under variable confining pressures. In general, the laboratory values are at least one order of magnitude smaller than the lower limits of the pulse test data.

Table 5-8. Hydraulic Property of EDZ

Borehole	Comments on EDZ
RT2HL	(TBM): no trend in EDZ
RT2IRD	(TBM): no EDZ visible
RD3VD	fractured zone with one high permeability value in first 20 cm, no other trend visible
RD4VD	high permeability zones in first 50 cm
RD7VD	no EDZ effect visible
RD7A05	detectable decrease of permeability at 55 cm
RD7ILD	decrease of permeability beyond 25 cm.
RD7IRD	high permeability zone at first 55 cm

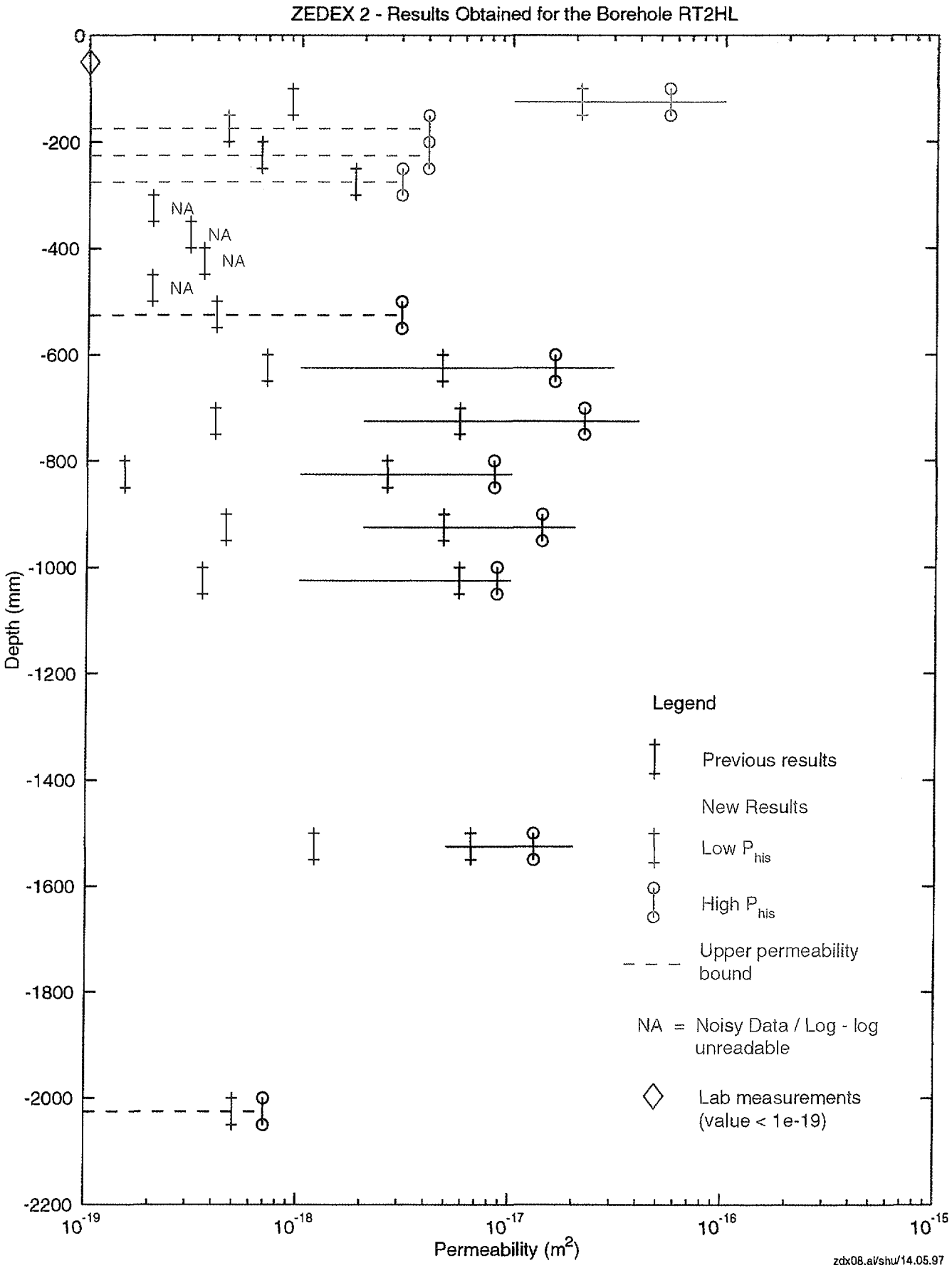

Figure 5-38. *Permeability profile with previous and new analysis results obtained for the borehole RT2HL.*

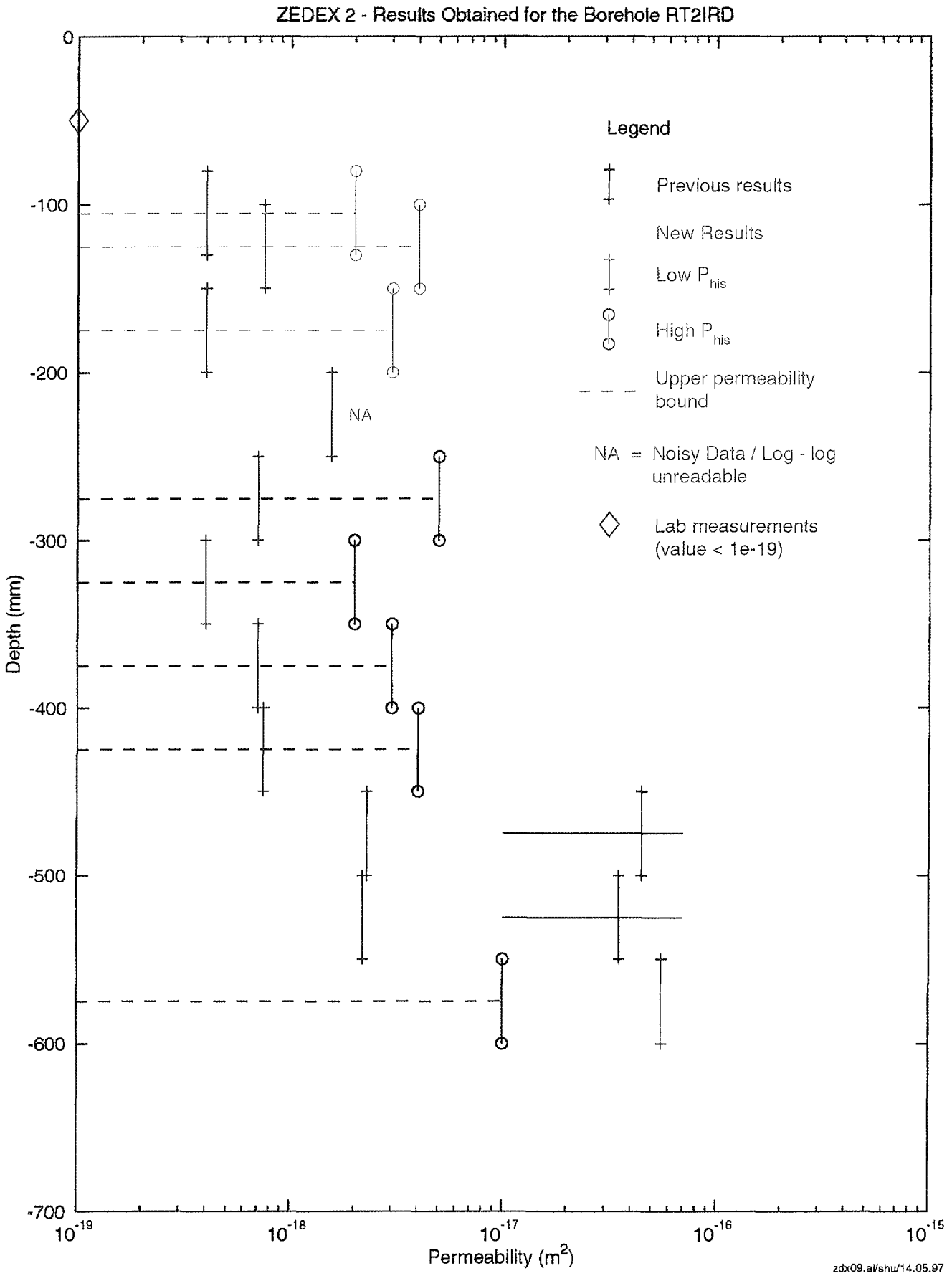

***Figure 5-39**. Permeability profile with previous and new analysis results obtained for the borehole RT2IRD.*

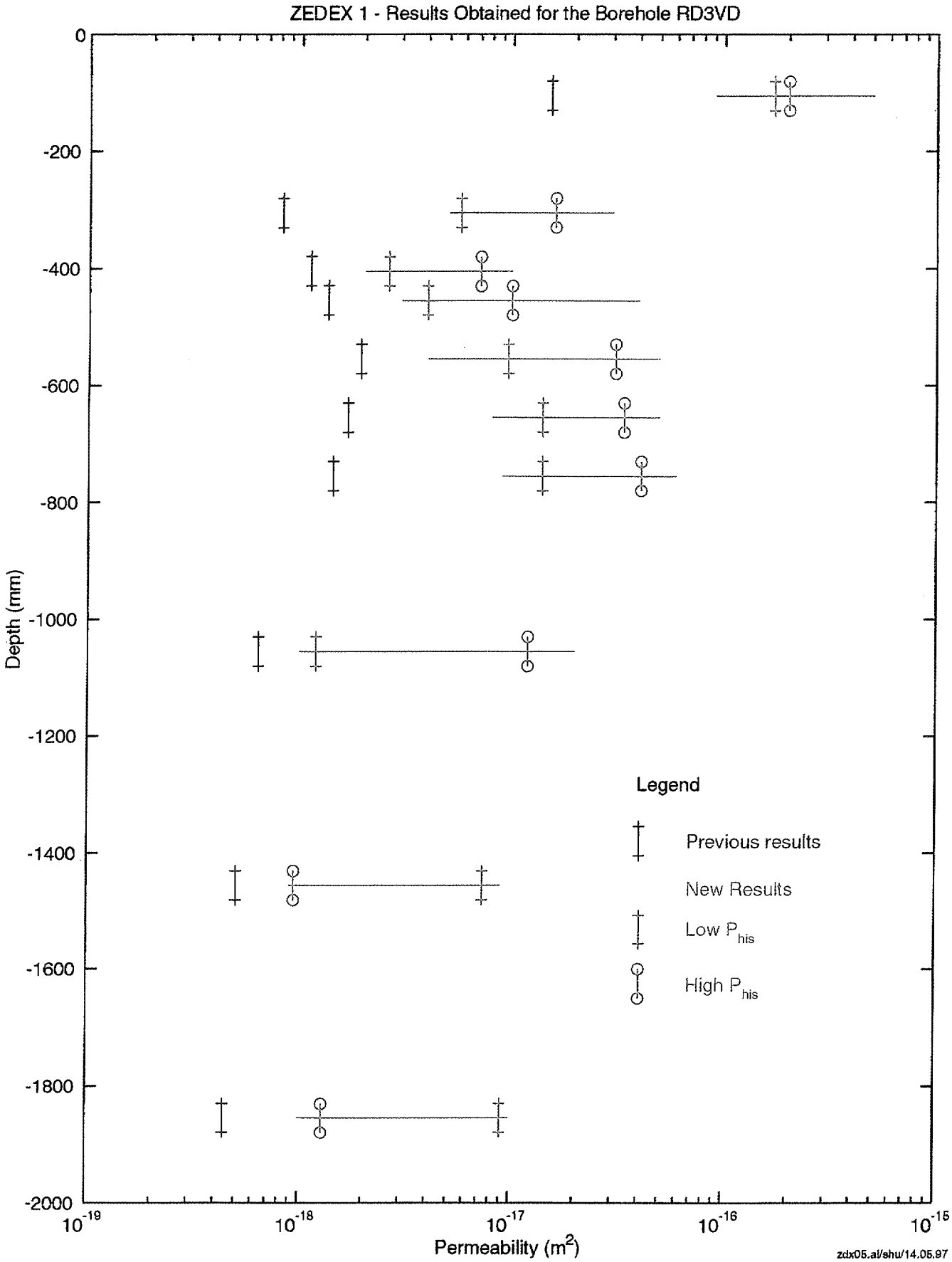

Figure 5-40. *Permeability profile with previous and new analysis results obtained for the borehole RD3VD.*

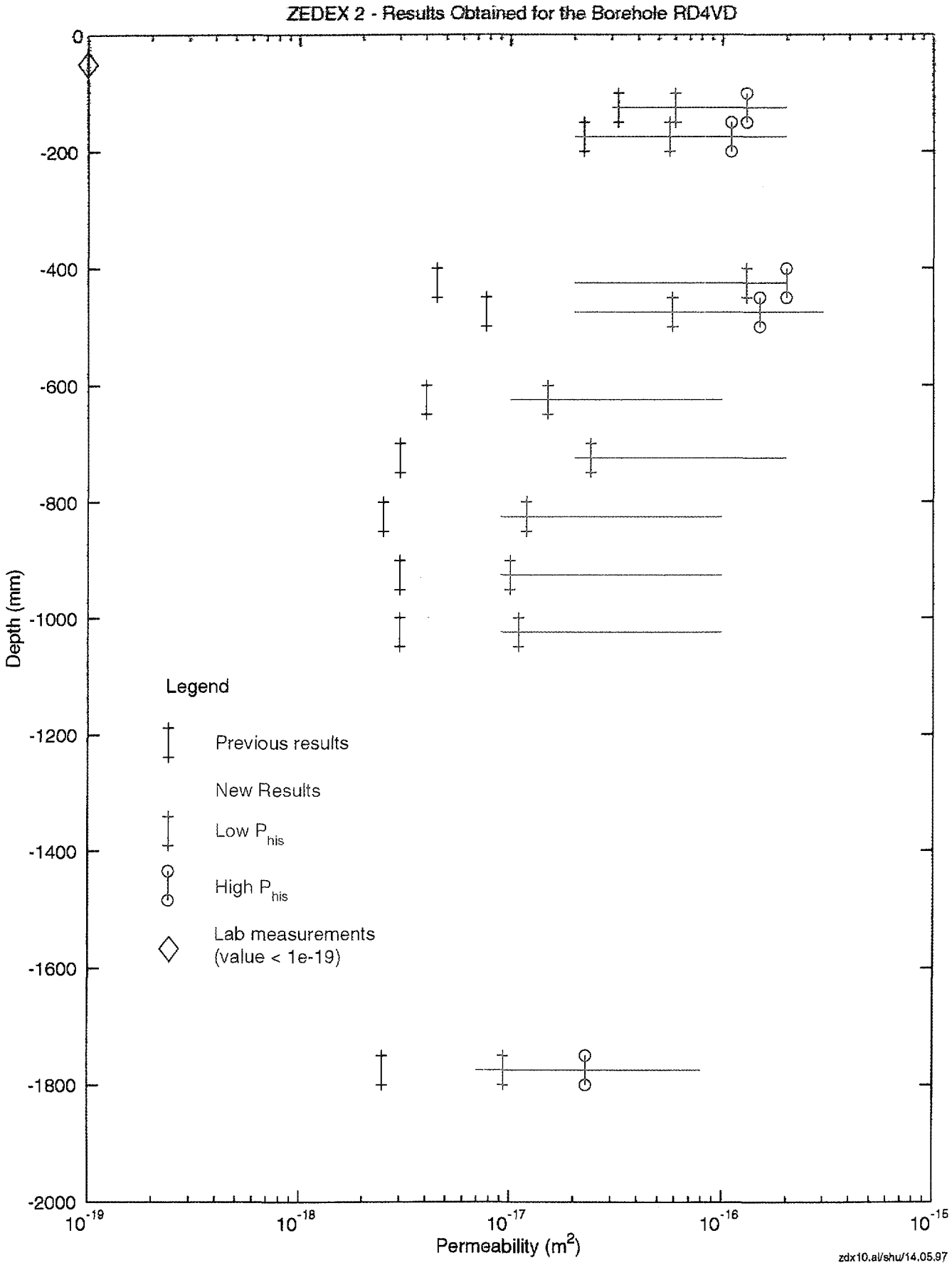

Figure 5-41. *Permeability profile with previous and new analysis results obtained for the borehole RD4VD.*

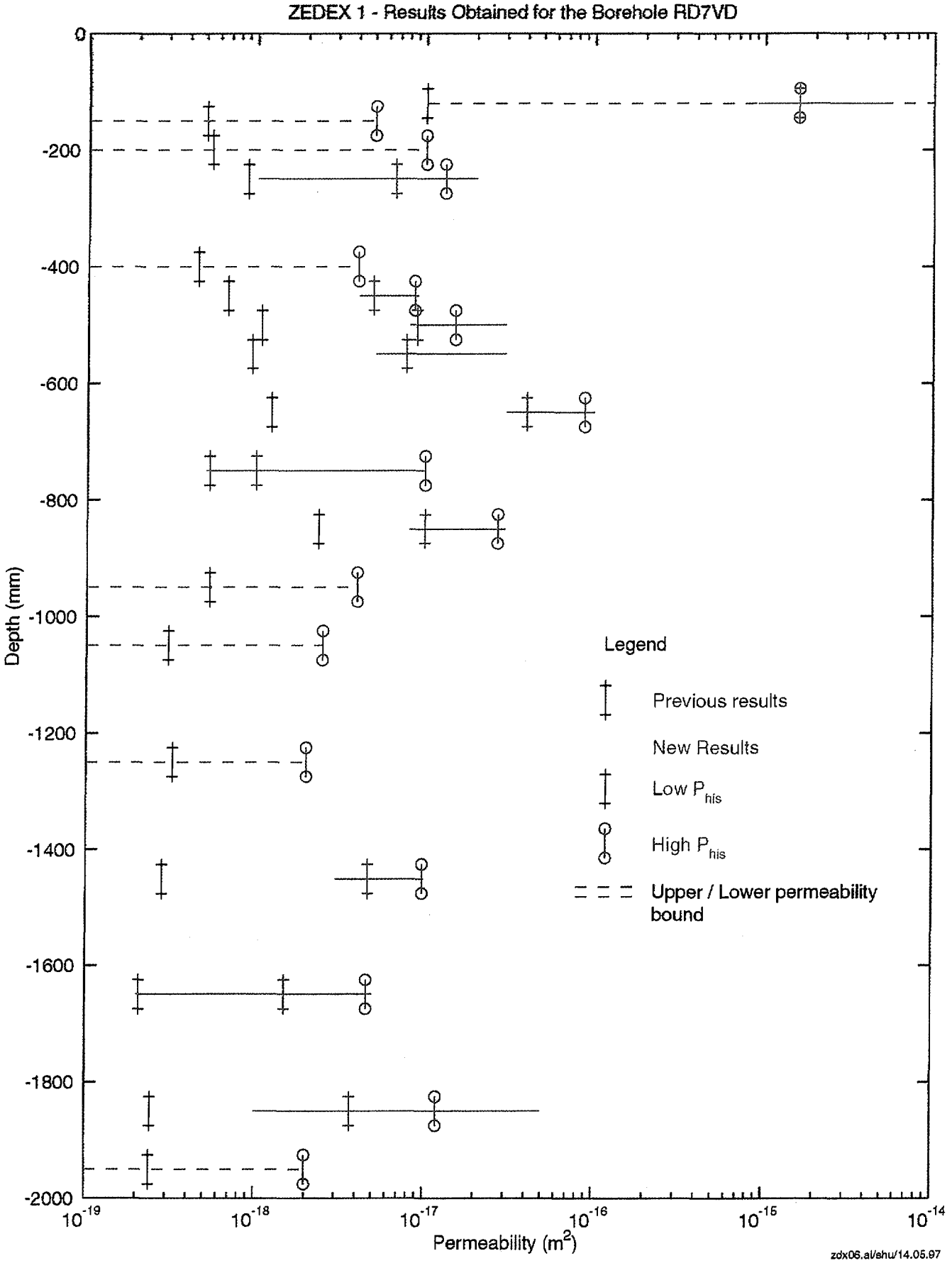

Figure 5-42. *Permeability profile with previous and new analysis results obtained for the borehole RD7VD.*

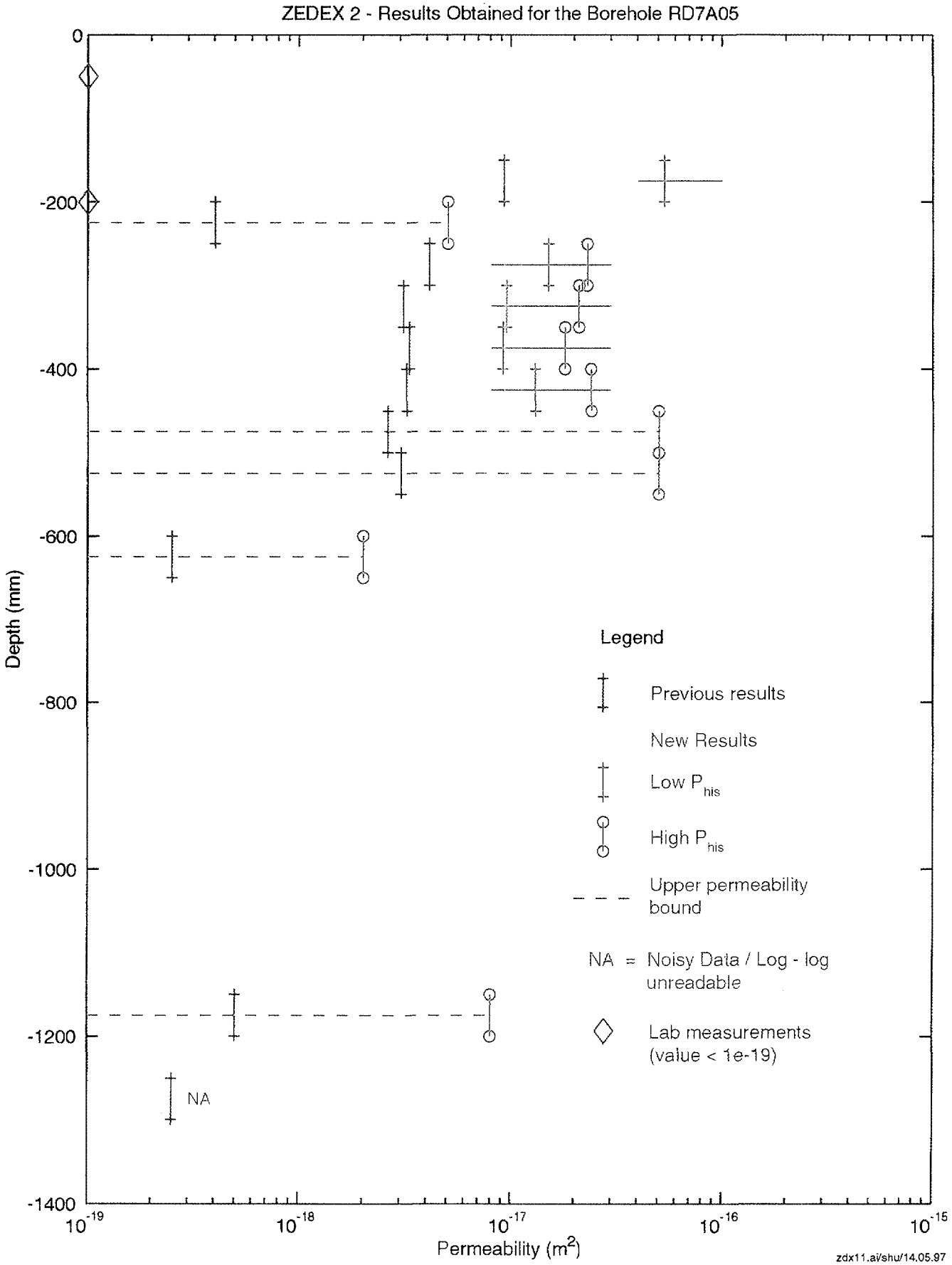

***Figure 5-43**. Permeability profile with previous and new analysis results obtained for the borehole RD7A05.*

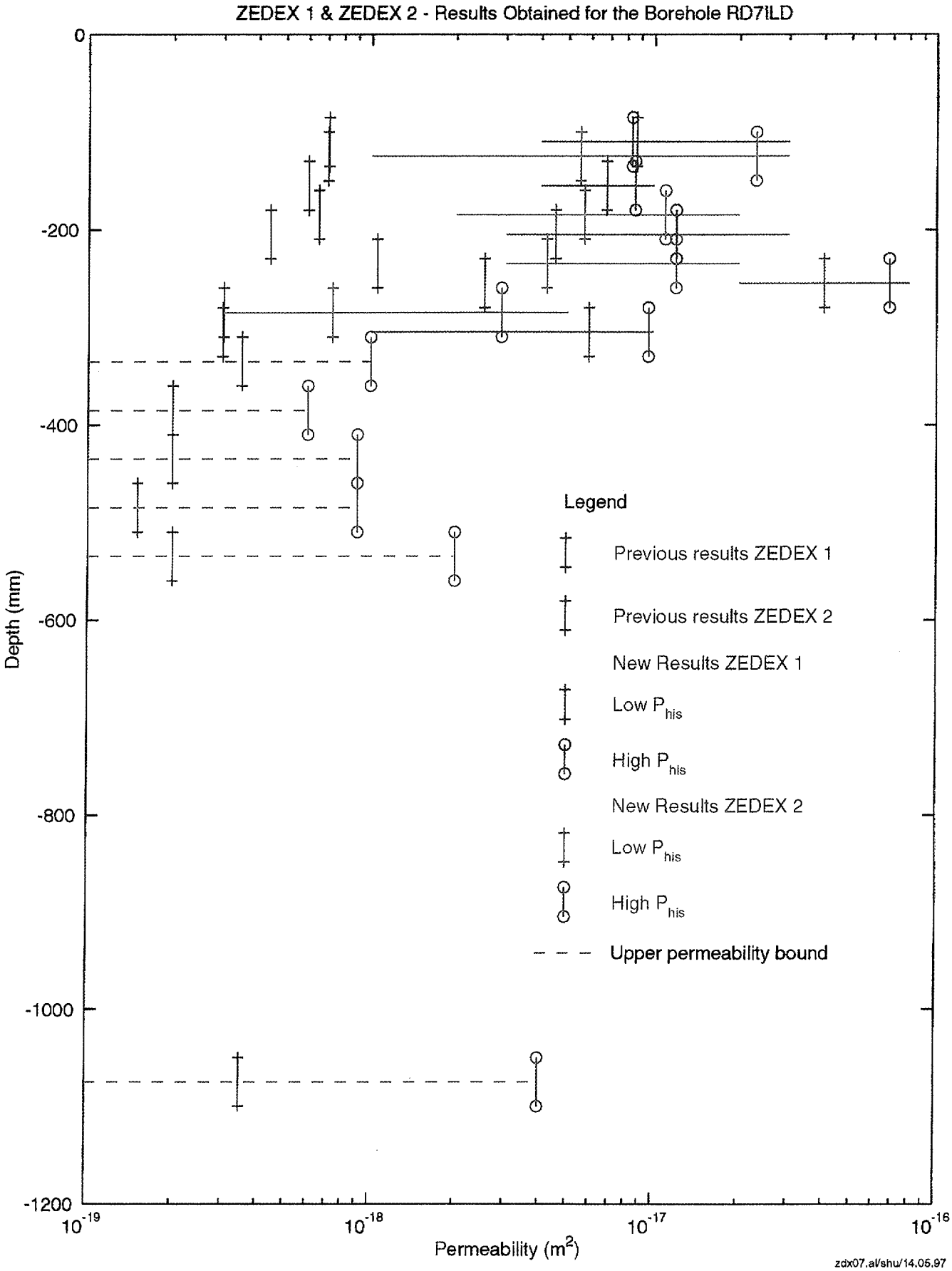

Figure 5-44. *Permeability profile with previous and new analysis results obtained for the borehole RD7ILD.*

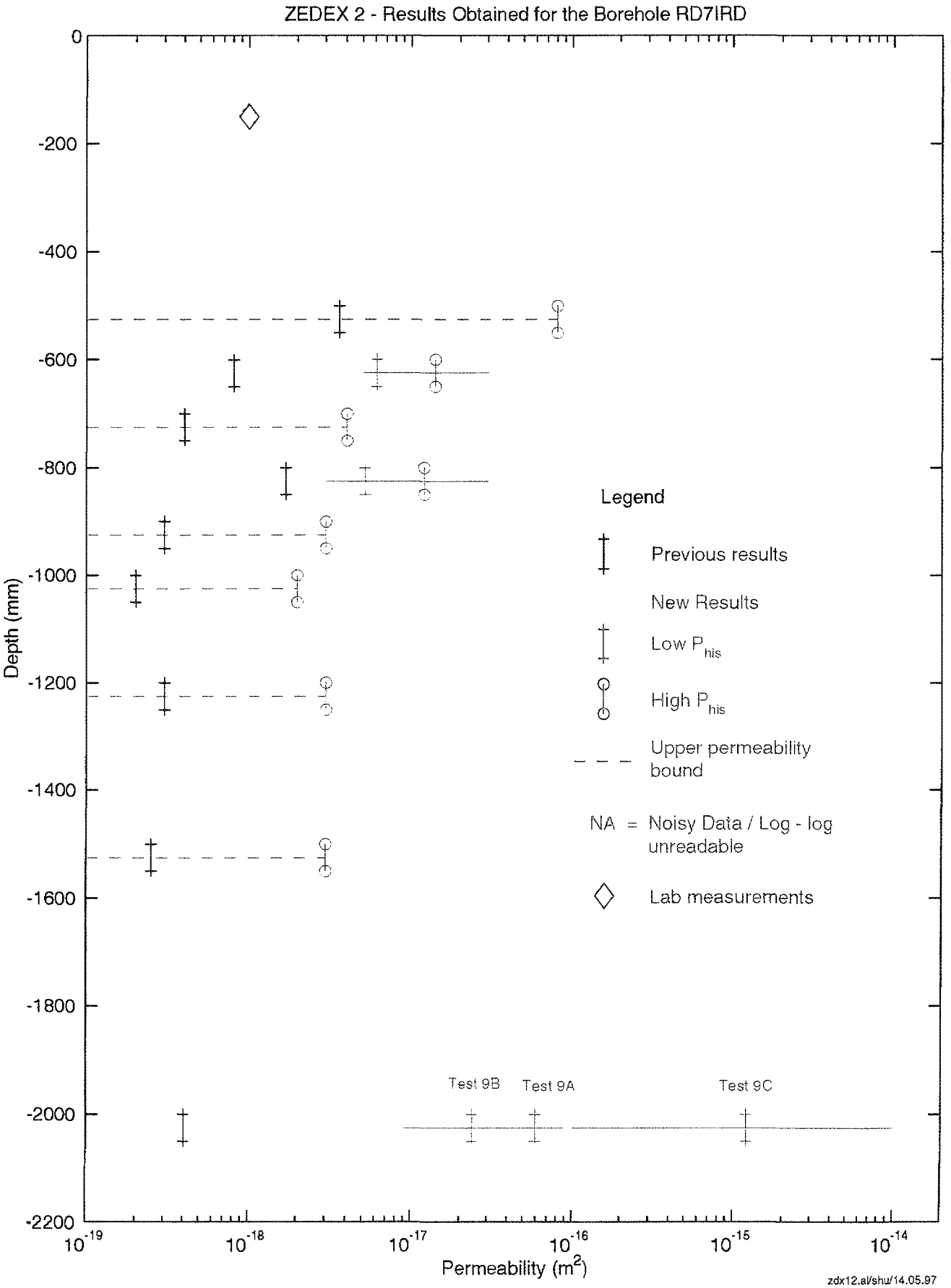

Figure 5-45. *Permeability profile with previous and new analysis results obtained for the borehole RD7IRD.*

Laboratory measurements

Laboratory measurements were performed on 13 oriented cubic samples cut from cores from the short radial holes in the TBM drift and 26 samples from the D&B drift. Laboratory measurements were also performed on 5 samples taken from the drift face.

Permeability tests

Each cubic sample was placed inside a rubber sleeve and set in a triaxial test cell. The tests were carried out under two conditions, steady state condition and pulse tests. The injection fluid used was dry nitrogen. In steady state conditions, the pressure was maintained at a constant level and the flow rate was measured. Pulse tests were conducted by instantaneously increasing the pressure. The pressure increase and time dependent recovery back to the initial hydraulic pressure were recorded by a computer. The data were analyzed using a finite difference method. The permeability was calculated as the average of 3 permeability values obtained on the 3 faces of the cubes.

The permeability decreases as a function of distance from the wall in the TBM drift (Figure 5-46). This is particularly clear in the samples from the inclined (RT1I) and horizontal (RT1H) borehole whilst the samples from the vertical (RT1V) borehole does not show any variation. Permeability values are generally low (1 10^{-20} m^2). A decrease of permeability with distance from the wall in the D&B drift can be observed in the inclined (RD3I, RD7I, RD2I and RD6I) and vertical (RD7V) boreholes (Figure 5-47). However, this trend does not appear in the samples from the horizontal (RD3H and RD7H) boreholes.

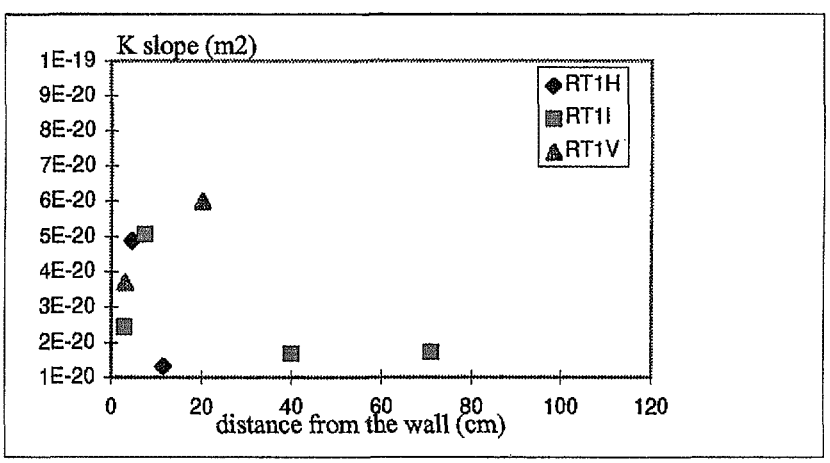

Figure 5-46. Permeability versus distance from the wall in the TBM drift in boreholes RT1H, RT1I and RT1V.

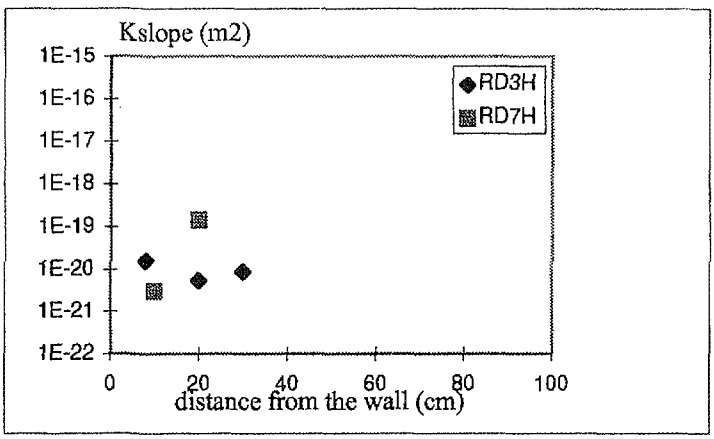

a)

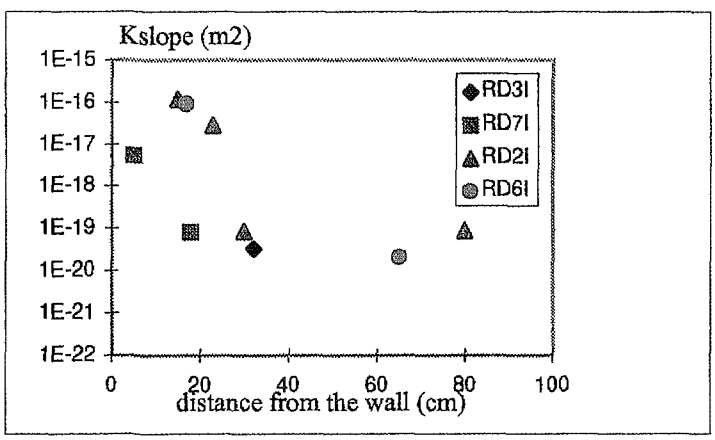

b)

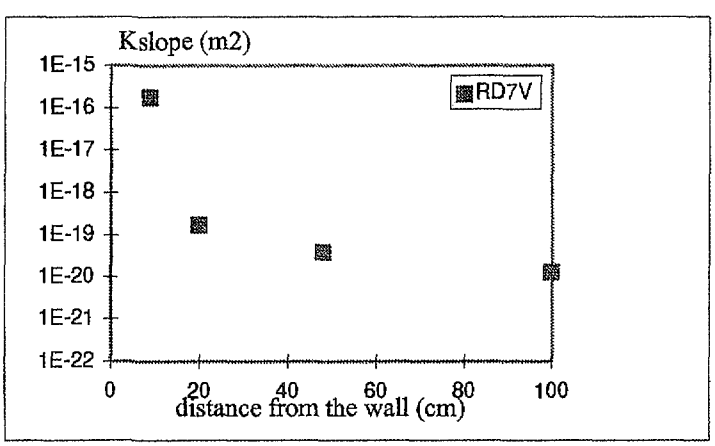

c)

Figure 5-47. *Permeability versus distance from the wall in the D&B drift. a) horizontal boreholes, b) inclined boreholes, c) vertical boreholes.*

Conclusions for the Damaged Zone Hydraulic Measurements

A large number of pulse test data were collected from 26 tested short radial boreholes. The re-analysis of pulse tests in 9 selected boreholes produced a new set of permeability data that characterises the rock properties in the damaged zone. The principal conclusions can be summarised as:

- the geomechanical conceptual model of the ZEDEX study, indicated that the effects of the EDZ in hard fractured rocks manifest through propagation of discrete fractures which are either pre-existing (and re-activated) or newly developed planes of weakness. Hence, any change of hydraulic properties in hard rock due to EDZ is attributed to the enhanced aperture and/or connectivity of discrete features and not to deformation or alteration of the rock matrix itself.

- as the method was only applied in boreholes drilled after the drift excavation precludes a direct comparison of before/after *in situ* properties and as such severely limits the interpretation of the significance of observations. It is not clear whether the measurements reflect primarily the drift excavation effect (EDZ) or rather a wellbore skin effect.

- the results suggest that there is no well defined and significant increase in permeability of the rock mass in the damaged zone in the vicinity of drift excavation which could be observed systematically in the analysed data even when taking the uncertainties identified into account.

- these data show that there is no significant distinction between the damage extent in D&B and TBM boreholes.

5.3.4 Visual indicators of damage

Dye penetration test

Blocks have been excavated by sawing, with a diamond saw, in two places in the D&B drift, at round R4 and R8 and in the TBM drift at chainage 3213 metres. In the D&B drift blocks were cut from both the right wall and in the floor (Figure 5-48). In the TBM drift blocks were excavated from the right wall.

Two horizontal cuts were made on each side of two half barrels. Then a number of vertical cuts were made in order to loosen the blocks. The depth of the cuts was about 0.5 metres and were designed to cross at least two horizontal half barrels along the length of the cuts.

After loosening the blocks, the cuts were sprayed with penetrant spray and a developer spray and the cuts were photographed. Cracks in the rock could then be studied and classified according to definitions specified in

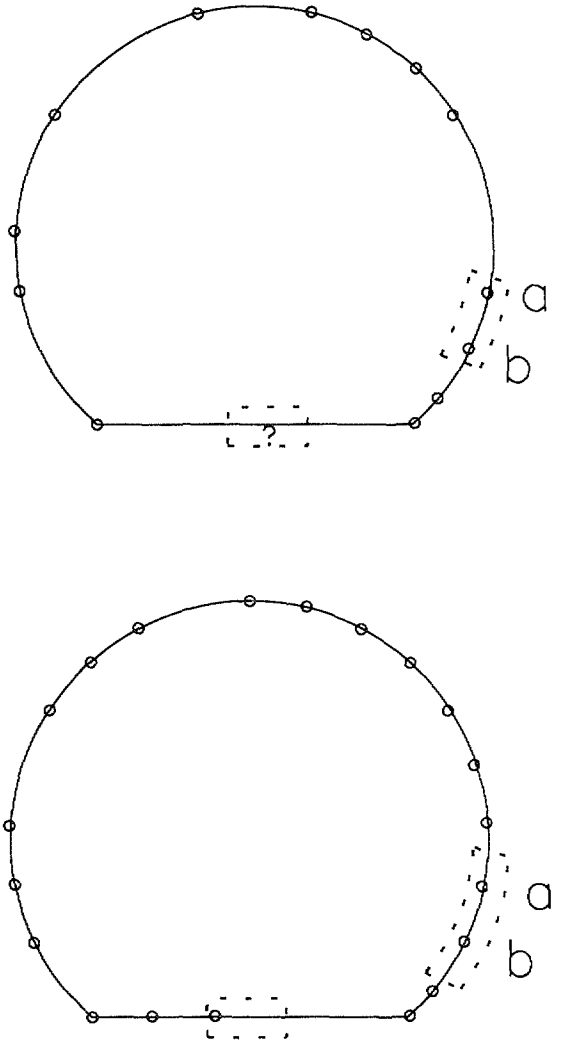

***Figure 5-48**. Half barrels and saw cuts for rounds R4 and R8.*

Figure 5-49. Crushing cracks were defined as cracks of length less than 0.1 metres.

On first inspection of the walls of the drift there were no apparent differences in fracturing between rounds R4 and R8, both of which were partially failed rounds. However, a closer analysis showed that there was a difference in crack length and frequency between the two rounds as shown in Figure 5-50. The average crack length in the walls in round R4 was 17 centimetres and in round R8 the crack length was on average 7 centimetres. In the floor the average crack length was 40 centimetres in round R4 and 30 centimetres in round R8. In the TBM drift no visible induced cracks were found.

Photographs of the cuts are shown in Figures 5-51 to 5-55.

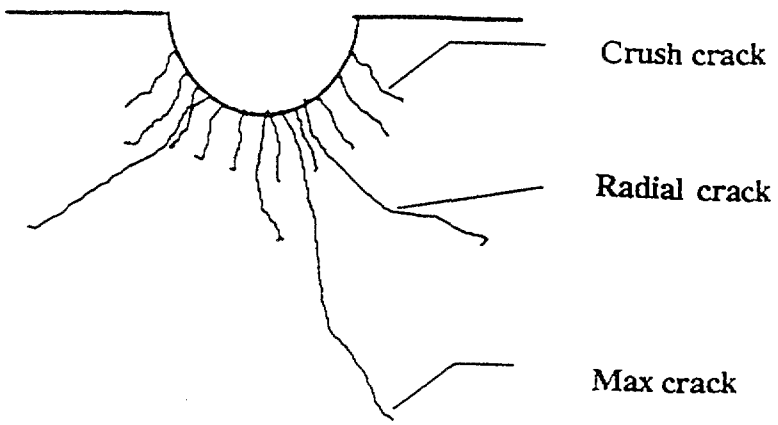

Figure 5-49. Definition of different crack types.

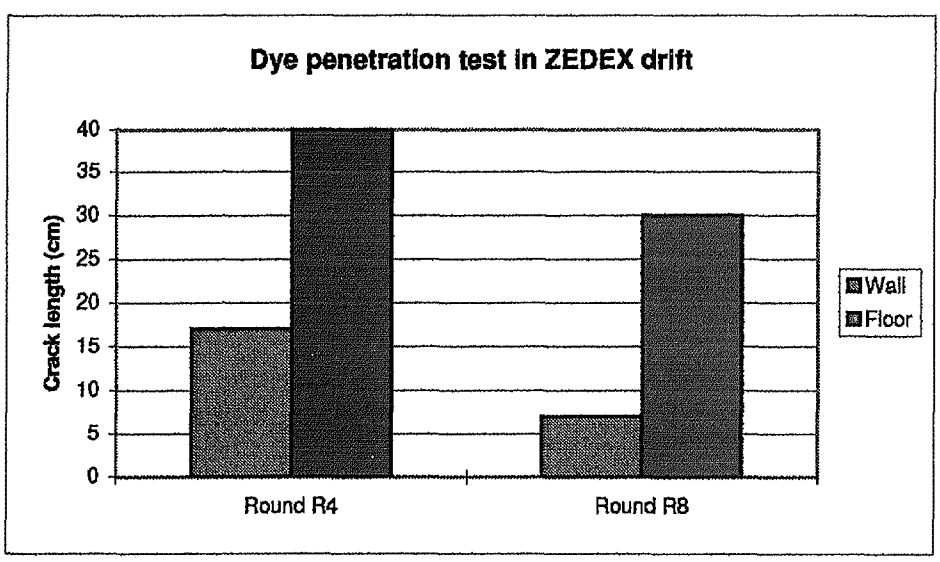

Figure 5-50. Crack length for the ZEDEX test.

***Figure 5-51**. Round R4, wall, ZEDEX D&B drift.*

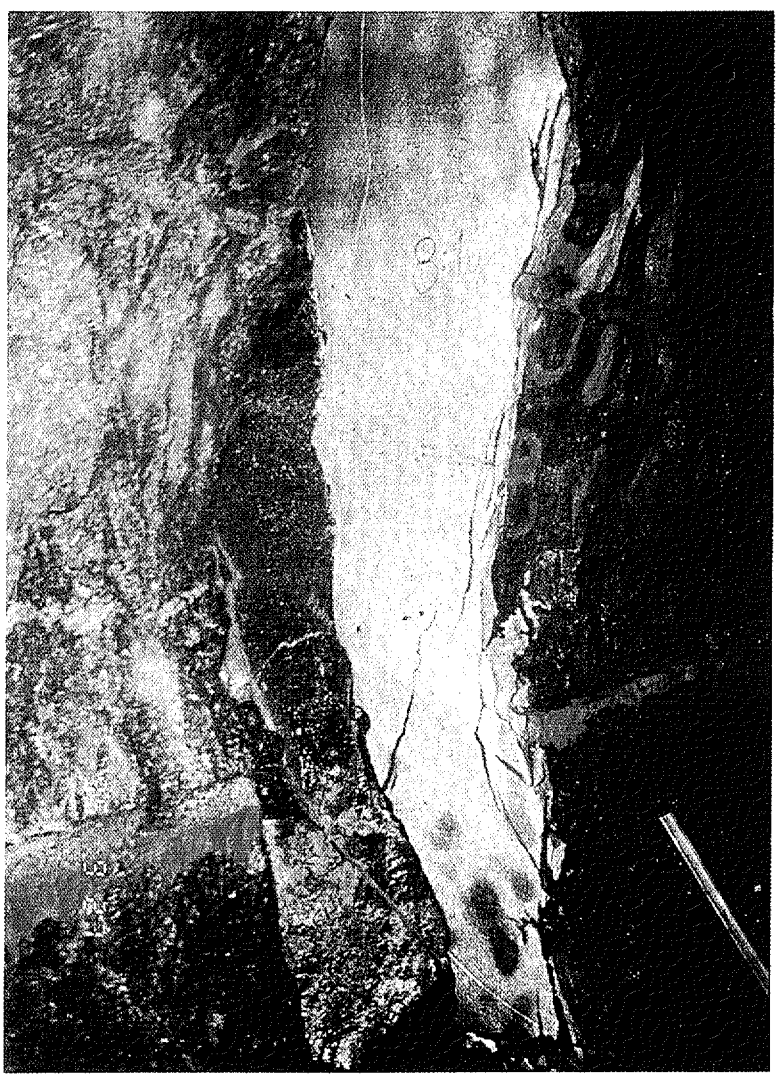

Figure 5-52. *Round R8, wall, ZEDEX D&B drift.*

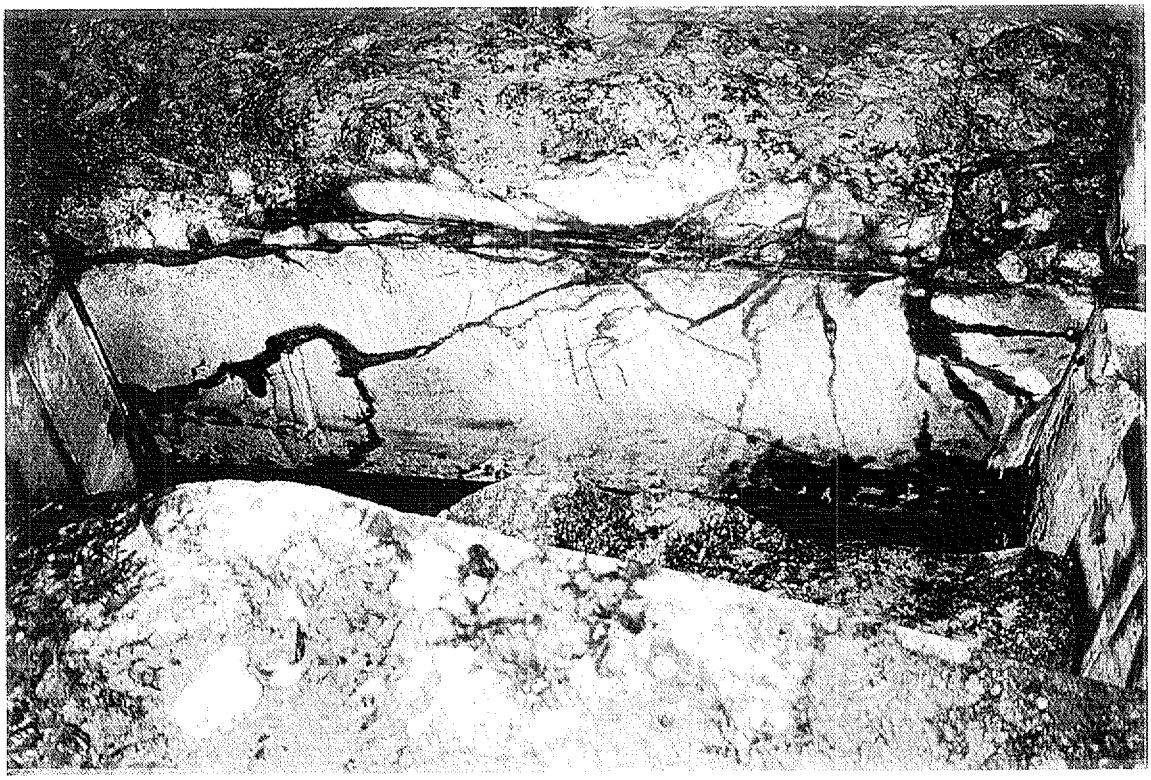

***Figure 5-53**. Round R4, floor, ZEDEX D&B drift.*

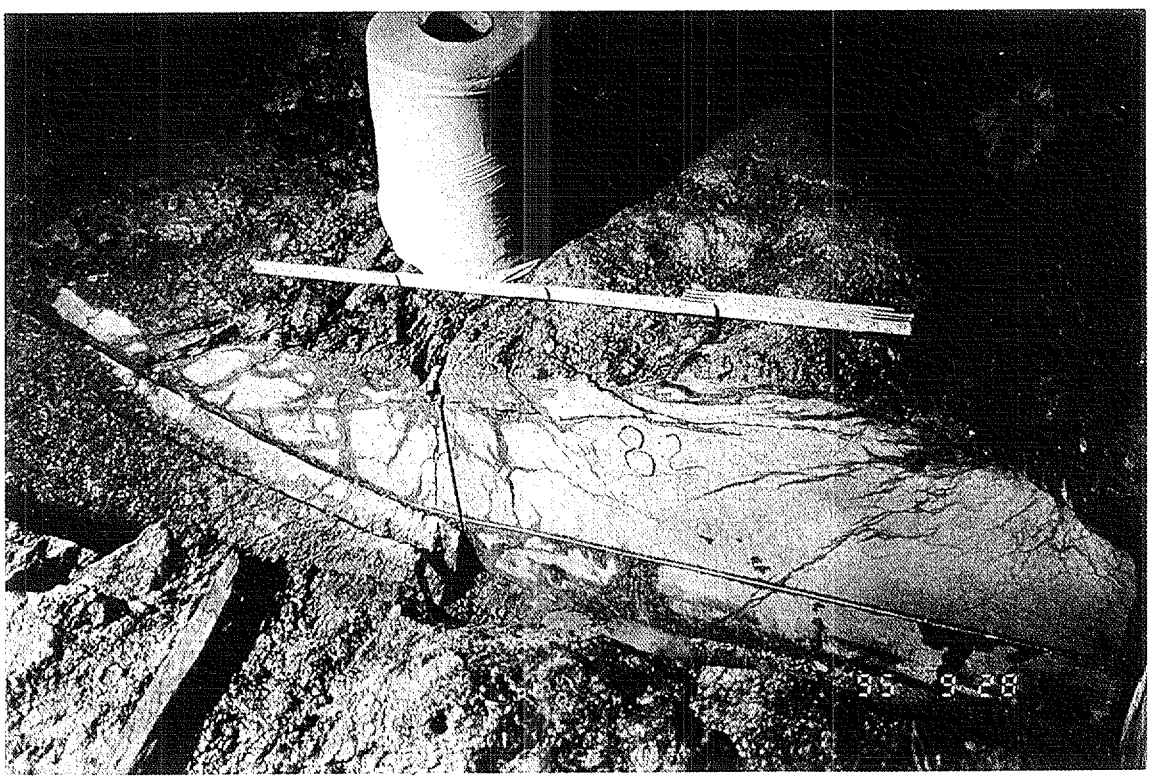

***Figure 5-54**. Round R8, floor, ZEDEX D&B drift.*

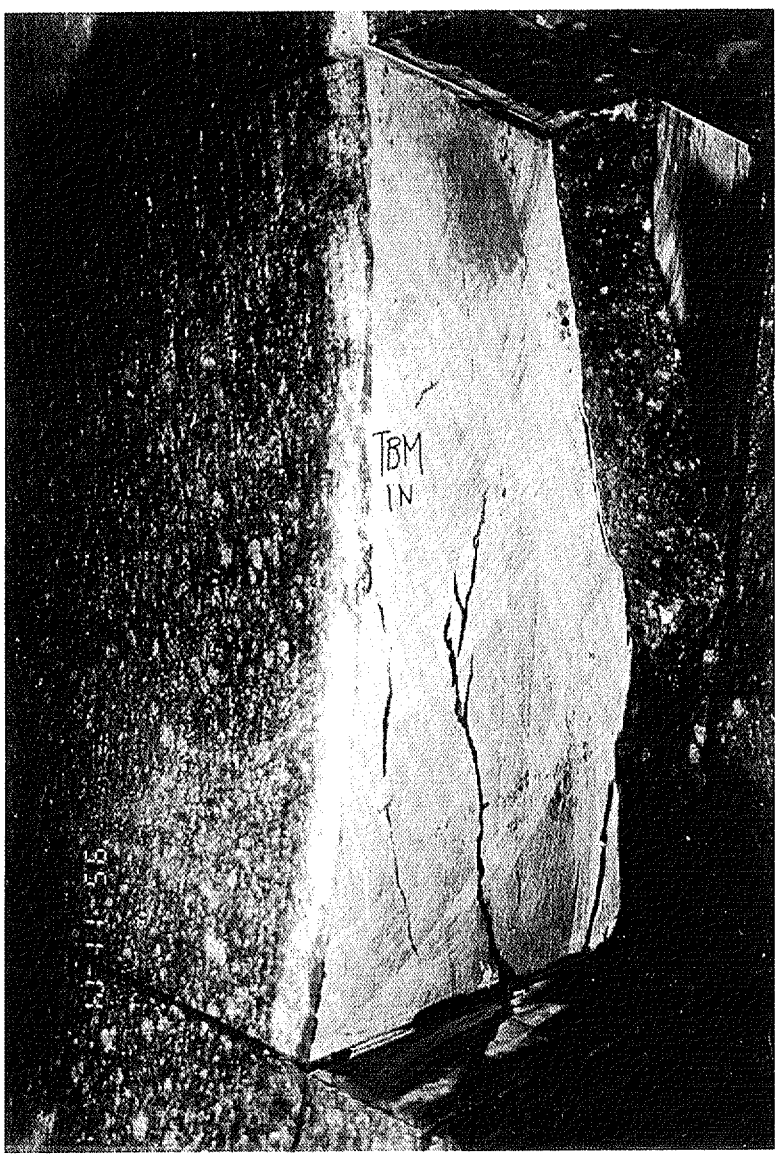

***Figure 5-55**. Section 3213 metres, wall, TBM drift.*

Crack Discrimination in Rock Samples

Rock samples were taken in the TBM drift wall and front and then treated in the laboratory to observe the cracks formed due to excavation (Figure 5-56, Tan *et al.,* 1997). A fluorescent method was used in the discrimination of cracks (Lindqvist *et al.*, 1994). A penetrant was applied on the surface and after treatment the samples were observed under high intensity black light. Photographs of each sample were taken, with an example shown in Figure 5-57 and the depth of the crushed zone, shown as whitish on the photographs and the length of side cracks were measured (Figure 5-58).

A whitish zone of about 2-5 millimetres was generally observed in the samples from the wall. Shallow grooves generated by the cutters were 2-5 millimetres deep and 10-20 millimetres wide. Only a few samples from the wall showed side cracks, 10- 20 millimetres long with a depth range of 2-5 millimetres.

Samples from the face of the TBM drift showed a whitish zone of 5-10 millimetres thick and side cracks were more dominant. The cracks tended to extend along a curved path to the free surface or to intersect with neighbouring cracks. The crack length was 10-60 millimetres and the depth ranged from 20-50 millimetres. The grooves were 10-40 millimetres wide and 2-10 millimetres deep which indicated that the face was subjected to deeper penetration and higher load than the side wall.

Mapping of the half-barrels

Missing and damaged sections of half-barrels from the perimeter boreholes can be used as an indication of damage (Figure 5-59). Mapping of the half-barrels showed an increased occurrence of a crushed zone at the end of the blast holes which can be correlated with priming of the charges using Dynamex cartridges.

A greater proportion of the half barrels were intact for the LSES rounds than for the NS blast rounds with the fraction of crushed zones and radial cracks running along the boreholes more pronounced in the NS design. In the re-blasted rounds highly fractured, almost crushed, sections along the core barrels were often observed. Nearly all of the ends of the core barrels in round R6, which was classified as a major misfire, were fractured. Fractures running along the core barrels were observed to be numerous and extended for the full length of the round. Some of these fractures running along the core barrels are almost perpendicular to the rock wall.

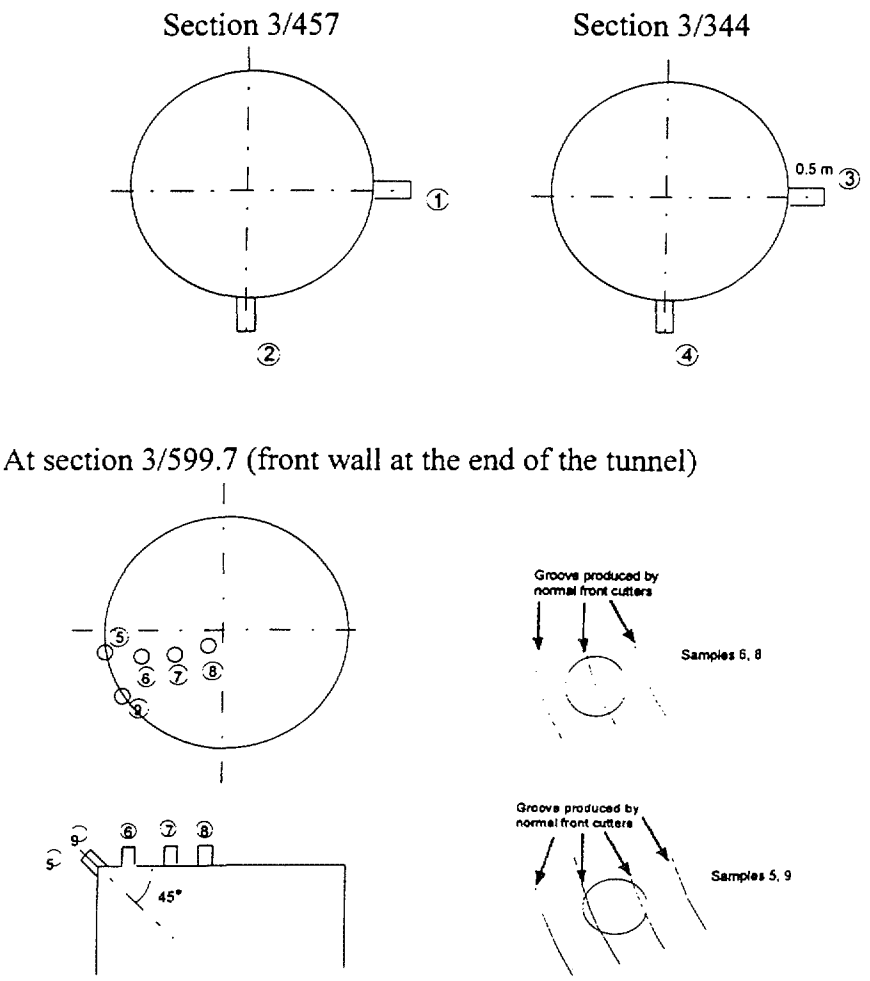

***Figure 5-56**. Sampling points from the TBM drift.*

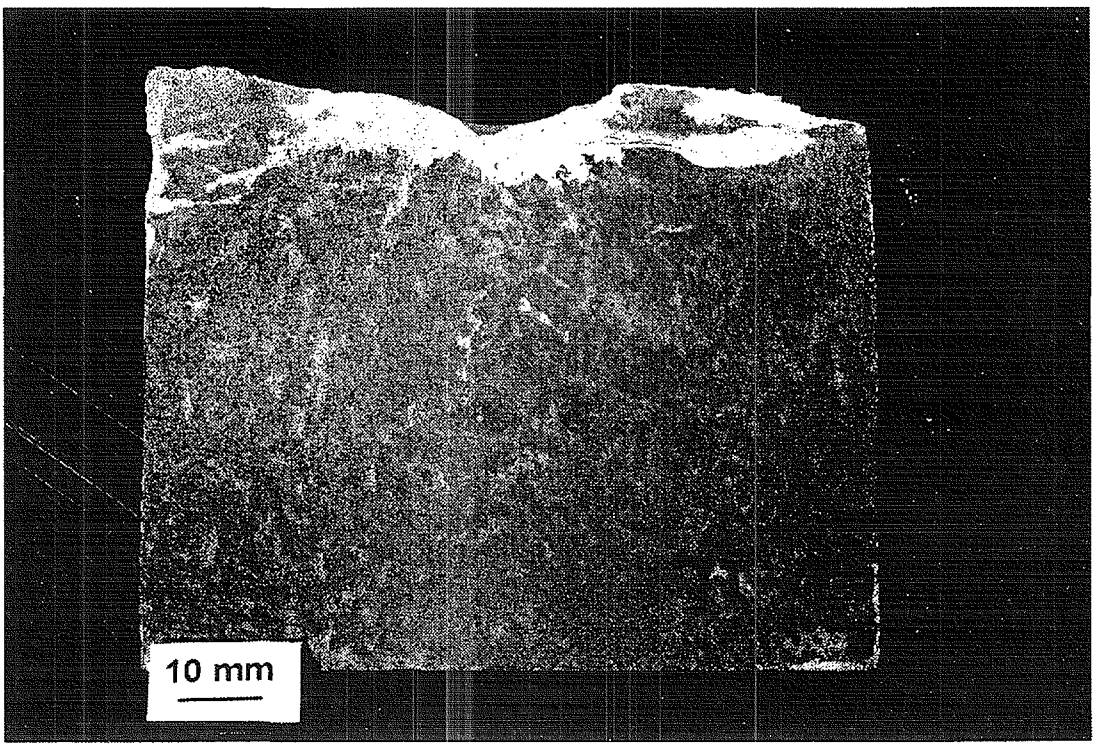

Figure 5-57. *Cracks observed from samples taken in the wall of TBM tunnel.*

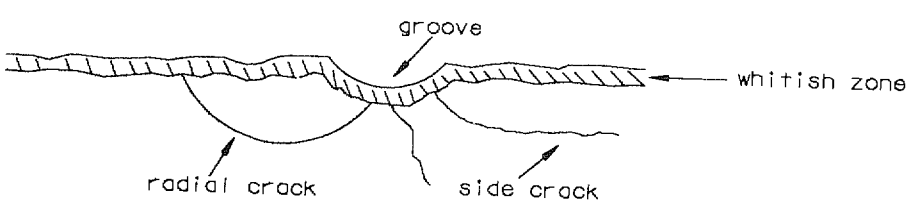

Figure 5-58. *Crack model modified from Lindqvist et al., 1994.*

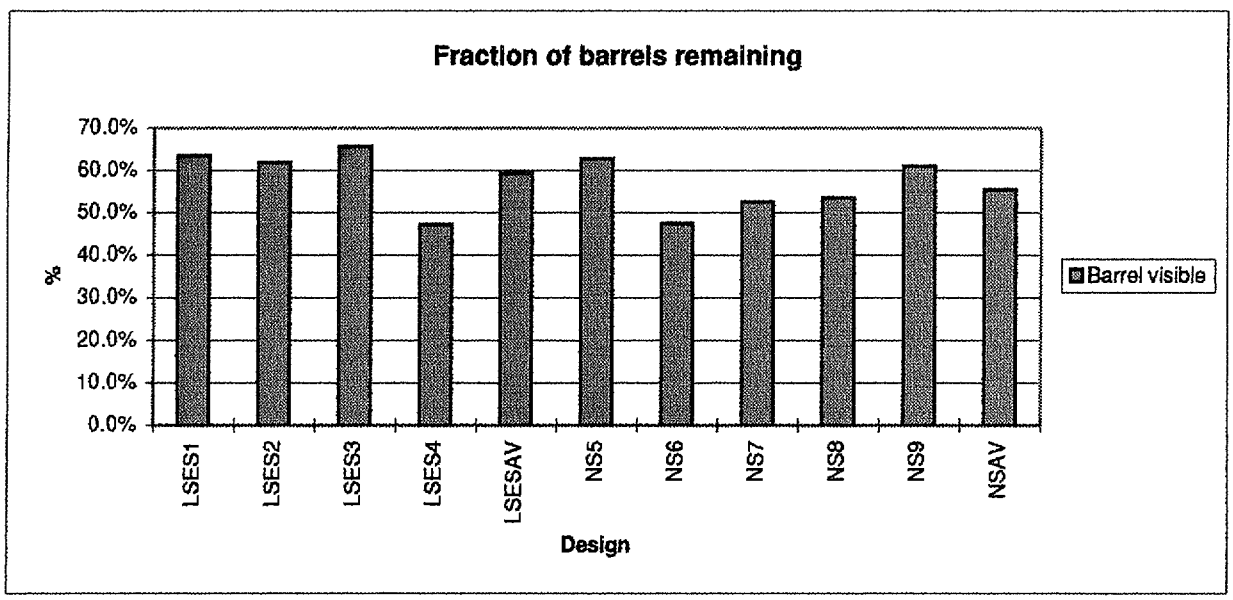

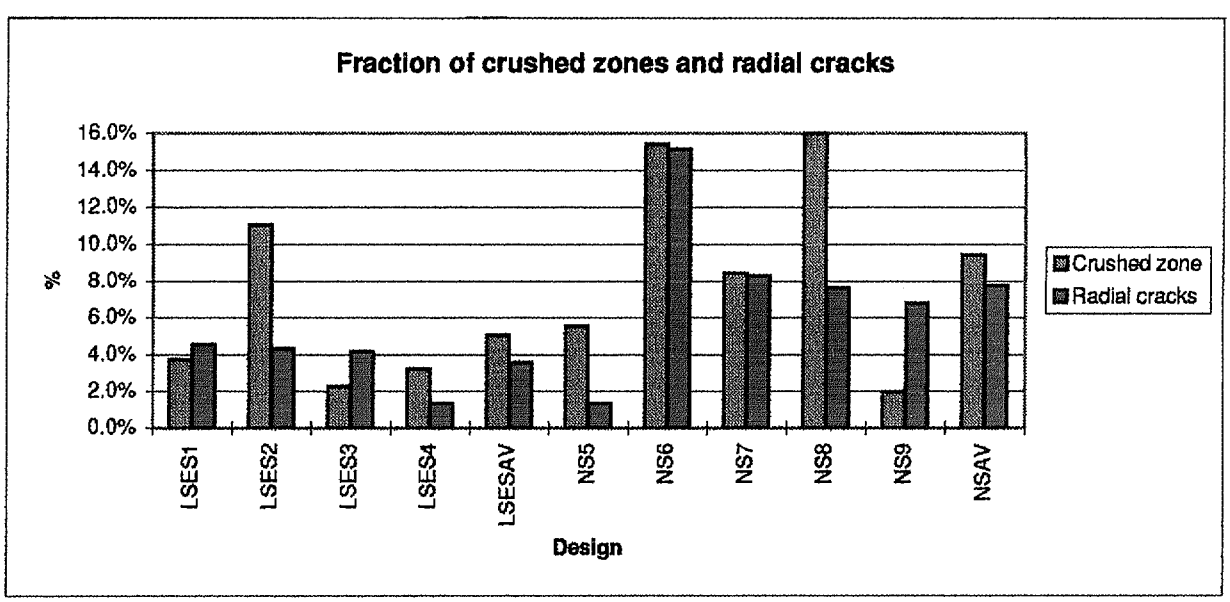

Figure 5-59. Fraction of barrels remaining and proportion of crushed zones and radial cracks along the barrels.

5.4 DISTURBED ZONE EFFECTS AND OBSERVATIONS

5.4.1 Acoustic Emissions

As discussed in Section 5.3.1 most of the AE activity was located within a thin skin of damage immediately surrounding the drift walls. However, a "second set" of AE events was recorded that were located further away from the drift walls and these were often found to occur in clusters of activity with some of this activity extending well into the disturbed zone. Examining the events from monitoring while the TBM was stopped 15 metres from its starting point, it can be seen that some of the events were located several metres from the drift (Figure 5-60) and were isolated from the main data set. Best fit planes were generated through the clusters, in three dimensional space, with two planes being determined (Figure 5-61). These planes have the same general direction as the main steeply dipping fracture set shown in Figure 4-5. The best fit planes constructed through the clustered events can be seen to approximately correspond to the position of two fractures mapped in the TBM drift. These more distant events therefore appear to be related to adjustment along existing fractures rather than cracking of intact rock.

It was observed that many of the more distant events from the drift surface were the highest amplitude events within the data set. Source mechanism modelling studies of three of these distal high amplitude events showed that the sources were consistent with shear-slip on a plane parallel to the predominant fracture direction at Äspö.

Other evidence of re-adjustment of fractures was seen from displacement results and may be tentatively concluded from the hydraulic tests results. The hydraulic tests in boreholes situated well away from the drifts suggested that there were changes in hydraulic conductivity in 13% of the tests associated with the D&B drift excavation and possible detectable changes were evident in 16% of the tests associated with the TBM drift. These changes may be attributed to opening and closing of some of these large, individual fractures. Furthermore, MPBX measurements showed inelastic displacement across certain fractures.

As was demonstrated from the factor of safety analysis for a plane parallel to the main fracture set (Figure 5-5), slip would be expected to occur extending out to distances over 3 metres from the drift at some locations. Many of the AE events away from the drift fall within the regions indicated in Figure 5-5 as having $FOS<1$. The stress models used in this analysis did not account for the additional stress perturbations around the fractures themselves. This may explain why we appear to have slip occurring further from the drift than predicted by stress modelling.

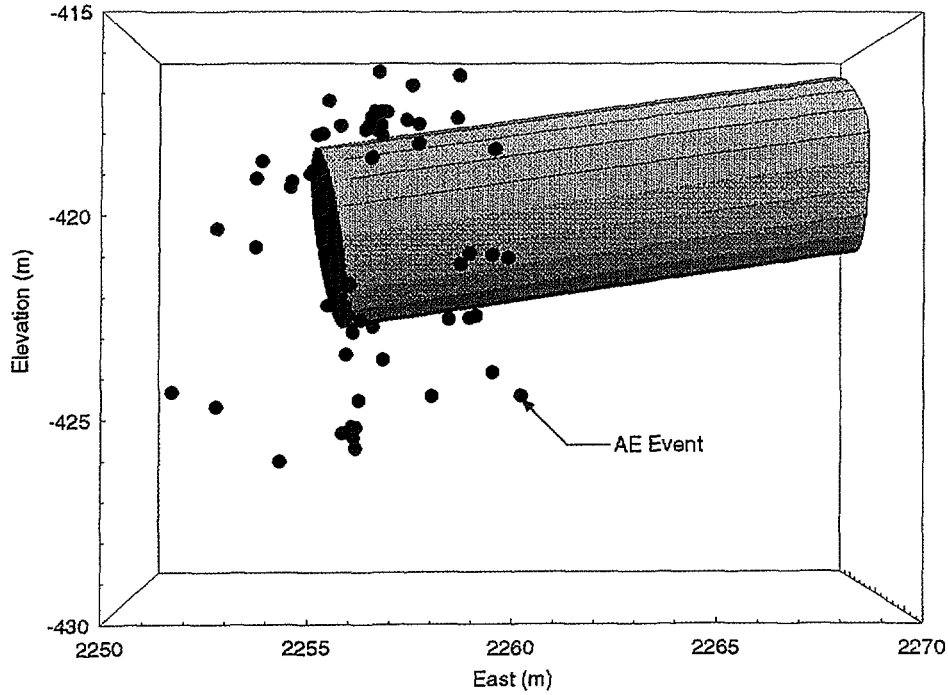

Figure 5-60. *Acoustic emission events recorded with the TBM stopped at 15 metres.*

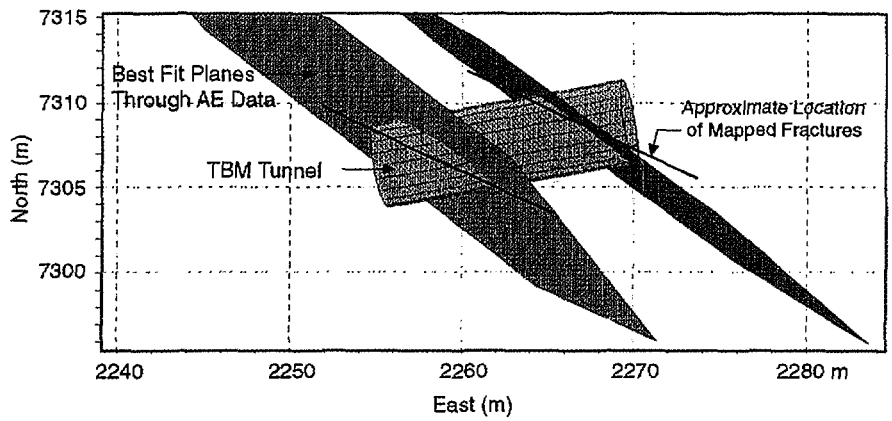

Figure 5-61. *Best fit planes through the clustered acoustic emission events recorded with the TBM stopped at 15 metres.*

5.4.2 Seismic Measurements

Tomography

Tomographic surveys were undertaken on two planes around the TBM drift and four planes around the D&B drift and the resulting data were inverted to produce P- and S-wave velocity tomograms and attenuation tomograms, Figure 5-62 provides an example of one of the P-wave tomograms. The tomographic surveys were undertaken both before and after excavation with the exception of the B1-B3 plane, as these boreholes were drilled after the excavation of the D&B drift.

In both the horizontal C4-C5 plane and the vertical C6-C7 plane around the TBM, there were no significant differences in the average velocity or anisotropy between the measurements made before and after the excavation of the drift. P-wave velocity difference tomograms were produced that showed changes of up to $\pm 30\ ms^{-1}$, however, the resolution of the technique was only about $\pm 100\ ms^{-1}$. Similarly the measurements made around the D&B drift showed no significant differences in the average velocities or anisotropy between the measurements made before and after the excavation of the D&B drift.

The mean P- and S-wave velocities and velocity variations calculated for each image plane acquired before and after excavation are listed in Table 5-9. After excavation, the reconstructed velocity images are seen to have the same values for mean velocities and variation as those images produced prior to excavation. Figures 5-63 and 5-64 show the spatial trends in P- and S-wave velocity for all horizontal tomographic planes.

Table 5-9. Average velocities and velocity spread in the tomographic sections.

Section	V_P before excavation (ms^{-1})	V_P after excavation (ms^{-1})	V_S before excavation (ms^{-1})	V_S after excavation (ms^{-1})
C4-C5	6060±100	6060±100	3460±120	3460±120
C6-C7	5960±100	5960±100	3390±150	-
A4-A5	6060±100	6060±100	3490±100	3490±100
A6-A7	6260±100	6260±100	3520±100	3520±100
B4-B2	6060±100	6060±100	3490±100	3490±100
B1-B3		5880±100		3330±100

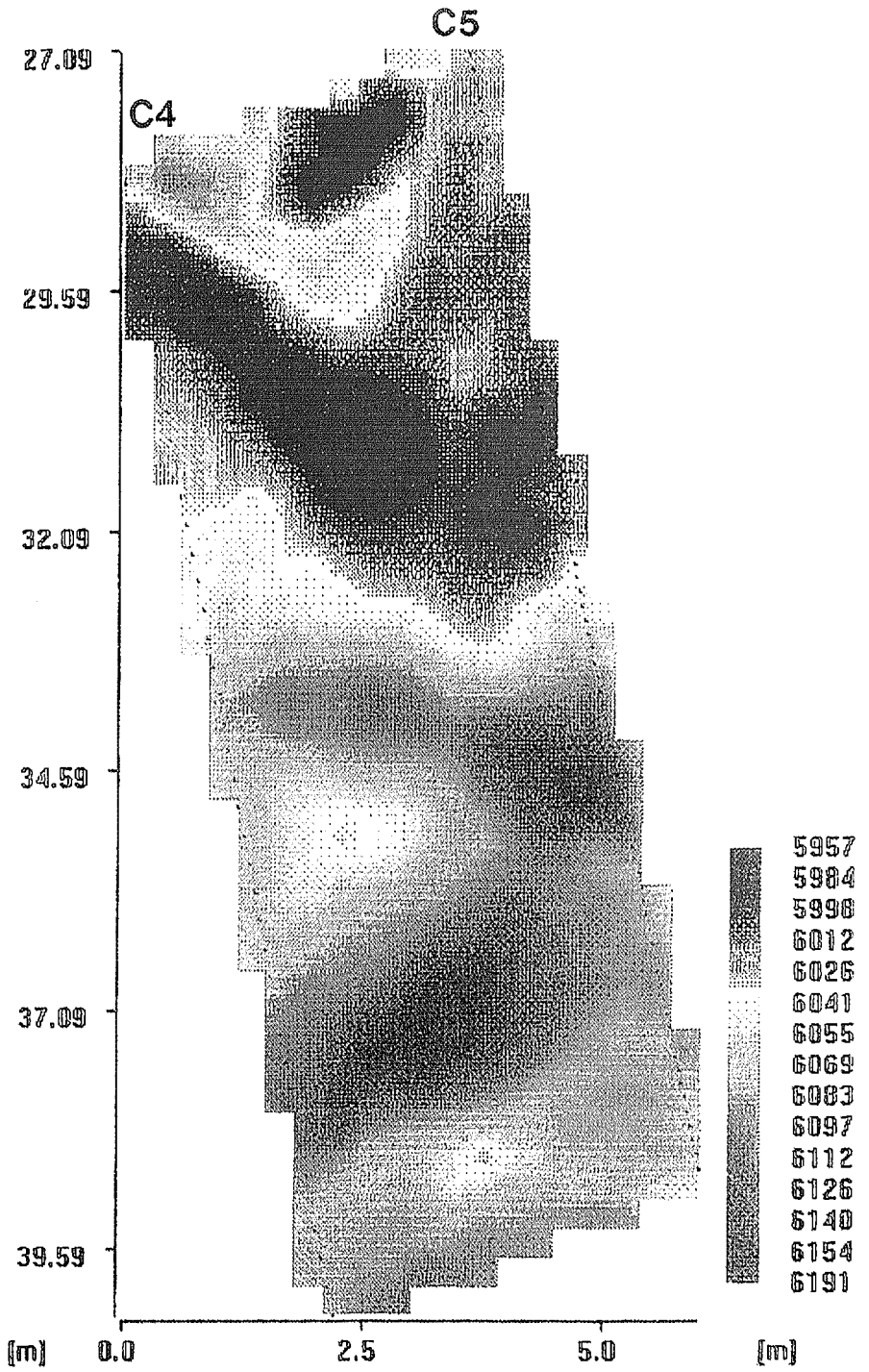

***Figure 5-62**. P-wave velocity tomogram for the horizontal plane between boreholes C4 and C5 before excavation.*

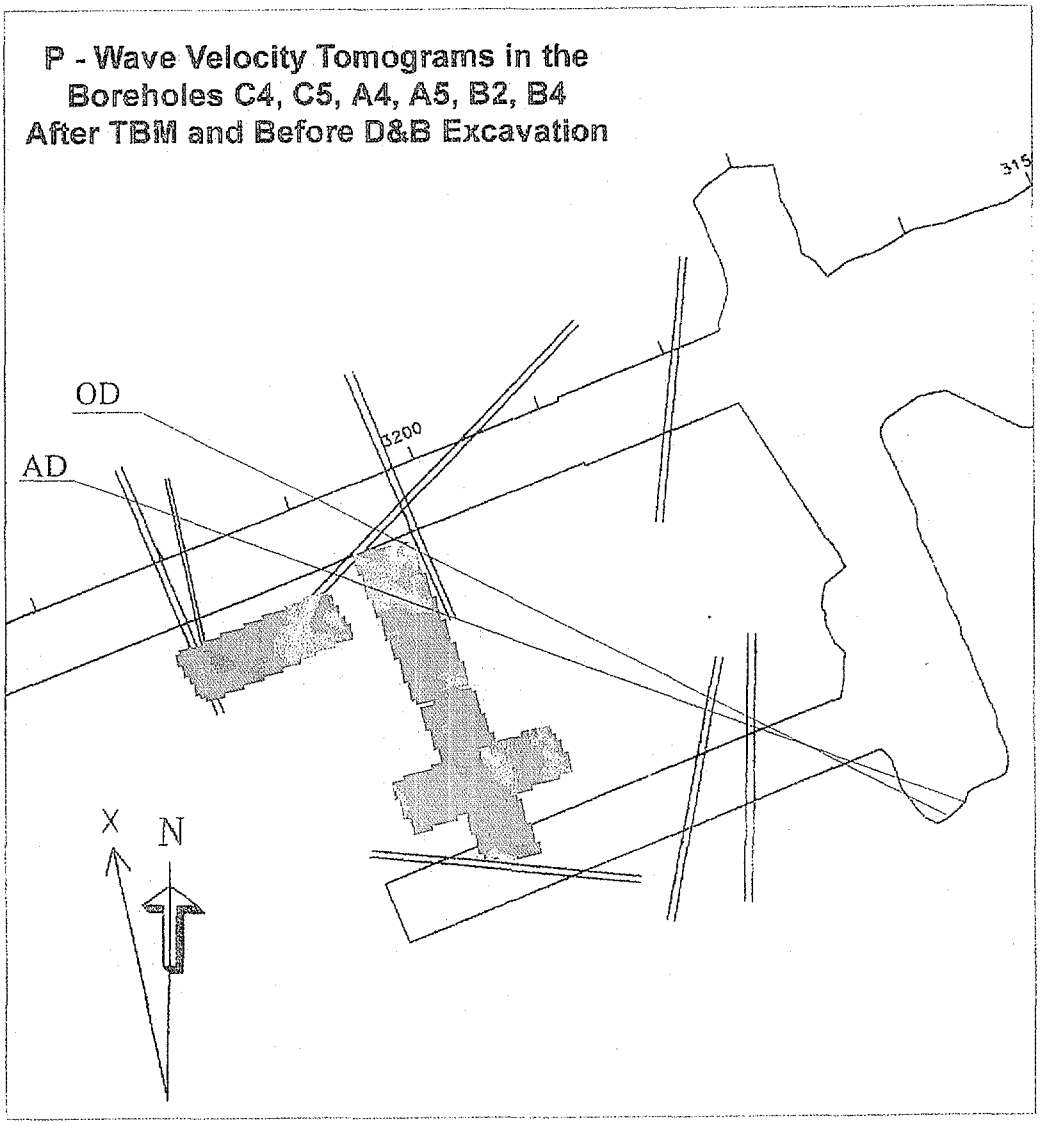

***Figure 5-63**. P-wave velocity tomograms in the boreholes A4-A5, B4-B2 (D&B and TBM) and C4-C5 after TBM and before D&B excavation. The colours do not indicate specific velocities and only the patterns should be considered. AD and OD are the interpreted more significant fractures observed in the drifts. Dykes of fine grained granite are shown by parallel lines.*

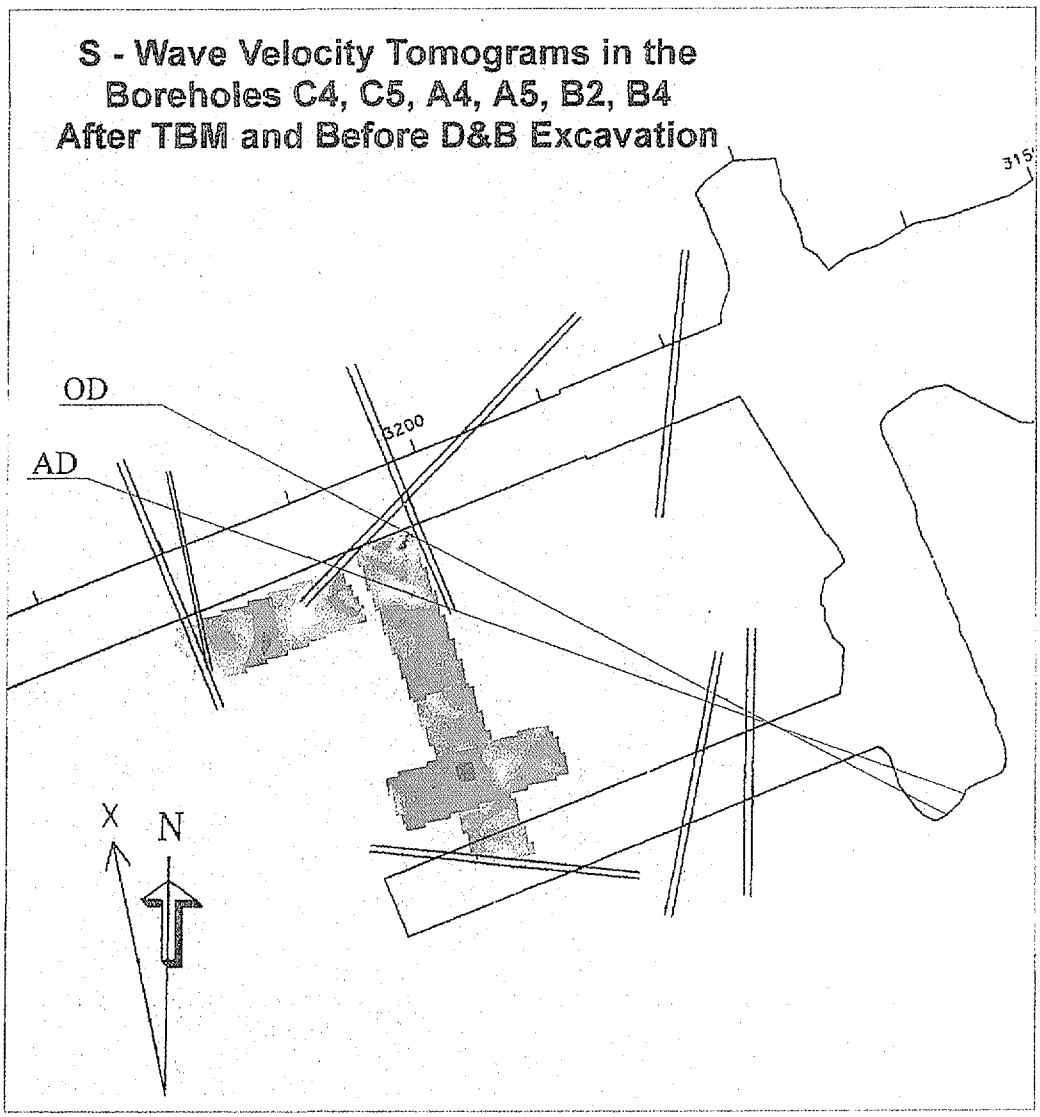

Figure 5-64. *S-wave velocity tomograms in the boreholes A4-A5, B4-B2 (D&B and TBM) and C4-C5 after TBM and before D&B excavation. The colours do not indicate specific velocities and only the pattern should be considered. AD and OD are the interpreted more significant fractures observed in the drifts. Dykes of fine grained granite are shown by parallel lines.*

It has not been possible to measure the effects of excavation using the seismic tomography method because the boreholes, forming the tomographic sections were further from the drifts than the interpreted extent of the damaged zone and were therefore within the disturbed zone. As the planes were too far from the drifts velocity changes should not have been determined and this is in agreement with the results presented in Table 5-9. This conclusion indicates that there are no material property changes occurring in the disturbed zone and whilst the measurements indicate a negative result, a positive conclusion may be drawn from these observations.

The exception to these observations, in terms of being within the damaged zone and imaging a low velocity zone, are the sections produced for the radial boreholes and sections B1-B3 and B4-B2. Inspection of these images, which commence in the damaged zone and transect the disturbed zone and continue into the virgin rock mass, suggests the presence of a low velocity zone between 0.5 and 1.5 metres from the wall of the drift (Figure 5-65 and 5-66). Interpretation of such images have to be treated with caution as the ray coverage in the area close to the drift wall is low and because this zone has been imaged at a lower resolution compared to the central portions of each tomographic image. The low velocity zone occurs in an area that was not imaged by the axial boreholes, which were located more than 2 metres away from the drift wall and therefore, it is not unexpected that tomographic images for these sections do not show any change in velocity resulting from the excavation.

Further, the P-wave velocity surveys made in conjunction with the AE survey indicated a drop in the average P-wave velocity as the TBM progressed of only about 5 ms^{-1} for several rays passing within 1 to 2 metres of the drift perimeter (Figure 5-67). The velocity change were of the order of 10 ms^{-1} for ray paths 1 to 2 metres from the D&B drift walls.

The three dimensional velocity measurements associated with the acoustic emission measurements showed a consistent pattern of velocity anisotropy, to those from the tomography surveys, with the fastest direction of V_P = 6063 ms^{-1} in the near vertical direction. In the horizontal plane the intermediate velocity axis (V_P = 5993 ms^{-1}) was oriented NW and the slow velocity direction (V_P = 5902 ms^{-1}) was oriented NE. The slow velocity direction is approximately normal to a common NW striking near vertical fracture set.

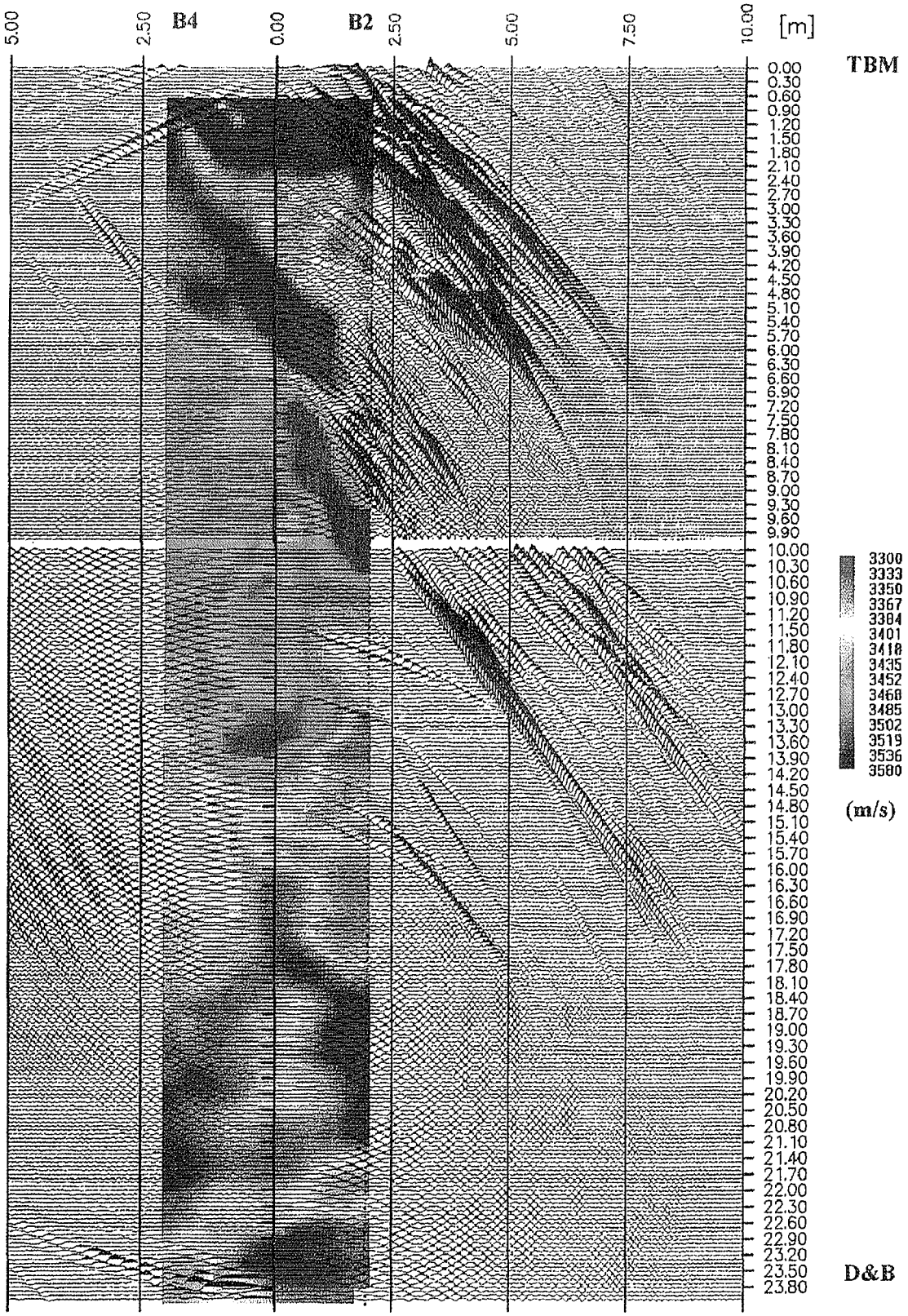

Figure 5-65. *Transmission and reflection seismic images for the measurements made in the boreholes B2-B4 (D&B and TBM) prior to excavation of the D&B drift.*

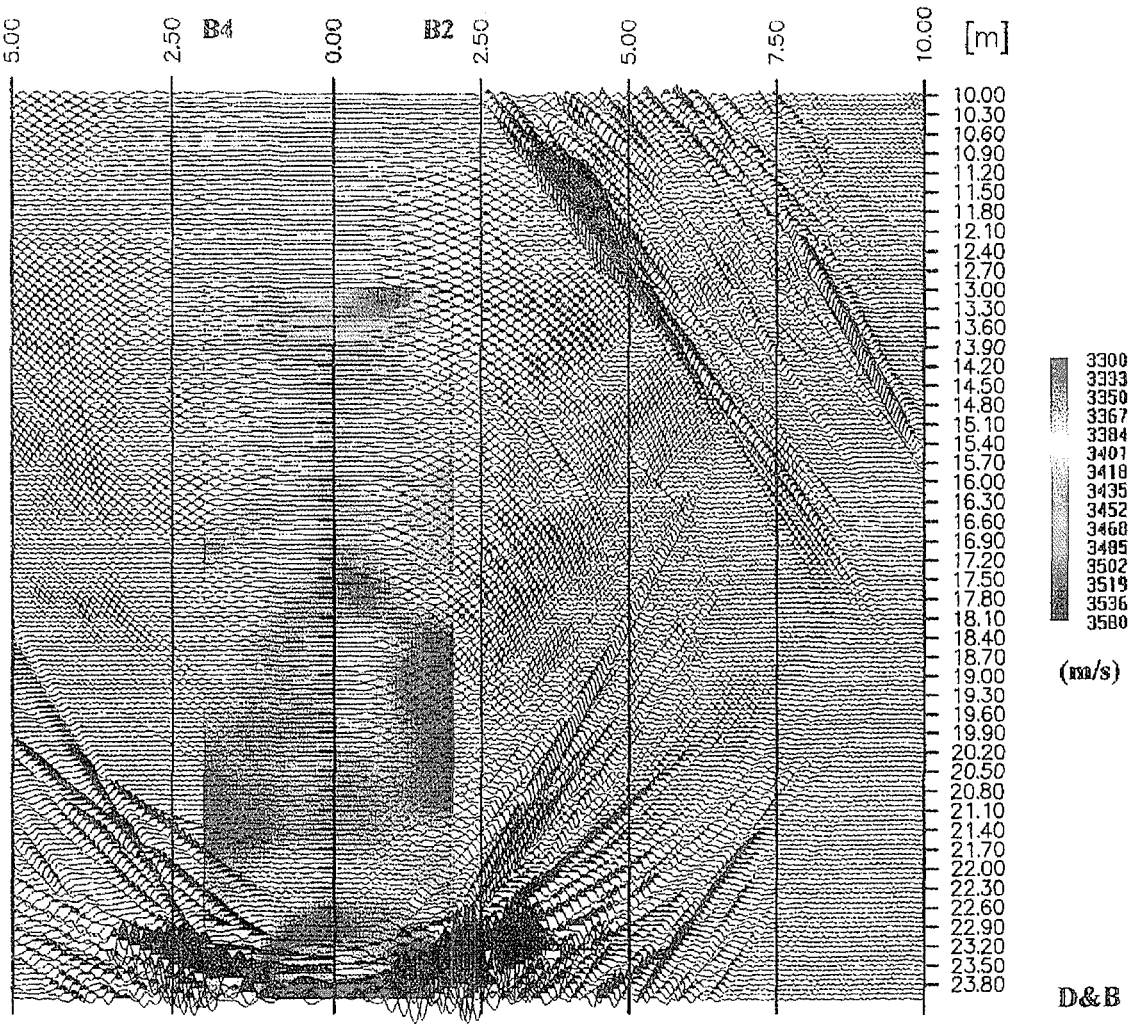

Figure 5-66. *Transmission and reflection seismic images for the measurements made in the boreholes B2-B4 (D&B and TBM) after the excavation of the D&B drift.*

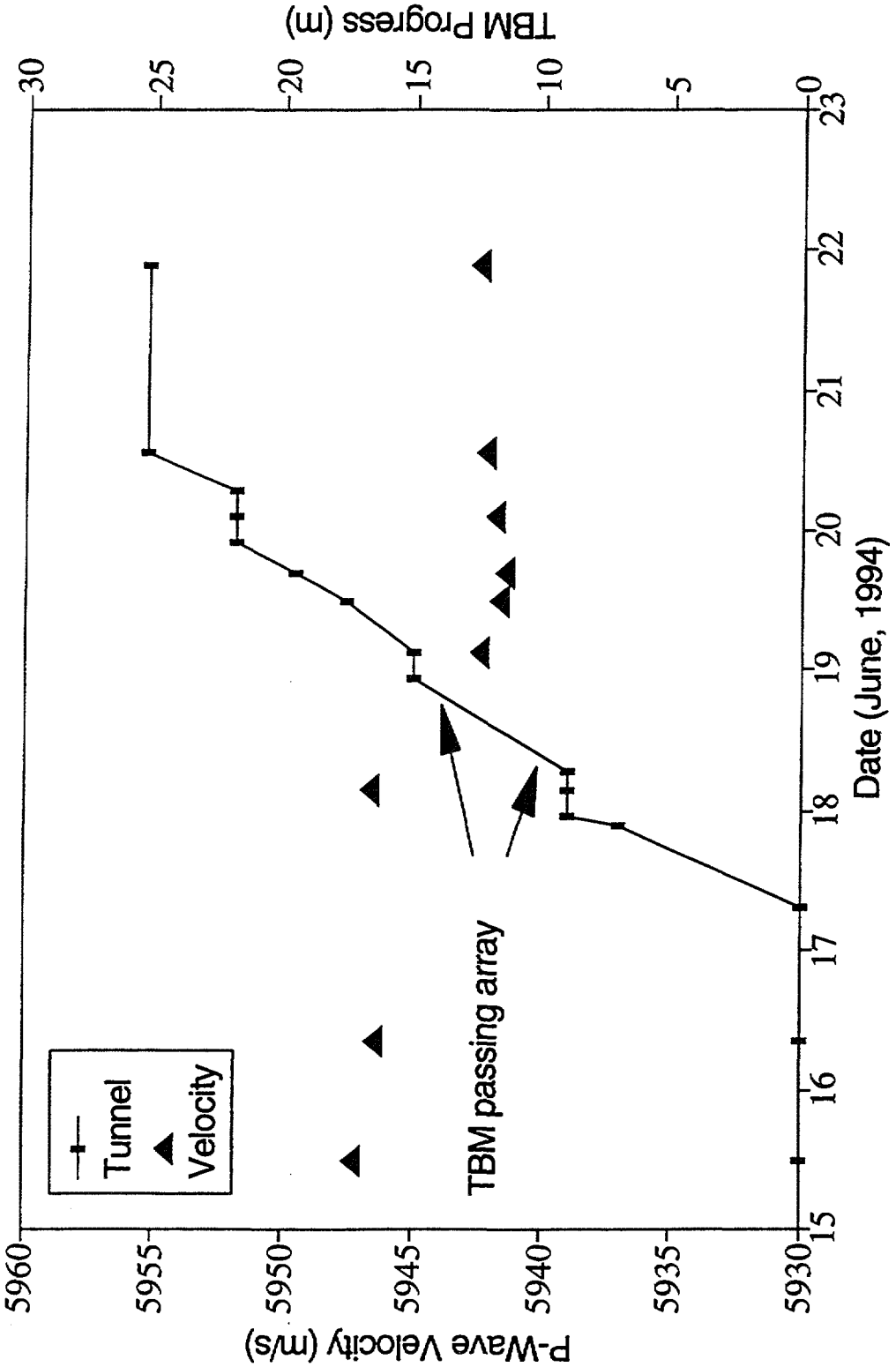

Figure 5-67. *Temporal changes in average P-wave velocity from velocity surveys associated with AE measurements. The drift face position, relative to the starting position of the TBM is also shown.*

Extended Reflection Analysis

Reflection analysis of the crosshole seismic tomographic transmission data sets shows structures and induced changes. The section between boreholes A4 and A5 was chosen which covered an area of approximately 12 x 4 metres close to the D&B drift. Figure 5-68 shows the migrated sections with azimuths of 0° and 180°. The position of the section with respect to the D&B drift and the boreholes is shown in the small index diagram. Two sets of reflectors were imaged, the first set (A) were interpreted to indicate fractures with a direction NW-SE dipping 90°, whilst the second set (B) is nearly parallel to the boreholes. After excavation (Figure 5-69) the reflectors (A) are still observed, whilst the reflectors (B) are not imaged and it may be interpreted that these were related to that part of the rock mass which was subsequently excavated. The major event in the section acquired after excavation is the reflection from the drift wall (T). Some weaker reflections (W) are also present and these may be due to fractures around the drift. The weak reflections at 2.5 metres from the median line seen before and after excavation, are possibly artefacts produced by the tail of the direct shear-wave.

Conclusions of Disturbed Zone Velocity Measurements

The velocity distribution in the disturbed zone appears to be smooth with no indications of any changes in the seismic properties resulting from the excavation of the two drifts.

The seismic measurements undertaken in the short radial boreholes provide additional information on the disturbed zone velocities. The pertinent velocity data derived from the measurements performed in the short radial holes, rounded to 100 ms^{-1} are given in Table 5-10 together with the average disturbed zone velocities from the tomographic surveys. The intact rock is well characterised having a P-wave velocities of 5900 to 6100 ms^{-1} and S-wave velocities of the order of 3500 ms^{-1}. It can be seen, that from the borehole logging (Downhole, Mini-sonic (low frequency), Micro-velocity logging (high frequency) (Section 5.3.2) that slightly lower velocities were obtained in comparison to those derived from the crosshole tomographic methods. This may be a function of resolution but it may also reflect drilling induced damage close to the borehole walls. Such local damage will have an insignificant influence on the average velocities derived from the crosshole methods as this will be small in comparison to the full ray path length.

Table 5-10. Summary of Disturbed Zone Velocity Measurements.

	TBM V_P (ms^{-1})	TBM V_S (ms^{-1})	D&B V_P (ms^{-1})	D&B V_S (ms^{-1})
Downhole logging	5900		5900	
Mini-sonic logging (low frequency)		3100		3100
Micro-velocity logging (high frequency)	6150	3200	6150	3200
Refraction seismics (aver)	6000		5800	
Velocity (max.)	6200	3600	6200	3600
Velocity (min.)	5600	3000	5600	3000
Radial hole tomography	6000		5940	3450
Disturbed Zone tomography	6060	3500	6060	3500

The anisotropy information and directions derived from the different measurements performed are summarised in Table 5-11. Generally the fast direction seen in the disturbed zone velocity field is NW-SE dipping and is steep to almost vertical.

Table 5-11. Directions of the maximum disturbed zone velocity field as derived from the various methods utilised.

	Fast Direction	Dip	P-wave velocity max ms^{-1}	S-wave velocity max ms^{-1}	Degree of Anisotropy
TBM					
Anisotropy	NW-SE	steep	6200	3600	5-10%
Radial hole tomography		vertical	6100	3550	2%
Disturbed zone tomography	NW-SE	steep	6200	3580	6%
D&B					
Anisotropy	NW-SE	moderate	6200	3600	5-10%
Radial hole tomography			5940	3450	0%
AE	NW-SE	steep	6060		2-3%
Disturbed zone tomography	NW-SE		6200	3580	2-6.5%

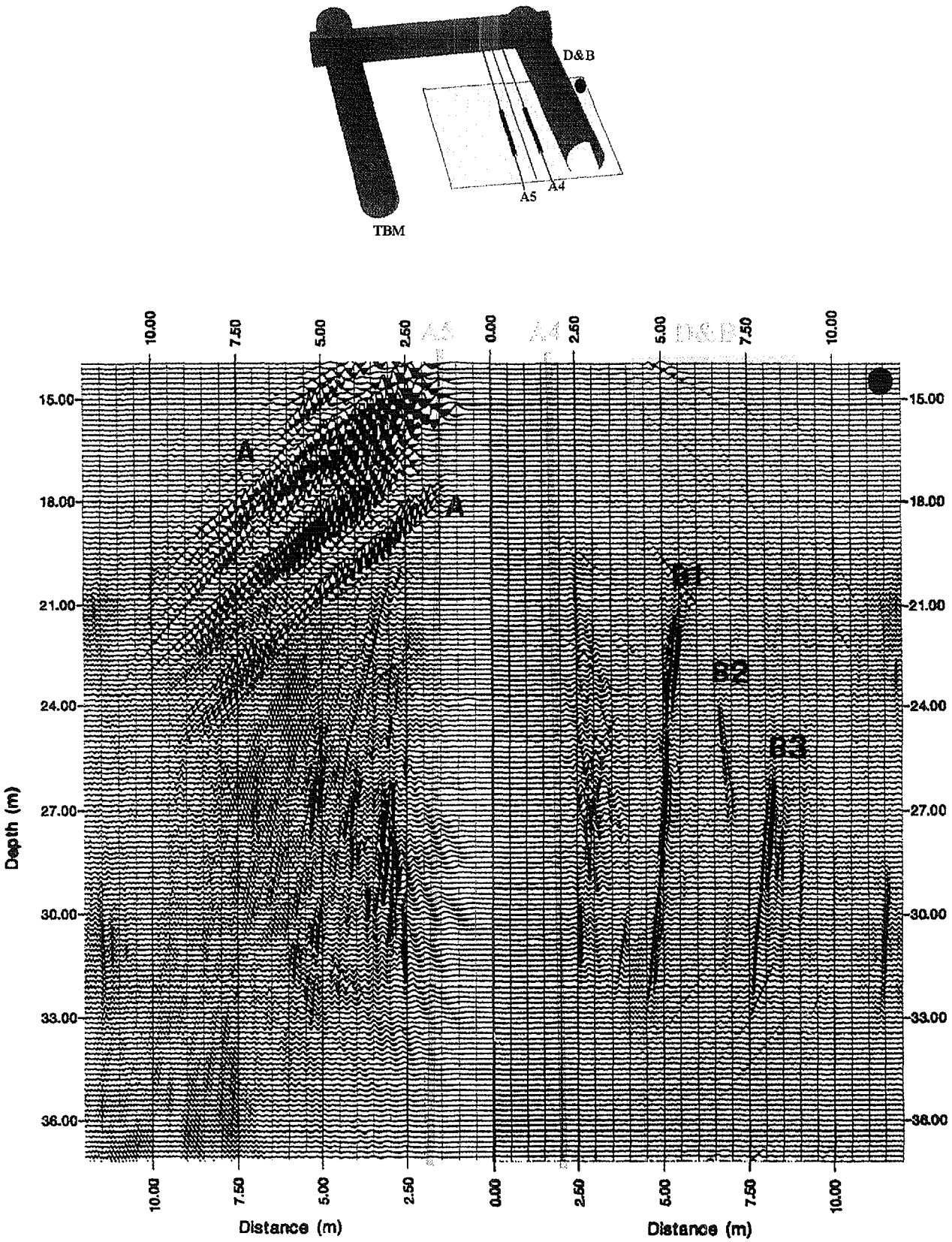

Figure 5-68. *The migrated sections before excavation. The index diagram shows the position of the sections with respect of the boreholes. The small dots indicate the orientation.*

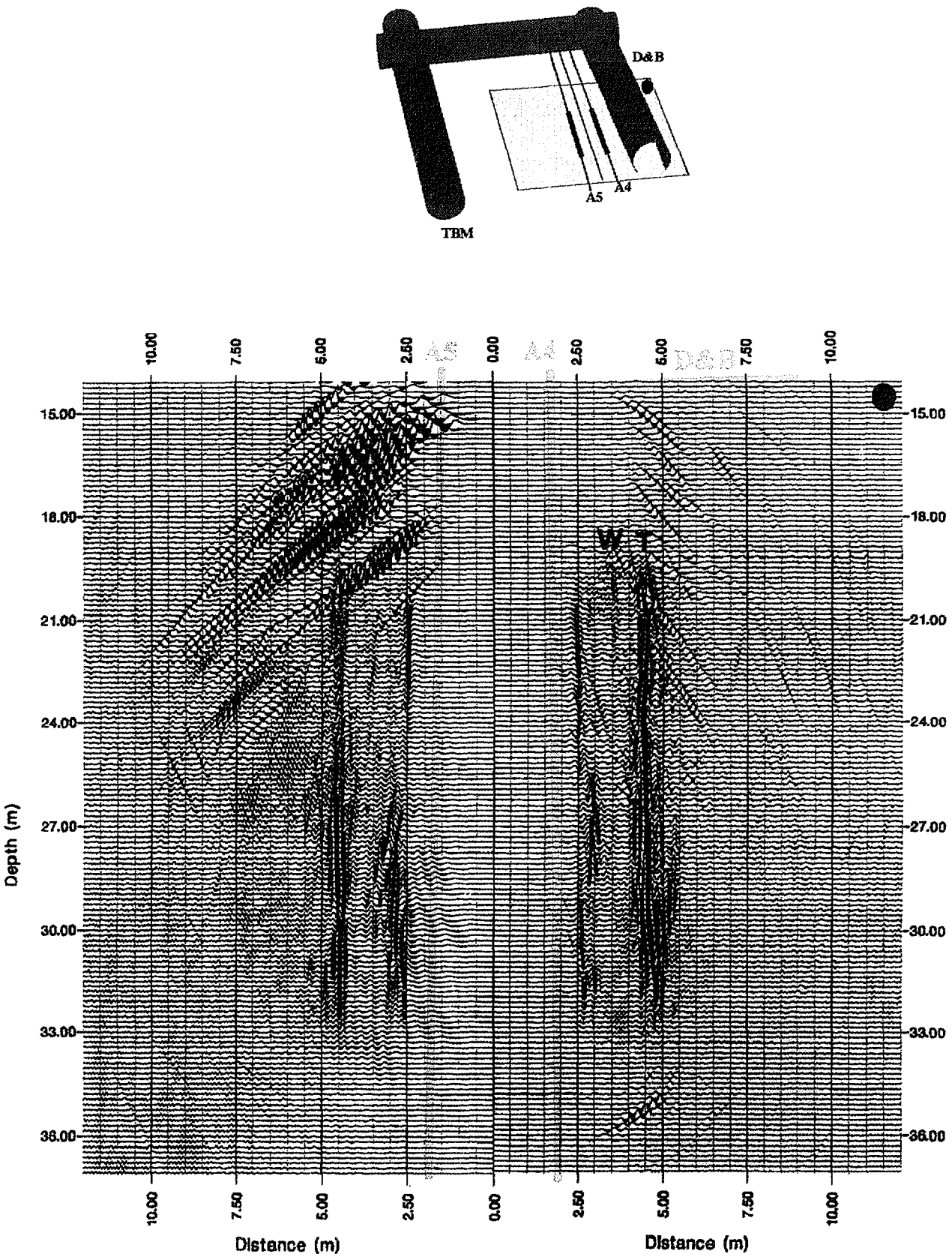

Figure 5-69. The migrated sections after excavation. The index diagram shows the position of the sections with respect of the boreholes. The small dots indicate the orientation.

The reflection analysis of the crosshole seismic transmission tomography data provides valuable information on the fractures of the rock and to some extent also provides an indication of changes in the rock mass in the close proximity of the drifts. These data may be interpreted to show that some fractures must have been within the rock mass excavated during the excavation of the D&B drift and that some fractures are close to the later walls of the drift. This may explain some of the low velocity zones found by logging the short radial holes in the D&B drift.

5.4.3 Hydraulic Measurements

Pressure build-up tests

In order to evaluate changes in hydraulic properties of the rock in the vicinity of the drift excavations, hydraulic borehole testing were performed before and after excavation in the following boreholes:

- boreholes B2 and B4: long radial boreholes, drilled from the TBM drift slightly up gradient, perpendicular to the drift axis and towards the D&B drift. No fractures were encountered, shown by core logging and no water outflows were observed during drilling.

- boreholes C4 and C5: long axial boreholes, drilled parallel to the TBM drift, slightly down gradient. C4 is 1.8 metres from the drift wall and C5 was slightly divergent and at its closest was 5 metres from the drift. Both boreholes encountered large outflows during the drilling (17 l/min in C4, 72 l/min in C5) and were grouted and re-drilled.

- boreholes A4 and A5: long axial boreholes, drilled parallel to the D&B drift, slightly down gradient. The lateral distance of A4 was 1.6 metres, A5 is slightly divergent and at its closest was 5 metres from the drift. The measured outflow from boreholes A4 and A5 was 0 and 16 l/min respectively.

A summary of the testing programme is presented in Table 5-12. Testing prior to excavation was performed a few days before the start of excavation work, with the tests being repeated approximately 2 to 3 months after the excavations. An alternative method, difference flow measurements, was performed about 4 to 11 months after excavation.

The hydraulic packer tests were performed as pressure build-up tests with a double packer configuration using an interval length of 3.5 metres for boreholes A4, A5, C4 and C5 and 1 metre for boreholes B2 and B4 (this configuration utilises two packers to packer off a section of the borehole, the test section also termed the test interval, which was either 1 or 3.5 metres in length). The equipment consisted of a double packer system with a downhole shut-in valve. The pressure was measured in the test section (P1) and in the connected sections above and below (P3). The difference in drawdowns in tests before and after excavation was sometimes over 200

metres and may cause significant stress effects in the wellbore vicinity and affect the comparison of hydraulic properties.

Table 5-12. Summary of hydraulic testing programme

Borehole/ Length	Orientation /Location	Number of intervals		Hydr. Packer Testing		Difference Flow Meter	
		Before	After	Before	After	Before	After
A4 40m	parallel to D&B	9	9	8	9	-	8
A5 41m	~parallel to D&B	10	10	10	10	-	10
B2 26m	long radial, from TBM	7	7	(7)*	5	-	-
B4 15m	long radial, from TBM	7	7	(7)*	5	-	-
C4 50m	parallel to TBM	10	10	10	(10)**	-	-
C5 50m	~ parallel to TBM	9	9	9	9	-	9

*: no pressure build-up in all tests

**: failure in 5 tests with no data obtained

Analysis

The main objective of hydraulic testing was to derive a value for the formation transmissivity and this was derived by three different methods.

The first technique is generally referred to as the "straight line" method and is applicable to homogeneous formations showing a cylindrical flow regime. Log-log and semi-log plots are used to diagnose the formation response and if a cylindrical flow response is identified, the transmissivity is calculated from this part of the data set using Jacob's semi-logarithmic approximation of the Theis well function.

Where the "straight line" method was not applicable, the transmissivity was derived from specific capacity, using an empirical linear correlation between the specific capacity and the formation transmissivity. The specific capacity was calculated by taking the average flowrate from the test interval prior to shut-in, divided by the change in hydraulic head. For the long radial boreholes B2 and B4, only the specific capacity data were evaluated due to lack of pressure build-up data in all tests prior to excavation.

All pressure build-up tests which showed responses beyond the effect of wellbore storage were re-interpreted (Enachescu *et al.*, 1996). This approach consisted of matching the entire data set with type curves that represented an appropriate flow model. Significant features of this approach are, that transmissivity can be derived without the presence of cylindrical flow through extrapolation of transitional data and non-linear regression and, the use of pressure derivative data on the log-log plot as a diagnostic tool to determine an appropriate flow model. The interpretation tool consisted of Golder Associates numerical package FlowDim. Selected tests were also analysed by SSI's Interpret/2™ program.

The first step in the analysis was to determine the best estimate for the input parameters and these are summarised in Table 5-13. Log-log diagnostic plots were computed for all tests with both pressure and pressure-derivative data. The pressure build-up periods were analysed as a shut-in event followed by a single constant rate period. An average rate was used to estimate the formation response during the flow period. Corrected rates were used in the re-analysis due to uncertainties in the rates considered in previous analyses. Borehole history was not accounted for and it is assumed that the test was performed at equilibrium.

Table 5-13. Interval information and input parameters

Parameter	Value	Source
Vertical depth	415.0[m]	measured
Borehole Radius	2.8 10^{-02}[m]	nominal
Interval Length		
A4, A5, C4, C5	3.5 [m]	measured
B2, B4	1.0 [m]	measured
Interval Volume		
A4, A5, C4, C5	8.6 10^{-03}[m^3]	calculated
B2, B4	2.5 10^{-03}[m^3]	calculated
Formation Fluid Temperature	14.0 [°C]	measured
Formation Porosity	0.41 [%]	estimated
Water Viscosity	1.3 10^{-03}[Pa s]	PVT correlation
Formation Volume Factor	1.0 [m^3/m^3]	PVT correlation
Water Compressibility	4.8 10^{-10}[1/Pa]	estimated
Formation Compressibility (rock and water)	1.0 10^{-09}[1/Pa]	estimated
Borehole Compressibility	1.0 10^{-09}[1/Pa]	assumed
Theoretical Wellbore Storage Constant for Shut-in Conditions		calculated from interval volume and assumed borehole compressibility
A4, A5, C4, C5	8.6 10^{-12}[m^3/Pa]	
B2, B4	2.5 10^{-12}[m^3/Pa]	

After examination of the responses on log-log plots, responses of similar formation character were categorised into groups. The comparison of formation responses in tests performed before and after excavation proved to be an important diagnostic feature when evaluating the changes in hydraulic properties due to drift excavation.

Results

The re-analysis of pressure build-up tests by matching all data using least squares regression has produced two major contributions:

- development of an overall understanding of the formation response,
- a semi-quantitative assessment of the confidence limits of the transmissivity values derived from type curve analyses.

The analysis of pressure derivative data on log-log plots is a very useful diagnostic tool; responses with similar formation character were categorised into groups. In many cases, observed changes in formation response in tests after excavation are the sole indicator for a change in hydraulic properties due to excavation. The defined groups of typical formation responses for build-up tests in boreholes A4, A5, B2, B4, C4, C5 are given in Table 5-14.

Table 5-14. Classification of formation responses observed in build-up tests in boreholes A4, A5, B2, B4, C4, C5

Response Type	Comments on log-log plot	Comments on derived T value
1	Response dominated by wellbore storage (WBS)	Data set must be extrapolated to derive T.
2	Response dominated by downward trend in derivative data after WBS and skin effects	T representative for distant formation
3	WBS and skin effects in early time, pseudo-radial flow stabilisation in mid time data	T derived from pseudo-radial flow stabilisation in mid time data.
4	Response dominated by tool effect, must be analysed as pulse	Results directly dependent on assumed WBS.
5	WBS and skin effect in early time, formation response in mid and late time data	appropriate flow model allows a reliable T derivation from the data set.
6	Large tool effect masks any formation response	No analysis possible

The results from the re-analysed pressure build-up tests are summarised for each borehole below and are presented in Figures 5-70 and 5-71. The transmissivity values derived from the re-analysed tests before and after the excavation are summarised in Table 5-15. In non-analysable tests the changes are reported as "not detectable". Some tests may show observable changes, their significance is not obvious and is described as "detectable".

Table 5-15. Summary of results, before and after excavation, of re-analysed pressure build-up tests, boreholes A4 and A5 (D&B)

Interval Top [m]	T [m^2/s] Before	T [m^2/s] After	Log [3] (T_A/T_B)	Response Type [1]		Significance of observed changes [2]
				Before	After	
A4 4.25	-	1.00E-11	-	1	1	not detectable
7.75	9.42E-10	7.26E-10	-0.10	2	5	not detectable
11.25	-	1.52E-10	-	-	1	not detectable
14.75	3.85E-10	1.39E-10	-0.40	4	3	not significant
18.25	6.29E-11	6.80E-11	0.00	4	1	not significant
21.75	3.52E-10	1.38E-10	-0.40	4	2	not detectable
25.25	1.03E-08	6.31E-10	-1.20	3	1	significant
28.75	5.30E-09	1.76E-09	-0.50	3	3	significant
32.25	-	1.29E-10	-	2	4	not detectable
A5 4.25	6.65E-11	1.40E-10	0.32	1	1	not detectable
7.75	1.87E-11	6.13E-10	1.52	1	2	significant
11.25	2.77E-06	3.89E-08	-1.85	5	3	significant
14.75	4.78E-07	3.70E-12	-5.11	3	1	significant?
18.25	1.15E-08	1.48E-10	-1.89	1	1	not detectable
21.75	1.48E-10	-	-	1	6	not detectable
25.25	7.46E-11	1.87E-09	1.40	1	4	not detectable
28.75	7.42E-11	2.92E-09	1.59	1	4	not detectable
32.25	-	3.18E-09	-	2	4	not detectable
35.75	7.01E-11	7.82E-10	1.05	4	4	not detectable

1. Type of response according to the definitions in Table 5-14.

2. Decision on significance is based on changes in both hydraulic properties or/and formation character, taking into account uncertainties in measured rates.

3. Log (T after excavation divided by T before excavation).

Boreholes A4 and A5 (D&B drift)

In A5, in two intervals at 11.25 metres and 14.75 metres depth large inflows were observed prior to excavation and a drastic decrease of flow and derived specific capacity (3 orders of magnitude at 14.75) after excavation (Figure 5-70). The total flow into the borehole dropped from about 1 l/min (before) to 0.19 l/min (after). This can be explained by the proximity of a NW trending fracture.

In A4 the derived transmissivity shows a range between $1\ 10^{-11}$ and $1\ 10^{-8}$ m^2/s. No significant changes in transmissivity were observed after excavation. The changes in hydraulic properties were evaluated as significant in the last three intervals based on formation character, although these tests were dominated by wellbore storage and partly by tool effects.

The transmissivity range in A5 is between $4\ 10^{-12}$ and $3\ 10^{-06}$ m^2/s. Results for tests before and after excavation were available for 8 intervals, of which 5 show an increase of transmissivity after excavation. However, only one of these results was deemed significant due to uncertainties in the rates used and due to tool effects. A significant reduction in rates and transmissivity was observed in two intervals, as above. For the 14.75 metres interval, a transmissivity drop by five orders of magnitude was reported in the re-analysis (Enachescu *et al.* 1996). However, this interpretation conflicts with flowmeter measurements (Figure 5-70).

In summary, 5 of 19 tests performed in boreholes A4 and A5 were seen to show a significant change in hydraulic properties, four show a reduction and one showed an increase in transmissivity in tests after excavation.

B2 and B4 (from TBM to D&B drift)

In boreholes B2 and B4, which showed no fractures and no detectable water inflows, no pressure recovery was achieved in the tests prior to excavation. In the tests performed after the excavation, pressure build-up data were available from the shut-in periods in most of the tests. No interval contained analysable responses for tests both before and after the excavation. Therefore the re-analysis was limited to tests performed after the excavation.

From the 10 tests available, seven were amenable to type-curve analysis. All analysed tests were dominated by wellbore storage and skin effects or wellbore history ("roll over" effect). Therefore, the transmissivity values obtained from the type-curve re-analysis are highly uncertain. As there are no transmissivity data from tests before the excavation, no comparison of derived hydraulic parameters is possible. It is concluded that the long radial boreholes B2 and B4, which were drilled in sound rock without any water-bearing fractures, do not provide any substantial contribution to the hydraulic characterisation of the formation.

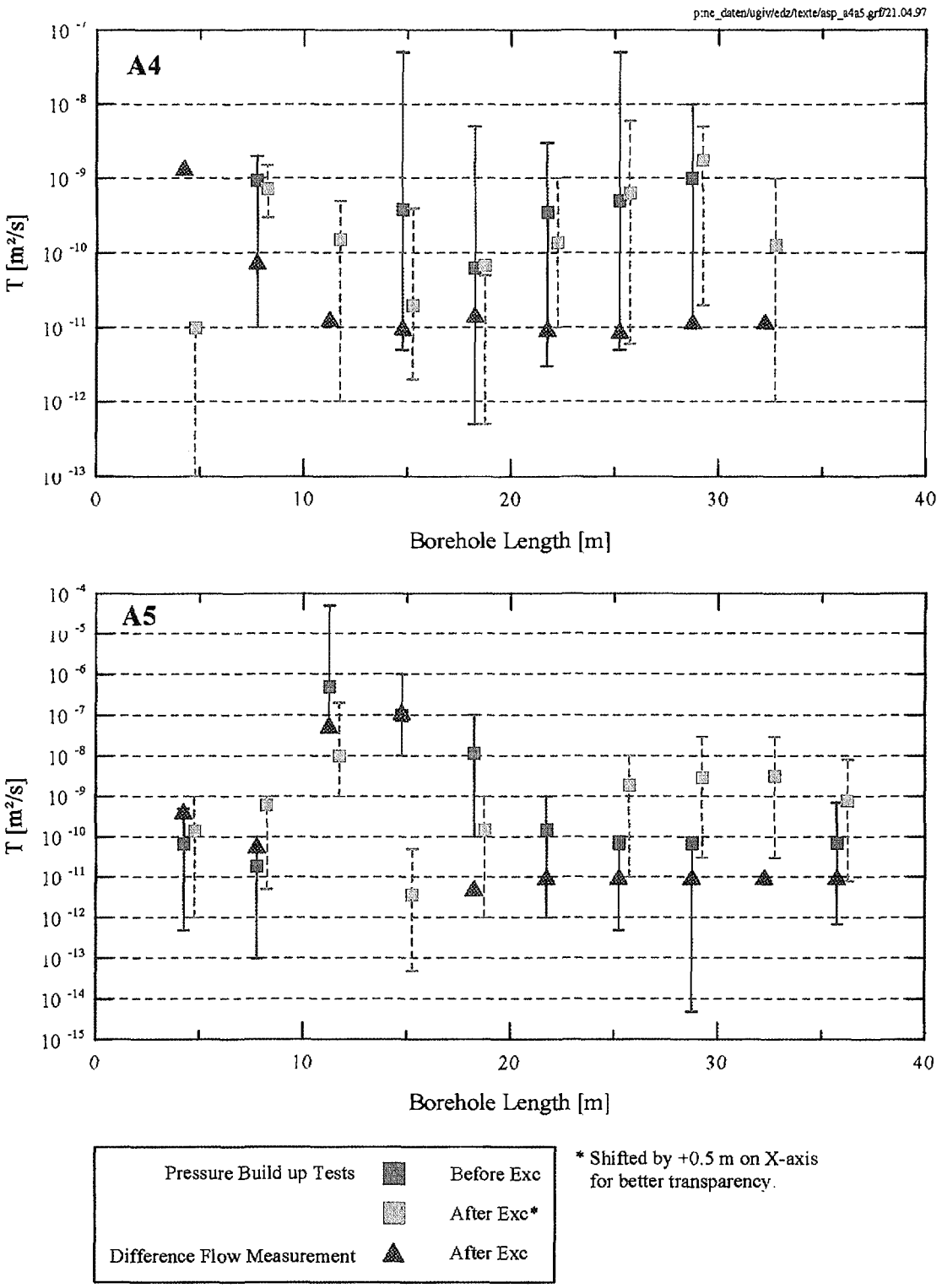

Figure 5-70. *Results of hydraulic testing in boreholes A4 and A5. Transmissivity T with indicated confidence limits.*

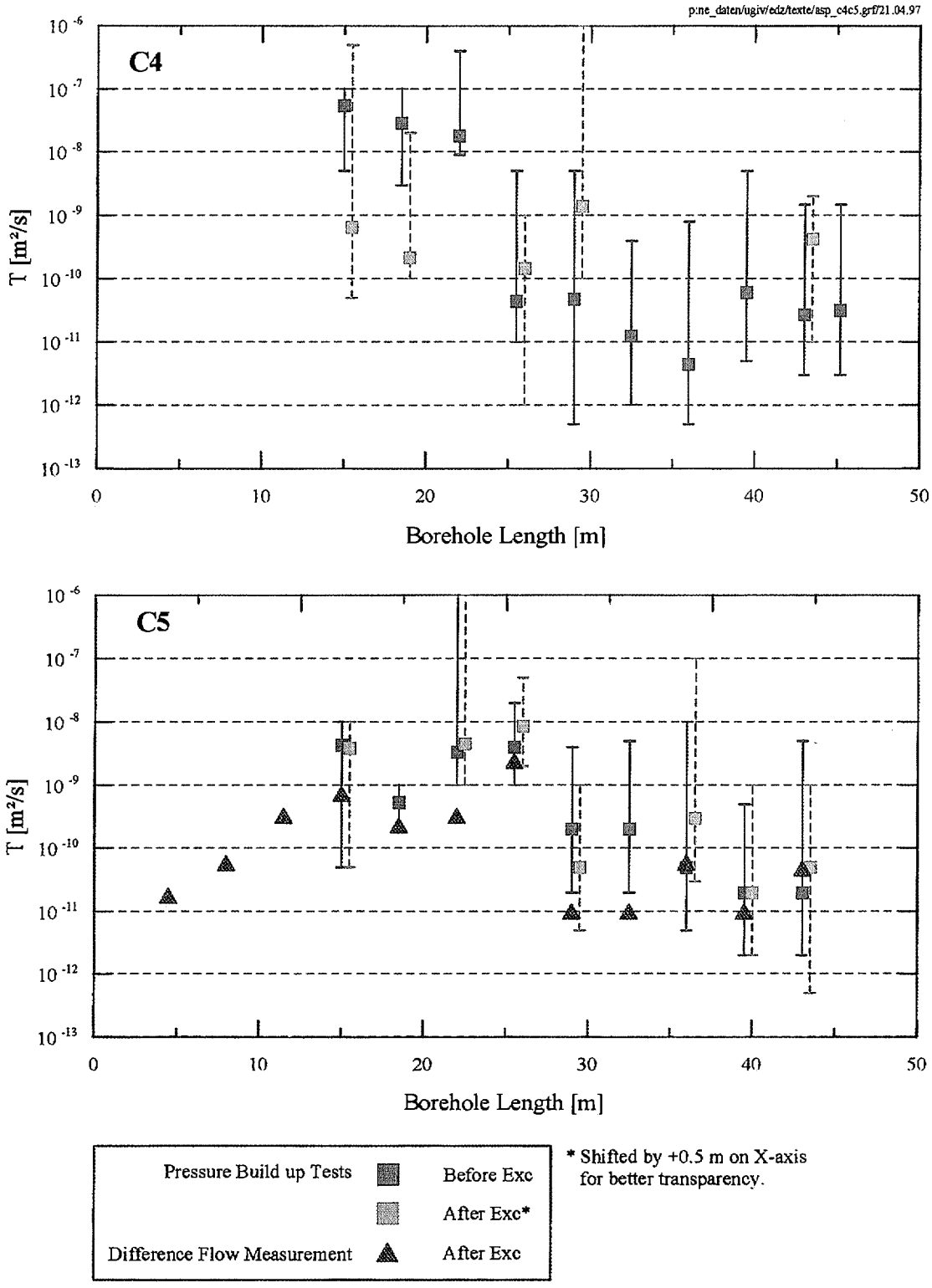

Figure 5-71. *Results of hydraulic testing in boreholes C4 and C5. Transmissivity T with indicated confidence limits.*

C4 and C5 (TBM drift)

Both boreholes produced significant flow during drilling and were grouted and re-drilled prior to testing.

The re-analysis of C4 and C5 build-up data has provided transmissivity values for all tests performed before excavation. In many tests, a high positive skin was selected to match the formation response, which was probably an effect of cementing the borehole. Only a few reliable transmissivity data are available from tests performed after excavation. The results of all re-analysed tests are given in Table 5-16 and presented in Figure 5-71.

Table 5-16. Summary of results, before and after excavation, of re-analysed pressure build-up tests, boreholes C4 and C5

Interval Top [m]	T [m^2/s] Before	T [m^2/s] After	Log [3] (T_A/T_B)	Response Type [1] Before	Response Type [1] After	Significance of observed changes [2]
C4 15.0	5.43E-08	6.60E-10	-1.92	2	2	not detectable
18.50	2.86E-08	2.13E-10	-2.13	2	2	not detectable
22.00	9.43E-09	-	-	5	-	not detectable
25.50	1.15E-09	1.46E-10	-0.90	3	2	not detectable
29.00	4.77E-11	1.39E-09	1.46	1	2	not detectable
32.50	1.90E-10	-	-	3	-	not detectable
36.00	4.26E-10	-	-	3	-	not detectable
39.50	1.11E-09	-	-	3	-	not detectable
43.00	6.85E-10	4.28E-10	-0.20	3	4	not detectable
45.20	7.17E-10	-	-	3	-	not detectable
C5 15.0	4.31E-09	3.83E-09	-0.05	2	2	detectable
18.50	5.34E-10	-	-	5	6	not detectable
22.00	3.31E-09	4.51E-09	0.13	2	2	not significant
25.50	4.00E-09	8.50E-09	0.33	2	2	detectable
29.00	1.58E-09	5.71E-10	-0.44	3	3	detectable
32.50	2.94E-10	-	-	3	4	not detectable
36.00	5.69E-10	-	-	3	2	detectable
39.50	2.40E-10	-	-	3	2	detectable
43.00	2.56E-09	-	-	3	2	detectable

1. Type of response according to definition in Table 5-14.

2. Decision on the significance is based on changes in both hydraulic properties or/and formation character, taking into account uncertainties in measured rates.

3. Log (T after excavation divided by T before excavation).

In C4, no build-up data were available for 5 tests performed after excavation due to a lack of measurable flow. From the five remaining tests, three show evidence for packer bypass and two tests are dominated by tool problems. As a result, no reliable information on transmissivity and on formation response is available from the tests performed after excavation. The significance of observed changes in all C4 test results was qualified as "not detectable" due to technical problems in the tests performed after excavation although this is in part dependent on an interpretation of the bypass events that occurred after excavation (i.e., formation related or equipment related).

In Borehole C5, transmissivity values were derived for 4 out of 9 tests performed after excavation. Only small changes in transmissivity were observed in these tests. Indications for change in formation character were observed in 6 tests, however, no conclusive interpretations could be made in most cases due to ambiguity in the analyses. The changes were classified as "detectable".

Overall, from 19 available test pairs in the boreholes in the vicinity of the TBM drift, no evident significant changes in hydraulic properties were observed. The evaluation was based on interpreted changes in formation response only, given that the derived transmissivity data are not reliable.

To summarise, the re-analysis of all pressure build-up tests using least squares fitting techniques provided useful information on the formation flow model. The responses were categorised into 5 principal types. Changes in formation character in tests before and after excavation are easily identified without being biased by subjectiveness involved in derivation of parameters. In particular, the large uncertainty in the flow rates used in the tests made it difficult to give conclusive statements on changes of hydraulic formation properties based exclusively on the derived transmissivities. In many cases, the determination of hydraulic properties was based solely on the response character. In tests where transmissivity changes could be evaluated with reliable rate data, about 80% of results show a reduction in transmissivity after excavation.

Difference flow measurements

This alternative technique was employed for the first time in underground conditions in boreholes A4 and A5 and C5 by using a specially designed downhole flowmeter (Rouhiainen, 1995). The objective was to test the suitability of the method to determine transmissivity in boreholes and to compare the results with those derived from previously performed pressure build-up tests.

The flowmeter tests were performed approximately 4 months (D&B drift) to 11 months (TBM drift) after excavation. The boreholes had been kept open in the meantime and the borehole history is much longer than for the build-up tests. During the flowmeter measurements all other boreholes were kept open. The tests were performed under two different borehole pressure conditions: first in the open hole and then under shut-in condition.

Flow measurements were made using the thermal pulse method and thermal dilution method.

Analysis of flowmeter data

The collected data were analysed with a steady-state equation; i.e., it is assumed that the radius of influence is stable and a constant-pressure boundary exists. Further, a cylindrical flow homogeneous model (without skin) is assumed. This assumption is consistent with the flow geometry used for the "straight line" analysis and least squares re-analysis of packer tests. To obtain the constant for cylindrical flow geometry which is required in the steady state equation, a radius to the constant-pressure boundary had to be assumed and a value of R=14 metres was chosen for the analysis (Rouhiainen, 1995).

Static hydraulic heads of the test sections were derived if there was non-zero flow in both measurements, i.e., under open-hole and shut-in conditions. Transmissivity could be derived if flow was detected in at least one measurement. In other cases, transmissivity was reported to be less than 1 10^{-11} m^2/s, corresponding to a detection limit of 0.1 ml/min.

Results of the flowmeter measurements

The calculated static hydraulic heads and transmissivities in the test intervals are compiled in Table 5-17 and transmissivities are presented in Figures 5-70 and 5-71. In total, 32 intervals in 3 boreholes were tested, with no measurable flow being detected in 10 intervals. The comparison of the derived transmissivity data with the results of pressure build-up tests is discussed below.

In view of the test assumptions, the calculated transmissivity should be regarded as an order of magnitude estimate. Possible sources of error include equipment problems, such as flowmeter accuracy (measurement limit exceeded in two tests in A5) or leakage around the rubber disks used instead of packer. It is also possible that some discrete water bearing features were missed during testing. This may be the case for borehole A4; the total measured flow in the flowmeter tests in the open borehole was approximately 2 ml/min, compared to the free total outflow from the borehole of 32 ml/min. This may be explained by the first part of the borehole which was not tested with the flowmeter.

Comparison of the two methods

The objective of the hydraulic testing was to provide data on the transmissivity distribution along the boreholes before and after the excavation of the drifts. In boreholes A4, A5 and C5, two principally different methods of testing were performed over the same intervals. Each analysis method contains a significant degree of uncertainty which is related to the input parameters, assumptions and the measured conditions. However, a comparison between the two methods is presented.

Table 5-17. Flow difference measurements. Calculated heads and transmissivities.

Borehole	Interval (top in m)	Head in Interval [m]	T of Interval [m^2/s]	Remarks
A4	4.25	-	-	Possibly missed fractures in A4
	7.75	13.7	1.4E-09	-
	11.25	33.0	7.7E-11	-
	14.75	-	1.3E-11	-
	18.25	-	<1E-11	below detection limit
	21.75	-	1.5E-11	-
	25.25	-	9.6E-12	-
	28.75	-	9.1E-12	-
	32.25	-	1.2E-11	-
	4.25	51.0	4.3E-10	-
A5	7.75	247.0	6.1E-11	-
	11.25	70.0	5.7E-08	erroneous due to flowmeter problem
	14.75	559.0	1.2E-07	erroneous due to flowmeter problem
	18.25	-	5.3E-12	-
	21.75	-	<1E-11	below detection limit
	25.25	-	<1E-11	below detection limit
	28.75	-	<1E-11	below detection limit
	32.25	-	<1E-11	below detection limit
	35.75	-	<1E-11	below detection limit
C5	4.50	-	1.8E-11	-
	8.00	212.0	5.8E-10	-
	11.50	175.0	3.3E-10	-
	15.00	289.0	7.3E-10	-
	18.50	178.0	2.3E-10	-
	22.00	125.0	3.3E-10	-
	25.50	119.0	2.4E-09	-
	29.00	-	<1E-11	below detection limit
	32.50	-	<1E-11	below detection limit
	36.00	233.0	5.9E-11	-
	39.50	-	<1E-11	below detection limit
	43.00	214.0	4.8E-11	-

Borehole A4

In five of six available tests, the pressure build-up tests show a higher transmissivity by up to two orders of magnitude. Only one test at 7.75 metres shows a smaller transmissivity by factor 2 (type 5).

Borehole A5

In the interval at 14.75 metres the analysis of the pressure build-up tests reported a drop in the flow rate and transmissivity by almost five orders of magnitude after the excavation. This observation is contradicted by the flowmeter measurement performed 4 months after the excavation, which showed a large inflow in this section and a transmissivity of the same order of magnitude as the packer test before the excavation. In this interval the discrepancy between the two methods exceeds 5 orders of magnitude after excavation. The flow period preceding the pressure build-up tests indicated a flow rate of about 600 ml/min before and only 0.5 ml/min after excavation. The discrepancy can probably be attributed to that the pressure build-up test after excavation did not include the critical water-bearing feature.

Two flowmeter tests in A5 show similar values to the packer tests, whereas the values in the remaining 6 tests are between 1 and 2 orders of magnitude smaller than those of the pressure build-up. All except one test, in which the flowmeter analysis reported a value of $<1\ 10^{-11} m^2/s$ (i.e. below the detection limit), are characterised by type 4 flow response.

Borehole C5

There were only three tests with results for both methods. All three tests correspond to response type 2 and show a somewhat lower transmissivity derived from the difference flow measurements.

Summary of the Comparison of the two methods

Apart from a few exceptions, the flowmeter measurements show consistently smaller transmissivity values of between half to two orders of magnitude, in comparison with the packer tests. However, it should be borne in mind that the boreholes remained open between the two sets of measurements and that the different starting conditions may bias the comparison.

Conclusions of the Disturbed Zone Hydraulic Tests

The re-analysis of pressure build-up tests contributed to developing a better overall understanding of the formation response in the disturbed zone. The significance of the changes in hydraulic properties of the disturbed zone was evaluated largely on the basis of observed changes in formation response. The transmissivity data obtained from interpretable test pairs before and after excavation are considered not to be reliable in most cases due to several sources of uncertainties.

In total, 38 pairs of pressure build-up tests were available for analysis. Significant changes in hydraulic properties of the disturbed zone were detected in 13 % of the tests, all of which are related to the D&B drift excavation. In the disturbed zone of the TBM drift, the observed changes were less evident; they were qualified as detectable in 16% of all tests. In

63% of test results, no decision on the significance of the changes in hydraulic properties can be made. A non-significant change was positively identified in 8% of results. No statement can thus be made regarding the trend in transmissive properties before and after excavation.

In general, changes in hydraulic properties due to drift excavation could not be evaluated on the basis of transmissivity values derived from the testing, given that the included uncertainties may completely bias any comparison.

6 CONCLUSIONS

To evaluate the results of the ZEDEX project and to assess how these results contribute to the understanding of the EDZ the results have been considered in relation to the original hypotheses and to the objectives established for the project at the design and planning stages. The objectives of the ZEDEX project were defined in the ZEDEX project plans and these are set out below:

- to understand the mechanical behaviour of the Excavation Disturbed Zone (EDZ) with respect to its origin, character, magnitude of property changes, extent and its dependence on excavation method,
- to perform supporting studies to increase understanding of the hydraulic significance of the EDZ and
- to test equipment and methodology for quantifying the EDZ.

To address these objectives and to determine the magnitude of property changes within the EDZ and to monitor the progressive development of the EDZ resulting from the excavation of both the TBM and D&B drifts a suite of measurements and observations were required and performed. In general, the measurements were undertaken before, during and/or after excavation. Two sets of measurements are available for the far-field but, measurements for the near-field were only made after excavation.

6.1 ZEDEX TESTED HYPOTHESIS

Based on earlier EDZ and rock mechanics research work the zone around an underground opening can be divided into three parts; failed, damaged and disturbed zones (Read, 1996). In the failed zone rock slabs detach completely from the rock mass as a result of progressive failure; whilst the damaged zone is characterised by changes in the material behaviour and in the pre-excavation stress state. However, in the disturbed zone the material properties remain essentially unchanged whereas changes in state are considered to be dominant. The relative extent of these zones and the magnitude of property changes is dependent on the magnitude of *in situ* stresses, the material properties, the geometry and orientation of the opening and the excavation method.

It is considered that in the near-field, encompassing the failed and damaged zones, the rock is damaged by the excavation method used and disturbed by the fact that the differential stress (σ_1-σ_3) may be highest in this region. In the far-field it is likely that the rock mass is disturbed by the stress redistribution and has a higher differential stress (σ_1-σ_3) than the

background value. In the near-field the damage will have changed the rock properties due to induced micro- and macro fracturing. If natural fractures are present, these may be deformed in both the near-field and far-field, involving aperture changes such as those caused by closure, opening, shearing and shearing induced dilation.

Detournay & St. John (1988) categorised failure modes around a circular unsupported tunnel (Figure 5-1). These categories may be applied to the rock mass around the ZEDEX drifts and using these it is suggested that the drifts would remain in a mainly elastic regime under the stress and material conditions determined for the Äspö site. The stress modelling undertaken for the ZEDEX volume is in agreement with these categories and showed that only very minor damage may be evident in the regions of maximum stress concentrations around the drifts. The modelling also indicated that damage due to stress relief should be confined to the boundaries of the drifts and that frictional sliding along pre-existing fractures may only occur up to 2.5 metres from the drift perimeters. But such stress re-distributions, by local slip, would be sparse occurrences within an elastic field. Thus the state of stress at Äspö is expected to cause only a minor stress induced damaged zone in addition to the disturbed zone.

The excavation process itself is expected to cause damage around the drifts and different excavation methods, as used in the ZEDEX project, should cause different amounts of damage. The excavation effects should be more dominant and more easily measurable if the stress induced damage is only small as postulated above.

From these considerations, the hypothesis established, at the design and planning stages for the ZEDEX project, was that in the near-field (then defined as distances of less than 2 metres) it was anticipated that disturbance or damage could be reduced by the application of an appropriate excavation method (smooth blasting or tunnel boring). The hypothesis also predicted that the far-field disturbance (then defined as distances greater than 2 metres) would be essentially independent of excavation method, as it would have been caused by stress redistribution, influenced by discontinuity geometry and the mechanical properties of the rock mass.

The results from the ZEDEX Project generally supported the hypothesis, but showed that the division based on near-field and far-field is not appropriate. Based on the ZEDEX results the following division has been found more appropriate:

- there is a damaged zone closest to the drift wall dominated by changes in rock properties which are mainly irreversible and

- there is a disturbed zone outside the damaged zone dominated by changes in stress state and hydraulic head and where changes in rock properties are small and mainly reversible and it is considered that there are no, or insignificant, material property changes.

These two zones, the damaged and the disturbed zones, are considered to form the EDZ. Thus the term EDZ is taken to mean the total disturbed zone that includes the failed and damage zones closest to the wall that are caused by the excavation method and also the disturbed zone outside the damaged zone. The change in rock properties and rock stress with distance from the wall of the excavation are gradational and there is hence no distinct "boundary" between the two zones and furthermore, an additional gradational boundary exists between the disturbed zone and the virgin rock mass.

6.2 EDZ CONCLUSIONS

The geological setting of the ZEDEX test site and initial interpretation of results obtained before, during and after excavation are presented in Olsson *et al.*, (1996b) and in the Äspö HRL Annual Report for 1995 (SKB, 1996).

In order to monitor the progressive development of the EDZ and address the objectives of the ZEDEX project of determining the magnitude of property changes within the EDZ, requires, in part, the identification of the boundary between the damaged and disturbed zones, which is recognised to be gradational in nature. From the measurements performed it should be possible to identify damaged and disturbed zones even if the changes are small, both in magnitude of property change and extent. The experimental data were therefore examined to determine significant changes in properties between the initial conditions and those properties measured after the excavation process.

Stress measurements performed in the pillar between the D&B and TBM drifts to study the variation in stress as a function of distance from the drift walls indicated that the magnitudes of the stresses measured at the ZEDEX site were significantly lower than the expected values based on an extrapolation of trends seen throughout the Äspö HRL. Previous studies at Äspö in deep boreholes using the same instrument (the Swedish State Power Board triaxial cell, Hallbjörn *et al.*, 1990) showed lower stress magnitudes compared to measurements made from the ramp using CSIRO overcoring methods. However, additional stress measurements undertaken in the pillar between the two drifts using the CSIRO overcoring method confirmed the earlier data. From the available data it was anticipated that the stress induced damage would be small and that excavation induced damage would be dominant but dependent on the method utilised and this was confirmed by the experimental data.

The initial conditions of the rock mass were characterised by several techniques including; drift mapping and core logging; the determination of geotechnical rock mass classification factors (Q, RMR), *in situ* seismic (P- and S-wave) velocity measurements and radar measurements. The rock mass response to excavation was observed by mapping induced fractures, multi-point borehole extensometers (MPBX) and convergence

measurements, laboratory testing on core samples and by acceleration, vibration, seismic velocity, permeability and Acoustic Emission (AE) measurements. Short radial holes were drilled in the drifts with additional sets of boreholes (fans) drilled at three locations and within these boreholes high resolution permeability, P- and S-wave interval velocities, seismic tomography and seismic velocity anisotropy measurements were performed. Lithological mapping undertaken in the drifts and core logging indicated that the lithology within which the drifts were excavated was similar; comprising diorite with Dykes of fine grained granites. Fractures having a north-west trend and steep dip intersected the ZEDEX volume, some of the fractures were water bearing. More fractures were observed in the TBM drift than in the D&B drift. The rock mass is competent and reasonably homogeneous with local differences in properties.

6.2.1 Conceptual understanding of the Damaged and Disturbed Zones

During excavation a force is exerted on the rock in order to break it so that a void of pre-determined size is created. The remaining rock surrounding the void should, particularly for smooth blasting, be left as intact as possible. The force needed to break the rock has during the ZEDEX experiment been exerted by explosives in blast holes and by TBM cutters.

The character of the damage to the rock by blasting and TBM excavation are quite similar as can be seen from Figures 5-49 and 5-58. There is normally a zone of crushed rock around the blast hole and the TBM groove from which radial cracks extend. The extent of the cracks is however significantly different being some tens of millimetres for TBM excavation compared to some tens of centimetres for blasting. The crushed parts of the rock and the parts with induced fractures constitute the damaged parts of the rock. As can be seen from, e.g., Figures 5-53 and 5-54 it is not trivial to define the extent of the damaged zone as induced cracks may extend far from the blast hole leaving pieces of intact rock in between. In this work the extent of the damaged zone has been taken to be the distance from the drift wall to which induced fractures extend. This can evidently vary depending on the point of observation due to the irregularity of the induced cracks and the sensitivity and resolution of the methods used. The damaged zone is potentially a zone of increased axial hydraulic conductivity due to the presence of cracks aligned axially with the drift in this zone.

Crushing and stress induced cracking may also occur if the void causes stress concentrations in excess of the breaking strength of the rock (Read, 1996, Detournay and St. John, 1988). This did not occur during the ZEDEX experiment due to the low stress levels compared to the rock strength.

In the disturbed zone, outside of the damaged zone, the stress redistribution caused by the void will cause block movements, aperture changes on natural fractures, and/or elastic deformation of the rock. In the disturbed zone changes in material properties such as seismic velocity, Young's modulus etc., are expected to be insignificant. Changes in hydraulic properties depend on aperture changes on natural fractures and hence on the

fracture orientations, extent and connectivity. No general statement can be made on the effect of a void on the hydraulic properties of the rock as it is strongly dependent on site specific conditions.

6.2.2 Conclusions for the Damaged Zone

The largest extent of the damaged zone was determined from the Acoustic Emission (AE) data, as this is the most sensitive method. Analysis of the Acoustic Emission (AE) events that occurred within the first 8 hours after excavation showed that AE events occur at deviatoric stress levels of 25 MPa, which is well below the typical range of crack initiation stresses. This, combined with source mechanism analysis of the AE events which showed that the great majority of events would fit shear-slip mechanisms, indicated that the events were generated by slip on pre-existing cracks or fractures. Other source mechanisms considered for the AE events were explosive (crack-opening) events and implosive (crack-closure) events. The partially failed rounds, number R2 and R6, had the highest proportion of implosive events. Much of the activity from these rounds occurred in the blasted but intact volume, which may have cracks initially opened by the blast gases. The implosive events recorded may represent the closure of such cracks.

The AE event density was approximately a factor of 10 higher for the D&B drift compared to the TBM drift. For the TBM drift the majority of AE-events occur at the face, i.e. inside the drift radius of 2.5 metres and within a few tens of centimetres from the drift wall. For the D&B the event density is high, out to one meter from the drift wall. Some events were detected at greater distances from the drifts but these events were interpreted as localised stress relaxation in an overall elastic environment.

Several seismic techniques were used to evaluate the rock properties in the damaged zone of the ZEDEX test drifts. All seismic methods showed a velocity decrease, velocity low, close to the drift surfaces. Generally it was found that the low velocity zone is extremely small (less than 10 centimetres) or even not present in the TBM drift, although it is recognised that this may be a function of measurement scale. Significant velocity reductions were observed around the D&B drift which exhibited a larger low velocity zone with an extent of about 30 centimetres and with a comparable low velocity zone of generally less than 5 centimetres around the TBM drift. Some single holes showed low velocities to a depth of 100 centimetres with these borehole being located in the floor of the D&B drift. The observed changes in seismic velocity indicates an increase in crack density. Cross-hole seismic measurements showed a maximum velocity anisotropy of about 15%, but no significant changes in velocity anisotropy were detected as a function of the excavation.

Visual indicators of damage, that include the dye penetration tests and micro-crack analysis of rock samples, also indicated that damage is confined to a narrow zone. The dye penetration tests performed in the slots cut from the drifts showed the extent of macro fracturing. From these

observations it would be inferred that the damage is confined to some 10 centimetres around the wall of the D&B drift, whilst in the floor of the D&B drift the fractures extend to about 50 centimetres. In the TBM drift no visible induced cracks were found. A more detailed analysis of cracks in rock samples from the TBM drift wall showed a crushed zone with an extent of about 10 to 20 millimetres and the presence of small grooves generated by the cutters.

The hydraulic measurements performed in the damaged zone indicates that there is little or no change in permeability of the rock matrix. The larger permeabilities observed have been associated with the induced and pre-existing fractures which intersected the radial holes. The high variability in fracture permeability made it impossible to quantify changes due to excavation. Induced fractures are believed to increase permeability in the damaged zone although it was not possible to quantify this within the project.

6.2.3 Conclusions for the Disturbed Zone

As discussed previously the boundary between the damaged and the disturbed zone is gradational, i.e. there is no distinct boundary but a change which may be defined as the boundary beyond which (at greater distances from the drift walls) any changes within the rock mass caused by the effects of the excavation are recoverable, thus the disturbed zone is an elastic region.

A large number of seismic measurements were performed mostly within the damaged zone. Those measurements made within the disturbed zone showed that there were no detectable changes in seismic velocity, attenuation or anisotropy between the measurements made before and those made after excavation and these observations were to be expected.

Acoustic Emission monitoring showed that within this zone some events, at distances of 3 to 4 metres from the drift walls, were clustered and appeared to be aligned with fractures. Source mechanism studies suggested that these events were consistent with shear-slip mechanisms on fractures parallel to the main fracture set. Qualitatively, there were approximately the same number of events sparsely distributed within the disturbed zone around both drifts. This again indicates that there would be no material property changes within the disturbed zone and that deformation was independent of the excavation method.

Analysis of stress measurements indicated that deformation around drifts would be confined to elastic deformation. Failure was not expected from high differential stress but possibly from relaxation or fracture extension although the crack initiation stress was not exceeded. The measurements obtained within the pillar are in reasonable agreement with the modelling performed, taking fractures into account.

Convergence measurements made within the drifts during excavation and displacements measured during excavation within the pillar between the

drifts indicated that the deformation was elastic. This result was expected from modelling work and the modelled displacements were in reasonable agreement with those measured.

Hydrogeological measurements showed no significant changes bearing in mind the limited data set and the uncertainties in the data. The measurements were performed in a low porosity and low permeability rock mass with some fractures with higher transmissivities. It must also be borne in mind that in the area of the TBM, grouting was performed and that the hydrogeological aspects were not a major goal of the project.

6.3 SUMMARY OF THE MAIN FINDINGS OF THE ZEDEX PROJECT

One of the objectives of the project was to understand the mechanical behaviour of the Excavation Disturbed Zone (EDZ) with respect to its origin, character, magnitude of property changes, extent and its dependence on excavation method. The ZEDEX experiment was performed in a rock mass with low stresses which has resulted in mainly elastic behaviour and no induced damage resulting from stress concentrations at the drift perimeter. The results and main findings of the project are summarised in Table 6-1.

The link between damage and the excavation method has been demonstrated although the difference between the two D&B methods, in terms of damage, could not be determined. As postulated, the damage observed around the D&B drift was greater than that observed around the TBM drift. A visual inspection of the rock close to the drift walls indicates that most of the newly developed connected cracks have been introduced by the excavation process. Results indicate that significant damage is caused by misfires or partially failed rounds and the reblasting required for the failed rounds. For example, misfires and partially failed rounds resulted in larger amounts of radiated seismic energy into the rock compared to successful rounds. This shows the importance of designing a blast pattern that with a high probability will result in a full pull in order to reduce the risk of damage to the rock. A modified design of the cut and consistent usage of electronic detonators with precise firing times could reduce damage significantly. Simultaneous detonation of all the contour holes have also been shown to reduce damage significantly (Olsson and Bergqvist, 1997) compared to detonation of the contour holes at different times as was used in the ZEDEX experiment.

Table 6-1. Summary of the pertinent results from the ZEDEX project

Technique	Excavation Method					
	TBM	LSES	NS	TBM	LSES	NS
	Damaged Zone			Disturbed Zone		
High resolution seismic tomography	no measurable velocity change	possible low velocity zone a few centimetres to 0.5 to 1.5 m from drift wall; fans of tomograms indicated a low velocity zone 0.2 to 0.5 m wide.		no measurable velocity change		
Permeability measurements (pressure build up tests)	not applicable			detectable change in 16% of tests, significance uncertain	change detected in 13% of tests, significance uncertain	
Difference flow measurements	not applicable			no conclusions can be drawn from the transmissivity values obtained		
Stress measurements	principal stress measurements lower than anticipated, rock mass in a mainly elastic regime, no stress induced failure expected; stress values lower near drift walls, σ_1 stress orientation more inclined to the vertical within 4 metres of the drifts and the maximum horizontal stress aligned more parallel to the drifts within 4 metres of the drifts					
Acoustic emission monitoring	activity within a few tens of centimetres from the drift wall	activity approximately ten times higher, event densities high out to 1 metre from the drift wall		sparse, clustered on fractures	sparse, qualitatively same numbers as around the TBM, source mechanisms suggest shear-slip on fractures	

Table 6-1 con't. Summary of the pertinent results from the ZEDEX project.

Technique	Excavation Method					
	TBM	LSES	NS	TBM	LSES	NS
	Damaged Zone			Disturbed Zone		
MPBX extensometers	not applicable	0.2 to 0.3 millimetres of convergence at the drift wall		not applicable	displacements evenly distributed with depth indicating that they were primarily elastic	
Convergence measurements (pins)	predominantly horizontal convergence, 0 to 4 mm	predominantly horizontal convergence, less than 1 mm, no difference between LSES or NS rounds		not applicable		
High resolution permeability measurements	no detectable trend	detectable changes in permeability in the first 0.5 metres, no changes in matrix permeability		no detectable change in permeability		
Laboratory testing	ultrasonic velocity measurements indicate micro-cracking near the drift wall			measurement indicate no detectable changes		
	under load largest change seen in the first 10 cm	under load largest change seen in the first 30 cm		measurement indicate no detectable changes		
Downhole P-wave velocity logging	velocity low 10-35 cm from drift wall	velocity low 10 to 100 cm from drift wall		velocity at background levels	velocity at background levels	
Acoustic resonance measurements	technique not sensitive enough to detect any excavation induced changes					

Table 6-1 con't. Summary of the pertinent results from the ZEDEX project.

Technique	Excavation Method					
	TBM	LSES	NS	TBM	LSES	NS
	Damaged Zone			Disturbed Zone		
Micro-velocity logging (high frequency)	velocity increase of between 250 to 400 ms^{-1} within the first metre or no change noted	velocity increase of between 300 to 400 ms^{-1} within the first metre or no change noted		no velocity change noted	velocity increase of between 300 to 600 ms^{-1} to distances of 4.5 metre from the drift wall	
Mini-sonic velocity logging (low frequency)	low velocity zone 0 to 10 cm	low velocity zone 0 to 15 cm	low velocity zone 0 to 30 cm†	no velocity change noted	no velocity change noted	no velocity change noted
Seismic Refraction	low velocity zone 10 cm wide	not applicable	low velocity zone 15 cm wide	not applicable		
Detailed mapping of half barrels	not applicable	more intact half barrels	more pronounced crushed zones and radial cracks	not applicable		
Crack Discrimination (TBM)	2 to 5 mm	not applicable		not applicable		
Dye penetrations tests	no visible cracks	average crack length 40 cm*	average crack length 30 cm	not applicable		

* Partially failed blast round
† Single cracks present

The damaged zone around the drifts, in particular the D&B drift was seen to be controlled, to some extent, by lithology; with the more brittle lithologies sustaining more damage. As expected the changes in rock properties induced by the stress field and those induced by relaxation are very small in magnitude and were mainly detected by the Acoustic Emission measurements. The results have enabled the subdivision of the EDZ into damaged and disturbed zones with the "boundary" interpreted from the acquired data.

The damaged zone, caused by the excavation methods applied, has been identified by several measurement techniques. Monitoring of AE events was the most sensitive method and may therefore produce a conservative estimate for the damaged zone, that indicates minor damage due to crack opening and slip. Sparse AE activity is not expected to correspond to measurable changes in rock properties. However, a large number of AE events, as observed around the D&B drift, indicates intense micro-cracking and is expected to produce a macroscopically detectable increase in crack density. For the D&B drift significant AE activity was observed up to 1 metre from the drift wall while the corresponding extent for the TBM drift is a few tens of centimetres. Changes in seismic velocity indicate a larger increase in crack density confirming the AE data. The dye penetration tests performed in the slots cut from the drift showed the extent of macro fracturing, that extended to about 50 centimetres in the floor of the D&B drift. The hydraulic measurements performed in the damaged zone showed little change in permeability of the rock matrix. The larger permeabilities observed being associated with the induced and pre-existing fractures intersecting the boreholes. It may be concluded that the damaged zone is characterised by changes in state and property changes, with the latter being dominant.

The disturbed zone is characterised by elastic displacements, changes in state and no induced fracturing. In this zone only a very few AE events were observed with a similar event density for both the TBM and D&B drifts. The source mechanisms suggested that the events resulted from shear-slip on existing fractures. The high resolution seismic tomography results showed no changes in seismic velocity and the displacement measurements indicated elastic behaviour. The hydraulic tests performed before and after excavation revealed no significant changes in hydraulic properties due to excavation. From these observations it may be concluded that the disturbed zone is characterised by changes in state, considered to be reversible.

The current view of the characteristics and extent of the damaged and disturbed zones are shown in Figure 6-1. The extent of the damaged zone is significantly greater around the drift excavated by blasting compared to the drift excavated by the tunnel boring machine. The extent of the damaged zone around the TBM drift is limited to about 3 centimetres from the drift wall. In the D&B drift the extent of the damaged zone is about 30 centimetres in the wall and about 80 centimetres in the floor. The damaged zone is characterised by irreversible changes in property due to excavation

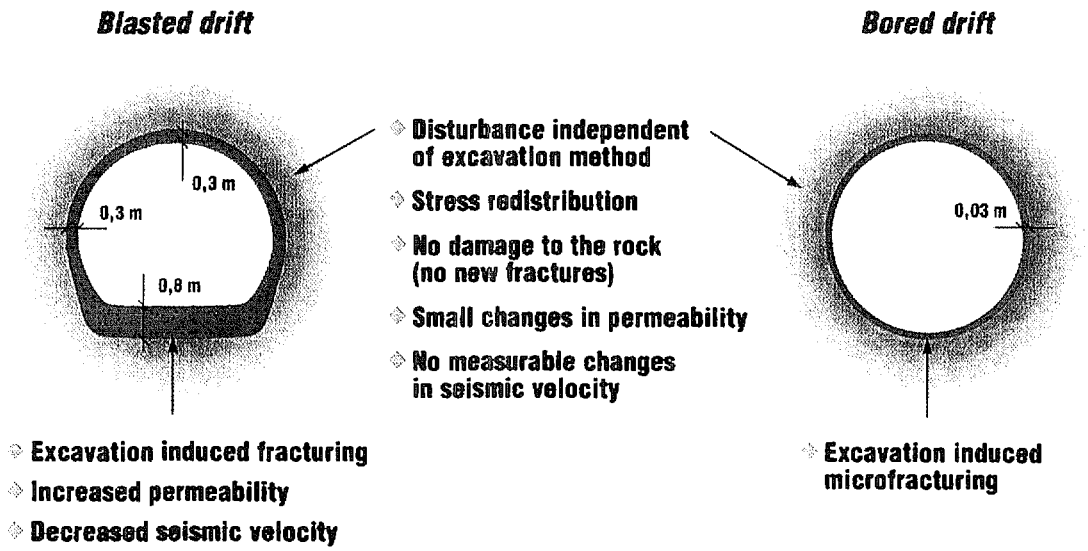

Figure 6-1. *Summary of the main findings of the ZEDEX Project. The extent of the damage zone is significantly greater in the drift excavated by blasting compared to the drift excavated by a tunnel boring machine.*

induced macro and micro fracturing resulting in decreased seismic velocity and increased permeability. Outside the damaged zone there is a disturbed zone where no changes in property has been observed. The disturbed zone is characterised by elastic displacements, changes in state and no induced fracturing. No measurable changes in seismic velocity has been found.

The ZEDEX project met the other objectives established for the project by performed supporting studies to increase understanding of the hydraulic significance of the EDZ and test equipment and methodology for quantifying the EDZ. It is, therefore, considered that as a result of the ZEDEX project it may be stated that "we understand the EDZ", certainly in the mechanical aspects in this stress regime at Äspö. However, studies examining connectivity and axial flow should be considered to fully characterise the EDZ. It is further considered that the project has contributed to the knowledge base on the development of the EDZ and the project has resulted in the publication of a number of reports and also a number of papers which are listed in Appendix 1.

6.4 METHODOLOGIES AND STRATEGY

The ZEDEX Project has been successful, particularly in the mechanical aspects and met the objectives set for the project. The conceptual model and hypothesis established prior to the commencement of the project were tested by the data obtained and validated through modelling. An integrated suite of measurement techniques was applied to the characterisation of the

damaged and disturbed zones and the results are in agreement with the initial concepts and hypotheses established. Great emphasis was placed on the integration of the different data sets, with the redundancy of data proving to be very useful and provided a consistency in the interpretation of the boundary between the damaged and disturbed zones developed around the drifts.

Whilst it can be seen that the problem investigated during this research programme is essentially a hydro-mechanical system, the ZEDEX project focused more on the mechanical aspects. It is considered that the adopted strategy was successful in determining the mechanical aspects of the system and the data obtained on the hydrogeological aspects was very useful, but it must be emphasised that this was not a major component of the planned investigation.

The results demonstrate that a reliable and conservative estimate of the extent of the zone of increased permeability can be derived from the velocity measurements. The area of increased permeability, if it exists at all around the ZEDEX drifts, is extremely small and the increase is low. However, the problems in performing hydraulic tests in the EDZ should be recognised.

The ZEDEX project tested a range of methods to characterise the EDZ and established experimental procedures for use at other HRL's. It is considered that the seismic velocity measurements and the Acoustic Emission measurements were the most robust methods.

Some of the results and conclusions reached may appear to conflict in terms of the reported extents and magnitudes of damage from the different methodologies. The reason for this apparent discrepancy lies in the different scales and sensitivities of the applied methods. For example the Acoustic Emission measurements are recognised as being the most sensitive method for indicating changes in a brittle material and in particular the method is sensitive to the smallest of microcrack adjustments and minor damage due to crack opening and slip. Rock mechanics experiments demonstrate, that only considerable Acoustic Emission activities indicate microcrack densities that cause velocity reductions. Therefore, where sparse Acoustic Emission activity is observed it would not be expected that there would be a measurable change in rock properties or the overall elastic behaviour of the rock. The velocity measurements are less sensitive and the reduction in velocity indicates a larger increase in crack density and therefore significant damage. However, it is not possible to determine, from the velocity measurements, whether or not the microcracks are connected. The velocity measurements of core samples performed under load proved to be a good indicator of damage produced more consistent results than velocity logging undertaken in the boreholes which were influenced by scale effects and sensitivity.

Similarly dye penetration tests and micro-crack analysis also show scale dependency. The dye penetration tests indicated the presence of a zone of interconnected cracks which were shown to increase the permeability

parallel to the wall of the D&B drift. Around the TBM drift no such zone was determined but a detailed analysis of rock samples from the wall of the TBM tunnel showed that the damage results from the excavation process and induced by stress concentrations at the cutters.

The laboratory measurements provided a check on the *in situ* measurements in terms of providing data on rock properties by alternative techniques. In general, the laboratory measurements corroborated the results obtained *in situ* and provided greater confidence in the interpreted extent of the damage zone. In addition, the laboratory measurements provided data on parameters such as micro-crack porosity, compressibility and micro-cracking not directly obtainable from *in situ* methods.

Of the methodologies utilised during the ZEDEX project it is considered that the borehole resonance method, Q and RMR logging and temperature measurements would not be performed in another, similar, project. Further, it is considered that modelling should be performed at an earlier stage in the project, at the design and planning stages. It is also considered that the axial boreholes were drilled too far from the projected locations for the drifts and consequently the tomographic sections were acquired entirely within the disturbed zone and were therefore not able to determine any changes in seismic velocity resulting from damage due to the excavation processes.

6.5 IMPLICATIONS FOR PERFORMANCE ASSESSMENT

The results from ZEDEX indicate that the role of the EDZ as a preferential pathway to radionuclide transport is limited to the damaged zone. The greatest extent of this zone was, at most, 1.0 metre around the D&B drift determined from the AE results and it is therefore considered to be a conservative figure. The clearly demonstrated link between the extent of the damaged zone, which is the hydraulically significant part and the excavation methodology, indicates that the damaged zone can therefore be limited through the application of an appropriate excavation method. Further, the limited extent of the damaged zone should also make it feasible to block any pathways in the damaged zone by plugs placed at strategic locations.

From the measurements performed it is possible to conclude that the damaged zone formed by the excavation of the D&B drift was greater in degree and extent than that caused by excavating the TBM drift. This damaged zone is characterised by induced fracturing, increased permeability and reduced seismic velocities. It was observed that the extent of the damage zone varied around the D&B drift and the maximum damage was observed in the floor. The damaged zone around a blasted drift can be reduced by further development of blast designs.

These conclusions are similar to those from the experiments carried out at the Edgar Mine by the Colorado School of Mines (CSM) which showed that by controlled blasting the extent of blast damage could be limited to 0.5 to 1 metres from the wall of the excavation (Ubbes *et al.*, 1989).

Further the Rock Sealing Project undertaken at Stripa showed that the EDZ affected by blasting was of the order of 0.0 to 0.8 metres from drift wall having a hydraulic conductivity of the order of 1.0×10^{-8} ms^{-1} whilst the conductivity in the floor was twice that in the wall which was attributed to the use of higher energy explosive charges. Whilst the EDZ affected by stress redistribution extended approximately from 0.8 to 3.0 metres from the drift wall and had a hydraulic conductivity of 3×10^{-9} ms^{-1} (Börgesson *et al.*, 1992). However, it should be recognised that this increase in hydraulic conductivity was not measured directly but inferred from modelling. The "Blasting Damage Investigation" carried out by SKB, to study the extent of the zone damaged by blasting for three different drill and blast schemes, showed that the damage in the floor of the drift was more extensive than in the walls for all drill and blast schemes used (Pusch and Stanfors, 1992).

An important aspect of the EDZ in performance assessments is the assumption that a zone of significantly increased permeability exists along the drift, however, limited evidence in support of this hypothesis exists (Winberg, 1995). The results of the ZEDEX Project have shown that there is little change in matrix permeability in the damaged zone close to the drift walls and that the larger permeabilities are the result of intersecting pre-existing or induced fractures. There appears to be no experimental evidence in support of an increased permeability in the disturbed zone affected by the stress redistribution caused by the void (Olsson and Winberg, 1996). The stress redistribution will of course lead to changes in fracture aperture, both opening and closure. In a general three-dimensional fracture network it is unlikely that fractures would open and connect in such a way that a permeable path opened along the drift. The risk of a connected pathway is of course greater if drifts are oriented parallel to one of the main fracture sets.

The ZEDEX experiment gives indirect evidence that the *damaged zone* around the drift has to be considered in performance assessments as a potential pathway of significantly increased hydraulic conductivity. As the hydraulically active part of the damaged zone consists of induced fractures it is not meaningful to describe its hydraulic properties in terms of hydraulic conductivity. Instead attempts should be made to estimate the transmissivity of the damaged zone for the entire drift cross-section. Unfortunately, the ZEDEX experiment did not include measurements for determining this value.

6.6 RECOMMENDATIONS

As discussed above it is considered that the ZEDEX project was successful and demonstrated the link between excavation and damage. Further, the project addressed the mechanical aspects of the development of the EDZ and was successful in determining the mechanical aspects of the system, additionally the project provided very useful data on the hydrogeological aspects of the system. As mentioned earlier it is recognised that the problem being investigated is essentially a hydro-mechanical system and as such it is considered that any future projects looking at the EDZ or specifically the damaged zone should address this as a combined system.

Therefore, it is considered that any further research work on the damaged zone surrounding drifts or tunnels should consider:

- the connectivity of the fractures generated and whether hydrogeological pathways maybe created
- having defined the connectivity of the system the effect of plugs and seals on the system should be investigated
- the temporal evolution of the EDZ and whether this affects the spatial evolution of the EDZ.

Further research should concentrate on the hydraulics and coupled hydro-mechanical aspects, including connectivity and axial flow, with integrated techniques providing the best capability of determining the boundaries of damage and disturbance. In addition research should be directed towards the use of non intrusive methods which should be developed to determine the amount of damage around underground openings and determine the boundaries between the damaged and disturbed zones. Such methods would not require additional boreholes to be drilled which create preferential pathways.

REFERENCES

Alheid H.J and Knecht M, 1996. Distribution of seismic wave velocities around underground drifts. In Proceedings of the Excavation Disturbed Zone Workshop. Canadian Nuclear Society International Conference on Deep Geological Disposal of Radioactive Waste, Winnipeg, Canada, 1996.

Barton N, 1996. Estimating rock mass deformation modulus for Excavation Disturbed Zone studies. In Proceedings of the Excavation Disturbed Zone Workshop. Canadian Nuclear Society International Conference on Deep Geological Disposal of Radioactive Waste, Winnipeg, Canada, 1996.

Bauer C, Homand F and Ben Slimane K, 1996a. Disturbed Zone assessment with permeability measurements in the ZEDEX tunnel. In Proceedings of the Excavation Disturbed Zone Workshop. Canadian Nuclear Society International Conference on Deep Geological Disposal of Radioactive Waste, Winnipeg, Canada, 1996.

Bauer C, Homand-Etienne F, Ben Slimane K, Hinzen K.G and Reamer S.K, 1996b. Damage zone characterization in the near field in the Swedish ZEDEX tunnel using in situ and laboratory measurements. In G. Barla (Ed.), Eurock '96, Torino. Prediction and performance in rock mechanics and rock engineering. Vol. 2, pp. 1345-1352. Associazione Geotechnica Italiana. Balkema, Rotterdam, Netherlands.

Boadu F.K and Long L.T, 1996 Effects of fractures on seismic-wave velocity and attenuation. Geophysical J. Int. 127, pp. 86-110.

Brace W. F and Byerlee J.D, 1968. Recent experimental studies of brittle fracture in rocks. In C. Fairhurst (Ed.), Proc, 8th U.S. Symp. On Rock Mechanics, Minneapolis, pp. 58-81. American Institute of Mining Engineers.

Börgesson L, Pusch R, Fredriksson A, Hökmark H, Karnland O and Sandén R, 1992. Final report of the Rock Sealing Project. Identification of zones disturbed by blasting and stress release. OECD/NEA International Stripa Project, Technical Report 92-08. Swedish Nuclear Fuel and Waste Management Company, Stockholm, Sweden.

Carlson S.R and Young R.P, 1993. Acoustic Emission and ultrasonic velocity study of excavation-induced microcrack damage at the Underground Research Laboratory. Int. J. Rock Mech. Min. Sci. & Geomech. Abstr., Vol. 30, pp. 901-907.

Chandler N.A, Kozak E.T and Martin C.D, 1996. Connected pathwys in the EDZ and the potential for flow along tunnels. In Proceedings of the Excavation Disturbed Zone Workshop. Canadian Nuclear Society

International Conference on Deep Geological Disposal of Radioactive Waste, Winnipeg, Canada, 1996.

Christiansson R and Hamberger U, 1991. Blasting damage investigation in access ramp section 0/526-0/565 m. No. 1, tunnel excavation and geological documentation. SKB Progress Report 25-91-12. Swedish Nuclear Fuel and Waste Management Company, Stockholm, Sweden.

Cosma C and Honkanen S, 1994. Seismic EDZ instrument development - Phase II. NGI report 931005.72/1, NGI, Oslo, Norway.

Curran J. H and Corkum B.T, 1993. EXAMINE3D - Three Dimensional Excavation Analysis for MINEs, Version 2.2. Users' manual. Toronto: University of Toronto, Department of Civil Engineering, Data Visualization Laboratory.

Detournay E and St. John C. M, 1988. Design charts for a deep circular tunnel under non-uniform loading. Rock Mech. and Rock Engin., 21 (2): pp. 119-137.

Enachescu C, Follin S and Wozniewicz J, 1996. Evaluation of two types of hydraulic tests performed in boreholes A4, A5 and C5 at the ZEDEX site, Äspö Hard Rock Laboratory. SKB Progress Report HRL-96-14. Swedish Nuclear Fuel and Waste Management Company, Stockholm, Sweden.

Emsley S.J, Olsson O, Stanfors R, Stenberg L, Cosma C and Tunbridge L, 1996. Integrated characterisation of a rock volume at the Äspö HRL utilised for an EDZ experiment. In G. Barla (Ed.), Eurock '96, Torino. Prediction and performance in rock mechanics and rock engineering. Vol. 2, pp. 1329-1336. Associazione Geotechnica Italiana. Balkema, Rotterdam, Netherlands.

Falls S.D, 1993. Ultrasonic Imaging and Acoustic Emission studies of microcrack development in Lac du Bonnet granite. Ph.D Thesis, Queen's University, Kingston, Canada, 227 pp.

Falls S.D and Young R.P, 1996. Examination of the excavtion-disturbed zone in the Swedish ZEDEX tunnel using acoustic emission and ultrasonic velocity measurements. In G. Barla (Ed.), Eurock '96, Torino. Prediction and performance in rock mechanics and rock engineering. Vol. 2, pp. 1337-1344. Associazione Geotechnica Italiana. Balkema, Rotterdam, Netherlands.

Fairhurst C and Damjanac B, 1996. The excavation damage zone - An international perspective. In Proceedings of the Excavation Disturbed Zone Workshop. Canadian Nuclear Society International Conference on Deep Geological Disposal of Radioactive Waste, Winnipeg, Canada, 1996.

Gustafson G, Stanfors R and Wikberg P, 1988. Swedish hard rock laboratory first evaluation of preinvestigations 1986-87 and target area

characterization. SKB Technical Report 88-16. Swedish Nuclear Fuel and Waste Management Company, Stockholm, Sweden.

Hallbjörn L, Ingeval K, Martna J and Strindell L, 1990. New automatic probe for measuring triaxial stress in deep boreholes. Tunnelling underground space technology, Vol. 5, pp. 141-145.

Hermansson J, 1995. Structural geology of water-bearing fractures. SKB Progress Report 25-95-23. Swedish Nuclear Fuel and Waste Management Company, Stockholm, Sweden.

Heuze F.E, 1981. Geomechanics of the Climax Mine-by, Nevada Test Site. Paper presented at the 22nd Rock Mechanics Symposium, MIT, Cambridge, MASS, June 29-July 2, 1981. Lawrence Livermore Laboratory, Preprint UCRL-85768.

Hoek E, 1965. Rock fracture under static stress conditions. CSIR Report Meg 383, National Mechanical Engineering Research Institute, Council for Scientific and Industrial Research, Pretoria, South Africa.

Hoek E and Brown E. T, 1980. Underground Excavations in Rock. The Institution of Mining and Metallurgy, London.

Hudson J.A, 1981. Wave speeds and attenuation of elastic waves in material containing cracks. Geophysical J. R. Astron. Soc. Vol. 64, pp. 133-150.

Johns R.T, 1995. MULTIFIT V1.0. Code description. Colenco internal memorandum. Colenco Power Engineering Ltd., Baden, Switzerland.

Kemeny J. M and Cook N. G. W, 1991. Micromechanics of deformation in rocks. In Toughening Mechanics in Quasi-Brittle Materials (Edited by S. P. Shaw), vol. 2 pp. 155- 188. Klewer Academic, The Netherlands.

Kornfält K.A and Wikman H, 1988. The rocks of the Äspö island. Description to the detailed maps of solid rocks including maps of 3 uncovered trenches. SKB Progress Report 25-88-12. Swedish Nuclear Fuel and Waste Management Company, Stockholm, Sweden.

Lee M, Bridges M and Stillborg B, 1993. Äspö virgin stress measurement results in sections 1050, 1190 and 1620 m of the access ramp. SKB Progress Report 25-93-02. Swedish Nuclear Fuel and Waste Management Company, Stockholm, Sweden.

Lee M, Hewitt T and Stillborg B, 1994. Rock stress measurement and laboratory testing of rock. SKB Progress Report 25-94-02. Swedish Nuclear Fuel and Waste Management Company, Stockholm, Sweden.

Leijon B, 1995. Summary of rock stress data from Äspö. SKB Progress Report 25-95-15. Swedish Nuclear Fuel and Waste Management Company, Stockholm, Sweden.

Lieb R.W *et al.*, 1989. Excavation responses in developing underground repositories in fractured rock in Switzerland. Proc. of the OECD/NEA Workshop on Excavation Response in Geological Repositories for Radionuclide Waste, Winnipeg, Canada 1988. OECD/NEA 1989.

Lindqvist P.A, Suarez del Rio L.M, Montoto M, Tan X.C and Kou S.Q, 1994. Rock Indentation Database. Testing procedures, results and main conclusions. SKB Progress Report 44-94-023. Swedish Nuclear Fuel and Waste Management Company, Stockholm, Sweden.

Litterbach N, Lee M, Struthers M and Stillborg B, 1994. Virgin stress measurement results - Boreholes KA2870A and KA3068A. SKB Progress Report 25-94-32. Swedish Nuclear Fuel and Waste Management Company, Stockholm, Sweden.

Martin C.D and Kozak E.T, 1992. Flow measurements in the excavation disturbed zone of Room 209. Atomic Energy of Canada Limited.

Martin C.D, Young R. P and Collins D. S, 1995. Monitoring progressive failure around a tunnel in massive granite, Proceedings of the 8th International congress of the International Society of Rock Mechanics, Tokyo, Japan, 1995.

Martin C.D, Dzik E.J and Read R.S, 1996. Designing an effective EDZ cutoff in high stress environments. In Proceedings of the Excavation Disturbed Zone Workshop. Canadian Nuclear Society International Conference on Deep Geological Disposal of Radioactive Waste, Winnipeg, Canada, 1996.

Martin C.D, 1997. Seventeenth Canadian Geotechnical Colloquium: The effect of cohesion loss and stress path on brittle rock strength. Canadian Geotechnical Journal. Volume 34, No. 5, pp. 698-725.

Munier R, 1995. Studies of geological structures at Äspö. Comprehensive summary of results. SKB Progress Report 25-95-21. Swedish Nuclear Fuel and Waste Management Company, Stockholm, Sweden.

Myrvang A.M, 1997. Evaluation of in-situ rock stress measurements at the ZEDEX test area. SKB Progress Report HRL-97-22. Swedish Nuclear Fuel and Waste Management Company, Stockholm, Sweden.

Olsson M and Bergqvist I, 1997. Crack propagation in rock from multiple hole blasting - Summary of work during the period 1993-96. SveBeFo Rapport 32, Stockholm, Sweden.

Olsson O (ed), 1992. Site characterization and validation - Final report. OECD/NEA International Stripa Project, Technical Report 92-22. Swedish Nuclear Fuel and Waste Management Company, Stockholm, Sweden.

Olsson O, Bäckblom B, Ben Slimane K, Cournut A, Davies N, Mellor D, 1996a. Planning, organization, and execution of an EDZ experiment while excavating two test drifts by TBM boring and blasting, respectively.

Eurock'96, Barla (ed.)Balkema, Rotterdam, 1996 (ISBN 90 5410843 6), pp. 1323-1327.

Olsson O, Emsley S, Bauer C, Falls S and Stenberg L, 1996b. ZEDEX. A study of the zone of excavation disturbance for blasted and bored tunnels. Volume 1-3. SKB International Cooperation Report 96-03. Swedish Nuclear Fuel and Waste Management Company, Stockholm, Sweden.

Olsson O.L and Winberg A, 1996. Current understanding of extent and properties of the excavation disturbed zone and its dependence of excavation method. In Proceedings of the Excavation Disturbed Zone Workshop. Canadian Nuclear Society International Conference on Deep Geological Disposal of Radioactive Waste, Winnipeg, Canada, 1996.

Patrick W.C, 1986. Spent Fuel Test - Climax: An evaluation of the technical faisability of geologic storage of spent nuclear fuel in granite. Lawrence Livermore Laboratory, Report UCRL-53702.

Pusch R and Stanfors R, 1992. The zone of disturbance around tunnels at depth. In J. Rock Mech. Min. Sci & Geomech. Abstr. Vol 29, No. 5, pp. 447-456, 1992. Pergamon Press Ltd.

Read R.S and Martin C.D, 1991. Mine-by Experiment Final Design Report. AECL, WNRE. AECL Technical Report AECL-10430.

Read R.S, 1996. Characterizing excavation damage in highly-stressed granite at AECL's Underground Research Laboratory. In Proceedings of the Excavation Disturbed Zone Workshop. Canadian Nuclear Society International Conference on Deep Geological Disposal of Radioactive Waste, Winnipeg, Canada, 1996.

Rhén I (ed), 1995. Documentatin of tunnel and shaft data. Tunnel section 2874 - 3600 m. Hoist and ventilation shafts 0-450 m. SKB Progress Report 25-95-28. Swedish Nuclear Fuel and Waste Management Company, Stockholm, Sweden.

Rhén I (ed), Gustafson G, Stanfors R and Wikberg P, 1997. Äspö HRL - Geoscientific evaluation 1997/5. Models based on site characterization 1986-1995. SKB Technical Report 97-06. Swedish Nuclear Fuel and Waste Management Company, Stockholm, Sweden.

Rouhiainen P, 1995. Difference flow measurements at the Äspö HRL, May 1995. SKB International Cooperation Report 95-04. Swedish Nuclear Fuel and Waste Management Company, Stockholm, Sweden.

Sehlstedt S, Stråhle A, Triumf C.A, 1990. Geological core mapping and geophysical borehole logging in the boreholes KBH02, KAS09, KAS11-14 and HAS18-20 at Äspö. SKB Progress Report 25-90-06. Swedish Nuclear Fuel and Waste Management Company, Stockholm, Sweden.

Simmons G.R, 1992. The Underground laboratory Room 209 Excavation Response Test - a summary report. Atomic Energy of Canada Limited, WNRE, AECL Technical Report AECL-10430.

Sjöberg J and Rådberg G, 1994. Three dimensional numerical analysis of stresses and displacements at the ZEDEX test area, Äspö HRL. SKB Progress Report 25-94-31. Swedish Nuclear Fuel and Waste Management Company, Stockholm, Sweden.

SKB, 1994. Äspö Hard Rock Laboratory. Test plan for ZEDEX - Zone of Excavation Disturbance Experiment. Release 1.0. SKB International Cooperation Report 94-02. Swedish Nuclear Fuel and Waste Management Company, Stockholm, Sweden.

SKB, 1995. Äspö Hard Rock Laboratory. Test plan for ZEDEX - Zone of Excavation Disturbance Experiment. Extension. Release 1.0. SKB International Cooperation Report 95-07. Swedish Nuclear Fuel and Waste Management Company, Stockholm, Sweden.

SKB, 1996. Äspö Hard Rock Laboratory. Annual Report 1995. SKB Technical Report 96-06. Swedish Nuclear Fuel and Waste Management Company, Stockholm, Sweden.

SKB, 1997. Äspö Hard Rock Laboratory. Annual Report 1996. SKB Technical Report 97-08. Swedish Nuclear Fuel and Waste Management Company, Stockholm, Sweden.

Sumerling T, 1996. An international comparison of disposal concepts and postclosure assessments for nuclear fuel waste disposal. Prepared for AECL, Whiteshell Laboratories, Canada. Safety Assessment Management, Reading, United Kingdom.

Tan X.C and Kou S.Q, 1997. Test report on crack discrimination of rock samples from Äspö TBM tunnel. SKB Progress Report HRL-97-09. Swedish Nuclear Fuel and Waste Management Company, Stockholm, Sweden.

Tauzin E, 1996. MULTISIM V1.0. Code description and results of first phase validation. Colenco Power Engineering Ltd., Baden, Switzerland.

Tauzin E and Johns R.T, 1997. A new borehole simulator for the analysis of well test data in low-permeability formations. IAMG'97. The annual conference of the International Association for Mathematical Geology, 22 - 27 September, 1997, Barcelona, Spain.

Ubbes W. F, Yow J. L and Hustrulid W. A, 1989. Application of the results of excavation response experiments at Climax and the Colorado School of Mine to the development of an experiment for the Underground research Laboratory. Proc. of OECD/NEA Workshop on Excavation Response in Geological Repositories for Radionuclide Waste, Winnipeg, Canada 1988. OECD/NEA 1989.

Wikberg P, Gustafson G, Rhén I and Stanfors R, 1991. Äspö Hard Rock Laboratory. Evaluation and conceptual modelling based on the pre-investigations 1986-1990. SKB Technical Report 91-22. Swedish Nuclear Fuel and Waste Management Company, Stockholm, Sweden.

Wiles T, 1996. Map3D User's manual version 3.6. Mine Modelling Limited, Copper Cliff Canada.

Winberg A, 1995. Overview and review of experiments on the excavation disturbed zone (EDZ). SKB Progress Report 25-95-17. Swedish Nuclear Fuel and Waste Management Company, Stockholm, Sweden.

Young R.P and Maxwell S.C, 1992. Seismic characterization of a highly stressed rock mass using tomographic imaging and induced seismicity. Journal of Geophysical Research, vol. 97, pp 12361-12373.

APPENDIX 1

LIST OF PAPERS AND ARTICLES PUBLISHED WITH REFERENCES TO THE ZEDEX PROJECT

Barton N
Estimating rock mass deformation modulus for Excavation Disturbed Zone studies.
In Proceedings of the Excavation Disturbed Zone Workshop. Canadian Nuclear Society International Conference on Deep Geological Disposal of Radioactive Waste, Winnipeg, Canada, September 20, 1996 (ISSN 0-919784-44-5).

Bauer C, Homand F, Ben Slimane K
Disturbed Zone assessment with permeability measurements in the ZEDEX tunnel.
In Proceedings of the Excavation Disturbed Zone Workshop. Canadian Nuclear Society International Conference on Deep Geological Disposal of Radioactive Waste, Winnipeg, Canada, September 20, 1996 (ISSN 0-919784-44-5).

Bauer C, Homand-Etienne F, Slimane K B, Hinzen K G, Reamer S K
Damage zone characterization in the near field in the Swedish ZEDEX tunnel using *in situ* and laboratory measurements.
Eurock '96, ISRM International Symposium, Torino, Italy, September 2-5, 1996.

Davies N, Mellor D
Review of excavation disturbance measurements undertaken within the ZEDEX project: Implications for the Nirex Rock Characterisation Facility.
Eurock '96, ISRM International Symposium, Torino, Italy, September 2-5, 1996.

Falls S D, Young R P
Examination of the excavation-disturbed zone in the Swedish ZEDEX tunnel using acoustic emission and ultrasonic velocity measurements.
Eurock '96, ISRM International Symposium, Torino, Italy, September 2-5, 1996.

Falls S D, Young R P
Comparison of excavation disturbance around deep tunnels in hard rock using acoustic emission and ultrasonic velocity methods.
In Proceedings of the Excavation Disturbed Zone Workshop. Canadian Nuclear Society International Conference on Deep Geological Disposal of Radioactive Waste, Winnipeg, Canada, September 20, 1996 (ISSN 0-919784-44-5).

Fairhurst C, Damjanac B
The excavation damage zone - An international perspective.
In Proceedings of the Excavation Disturbed Zone Workshop. Canadian Nuclear Society International Conference on Deep Geological Disposal of Radioactive Waste, Winnipeg, Canada, September 20, 1996 (ISSN 0-919784-44-5).

Martin C D, Dzik E J, Read R S
Designing an effective EDZ cutoff in high stress environments.
In Proceedings of the Excavation Disturbed Zone Workshop. Canadian Nuclear Society International Conference on Deep Geological Disposal of Radioactive Waste, Winnipeg, Canada, September 20, 1996 (ISSN 0-919784-44-5).

Mellor D, Cournut A
Measurement of the Excavation Disturbed Zone in the ZEDEX project in the Context of Repository Post-Closure Performance Assessment.
In Proceedings of the Excavation Disturbed Zone Workshop. Canadian Nuclear Society International Conference on Deep Geological Disposal of Radioactive Waste, Winnipeg, Canada, September 20, 1996 (ISSN 0-919784-44-5).

Olsson O
ZEDEX- An *in situ* study at Äspö of the excavation disturbed zone for a TBM and drill and blast excavation. ZEDEX - En studie i Äspö av störda zonen för sprängd respektive borrad tunnel.
Bergmekanikdagen, SveBeFo, Stockholm, Mars 15, 1995.

Olsson O, Bäckblom G, Slimane K B, Cournut A, Davies N, Mellor D
Planning, organization, and execution of an EDZ experiment while excavating two test drifts by TBM boring and blasting, respectively.
Eurock '96, ISRM International Symposium, Torino, Italy, September 2-5, 1996.

Olsson O, Emsley S J, Cosma C, Tunbridge L, Stanfors R, Stenberg L
Integrated characterisation of a rock volume at the Äspö HRL utilised for an EDZ experiment.
Eurock '96, ISRM International Symposium, Torino, Italy, September 2-5, 1996.

Olsson O, Winberg A
Current understanding of extent and properties of the excavation disturbed zone and its dependence on excavation method.
In Proceedings of the Excavation Disturbed Zone Workshop. Canadian Nuclear Society International Conference on Deep Geological Disposal of Radioactive Waste, Winnipeg, Canada, September 20, 1996 (ISSN 0-919784-44-5).

Äspö Hard Rock Laboratory.
10 years of research. 1996. SKB, Stockholm.

List of SKB reports

Annual Reports

1977-78
TR 121
KBS Technical Reports 1 – 120
Summaries
Stockholm, May 1979

1979
TR 79-28
The KBS Annual Report 1979
KBS Technical Reports 79-01 – 79-27
Summaries
Stockholm, March 1980

1980
TR 80-26
The KBS Annual Report 1980
KBS Technical Reports 80-01 – 80-25
Summaries
Stockholm, March 1981

1981
TR 81-17
The KBS Annual Report 1981
KBS Technical Reports 81-01 – 81-16
Summaries
Stockholm, April 1982

1982
TR 82-28
The KBS Annual Report 1982
KBS Technical Reports 82-01 – 82-27
Summaries
Stockholm, July 1983

1983
TR 83-77
The KBS Annual Report 1983
KBS Technical Reports 83-01 – 83-76
Summaries
Stockholm, June 1984

1984
TR 85-01
Annual Research and Development Report 1984
Including Summaries of Technical Reports Issued during 1984. (Technical Reports 84-01 – 84-19)
Stockholm, June 1985

1985
TR 85-20
Annual Research and Development Report 1985
Including Summaries of Technical Reports Issued during 1985. (Technical Reports 85-01 – 85-19)
Stockholm, May 1986

1986
TR 86-31
SKB Annual Report 1986
Including Summaries of Technical Reports Issued during 1986
Stockholm, May 1987

1987
TR 87-33
SKB Annual Report 1987
Including Summaries of Technical Reports Issued during 1987
Stockholm, May 1988

1988
TR 88-32
SKB Annual Report 1988
Including Summaries of Technical Reports Issued during 1988
Stockholm, May 1989

1989
TR 89-40
SKB Annual Report 1989
Including Summaries of Technical Reports Issued during 1989
Stockholm, May 1990

1990
TR 90-46
SKB Annual Report 1990
Including Summaries of Technical Reports Issued during 1990
Stockholm, May 1991

1991
TR 91-64
SKB Annual Report 1991
Including Summaries of Technical Reports Issued during 1991
Stockholm, April 1992

1992
TR 92-46
SKB Annual Report 1992
Including Summaries of Technical Reports Issued during 1992
Stockholm, May 1993

1993
TR 93-34
SKB Annual Report 1993
Including Summaries of Technical Reports Issued during 1993
Stockholm, May 1994

1994

TR 94-33

SKB Annual Report 1994

Including Summaries of Technical Reports Issued during 1994

Stockholm, May 1995

1995

TR 95-37

SKB Annual Report 1995

Including Summaries of Technical Reports Issued during 1995

Stockholm, May 1996

1996

TR 96-25

SKB Annual Report 1996

Including Summaries of Technical Reports Issued during 1996

Stockholm, May 1997

List of SKB Technical Reports 1997

TR 97-01

Retention mechanisms and the flow wetted surface – implications for safety analysis

Mark Elert

Kemakta Konsult AB

February 1997

TR 97-02

Äspö HRL – Geoscientific evaluation 1997/1. Overview of site characterization 1986–1995

Roy Stanfors[1], Mikael Erlström[2], Ingemar Markström[3]

[1] RS Consulting, Lund

[2] SGU, Lund

[3] Sydkraft Konsult, Malmö

March 1997

TR 97-03

Äspö HRL – Geoscientific evaluation 1997/2. Results from pre-investigations and detailed site characterization. Summary report

Ingvar Rhén (ed.)[1], Göran Bäckblom (ed.)[2], Gunnar Gustafson[3], Roy Stanfors[4], Peter Wikberg[2]

[1] VBB Viak, Göteborg

[2] SKB, Stockholm

[3] VBB Viak/CTH, Göteborg

[4] RS Consulting, Lund

May 1997

TR 97-04

Äspö HRL – Geoscientific evaluation 1997/3. Results from pre-investigations and detailed site characterization. Comparison of predictions and observations. Geology and mechanical stability

Roy Stanfors[1], Pär Olsson[2], Håkan Stille[3]

[1] RS Consulting, Lund

[2] Skanska, Stockholm

[3] KTH, Stockholm

May 1997

TR 97-05

Äspö HRL – Geoscientific evaluation 1997/4. Results from pre-investigations and detailed site characterization. Comparison of predictions and observations. Hydrogeology, groundwater chemistry and transport of solutes

Ingvar Rhén[1], Gunnar Gustafson[2], Peter Wikberg[3]

[1] VBB Viak, Göteborg

[2] VBB Viak/CTH, Göteborg

[3] SKB, Stockholm

June 1997

TR 97-06

Äspö HRL – Geoscientific evaluation 1997/5. Models based on site characterization 1986–1995

Ingvar Rhén (ed.)[1], Gunnar Gustafson[2], Roy Stanfors[3], Peter Wikberg[4]

[1] VBB Viak, Göteborg

[2] VBB Viak/CTH, Göteborg

[3] RS Consulting, Lund

[4] SKB, Stockholm

October 1997

TR 97-07

A methodology to estimate earthquake effects on fractures intersecting canister holes

Paul La Pointe, Peter Wallmann, Andrew Thomas, Sven Follin

Golder Associates Inc.

March 1997

TR 97-08

Äspö Hard Rock Laboratory Annual Report 1996

SKB

April 1997

TR 97-09

A regional analysis of groundwater flow and salinity distribution in the Äspö area

Urban Svensson

Computer-aided Fluid Engineering AB

May 1997

TR 97-10
On the flow of groundwater in closed tunnels. Generic hydrogeological modelling of nuclear waste repository, SFL 3–5
Johan G Holmén
Uppsala University/Golder Associates AB
June 1997

TR 97-11
Analysis of radioactive corrosion test specimens by means of ICP-MS. Comparison with earlier methods
R S Forsyth
Forsyth Consulting
July 1997

TR 97-12
Diffusion and sorption properties of radionuclides in compacted bentonite
Ji-Wei Yu, Ivars Neretnieks
Dept. of Chemical Engineering and Technology, Chemical Engineering, Royal Institute of Technology, Stockholm, Sweden
July 1997

TR 97-13
Spent nuclear fuel – how dangerous is it? A report from the project "Description of risk"
Allan Hedin
Swedish Nuclear Fuel and Waste Management Co,
Stockholm, Sweden
March 1997

TR 97-14
Water exchange estimates derived from forcing for the hydraulically coupled basins surrounding Äspö island and adjacent coastal water
Anders Engqvist
A & I Engqvist Konsult HB, Vaxholm, Sweden
August 1997

TR 97-15
Dissolution studies of synthetic soddyite and uranophane
Ignasi Casas[1], Isabel Pérez[1], Elena Torrero[1], Jordi Bruno[2], Esther Cera[2], Lara Duro[2]
[1] Dept. of Chemical Engineering, UPC
[2] QuantiSci SL
September 1997

TR 97-16
Groundwater flow through a natural fracture. Flow experiments and numerical modelling
Erik Larsson
Dept. of Geology, Chalmers University of Technology, Göteborg, Sweden
September 1997

TR 97-17
A site scale analysis of groundwater flow and salinity distribution in the Äspö area
Urban Svensson
Computer-aided Fluid Engineering AB
October 1997

TR 97-18
Release of segregated nuclides from spent fuel
L H Johnson, J C Tait
AECL, Whiteshell Laboratories, Pinawa, Manitoba, Canada
October 1997

TR 97-19
Assessment of a spent fuel disposal canister. Assessment studies for a copper canister with cast steel inner component
Alex E Bond, Andrew R Hoch, Gareth D Jones, Aleks J Tomczyk, Richard M Wiggin, William J Worraker
AEA Technology, Harwell, UK
May 1997

TR 97-20
Diffusion data in granite Recommended values
Yvonne Ohlsson, Ivars Neretnieks
Department of Chemical Engineering and Technology, Chemical Engineering, Royal Institute of Technology, Stockholm, Sweden
October 1997

TR 97-21
Investigation of the large scale regional hydrogeological situation at Ceberg
Anders Boghammar[1], Bertil Grundfelt[1], Lee Hartley[2]
[1] Kemakta Konsult AB, Sweden
[2] AEA Technology, UK
November 1997

TR 97-22
Investigations of subterranean microorganisms and their importance for performance assessment of radioactive waste disposal. Results and conclusions achieved during the period 1995 to 1997
Karsten Pedersen
Göteborg University, Institute of Cell and Molecular Biology, Dept. of General and Marine Microbiology, Göteborg, Sweden
November 1997

TR 97-23
Summary of hydrogeologic conditions at Aberg, Beberg and Ceberg
Douglas Walker[1], Ingvar Rhén[2], Ioana Gurban[1]
[1] INTERA KB
[2] VBB Viak
October 1997

TR 97-24
Characterization of the excavation disturbance caused by boring of the experimental full scale deposition holes in the Research Tunnel at Olkiluoto
Jorma Autio
Saanio & Riekkola Oy, Helsinki, Finland
September 1997

TR 97-25
The SKB Spent Fuel Corrosion Programme.
An evaluation of results from the experimental programme performed in the Studsvik Hot Cell Laboratory
Roy Forsyth
Forsyth Consulting
December 1997

TR 97-26
Thermoelastic stress due to a rectangular heat source in a semi-infinite medium. Application for the KBS-3 repository
Thomas Probert, Johan Claesson
Depts. of Mathematical Physics and Building Physics, Lund University, Sweden
April 1997

TR 97-27
Temperature field due to time-dependent heat sources in a large rectangular grid. Application for the KBS-3 repository
Thomas Probert, Johan Claesson
Depts. of Mathematical Physics and Building Physics, Lund University, Sweden
April 1997

TR 97-28
A mathematical model of past, present and future shore level displacement in Fennoscandia
Tore Påsse
Sveriges geologiska undersökning, Göteborg Sweden
December 1997

TR 97-29
Regional characterization of hydraulic properties of rock using well test data
David Wladis, Patrik Jönsson, Thomas Wallroth
Department of Geology, Chalmers University of Technology, Göteborg, Sweden
November 1997